SD98-06-F

South Dakota
Department of Transportation
Office of Research

U.S. Department
of Transportation
Federal Highway
Administration

Evaluation of High Performance Concrete in Four Bridge Decks as well as Prestressed Girders for Two Bridges

Study SD98-06
Final Report

Prepared by
Dr. V. Ramakrishnan
Distinguished Professor, SDSM&T.
501 East St. Joseph Street
Rapid City, SD 57701-3995 (605) 394 - 2439
&
Dr. Arden Sigl
Professor, SDSU.
Brookings, SD 57007-1098 (605) 688-6526

December 2001

DISCLAIMER

The contents of this report reflect the views of the authors who are responsible for the facts and accuracy of the data presented herein. The contents do not necessarily reflect the official views or policies of the South Dakota Department of Transportation, the State Transportation Commission, or the Federal Highway Administration. This report does not constitute a standard, specification, or regulation.

ACKNOWLEDGEMENTS

This work was performed under the supervision of the SD98-06 Technical Panel:

William Brinkman..... SD ACPA
Mark Clausen ..... FHWA
John Cole.....Bridge Design
Dan Johnston.....Office of Research
Corey Haeder……SD Concrete Products
Ron McMahon-Office of Materials& Surfacing
Craig Smith ..... Sioux Falls Area
Daniel Strand.....Office of Research
Tammy Williams.....Custer Area

The work was performed in cooperation with the United States Department of Transportation Federal Highway Administration.

TECHNICAL REPORT STANDARD TITLE PAGE

1. Report No. SD1998-06-F	2. Government Accession No.	3. Recipient's Catalog No.
4. Title and Subtitle Evaluation of High Performance Concrete in Four Bridge Decks as well as Prestressed Girders for Two Bridges		5. Report Date December 31, 2001 6. Performing Organization Code
7. Author(s) Dr. V. Ramakrishnan & Dr. Arden Sigl*		8. Performing Organization Report No.
9. Performing Organization Name and Address Department of Civil & Environmental Engineering 501 East St. Joseph Street Rapid City, SD 57701-3995 (605) 394 – 2439 *Department of Civil & Environmental Engineering SDSU. Brookings, SD 57007-1098 (605) 688 - 6526		10. Work Unit No. 11. Contract or Grant No. 310560
12. Sponsoring Agency Name and Address South Dakota Department of Transportation Office of Research 700 East Broadway Avenue Pierre, SD 57501-2586		13. Type of Report and Period Covered Final Report 12/29/97 to 12/31/01 14. Sponsoring Agency Code
15. Supplementary Notes Project Monitor: Dan Strand		

16. Abstract

The South Dakota Department of Transportation constructed two three span high performance concrete (HPC) bridges in the summers of 1999 and 2000. The twin prestressed girder bridges are located along Interstate 29 near Sioux Falls, South Dakota. In each bridge instrumentation was installed in two end span girders and in the deck of an end span of these structures. This report presents the results of the laboratory trial batches and testing to optimize HPC mix designs for the girders and the decks. Detailed strain histories in the girders and in the decks, and deflections of the girders prior to installation in the bridge and after they were installed in the bridge over the two year period are also reported.

For the high performance bridge deck concrete two different coarse aggregates were used (quartzite and limestone) and ten mixes were cast with each aggregate. In each mix the percentage replacement of cement by weight with silica fume and fly ash was varied, keeping the w/c ratio constant. For the high-strength bridge girder concrete, twelve mixes were cast varying both the percentage replacement of cement with silica fume and the w/c ratios. The percentage replacements of silica fume investigated were 7%, 10% and 12% and the w/c ratios investigated were 0.28, 0.30, and 0.32. All concretes were tested for compressive strength, static modulus, modulus of rupture and chloride permeability. The addition of fly ash and silica fume reduced the chloride permeability of concrete significantly while increasing the compressive strength. Based on the analysis of results obtained, one mix was chosen, as the best mix having all the properties required for a high performance bridge deck. Another high strength HPC mix was selected for the girders to satisfy the strength requirements for the early release of prestress strands and at 28 days. Detailed compressive strength time histories out to ages of one year were developed for the concrete used in the structures. Tests to determine the modulus of elasticity for both the girder and deck concrete were conducted at selected ages out to one year. Shrinkage blocks were cast and instrumented in order to monitor the development of shrinkage strains in the girders and the bridge decks. The total cost of the HPC bridges and the standard SDDOT present design bridges is almost the same. However the life-cycle cost may be cheaper because of the anticipated longer life and reduced maintenance costs for the HPC bridges. Conclusions and recommendations are included in the report.

17. Keywords Bridge deflections, Bridge strains, Chloride permeability, Fly ash, High performance concrete, Silica fume.	18. Distribution Statement No restrictions. This document is available to the public from the sponsoring agency.

19. Security Classification (of this report) Unclassified	20. Security Classification (of this page) Unclassified	21. No. of Pages # of pages	22. Price

CONTENTS

LIST OF FIGURES

Chapter 3

Chapter 4

LIST OF TABLES

Chapter 3

Chapter 4

Appendix A

Appendix B

GLOSSARY

The following is a glossary of terms for High performance concrete (HPC) used in this report.

0.1 General Terms

High Performance Concrete - Concrete in which certain desired properties have been enhanced, for a given application, beyond the properties for plain concrete.

High Strength Concrete - Concrete with compressive strength in excess of 42 MPa (6000 psi) is referred to as high strength concrete.

Admixtures – Admixtures are materials other than water, aggregate, or hydraulic cement, which are added to the batch immediately before or during the mixing operation. Their function is to modify properties of concrete so as to make it more suitable for the work at hand, or for economy, or for other purposes such as saving energy.

Fly ash - Fly ash is a finely divided residue, which is the by-product of the combustion of ground or powdered coal exhaust fumes of coal-fired power stations.

Silica fume - Silica fume is a by-product resulting from the use of high purity quartz with coal in the electric arc furnace in the production of silicon and ferro silicon alloys

Chloride Permeability of Concrete - Measure of concretes ability to resist penetration of chloride ions.

Flexural Toughness - The area under the flexural load-deflection curve obtained from a static test of a specimen up to a specified deflection. It is an indication of the energy absorption capability of a material.

Impact Strength - The total energy required to break a standard test specimen of a specified size under specified impact conditions, as given by ACI Committee 544.

Static Modulus - The value of Young's modulus of elasticity obtained from measuring stress-strain relationships derived from other than dynamic loading.

Accelerated Curing – Curing concrete using warm water to accelerate strength gain.

0.2 Acronyms Used

ACI – American Concrete Institute

PCC – Portland Cement Concrete

ASTM – American Society of Testing of Materials

AASHTO – American Association of State Highway and Transportation Officials

FHWA – Federal Highway Administration

SDDOT – South Dakota Department of Transportation

HPC – High Performance Concrete

HSC – High Strength Concrete

MRWR – Medium Range Water Reducer

HRWR – High Range Water Reducer

RCPT – Rapid Chloride Permeability Test

AEA – Air Entraining Agent

SDSM&T – South Dakota School of Mines & Technology

SDSU – South Dakota State University

SSD – Saturated Surface Dry

0.3 ASTM Specifications

C 31 - Practices for Making and Curing Concrete Test Specimens in the Field

C 39 - Test Method for Compressive Strength of Cylindrical Concrete Specimens

C 78 - Test Method for Flexural Strength of Concrete (Using Simple Beam with Third-point Loading)

C 94 - Specification for Ready-Mixed Concrete

C138 - Test for Unit Weight, Yield and Air Content (gravimetric) of concrete

C 143 - Test Method for Slump of Portland Cement Concrete

C 172 - Method of Sampling Freshly Mixed Concrete

C 173 - Test Method of Air Content of Freshly Mixed Concrete by the Volumetric Method

C 231 - Test Method for Air Content of Freshly Mixed Concrete by the Pressure Method

C 469 - Test Method for Static Modulus of Elasticity and Poisson's Ratio of Concrete in Compression

C 1064 – Standard Test Method for Temperature of Freshly Mixed Portland Cement Concrete

C 1202 - Test Method for Electrical Indication of Concrete's Ability to Resist Chloride Ion Penetration

C 666 - Test Method for Resistance of Concrete to Rapid Freezing and Thawing

CHAPTER 1.0

EXECUTIVE SUMMARY

1.1 Problem Description

Due to tightening budget constraints, transportation engineers are challenged to construct transportation facilities economically with an increase in performance. However, simultaneous improvements in cost and performance are unlikely unless material properties or construction methods can be enhanced. High performance concrete (HPC) may be utilized to enhance the desired concrete properties for a given application.

These are the times when bridge designers are concerned with overhead clearances for highways beneath bridges, the need for increased span lengths, without increasing girder depth, or may desire to reduce the number of girders for a bridge, all of which would require HPC. In South Dakota, de-icing chemicals are used to assist in the removal of ice from driving surfaces. These chemicals pose problems on pavements and bridge decks. Due to the concrete's permeability as well as any cracking, chemicals can penetrate the concrete causing rebar corrosion and concrete deterioration over time in bridge decks shortening deck life.

Understanding the possible benefits of HPC, SDDOT's bridge designers wanted to construct and evaluate two bridge decks as well as prestressed girders for two bridges. Therefore, trial HPC batches were prepared and the necessary testing of fresh and hardened concrete properties were conducted to ensure that the desired concrete properties were achieved. Some of the fresh and hardened concrete properties for each HPC mix were unknown and needed to be determined prior to the construction of girders and decks. Some properties in question for HPC's were: 28-day compressive strength, obtaining strand release strength in a specified time, thermal properties, creep, shrinkage and elastic shortening for high strength concrete with limestone and quartzite aggregates; permeability and crack potential of concrete utilizing fly ash, silica fume, or a combination of fly ash and silica fume with limestone and quartzite aggregate; etc.

1.2 Research Objectives

1. To recommend HPC mix designs for use in bridge decks and prestressed girders.
2. To evaluate the constructability and performance of HPC in bridge decks and prestressed girders.

1.3 Details of Bridges

The two railroad overpass bridges constructed and evaluated for the HPC Research project are located in Minnehaha County approximately one mile north of the interchange between I-29 and I-90. Bridge no. 1, as it is referred to in this report, carries I-29 northbound traffic over the Burlington-Northern Railroad track. The second bridge, referred to as bridge 2 in

this report, carries I-29 southbound traffic over the same railroad track. Bridge 1 was constructed in the summer of 1999 and bridge 2 was constructed in the summer of 2000.

The location was chosen mainly because high traffic counts and heavy use of deicing salts provided a true test of the strength and durability of HPC. Also, more clearance was needed for that railroad. The bridges are 52.36 m (171.8 ft) in length, have a 27° left-hand forward (LHF) skew, and are designed for a 12.19 m (40-foot) roadway. Each bridge has three spans with four girder lines of AASHTO Type II prestressed girders (total of twelve girders). Eight of the prestressed girders are 16.38 m (53.75 ft) long and are used on the 16.46 m (54 ft) end spans. The other four girders are 18.36 m (60.25 ft) long and are used in the 18.59 m (61 ft) long center span. The South Dakota Department of Transportation inventory numbers for these bridges are 50-181-155 for bridge 1 and 50-180-155 for bridge 2.

The girders are spaced 3.49 m (11.42 ft) center to center with an overhang of 1.28m (4.208 ft) on each side of the bridge. When the deck was placed, abutment concrete is cast around the ends of the girders, which made the girders integral with the abutment. At the bents fairly thick diaphragms were cast around the girder ends, which helps continuity between spans. The use of HPC allowed designers to reduce the number of girders in each span from five to four. Design compressive strength of the girder concrete was 68.3 MPa (9900 psi) with a strength of 56.9 MPa (8250 psi) required at release of the prestressing strands.

1.4 Literature Review

A comprehensive literature review relevant to HPC' s use for bridge decks and prestressed girders as well as instrumentation methods to monitor them was conducted which helped in the planning and conducting the research project.

1.5 Trial Mixes

The aim was to design, evaluate and recommend mixture proportions for the bridge deck and the prestressed girder concrete. For the high performance bridge deck concrete two different coarse aggregates were used (quartzite and limestone) and ten mixes were cast with each aggregate. In each mix the percentage replacement of cement by weight with silica fume and fly ash was varied, keeping the w/c ratio constant. The specimens were tested for compressive strength, static modulus, modulus of rupture and chloride permeability. For the high-strength bridge girder concrete, twelve mixes were cast varying both the percentage replacement of cement with silica fume and the w/c ratios. The percentage replacements investigated were 7%, 10% and 12% and the w/c ratios investigated were 0.28, 0.30, and 0.32. The specimens cast were tested for compressive strength and static modulus.

It was found that the addition of fly ash and silica fume reduces the chloride permeability of concrete significantly while increasing the compressive strength. Based on the analysis of results obtained, one mix was chosen, as the best mix having all the properties required for a high performance bridge deck. The results obtained from the tests carried out on the high

strength concrete mixes were analyzed thoroughly and one mix was selected based on the strength requirements at release of prestress. This mix was cast again and tests were conducted to confirm the results. Additionally the rapid chloride permeability test was also conducted on this mix.

1.6 The field sampling program

The sampling frequency for the project was selected in order to provide the necessary information to permit the evaluation of the concrete properties of interest. All the standard routine tests were performed on the fresh concrete samples. Detailed strength histories of the concretes were developed by performing compressive tests at concrete ages of 1, 3, 7, 14, 28, 56 (or 90), 180 days and one year. For the instrumented girders, both a companion cured series and a laboratory-cured series were employed. A partial series was fabricated for girders that did not carry instrumentation. The deck concrete was sampled at each midspan and at each bent. This resulted in five samples and five series were fabricated for each deck.

1.7 Instrumentation for Girders and Bridge Decks

The instrumentation was developed for taking of measurements of strains, temperatures, and deflections in both the girders and the decks. Two girders in the end span of these structures were selected to receive instrumentation. In each bridge the instrumented girders are located in the north end-span and are the west side edge girder and the adjacent interior girder. Strains were measured with Geokon Model VCE 4200 vibrating wire strain transducers. Each vibrating wire transducer is capable of providing a temperature measurement in addition to a strain measurement. Several thermistors were included in the concrete decks in order to measure additional temperatures.

In order to measure the strains in the girders, four strain transducers were located at the mid-span of each girder and were distributed more or less uniformly through the depth of the girder. To enable the measurement of deflections, full depth rods were embedded in the girders at the center, ends and the quarter points of the beams. These full-depth rods permitted the measurement of deflections over the top of the girders and the later measurement of the deflections of the girders and thus the bridge from underneath the structure.

A shrinkage block of 152×152×304 mm (6 x 6 x 12 inches) with an embedded vibrating wire strain transducer was cast with each instrumented girder in order to track the time dependent behavior of the concrete.

In the bridges additional strain transducers were placed at the bent in the gap between the end of an instrumented girder and the following center-span girder. Three transducers were distributed in this space through the depth of the girder. The deck instrumentation was set up to permit the measurement of deck strains at eight additional locations. Two locations were directly above the instrumentation in the girders and distributed through the thickness of the deck. Two additional locations were at mid-span of each instrumented girder but 90 degrees to

the girder' s longitudinal axes and midway between the girder lines. At the bents four additional locations were established along the centerline of the abutment. Two of these locations were directly above the transducers within the bent and two were located midway between the girder lines. At each of these eight locations, two vibrating wire transducers and one thermistor were installed. The vibrating wire transducers were positioned at the level of the top and bottom mat of steel with the thermistor located midway between the strain transducers. In order to measure the deck-concrete shrinkage strains, two shrinkage blocks were cast from the deck concrete. These blocks were of the same dimensions as the girder blocks, and each carried a strain transducer.

There was interest in taking measurements of impedance in the deck concrete. Parallel plate devices were fabricated and embedded in the decks in order to permit these measurements. A total of six were embedded in each deck. These were distributed in the north end-span of the bridges and located randomly across the width of the deck. In each set of three, two were stacked vertically such that one was at the level of the bottom mat of steel and the other was located at the top mat of steel. The third device was located a short distance away and positioned at the level of the top mat of steel. With only minor interruptions the instrumented girders and decks had been continuously monitored from the time the concrete was placed

1.8 Tests on Hardened Concrete Field Samples

For the two bridges, a total of 796 cylinders were prepared. Of this number approximately 92 cylinders were assigned to the rapid chloride test. In total, 701 cylinders were tested in compression (Three were not tested.). To document the modulus of elasticity 102 tests were performed.

The girder mixes employed silica fume in the concrete mix. The range in compressive strength at 28 days ranged from a low of 91.0 MPa (13,200 psi) to a high value of 108.2 MPa (15,700 psi). The average value being 99.28 MPa (14,400 psi) with a standard deviation of 6.8 MPa (990 psi). The stress at transfer was specified to be not less than 58.6 MPa (8,520 psi) with a minimum compressive strength at 28 days of 68.26 MPa (9,900 psi). It took about three days to obtain the needed compressive strength in order to permit prestress transfer to the girders.

Two different deck mixes were employed. A silica fume mix was used on the bridge built in 1999 and a fly ash mix was used for the bridge built in 2000. The results from the five compressive strength series for the silica fume deck produced a range in compressive strength at 28 days from 46.54 MPa to 48.75 MPa (6750 to 7070 psi). The mean of the 28 day tests was 48.75 MPa (7070 psi) with a standard deviation of 2.28 MPa (330 psi).

The results for the fly ash mix for the deck on bridge 2 yielded a range at 28 days from 43.6 MPa to 49.0 MPa (6330 to 7110 psi). At 28 days, the mean was 46.6 MPa (6,760 psi) with a standard deviation of 2.2 MPa (320 psi).

In the design of prestressed concrete structures, it is important to have a reliable estimate of the modulus of elasticity for the concrete. The equation that is recommended for use with high strength concrete will be referred to as the ACI 363 equation.

$$E_c = \left(40{,}000\sqrt{f_c'} + 1{,}000{,}000\right)\left(\frac{w_c}{145}\right)^{1.5}$$

E_c = Modulus of Elasticity (psi units).

w_c = Unit weight of the concrete (lbs/ft^3).

f_c' = Compressive strength of the concrete (psi units.)

In total, 98 modulus of elasticity tests were performed on the concrete sampled from the girders and the decks. The conclusion reached from the present work is that the above equation can be used to estimate the modulus of elasticity for the concrete in this study if the constant of 6895 MPa (1,000,000 psi) is replaced by the constant 13,790 MPa (2,000,000 psi). This result is not unexpected. The work that was done to develop the ACI 363 equation utilized limestone aggregates. The mixes in this study made use of quartzite aggregate and quartzite is a much harder aggregate. This equation can be used on the deck concretes as well. It should be noted that, at the present time, high strength concrete is a concrete with a 28-day compressive strength greater than 41.37 MPa (6,000 psi).

The rapid chloride permeability test (RCPT) was conducted as per ASTM C 1202. A total of 60 specimens from bridge 1 and 32 specimens from bridge 2 were tested. The permeabilities for the silica fume bridge deck varied from 398 to 621 coulombs, with an average value (for 24 specimens) of 462 coulombs. For the fly ash bridge deck concrete, the permeabilities varied from 708 to 1404 coulombs with an average value of (for 24 specimens) 1038 coulombs. These variations were less than others experienced for field concrete and it indicated a good quality control in the production of concrete.

The major purpose of this project is to develop the concrete mix design to minimize the intrusion of chloride ions so that rebar corrosion is reduced. The project' s requirements stated that “the bridge deck permeability should be reduced to a significant amount (50%) as compared to SDDOT' s standard bridge deck mix”. The permeability of SDDOT' s standard bridge deck mix (laboratory mix) was 4158 coulombs. There was a 88.9% reduction in permeability for silica fume bridge deck concrete and 75% reduction in permeability for the fly ash concrete. However the fly ash concrete had 123% higher permeability than the silica fume concrete.

The high strength HPC mix used for the fabrication of the girders had very low permeabilities, 65 coulombs for bridge 1 and 87 coulombs for bridge 2, which are according to ASTM C 1202 are "Negligible". The high strength HPC used for girders was almost impermeable and the steel tendons would not corrode due to the chloride penetration.

1.9 Performance of HPC Bridge Girders and Decks

1.9.1 Deflection Measurements: The initial set of deflection measurements was taken immediately after the transfer of prestress to the girders. Observations continued to be taken at close, but increasing time intervals out to one month, thereafter readings were taken approximately monthly. After the concrete deck was placed readings were taken from the underside of the girders. The three wire leveling technique employed is expected to yield results within ± 0.46 mm (± 0.018 in.).

The average maximum instantaneous camber (upward deflection) after the transfer of prestress to the two girders from bridge 1 was 17.8 mm (0.70 inches). The corresponding value for the girders for bridge 2 is 16.8 mm (0.66 inches). About a month later the maximum camber that was exhibited averaged 24.4 mm (0.96 inches) for the girders for bridge 1 and 30.7 mm (1.21 inches) for the girders for bridge 2. This difference in camber is 45 percent or 31 percent depending which girder is selected as the base for comparison. The displacements due to deck placement were –8. 6 mm (–0.34 inch) for bridge 1 and –11.2 mm (–0.44 inch) for bridge 2. This is an interesting result since the decks were designed to have the same thickness. Two different concretes were used in the two decks but their densities would not differ by this amount.

Since the decks have been placed, the long-term deflections are not changing significantly. Bridge 2 is exhibiting about double the long-term upward camber as compared to bridge 1, 12.7 and 6.35 mm (0.50 and 0.25 inches) respectively.

1.9.2 Impedance measurements: The measurements of impedance in the silica fume concrete have shown a tremendous degree of variability. This is particularly true during the winter. Average values in the winter tend to be up around 45,000 ohms and about 15,000 to 20,000 ohms in the summer. The fly ash concrete has not shown this variability, averaging perhaps 5,000 ohms over both the winter and the summer. The readings from the fly ash deck also tend to increase slightly during the winter months, but not as dramatically as the readings from the silica fume deck.

1.9.3 Thermal and shrinkage strains: In order to analyze the strains in the girders and in the deck, a reliable estimate of the coefficient of thermal expansion is needed. To obtain this estimate shrinkage blocks were cast– one for each girder and two for each deck. Early in the history of these blocks the shrinkage is superimposed on the thermal changes taking place and are of the same order of magnitude. For this reason, one must wait several months in order for the shrinkage rate to slow, so that a reliable estimate of the coefficient of thermal expansion can be made. It was noted that the winter months did not produce satisfactory estimates for the coefficient of thermal expansion. It appeared as if the freeze-thaw effects were affecting the expansion and contraction of the blocks.

It was decided to use only summer months to estimate the thermal coefficient. In addition, in order to add reliability to the results, a diurnal temperature change of not less than 18 Fahrenheit degrees would be required before this temperature change would be used to estimate the coefficient of thermal expansion.

It had been decided, based on some of the year 2000 results and before all of the data was available, that a coefficient of thermal expansion equal to $7.50 \times 10^{-6}/^{o}F$ would be used for the project. As it turned out this value may have been a little low, but, in any case, it was used. The strain analysis is not that sensitive to the exact value of the coefficient of thermal expansion. The value selected for use does fit within the range of values that are quoted for quartzite aggregate concrete in ACI Publication 209R-92 ($6.50 \times 10^{-6} / {}^{o}F - 8.11 \times 10^{-6} / {}^{o}F$

Having a value for the coefficient of thermal expansion, the thermal strains were filtered from the shrinkage block strain histories. This isolates the shrinkage strain and permits the analysis of the time variation of the shrinkage strains. The classic increase in shrinkage strain with time during the early age of the concrete was observed. After this more rapid development of shrinkage strains the shrinkage strains level off and, in theory, asymptotically approach a limiting maximum value. For the sake of discussion, the early-age will refer to the first 100 days and later-age will refer to the time period later than 100 days.

All strain histories appear to exhibit a significant seasonal effect after the initial shrinkage occurs. The shrinkage decreases over the winter months and then rises to a maximum value during the summer months. The reason for this phenomenon is not fully understood. It is likely that the concrete actually gains back a portion of the initial shrinkage when water from rain or melted snow permeates into the blocks. A further complicating factor in the behavior of the blocks is the effect of freezing and subsequent thawing, or the effect of several of these cycles. In addition, the support conditions may have been an issue. Further monitoring of the bridges is needed in order to determine whether this variation in the shrinkage is a seasonal phenomenon due to the interaction of the blocks with the environment, or something different.

The girder concrete for bridge 1 demonstrated a maximum early-age shrinkage of about 150 με (microstrain = 10^{-6} in/in) the corresponding value for the girders for bridge 2 is 200 με. This difference is about 25 to 30 percent depending on how one elects to express the difference. What is interesting is that there is not nearly this variation between the two shrinkage blocks. It may be indicative of the variation inherent in dealing with a silica fume mix. This difference in shrinkage contributes to the increased camber that developed in the girders for bridge 2.

The deck concretes present a little different picture. The early period shrinkage for the silica fume concrete making up the deck is about 240 to 250 με. The corresponding fly ash concrete early period (first 100 days) shrinkage is about 150 με. This difference is significant. The silica fume concrete exhibited about 1.6 times as much early period shrinkage as the fly ash concrete. This difference holds true for the late shrinkage as well.

1.9.4 Developing the strain time histories: In order to analyze the strain time series several adjustments were made to the basic data. The strain transducers yield raw strain measurements. In order to analyze the results the data was converted to a base temperature of 72 Fahrenheit degrees. In all cases a time zero was selected about two days after the concrete was initially placed in the forms. The selection of the time zero does influence the subsequent time histories, but a half day one way or the other does not have a great affect on the results.

After the time histories are generated, the results from the shrinkage blocks are used to factor out the shrinkage strains. These resulting strain histories are subjected to further analysis.

1.9.5 The girder strain time histories: As has been stated, a total of four strain transducers are located at the mid-span cross-section of each instrumented girder. At each time for which readings were taken, a regression analysis was carried out on the results from these four transducers. From this regression result, a strain is computed at the top fiber of the girder, at the bottom fiber of the girder and at the centroid of the girder.

From the measurements, the following observations can be made. The average initial compressive strain at the centroid of the girders for bridge no. 1 is about 425 με. Since this strain is at the centroid of the section, it is an indicator of the initial prestress force, P_i. In Bridge 2, it is observed that the initial compressive strain at the centroid is about 525 με. The difference between these two values is about 19 percent. This difference seems large considering the agreement in the initial deflections.

The time variation change in the strain due to creep from the time the girder was cast until the deck was placed is about 25 με in Bridge 1 and about 75 με in Bridge 2. These values represent a change of about 5.9 percent in the initial prestress in the girders for bridge 1 and about a 14.0 percent change in the initial prestress for bridge 2. This change in strain occurs over an approximate two-month period.

There is no significant long-term change in the strains measured in bridge 1 from August 1999, through March 2000. After March 2000, there is an apparent long-period seasonal change or perhaps a nonrecurring change, which of the two that it is cannot be determined. More data is needed in order to determine what is occurring. This indicates that the total losses due to creep and relaxation is about 6.0 percent for bridge 1. This analysis is complicated by the variation noted above.

After the deck is in place on bridge 2, there is a small but continued development of creep strain. This is about 20 to 30 με. This strain developing over an 11-month period. This is indicative of an additional 4 to 5 percent loss in initial prestress force. This brings the total loss due to creep and shrinkage to date to 18.0 percent for bridge 2. More analysis is needed in order to give a more definitive result for the losses in these bridges.

1.9.6 Girder mid-span curvatures and bent curvatures: The curvature at a cross-section of a beam is the reciprocal of the radius to which the beam is bent at that point in the beam. This can

be calculated from measured strains. This was done for each of the instrumented girders. After they were computed for each girder the values were averaged for the girders for each bridge. The average curvature that developed after prestress transfer is about 20.0 με/in for the girders in bridge 1 and about 25.0 με/in for the girders in bridge 2. These reflect a difference of 20 to 25 percent, again, depending upon which value is used to make the comparison. These percentages are in reasonable agreement with the difference in the strains at the centroid of the section, which they should be, because the prestress that is applied causes the initial curvature.

At the bent in the space between the girder ends a set of three vibrating wire transducers were arranged in a stacked array. These transducers were used to compute the curvature at the bent. Two installations of this type were made in each bridge. The two sets installed in bridge 1 provide good results. The set in bridge two at the exterior girder was damaged during deck placement. The other installation at the bent in bridge 2 is working okay. The curvatures were computed for the remaining three sets of transducers.

The curvatures at the bent in bridge 1, demonstrate an almost linear reduction in curvature over the two years since the bridge was constructed. The change is from a value of about 9.5 με/in to a minimum value in August of 2001 of about 4.5 με/in. There is not as much data available for bridge 2 but it appears to be behaving in a similar manner. This change in curvature may be caused by the tendency of the decks to shrink and thus change the curvature between the girders. More data is needed in order to see exactly what is happening at these locations in the bridges. This is a puzzling but interesting phenomenon.

1.9.7 Deck strains: The analysis of the strains in the decks proceeded in the manner discussed for the girders with the exception that only strains at the mid-thickness of the decks were computed for each of the eight instrumented locations in the deck. The results from the four locations at mid-span were then averaged. The four locations at the bent were also averaged. Focusing on the net strains after the shrinkage strains have been factored out, the following observations can be made. The tensile strains are significantly higher in the silica fume deck of bridge 1 as compared to the fly ash deck of bridge 2. Bridge 1 has an average tensile strain of about 160 με at mid-span. The corresponding value over the bent is about 420 με. Similar results for Bridge 2 are 60 με at mid-span and 250 με over the bent. If one averages the 160 and the 420 and divides this number by the average of the 60 and the 250, the result obtained indicates that the bridge 1 has tensile strains about 1.9 times greater than bridge 2.

The strains in the deck are interesting, but difficult to explain. They are consistent with the developing data that indicates that the silica fume deck exhibited a greater tendency to shrink and thus develop tensile stresses. On the other hand, as will be seen, there are about twice as many transverse cracks in the silica fume deck as compared to the fly ash deck, thus with cracking, the tensile stresses should be reduced. The data is consistent with a highly restrained element, which the deck seems to be. Not much is known about the creep of concrete in tension

except that it certainly takes place. Additional data and further detailed analysis is needed before additional comments can be made.

1.9.8 Underside deck crack surveys: Significant transverse deck cracking was noted in bridge 1 during the first winter (Early January 2000) after it was constructed. Transverse deck cracking was also noted in bridge 2 during this bridge' s first winter. In August of 2001, underside deck surveys were conducted on these two bridges. The number of cracks was counted between each girder and along the overhangs.

These cracks have been observed to seep moisture during the winter. This is easily observed during the winter months and was the reason that the cracks were first noted in January of 2000. Nearly all of these cracks are exhibiting calcium carbonate precipitate.

The crack spacing in the end spans of the bridge 1 is about double the spacing observed in the center span. For bridge 2 this same relative spacing is observed. This indicates, which makes sense, that there is more restraint in the center span which contributes to greater cracking. Overall, the average crack spacing in bridge 1 is about 1.37m (4.5 feet). The corresponding value for bridge 2 is about 2.32m (7.6 feet). The ratio of the crack spacing in bridge 2 to the crack spacing in Bridge 1 is 1.7. This is in general agreement with the shrinkage data from the two bridges. This ratio, as previously cited, is 1.6. The basic point is that there is significantly more cracking in the silica fume deck as compared to the fly ash deck and this is supported by the data that has been taken.

1.10 Cost Comparison

In the twin HPC bridges constructed, only 4 girders were used instead of 5 used in similar bridges in SDDOT present design. Therefore the girder spacing had increased necessitating an increase in deck slab thickness. A comparison of the costs for the girders and decks for the HPC in the year 1999 and 2000 and the present SDDOT design is shown below.

	Conventional Concrete	High Performance Concrete (1999)	High Performance Concrete (2000)
Girders	$94, 778.75	$50, 459.2	$91, 660
Deck	$72, 587. 27	$81, 972	$85, 536

The total cost comparison between HPC bridges in 1999 and 2000, and the standard concrete bridge in 1999 is shown below:

	1999-First Year Bid Cost	2000-Second Year Bid Cost
Conventional Concrete Bridge		
Girders	$94, 778.75	
Deck	$72, 587. 27	
Total	**167366.02**	
HPC Bridge		
Girders	$50, 459.2	$ 91, 660
Deck	$81, 972	$ 85, 536
Total	**132431.2**	**177196**

In the year 1999, the girder cost was well below the average (standard concrete) and the total bridge cost was also below average because for the 1999 bridge, the prestressed girders were purchased by SDDOT directly from the fabricator and supplied to the contractor.

1.11 Conclusions

Based on the test results and the observations made during the course of this investigation, the following conclusions are offered.

1.11.1 High Strength HPC Mix and Performance of Prestressed Girders

- The silica fume high strength HPC mix developed by the laboratory trial mixes and slightly modified for the field conditions and used in the fabrication of prestressed girders performed well both in the fresh and hardened states. The selected mix had 403.24 kg/m^3 (680 lb/cu.yd) cement and 49.81 kg/m^3 (84 lb/cu.yd) of silica fume with a water to cement ratio of 0.28 and water to cement + silica fume ratio of 0.25. This mix gave the required 127 to 178 mm (5 to 7 inches) slump and 4.0±1.0 % air. The coarse aggregates consisted of 19 mm (3/4 inch) Sioux falls quartzite aggregate. There was a significant increase in the compressive strength due to the addition of silica fume. This mix exceeded the specified design strength requirements of 56.9 MPa (8520 psi) at release of the strands and 68.3 MPa (9900 psi) at 28 days. This mix developed a range in stress at 28 days of 89.64 MPa (13, 000 psi) to 108.25 MPa (15,700 psi). Based on the results obtained from the field concrete used in the fabrication of the girders this high strength HPC mix could be used with design strength (28 days) conservatively set at 82.7 MPa (12,000 psi). This predicts that 95 percent of the results would break at, or higher than the design strength. This statement assumes that three cylinders be used and averaged to produce one test result, and that the test results are normally distributed.

- The modulus of elasticity of the high strength HPC mix with quartzite aggregate was higher than the SDDOT standard mixes used for prestressed girders. The modulus of elasticity for this mix can be estimated by the recommended ACI 363 equation with the substitution in this equation of 13790 MPa (2,000,000 psi) for the 6895 MPa (1,000,000 psi) constant.
- The modulus of elasticity of the high strength HPC mix with quartzite aggregate was higher than the SDDOT standard mixes used for prestressed girders. The current equation that is recommended for evaluating the modulus of elasticity of HSC is the ACI 363 equation. It has the form-

  ACI equation 363:

$$E_c = \left(40{,}000\sqrt{f_c'} + 1{,}000{,}000\right)\left(\frac{w_c}{145}\right)^{1.5} \qquad \text{eq. 4-2}$$

  An equation to predict the modulus of elasticity for HSC is not provided in either the current AASHTO or ACI 318 specifications. Based on the tests conducted as part of this research, and limited to mixes containing Sioux Quartzite aggregate, it is concluded that the above equation be used with the modification that the 1,000,000 constant be changed to 2,000,000. The resulting form is –

$$E_c = \left(40{,}000\sqrt{f_c'} + 2{,}000{,}000\right)\left(\frac{w_c}{145}\right)^{1.5} \qquad \text{eq. 4-3 .}$$

- The girders in bridge 1 exhibited a maximum early age (first 100 days) shrinkage of 150 με, the corresponding value for the girders of bridge 2 was 200 με. This is a variation of 25 to 30 percent. It is likely to be indicative of the variation in shrinkage that can be expected in silica fume high strength HPC. This was observed to be about half of that predicted for "so-called", standard concrete (Using the recommendations as suggested by the ACI 209 committee.)
- The loss in initial prestress for the girders due to the combined effect of creep and relaxation up to the time the deck was cast, was about 6 percent for the girders in bridge 1, and about 14 percent for the girders in bridge 2. The girders in bridge 2 exhibited an additional 4.8 percent loss from the time that the deck was placed up to the time that the girders were one year of age. Due to the form of the data record for bridge 1 it is not possible to estimate the losses in bridge 1 after the deck placement (More data is needed as the record is developing a possible

periodic component). It is expected that additional losses (It is believed that their magnitude is not large.) have occurred, but their magnitude cannot be estimated at this time. Additional data and further analysis will be needed to determine a more reliable estimate of the time-dependent losses in these girders.

- The long-term curvature in bridge 2 is about double the curvature exhibited in bridge 1. This conclusion is consistent with the measured deflections. With the decks in place, these structures have not shown a tendency to develop increasing long-term deflections. It can be concluded that this is due to the shrinkage that is occurring in the deck, which counteracts the tendency for the girders to exhibit increased camber. This conclusion is based on limited data.
- The measured curvatures taken in the gap between the girders at the bent demonstrate significant reduction over time. In bridge 1 it has been reduced from 9.5 to 4.0 (Curvature units in^{-1}, the values have been multiplied by 10^6.) over a two year time period. The results for bridge 2 show a similar trend but it is not as dramatic. The problem is that only one year of data is available from bridge 2 and more data will be needed to assess this behavior. The trend in the curvatures at the bents is difficult to explain.
- The average chloride permeability for the girders in bridges 1 and 2 were 65 and 87 coulombs respectively. According to ASTM C 1202, the chloride ion penetrability for both bridge girders is "Negligible". Therefore the high strength HPC could be considered as impermeable and the corrosion potential of the prestressed steel tendons is negligible.

1.11.2 Bridge Deck Concrete and Performance of the Decks

Based on the analysis of the trial mixes the following conclusions are made:

- The compressive strengths of concretes containing silica fume and fly ash were significantly higher when compared to plain concretes at the same w/c ratio and age. The increase in strength due to the addition of mineral admixtures was more prominent at later ages (28 day).
- There was no significant change in the modulus of rupture values for concretes containing silica fume and fly ash when compared to plain concretes at the same w/c ratio.
- The increase in static modulus values was more prominent in concretes containing just silica fume when compared with plain concrete at the same w/c ratios.

- There was no significant change in the compressive strength due to variation in the type of coarse aggregate used. Almost all the mixes containing limestone aggregate showed higher modulus of rupture values when compared to the same mixes containing quartzite aggregate.
- There was a significant reduction in the chloride permeability values in concretes containing silica fume when compared to plain concretes at the same w/c ratios. The reduction was more prominent in the concretes containing just silica fume than the concretes containing a combination of silica fume and fly ash. Concretes containing just fly ash showed higher chloride permeabilities when compared to concretes with silica fume but lower chloride permeabilities when compared to plain concretes.
- The results of the rapid chloride permeability tests carried out on specimens, subjected to accelerated curing showed a good correlation with the results obtained from the tests carried out at 90-days.
- All mixes containing mineral admixtures showed low workability and hence water reducers were used to obtain the required workability. The addition of the water reducers did not affect the strength.

Based on the test results of the field concrete used in bridge 1 and 2, the following conclusions are offered:

- The 28 day compressive strengths obtained were, silica fume trial mix 61.5 MPa (8910 psi), silica fume mix for bridge 1- 48.8 MPa (7070 psi), fly ash mix for bridge 2 - 46.6 MPa (6760 psi). At 90 days, both concretes had the same compressive strength 53.5 MPa (7760 psi). The 1-year compressive strengths were silica fume mix for bridge 1-57.6 MPa (8350 psi), fly ash mix for bridge 2- 62.4 MPa (9040 psi). Both mixes had much higher strength than the design 28-day strength 31 MPa (4500 psi). This is about 50% higher strength than the required strength. At 28 days, the silica fume mix used in the bridge deck yielded a 5 percent greater strength than the fly ash mix used in bridge deck no. 2. At one year the fly ash mix yielded compressive strength results 7 percent higher than the silica fume mix. This was as expected.
- The silica fume deck concrete exhibited 1.6 times more early age shrinkage strain than the fly ash concrete mix. This had contributed to the greater deck cracking than was observed in the fly ash deck concrete.

- Both decks tended to develop significant tensile strains. On average the silica fume deck developed average tensile strains 1.9 times greater than the average tensile strains that were measured in the fly ash deck.
- There was a higher heat of hydration and higher temperatures during the early curing period in silica fume concrete as compared to the fly ash concrete.
- A coefficient of thermal expansion of $13.5 \times 10^{-6}\ ^{o}C^{-1}$ ($7.5 \times 10^{-6}\ ^{o}F^{-1}$) can be used with confidence for silica fume and fly ash mixes representative of those studied in this research.
- The crack survey data demonstrate that there was 1.7 times more cracking in the silica fume deck as compared to the fly ash deck. This is in general agreement with the deck tensile strain data.
- The fly ash mix is considered to be better for deck use than the silica fume mix because of the fly ash concrete' s tendency to develop lower shrinkage strains and thus develop fewer cracks. A further negative for the silica fume mix is that it requires much more care during the placing and curing of the concrete. For this reason, silica fume concrete is likely to cost more than fly ash concrete.
- The rapid chloride permeabilities as measured from the ASTM C 1202 test for the silica fume bridge deck concrete ranged from 393 to 621 coulombs and for fly ash concrete used in bridge deck 2 varied from 708 to 1404 coulombs. The average permeability (24 specimens) for silica fume concrete was 462 coulombs whereas the permeability of SDDOT' s standard bridge deck concrete was 4158 coulombs. This is 88.9 % reduction which had far exceeded the required 50% reduction. The average permeability (24 specimens) for the fly ash concrete was 1038 coulombs which was a reduction of 75%. The permeability of fly ash concrete was 123 % higher than that of the silica fume concrete containing 7 percent silica fume.
- According to ASTM C1202, the chloride ion penetrability is "very low" for the silica fume concrete and "low" for the fly ash concrete. It is concluded that the potential for rebar corrosion is low for both silica fume and fly ash concretes.

1.11.3 Cost

- The cost of the superstructure for the bridges was the same on a first cost basis for both the HPC bridge and the normal concrete SDDOT present design bridge. However the life cycle

cost might be cheaper for the HPC bridge because of the anticipated longer life and reduced maintenance cost.

- The use of HPC allowed designers to reduce the number of girders in each span from five to four. However the thicker deck needed due to the wider girder spacing negated the savings realized in the girders.

1.12 Recommendations

Prestressed Girders:

1. For the fabrication of prestressed girders, when compressive strengths greater than 62 MPa (9000 psi) are required, the high strength silica fume HPC should be specified. The 28-day design compressive strength could be specified as high as 82.7 MPa (12,000 psi), but the fabricator would want the concrete to reach the release strength in a few days for production purposes. Therefore the mix should be designed to reach the fabricator' s required release strength in the specified number of days.

   The feasibility of producing and using high strength silica fume HPC mix had been successfully demonstrated in this project. The concrete was almost impermeable and hence the corrosion potential was eliminated. The anticipated benefits are less number of girders, less deflection, less prestress loss due to creep and shrinkage.

2. Based on extensive testing of trial mixes and analysis, the following mix proportions are recommended for high strength girder concrete. This mix was used for a design strength (f_c') of 68.3 MPa (9900 psi) and the average strength obtained was 99.3 MPa (14,400 psi). The fabricator wanted to achieve the specified strand release strength of 56.9 MPa (8250 psi) in 3 days.

Cement (Type II)	403.24 kg/m^3	680 lbs./pcy
Water included from		
Silica fume slurry and HRWR	112.67 kg/m^3	190 lbs./pcy
Coarse aggregate (3/4" quartzite)	1082.23 kg/m^3	1825 lbs./pcy
Fine aggregate (S.S.D)	683.16 kg/m^3	1200 lbs./pcy
Silica fume	49.81 kg/m^3	84 lbs./pcy
Air Content	4.0±1.0%	4.0±1.0%
Water to Cement ratio	0.28	0.28
Water/C+S.F. ratio	0.25	0.25

Note: The recommended slump was 127 to 178 mm (5 to 7 inches). The dosage of High Range Water Reducer (HRWR) and/or water reducer should be adjusted according to the field conditions to achieve the specified slump. The 19mm (3/4 inch) quartzite aggregate used in this project conformed to the standard specifications for Roads and

Bridges, Section 820 for Size No. 1 (SDDOT). The mixing water should be adjusted taking into account the excess water present in the silica fume slurry and the high range and mid range water reducers.

3. The equation currently recommended for calculation of modulus of elasticity (E_c) for HSC is the ACI 363 equation:

$$E_C = \left(40{,}000\sqrt{f_c'} + 1{,}000{,}000\right)\left(\frac{w_C}{145}\right)^{1.5}$$

Based on the modulus of elasticity (ASTM C469) tests conducted as part of this research and limited to mixes containing Sioux Quartzite aggregate, it is recommended that the above equation be modified by changing the 1,000,000 constant to 2,000,000. Therefore the recommended formula becomes:

$$E_c = \left(40{,}000\sqrt{f_c'} + 2{,}000{,}000\right)\left(\frac{w_c}{145}\right)^{1.5}$$

It is recommended that the ACI 363 equation be used without modification for mixes containing limestone aggregates since the research was not conducted on mixes containing limestone aggregate.

Bridge Deck:

4. For the construction of bridge decks, the Class F fly ash concrete which was successfully used in the construction of bridge deck 2, should be specified for future deck concrete. Compared to plain deck concrete, the benefits of using fly ash deck concrete as demonstrated in this project, are substantial reduction in the chloride ion penetrability (a "low" value as per ASTM C1202), reduced corrosion potential, higher modulus concrete, reduced plastic shrinkage, reduced drying shrinkage, reduced restrained shrinkage cracking in the underside of the deck slabs, reduced early temperature rise due to the hydration activity, less micro-cracking, higher durability, better workability, and good finishability. This fly ash concrete developed smaller tensile stress in the deck than the silica fume concrete. All these benefits could be realized without an increase in cost.
5. The recommended bridge deck concrete mix proportions are given below.

Cement (Type I/II)	349.87 kg/m^3	590 lbs./cu.yd.
Fly ash (Class F)	74.53 kg/m^3	124 lbs./cu.yd.
Water	151.22 kg/m^3	255 lbs./cu.yd.
Fine aggregate (sand)	724.65 kg/m^3	1222 lbs./cu.yd.
Coarse aggregate (rock)	968.96 kg/m^3	1634 lbs./cu.yd.

Percent air	6.5%±1.0%	6.5%±1.0%
Water/C ratio	0.432	0.432
Water/C+FA ratio	0.357	0.357

Note: Appropriate quantity of water reducer either mid range or high range should be used to obtain the specified slump. The mixing water should be adjusted taking into account the excess water in the water reducer used. An appropriate amount of air entraining agent should be used to obtain an air content of 6.5±1 %.

The 28-day design compressive strength could be specified as 37.9 MPa (5500 psi) because this mix gave an average compressive strength of 46.2 MPa (6700 psi) at 28 days. According to ACI 318, for a design strength (f_c') of 37.9MPa (5500 psi), the required average strength would be (5500+1200) 6700 psi. This higher design strength could be used in the design of the deck slab to reduce the thickness. Based on the performance of the bridge decks in bridges 1 and 2, the fly ash mix is deemed better for deck use than silica fume mix. There is apparently no economical way to efficiently control the shrinkage, and thus the tendency to produce cracks in the silica fume mix.

6. Where higher strength concrete is not needed and when the design compressive strength of 31 MPa (4500 psi) is required then the following Class F fly ash concrete could be used for both limestone and quartzite aggregate. This recommendation is based on the ongoing research "Determination of Optimized Fly Ash Content in Bridge Deck and Bridge Deck Overlay Concrete: SD00-06". When this mix is used the chloride ion permeability at 90 days (ASTM C1202) would be reduced more than 50 percent compared to Class A bridge deck concrete currently used.

Cement Type I/II	291 kg/m^3	491 lbs./cu.yd.
Fine Aggregate	652 kg/m^3	1100 lbs./cu.yd.
Coarse Aggregate	1023 kg/m^3	1725 lbs./cu.yd.
Water	155 kg/m^3	262 lbs./cu.yd.
Fly Ash	97 kg/m^3	164 lbs./cu.yd.
Percent air	6.5%±1.0%	6.5%±1.0%
Water to Cement ratio	0.53	0.53
Water/C+S.F. ratio	0.40	0.40

Note: The appropriate amount of air entraining agent should be used by the contractor to obtain the specified air content.

7. For bridge deck concrete, the rapid chloride permeability at 90 days, as determined by the ASTM C 1202 test, should be specified for accepting the concrete. The specification should require that the charge passed should be less than 2000 coulombs at 90 days testing, which ensures the "low" chloride ion penetrability. The major objective of this project was to

develop a mix proportion to reduce the chloride permeability by 50 percent. The fly ash deck concrete used in the project achieved a 75% reduction in the chloride permeability.

8. In cases where the w/c ratios are very low (in the range of 0.28 to 0.32) and mineral admixtures such as silica fume and fly ash are in use, high range water reducers are recommended. In cases where the w/c ratio is around 0.40, mid range water reducers may be sufficient. Addition of large quantities of mid range water reducers lowers the rate of strength gain.
9. It is strongly recommended that, whenever silica fume is used in bridge deck concrete, a proper 100% humid curing for 5 to 7 days is necessary to minimize shrinkage cracking. This could be achieved with continuous water sprays or misting and/or fogging devices. The same construction procedures for mixing, transporting, placing, consolidating, finishing and tining used for construction with standard concrete should be followed. The same construction techniques and equipment without major modification could be used for the construction of HPC bridge decks.

General:

10. When silica fume is used in a slurry form, the slurry should be sampled and tested while being continuously agitated, before use and at specified intervals during the concrete production. The amount of silica fume in the slurry could be determined by the hydrometer test. Because the silica fume is suspended in water (not dissolved), there is an inevitable tendency for the silica fume to settle to the bottom. To avoid this a continuous agitation of the liquid with proper instruments is recommended. The water in the slurry should be accounted for and the mix water should be adjusted.
11. When HPC mixes are used, it is recommended that the following quality control tests should be conducted in the field using ASTM test procedures for the fresh concrete: slump, unit weight, air content, and the concrete temperature. The ambient temperature, humidity, and the wind velocity should be recorded during the bridge deck concrete placement or the fabrication of the prestressed girders. The compressive strength and static modulus tests should be conducted on the field samples collected and cured according to the ASTM standard procedures at 28 days. When HPC is used for fabricating prestressed girders, it is recommended that companion cylinders (preferably 102 mm × 204 mm (4" × 8")) should be placed near the girder and cured under identical conditions as the girders, to determine when

the prestressed strands can be released as per specifications. When chloride permeability is specified, the hardened concrete samples made from the actual concrete placed should be tested for rapid chloride permeability at 90 days as per ASTM C 1202. The cylinder samples can be made in the field and cured as per standard ASTM procedures for 28 days.

12. These two bridges should continue to be monitored by using the already installed instrumentation and by visual observation. Only limited data, (one-year for bridge 2, and two years for bridge 1) have been gathered. To determine the long term behavior, several years of monitoring is required.

CHAPTER 2.0

PROBLEM DESCRIPTION AND OBJECTIVES

2.1 Problem Description

Due to tightening budget constraints, transportation engineers are challenged to construct transportation facilities economically with an increase in performance. However, simultaneous improvements in cost and performance are unlikely unless material properties or construction methods can be enhanced. High performance concrete (HPC) may be utilized to enhance the desired concrete properties for a given application. Recently, HPC was redefined and, although this definition is several pages long, may be summarized as "the enhancement of certain desired concrete properties for a given application beyond the properties for plain concrete."

These are the times when bridge designers are concerned with overhead clearances for highways beneath bridges, the need for increased span lengths, without increasing girder depth, or may desire to reduce the number of girders for a bridge, all of which would require HPC. In South Dakota, de-icing chemicals are used for removing ice from driving surfaces. These chemicals pose problems on pavements and bridge decks. Due to the concrete's permeability as well as any cracking, chemicals can penetrate the concrete causing rebar corrosion and concrete deterioration over time in bridge decks shortening deck life.

Understanding the possible benefits of HPC, SDDOT's bridge designers wanted to construct and evaluate two bridge decks as well as prestressed girders for two bridges. While HPC may appear to have higher initial costs, these higher costs may be offset through reduced girder depths, reduced number of girders, reduced number of substructure units, or reduced concrete deck thickness. HPC in concrete deck surfaces can result in higher resistance to chloride intrusion, less surface cracking and greater resistance to freeze-thaw deterioration. Therefore, where HPC is utilized, there is a potential to reduce repair and replacement costs. SDDOT took the opportunity to incorporate HPC into two bridge decks on I-229 in Sioux Falls as well as the decks and prestressed concrete girders for two additional bridges on I-29 north of Sioux Falls. Trial HPC batches were prepared and the necessary testing of fresh and hardened concrete properties were conducted to ensure that the desired concrete properties were achieved. Some of the fresh and hardened concrete properties for each HPC mix were unknown and needed to be determined prior to the construction of girders and decks. Some properties in question for HPC's are: 28-day compressive strength, obtaining strand release strength in a specified time, thermal

properties, creep, shrinkage and elastic shortening for high strength concrete with limestone and quartzite aggregates; permeability and crack potential of concrete utilizing fly ash, silica fume, or a combination of fly ash and silica fume with limestone and quartzite aggregate.

2.2 Research Objectives

1. To recommend HPC mix designs for use in bridge decks and prestressed girders.
2. To evaluate the constructability and performance of HPC in bridge decks and prestressed girders.

2.3 Materials

2.3.1 Cement: Type I/II portland cement satisfying the requirements of ASTM C150 was used for all mixes. The cement was supplied by Dacotah Cement.

2.3.2 Coarse Aggregate: The coarse aggregate used was crushed limestone and quartzite. The maximum size of the coarse aggregate was ¾ in. with absorption coefficient of 0.45 %. The specific gravity of the limestone aggregate was 2.68 and that of the quartzite aggregate was 2.63. The quartzite aggregate was supplied by Winters Concrete & L.G. Everest and the limestone aggregate was obtained from Hills Material, Rapid City, South Dakota.

2.3.3. Fine Aggregate: The fine aggregate used was natural sand with a water absorption coefficient of 1.6%. It was obtained from Birdsall Sand and Gravel, from their sites at Igloo and Oral, South Dakota, and supplied by Winters Concrete & L.G. Everest.

2.3.4 Water: The water used was tap water from the Rapid City Municipal water supply system.

2.3.5 Admixtures: The mineral admixtures used were Coal Creek Fly Ash (Class F) supplied by JTM Industries, WashBurn, North Dakota and Densified Silica Fume supplied by Norchem Concrete Products, Inc. The chemical admixtures used were Standard Air Entraining Agent (AEA) - MB-VR (Master Builders), High Range Water Reducer (HRWR) Rheobuild 1000 (Master Builders), Medium Range Water Reducer (MRWR) -Polyheed-997 (Master Builders).

2.4 Quality Control Tests

2.4.1 Tests on Fresh Concrete: The freshly mixed concrete was tested for slump (ASTM C143), air content (ASTM C231), fresh concrete unit weight (ASTM C138), and concrete temperature (ASTM C 1064). The ambient temperature and humidity were also recorded.

2.4.2 Tests on Hardened Concrete:

2.4.2.1 Compressive Strength and Static Modulus: Cylinders were tested for static modulus (ASTM C 469) and compressive strength (ASTM C 39) at 14 and 28 days. Prior to the compression test, the cylinders were also tested for the static modulus of elasticity (ASTM C 469) and for dry unit weight. The dry unit weight was obtained by dividing the weight of the specimen by the measured volume of the specimen. The size of the cylinders was 150 mm x 300 mm (6 in. x 12 in.).

2.4.2.2 Modulus of Rupture Test (Static Flexural Strength): Beams were tested at 14 and 28 days for the flexural strength in accordance with the ASTM C 78, which was a load-control test. The beams were tested over a simply supported span of 300 mm (12 inches) and third point loading was applied to the beams. The size of the beams was 100 mm x 100 mm x 350 mm (4x4x14 - inch).

2.4.2.3 Rapid Chloride Permeability Test (RCPT): The RCPT (1,2) was conducted in accordance with the procedure given in ASTM C 1202. A brief summary of the procedure followed is given below:

Test Specimen: The 100 mm x 200 mm (4 in. x 8 in.) cylinders were cut to a thickness of 50 mm (2 in.) from the top (finished) surface by using a concrete saw (the saw used was a diamond saw). This slice was used as the test specimen.

Conditioning

- Two liters of tap water were boiled vigorously and then allowed to cool to the room temperature.
- The specimens were allowed to dry for one hour. A sufficient amount of two-part epoxy was mixed in a plastic container. This epoxy was then coated on the circumferential sides of the specimens using a brush. The epoxy used was DEVCON High Strength epoxy resin (5 minute fast drying), 2,4,6-TRI (Dimethylaminomethyl) Phenol and Amine/Mercaptan hardener. The epoxy was allowed to cure thoroughly.
- The specimens were then placed in the vacuum dessicator (PR-1070-L for humidifying 8 samples bought from Germann Instruments) bowl such that both ends of each specimen were exposed. The edges of the lid were cleaned and lightly oiled.

The lid was then placed on the dessicator and the vacuum pump was turned on. The vacuum was maintained at -0.8 BAR (-13 psi) for 3 hours.

- After three hours, the separatory funnel was filled with deaerated water. With the vacuum pump still running, the water stopcock was opened and sufficient water was let into the dessicator to completely submerge the specimens. The stopcock was then closed and the vacuum pump was run for one additional hour.
- At the end of the additional hour the vacuum pump was turned off and the vacuum line stopcock was opened to let in the air and the specimens were allowed to soak under water for 18±2 hours.

Test Procedure

- The specimens were removed from the vacuum dessicator and were prevented from drying by enclosing the specimens in a plastic bag and pouring water into it.
- The inside surface of the vulcanized rubber gaskets (100 mm [4 in.] outside diameter and 75 mm [3 in.] inside diameter and 6mm [0.5 in.] thick) were coated with a cell sealant. The sealant used was SILICONE (Dow Corning Brand) available in 82.8 ml (2.8 fl.oz.) tubes.
- One of the gaskets (PR-1010M sealing rings bought from Germann Instruments) was placed in the space above the mesh. Then the specimen was pushed into the gasket. The spacer was placed over the specimen and the other gasket was positioned at the end of the specimen. Finally, the second half of the cell was positioned over the gasket with bolts going through the attachment holes. The washers and the nuts were attached to the bolts and tightened.
- The specimen was positioned in the measuring cell (PR-1000 Measuring Cell, complete with two connecting cables and temperature probe bought from Germann Instruments) containing a fluid reservoir for each end of the specimen. One reservoir was filled with 3% sodium chloride (NaCl) solution and the other with 0.3 N sodium hydroxide (NaOH) solution. The specimen was positioned such that the finished surface of the specimen was facing the NaCl reservoir and the cut surface facing the NaOH reservoir. The reservoir containing NaCl is connected to the negative terminal; the NaOH reservoir is connected to the positive terminal of the power supply.

- The lead wires were attached to cell electrical connectors and the cells were connected to the power supply. The power supply used was PROOVE IT (PR-1050 bought from Germann Instruments, Inc.) power supply with microprocessor and circuits for measuring the voltage and the current on each attached cell. The voltage supplied to the power supply unit was 230V AC or 115V AC, frequency 50 or 60 Hz. The voltage output from the power supply unit was 10/20/30/60 VDC, selected by the microprocessor (we used 60 VDC). The power supply can test a maximum of 8 cells at a time. The built-in A/D converter was controlled by the microprocessor, which in turn transferred the data to the computer, where the data was processed and stored for a later printout.
- The power supply was turned on and the voltage value was set to 60 VDC. The computer program used (PR-1040 Software supplied by Germann Instruments) recorded the current (in mA) and temperature (in ^{o}C) values every 5 minutes.
- The test was terminated after six hours. The specimen was removed and the cells were rinsed thoroughly in tap water and the residual sealant was stripped out and discarded.

2.5 Test Specimens

The specimens cast for each mix are as follows:

- Eight 100 mm x 100 mm x 350 mm (4 in. x 4 in. x14 in.) beams - Four to be tested at 14 and four at 28-days for static flexural strength.
- Six 150 mm x 300 mm (6 in. x 12 in.) cylinders – Three to be tested at 14 and three at 28-days for static modulus and compressive strength.
- Ten 100 mm x 200 mm (4in. x 8 in.) cylinders – To be used in the Chloride Permeability Tests.

All the beams were cast in wooden molds and all the cylinders in plastic molds. All the molds were oiled prior to the casting. The specimens were covered with plastic sheets for twenty-four hours after casting at room temperature. They were then demolded and placed in a lime saturated water tank for curing. The beams and cylinders remained in the curing tanks until testing at either 14 or 28-days.

2.6 Details of Bridges

The two railroad overpass bridges constructed and evaluated for the HPC Research project are located in Minnehaha County approximately one mile north of the interchange between I-29 and I-90. Bridge no. 1, as it is referred to in this report, carries I-29 northbound traffic over the Burlington-Northern Railroad track. The second bridge, referred to as bridge no. 2 in this report, carries I-29 southbound traffic over the same railroad track. Bridge 1 was constructed in the summer of 1999 and bridge 2 was constructed in the summer of 2000.

The location was chosen mainly because high traffic counts and heavy use of deicing salts provided a true test of the strength and durability of HPC and to provide more clearance for the railroad below.

The bridges are 52.36 m (171.8 ft) in length, have a 27° left-hand forward (LHF) skew, and are designed for a 12.19 m (40-foot) roadway. Each bridge has three spans with four girder lines of AASHTO Type II prestressed girders (total of twelve girders). Each bridge has eight prestressed girders, which are 16.38 m (53.75 ft) long and are used on the 16.46 m (54 ft) end spans. In addition each bridge has four girders 18.36 m (60.25 ft) long and are used in the 18.59 m (61 ft) long center span. The South Dakota Department of Transportation inventory numbers for these bridges are 50-181-155 for bridge 1 and 50-180-155 for bridge 2.

The girders are spaced 3.49 m (11.42 ft) center to center with an overhang of 1.28m (4.208 ft) on each side of the bridge. When the deck was placed, abutment concrete was cast around the ends of the girders, which made the girders integral with the abutment. At the bents fairly thick diaphragms are cast around the girder ends, which help to produce continuity between spans.

The use of HPC allowed designers to reduce the number of girders in each span from five to four. Design compressive strength of the girder concrete was 68.3 MPa (9900 psi) strength of 56.9 MPa (85200 psi) required at release of the strands.

CHAPTER 3.0

TASK DESCRIPTION

3.1 Task 1- Review and summarize literature relevant to HPC's use for bridge decks and prestressed girders as well as instrumentation methods used to monitor them.

3.1.1 High Performance Concrete: High Performance Concrete (HPC) has many definitions. The Federal Highway Administration (FHWA) definition states that "HPC is a concrete that has been designed to be more durable and if necessary, stronger than conventional concrete" (1). A Strategic Highway Research Program (SHRP) study (2) defined HPC for concrete as

1. A maximum water–cementitious ratio of 0.35
2. A minimum durability factor of 80% as determined by ASTM C 666, and
3. A minimum strength criteria of either
    - 21 Mpa (3000 Psi) within 4 hours after placement (Very Early Strength),
    - 34 Mpa (5000 Psi) within 24 hours (High Early Strength) or
    - 69 Mpa (10,000 Psi) within 28 days (Very High Strength)

In a SDDOT study SD94-04 (3); HPC was defined "as a concrete with highly enhanced (or improved) desirable properties for the specific purpose and function for which it is used". It need not necessarily be high-strength concrete. HPC for the bridge deck overlay, pavement, and white topping will have enhanced ductility, impermeability, fatigue strength, impact resistance, toughness, wear resistance and durability. The American Concrete Institute (ACI) defined HPC as "Concrete meeting special combinations of performance and uniformity requirements that cannot always be achieved routinely using conventional constituents and normal mixing, placing, and curing practices" (1). In other words, (3-10) high performance concrete (HPC) is any concrete, which has one, or more of its attributes enhanced beyond that of ordinary concrete to meet the performance need for a specific application. The use of fly ash, silica fume and slag in various types of concretes including high strength concretes is essential today. In order to achieve workability, uniformity, strength and durability, such additives are more readily used in today's structural applications. Additionally, environmental needs require the disposal of these ingredients and their use in concrete achieved cost-effective enhancement of the concrete properties. If concretes of compressive strengths in excess of 83 Mpa (12,000 psi) have to be

achieved then the use of these ingredients become essential. Examples of characteristics that may be considered critical for an application are:

- Ease of placement
- Compaction without segregation
- Early age strength
- Long term mechanical properties
- Permeability
- Density
- Heat of hydration
- Toughness
- Volume stability
- Long life in severe environments

Because many characteristics of high performance concrete are interrelated, a change in one usually results in changes in one or more of the other characteristics. Consequently, if several characteristics have to be taken into account in producing concrete for the intended application, each of these characteristics must be clearly specified.

HPC has many useful applications and potential benefits to the highway industry, which include:

- Better performance and service life of highway facilities.
- Less maintenance, because of enhanced concrete durability.
- Lower life-cycle cost.
- Less construction time, as in repairs and fast track construction.
- Higher productivity and quality of pre-cast and prestressed products.
- Less consumption of cement and more conservation of resources

High-performance concrete for bridges (4-10) is a new approach to concrete materials engineering which places increased emphasis on both strength and durability. Although compressive strength has typically been the main consideration in concrete mix design, specified compressive strengths are usually much lower than what can be currently achieved. In addition, durability concerns have often been limited to providing protection from freeze-thaw deterioration.

The durability of concrete (11-13) depends largely on its ability to resist the penetration of water and aggressive compounds. Four major types of environmental distress occur in reinforced concrete: corrosion of reinforcement, alkali aggregate reactivity, freeze-thaw deterioration, and attack by sulfates. Corrosion of steel occurs most extensively.

In each case, water or solutions penetrating the concrete initiate or accelerate the distress, making costly repairs necessary. Air-entrained concretes with low permeability are required to resist the infiltration of harmful solutions and provide the necessary durability when exposed to the environment. Low-permeability concretes perform better in severe environments than ordinary portland cement concretes (PCC) and can be categorized as high-performance concrete (HPC).

The laboratory and field studies conducted by the Virginia Department of Transportation (VDOT) indicate that bridge deck concrete with a conventional w/c ratio of 0.45 or less provide the coulomb values specified by VDOT (11,14) as long as a pozzolan or slag is used. Proper construction practices are needed to produce quality concrete elements. The rapid chloride permeability test (RCPT) provides satisfactory results and is used in the specifications for accepting concrete.

A high performance bridge deck was constructed in New Hampshire (12). The University of New Hampshire (UNH) performed field and laboratory testing on three different mix proportions as a part of the project research work. The requirements for the three mixes were: design strength of 42 Mpa (5945 psi); 28-day cylinder strength of 50 Mpa (7200 psi); and a maximum chloride ion permeability of 1000 coulombs at 56 days. Test slabs representing each mix were installed at a UNH bridge deck testing facility located in Rochester, New Hampshire. The slabs were subjected to heavy truck traffic with recorded weights upto 59,000 kgs (65 tons) for a period of 6 months during the winter season. The mix that exhibited the best performance was ultimately selected as a basis for the HPC bridge deck specification. The final product exceeded expectations. No visible cracks on the top surface of the deck were found during several post-construction reviews conducted by research, construction and design personnel. The 28-day concrete strength exceeded the specification requirement. However, the modulus of elasticity was lower than expected. The freeze-thaw durability, chloride-ion permeability, and scaling tests revealed excellent results. Based on preliminary evaluations, it was concluded that

the concrete deck would be highly resistant to chloride intrusion and freeze-thaw deterioration and would provide superior long-term service (12).

Phase II of the Purdys Wharf development (55) on the Helifax Waterfront consists of a 22-story office tower founded on drilled caisson piles. There are 32 caissons of 1220-mm (48.03 in.) diameter and 30 caissons of 1066-mm (41.97 in.) diameter. The average length of a caisson is about 21 m (68.85 ft.). The piles are socketed into bedrock for a depth of 1.8 m (5.9 ft.). The piles were heavily reinforced, thus a 14 mm (0.55 in.) nominal size of aggregate was proposed for use. A superplasticizer was specified to increase the workability. The contract specification for the pile required a compressive strength of 45 Mpa (6525 psi) at 28 days. Concrete containing high volumes of low-calcium fly ash was selected for part of this project. The maximum size of coarse aggregate was 14 mm (0.55 in.). Compressive strengths of the order of 32 (4640 psi) and 55 Mpa (7975 psi) at 7 and 28 days, respectively were obtained for this concrete. In situ tests were also performed to determine the bond strength between concrete and rock. Bond strength development was shown to be quite satisfactory, with values of greater than 3 Mpa (435 psi) - about 2.5 times the design criterion of 1.2 Mpa (174 psi).

In Texas (15) two overpasses have been constructed with HPC in projects sponsored by the Federal Highway Administration (FHWA) and the Texas DOT in cooperation with the Center for Transportation Research at the University of Texas at Austin. Using the knowledge gained from these two projects, the researchers at the University of Texas at Austin and the Texas DOT personnel developed a permeability specification for bridge decks and substructures. The current permeability specification for HPC bridge decks in Texas requires a maximum of 2000 coulombs passed at 28 days, as per AASHTO T277, and 5 to 8 percent total air in place. The permeability requirement at 28 days should be consistent with the strength requirement of 28 MPa (4000 psi) for the cast-in-place topping and 34 Mpa (5000 psi) for precast subdeck panels. Difficulty in obtaining permeabilities less than 2000 coulombs passed at the early age of 28 days has resulted in the evaluation of an accelerated curing method for permeability testing that was used in Virginia (14) to approximate field permeabilities at one year.

Malhotra et al (47) worked on producing high-volume fly ash-blended cements. CANMET developed high-volume fly ash (HVFA) concrete in which 55 to 60% of the Portland cement is replaced by a low-calcium fly ash. This type of concrete has demonstrated excellent mechanical properties and long term durability and is slowly gaining acceptance worldwide.

Currently fly ash has to be added at a ready-mixed concrete batch plant to produce HVFA concrete; this necessitates additional storage silos and quality control at ready-mixed concrete plants. To address these issues major projects were undertaken to develop a blended cement incorporating high volumes of ASTM Class F fly ash. The blended cement is made by inter grinding approximately 55% of a low-calcium fly ash and 45% of ASTM Type I or Type III cement clinker together with small amounts of gypsum and a dry high-range water-reducing admixture.

The mechanical properties of concrete made with the HVFA-blended cements depend primarily on the type of fly ash used in the blended cements. In general, these properties are excellent because of the dense microstructure and the low water content of the concrete made with this type of cement.

Malhotra et al (47) concluded that Concrete made with the HVFA- blended cements showed higher resistance to the chloride-ion penetration than the conventional portland cement concrete of similar strength in the tests performed according to ASTM C 1202. For example, the 28-day value of the total charge passed in coulombs, a measure of the resistance of concrete to the chloride-ion penetration ranges from 300 to 2000 for the concrete made with the HVFA-blended cements, versus 2500 to 6000 coulombs for the control portland cement concrete. A value of less than 1000 coulombs is indicative of concrete with very low permeability.

The cost of the blended cements discussed above will depend on the cost of the cement clinker, fly ash, and the energy required for grinding. Although no detailed data have developed on this issue, it is believed that the cost of the blended cements should be lower than the cost of normal portland cement.

HVFA-blended cements can be produced with the cement clinkers and fly ashes having a wide range of chemical compositions and physical properties as shown by Bouzoubaa et al (48). Most of the blended cements produced can meet the ASTM requirement for blended cements if an appropriate grinding procedure is used. Concrete made with HVFA-blended cements has adequate early-age and excellent later-age mechanical properties and demonstrates remarkable performance in durability aspects, such as resistance to freezing and thawing and chloride-ion penetration (49-51). Because of low cement content, the temperature rise in concrete made with the HVFA-blended cements is rather low. Thus, HVFA-blended cements are ideal for concrete structures where high heat of hydration is a concern.

High content of fly ash is being tried in extruded cementitious composites (52). There is a growing interest in the use of the extrusion process in the fiber-reinforced cement composites industry. To minimize defects in extrudable mixtures, additives and admixtures, such as fly ash could be used. The advantage of using extrusion in cement product processing is that the fiber can be aligned in the load-bearing direction, the matrix and fiber packing can be optimized to achieve low porosity, and the fiber-matrix bond can be improved. Composites containing different percentages of fly ash as a replacement for cement have been fabricated. The use of fly ash improves both the strength and toughness of the composite. This improved performance, however, was observed only when fibers were incorporated into the mixture, and is dependent on the type of fiber. The reduction in the fiber-matrix bond strength changed the mode of failure from fiber fracture for composites without fly ash to fiber pullout for composites with fly ash. This results in ductile behavior of the composites with fly ash, as opposed to more brittle behavior of those without fly ash.

Investigation on long-term mechanical properties and durability characteristics of high-strength/high-performance concrete incorporating supplementary cementing materials under both laboratory and outdoor exposure conditions has been carried out (53). After ten years, the compressive strength of the cores drilled from the column elements of the control portland cement concrete and concrete incorporating various supplementary cementing materials ranged from 86.4 to 110.3 MPa (12528 to 15993.5 psi). The highest strength was obtained for the concrete with fly ash. The fly ash concrete had lower strength at ages up to 28 days than the other concretes, but it had the highest strength gain of more than 120 % between 28 days and 10 years. In tests performed according to ASTM C 1202, the charge passed through all the concretes at 10 years was less than 1000 coulombs, indicating very high resistance of the concretes to chloride-ion penetration (52). Whereas the concrete incorporating silica fume has the highest compressive strength at ages up to 28 days, but it had a strength gain of only 18 % beyond that age.

Under high- performance concrete we have a new category of concrete known as the self-consolidating concrete (SCC) which is characterized by its ability to spread readily into place and self-consolidate without exhibiting any significant separation of constituents (53). The use of self-consolidating concrete can enable the reduction of labor demand for vibration and surface finishing, accelerated placement rate of concrete, and secure superior surface quality.

Investigation has been carried out on mixture proportioning of air entrained SCC suitable for filling congested sections, such as in the case of repair of the underside of bridge deck girders, and conventional non-restricted elements. Such concretes have been used in densely reinforced beam in parking structures and moderately reinforced beam-wall element with restricted access in powerhouses.

Khayat (54) has shown that the air-entrained mixtures optimized for field repair exhibit high resistance to surface settlement, low temperature rise, adequate strength development, moderate shrinkage and permeability, and excellent durability to freezing and thawing and to deicing salt scaling. When properly proportioned, such high-performance SCC can offer an effective option to repair damaged structural sections that present difficulties for concrete placement and consolidation.

The similarities in the above mentioned projects are listed below:

- Reduced life-cycle costs based in part on longer lasting bridge decks and reduced maintenance are anticipated with the use of HPC.
- The emphasis on HPC for bridge decks is for improved durability and consistently good constructability rather than higher strength.
- To the maximum extent possible, local materials and conventional methods are used.
- Multiple laboratory and field trial mixes were developed and batched. Performance characteristics varied depending on type, brand, and combination of mix constituents.
- In addition to use of a uniform consistent product with enhanced properties, proper construction practices are essential for long lasting concrete structures.
- Where special problems are expected, such as in areas having alkali-reactive aggregates and in areas having high sulfates, special tests are needed to check chemical durability.

3.1.2 High Strength Concrete

Production of high strength concrete (defined as concrete with specified compressive strength higher than 6000 psi (49 Mpa)) requires special considerations. The use of high strength concretes began in the 1960’s and has progressed steadily since then. Today, concretes with compressive strengths of 69 Mpa (10000 psi) can be routinely produced. The initial applications of high strength concretes were in columns of high-rise buildings. The availability of high-

strength concrete made it possible to achieve greater heights, to reduce column sizes and to provide greater stiffness to buildings. The focus of applications has now shifted to bridges where potential applications in pre-stressed concrete are now being pursued. The improved durability, which occurs with low permeability, has led to broader applications such as design of longer life highways and parking structures (4).

High-strength concrete (16-18) can be used to increase the span length of girders, reduce the number of girders required in a given bridge or allow for the use of shallower sections. The use of high-strength high performance concrete in bridge girders has, generally, reduced the number of girders required for a given span length or has resulted in the ability to increase span lengths.

When high strength concretes were produced from the basic ingredients of cement, aggregate and water, the maximum achievable compressive strength was limited to 62 Mpa (9000 psi). However, with the availability of mineral admixtures in the form of fly ash, slag, and silica fume, and with the advent of high-range water-reducing agents, compressive strengths as high as 135 Mpa (20,000 psi) can now be achieved with concretes that are easy to place. The availability of high-range water reducing admixtures has enabled concrete mixes to be designed with even lower water-cementitious ratios than was previously possible (16-18).

ACI 363R and other ACI guidelines address some recommendations on placing, compacting and curing of high strength concrete. These documents also disclose some general principles of mix design. However, design of concrete entails detailed knowledge of properties of local materials, i.e., aggregates, cement, and pozzolanic admixtures.

3.1.3 Fly Ash

Fly ash is a finely divided residue, which is the by-product of the combustion of ground or powdered coal exhaust fumes of coal-fired power stations. It is composed of siliceous and aluminious ingredients and possesses limited cementitious properties unless so finely divided that its fineness is equal to or less than the fineness of the cement with which it is mixed. In the presence of the water in the mix, it reacts with the calcium hydroxide at ordinary temperatures, thereby forming compounds that have high cementitious quality (18).

ACI Committee 226 (17,19) has published a report on fly ash in concrete. Whenever fly ash is used, the volume of paste in the concrete mix would normally exceed that in a no-fly ash

concrete mix. The increased volume of paste produces better workability. As a result, a smaller water content is needed in mixes with fly ash than in mixes where fly ash is not used. Fly ash reduces bleeding and retards the time of set. Superplasticizers are necessary in high volume fly ash concrete where the W/C+F ratio is about 0.3. The dosage of fly ash required is generally about 15 percent of the total cementitious material (17).

The use of ASTM Class F fly ash can result in a lower compressive strength at early ages (3-7 days). Thereafter, as the strength contribution rate of the portland cement decreases, the continued pozzolanic activity of the fly ash content in the hardening mix contributes to higher strength gain at later ages. This higher rate of strength gain continues with time, resulting in higher ultimate strengths compared to concretes without fly ash content (20). From the report of ACI Committee 226 (19) it can be deduced that the modulus of elasticity of fly ash concrete, particularly at early ages, is slightly higher than plain concrete.

Long-term behavior is measured by creep and drying shrinkage deformations. Creep is the transverse flow of the material under external load or stress. But it is affected also by the duration of the load, the strength of the concrete, the aggregate content, temperature effects, and moisture conditions. However, many investigations have demonstrated that fly ash concretes generally exhibit lower long-term creep strains because of their higher rate of late age strength gain. Drying shrinkage is influenced by environmental conditions such as ambient temperatures, humidity, cement content and type, water/cementitious ratio, and aggregate type. The use of fly ash in concrete helps to replace a part of its cement content resulting in the modification of its properties.

Benefits of Fly ash in Fresh Concrete

- Increase in the initial setting and final setting time
- Change in workability
- Reduced segregation and bleeding
- Decrease in peak temperature due to reduction in cement content

Benefits of Fly ash in Hardened concrete

- Increase in long term strength due to continued pozzolonic reaction of fly ash in the presence of moisture

- Reduced strength at early ages. The modulus of elasticity of fly ash concrete is a little lower at early ages and higher at later ages
- Improves creep behavior of concrete particularly at early ages
- Improves the bond interaction of the concrete constituents as it reduces bleeding in fresh concrete
- Reduces the concrete permeability
- Reduces alkali silica reaction
- Increase in the sulphate resistance

3.1.4 Silica fume

Silica fume is a by-product resulting from the use of high purity quartz with coal in the electric arc furnace in the production of silicon and ferro silicon alloys (18). It is generally accepted as an efficient admixture for high-strength concrete mixes. Its main constituent, fine spherical particles of silicon dioxide makes it an ideal cement replacement simultaneously raising the concrete strength. The diameter of silica fume particles is 0.1 – 0.12μm (3.94 – 4.73μin.) and their surface area is 15 – 20 m^2/g (703840 $in^2/lb.$). In comparison, ASTM conforming portland cement or fly ash sizes are almost two orders of magnitude larger than silica fume particles i.e. 10- 12μm (39.4 – 47.3μin.). Being a waste product with relative ease in collection as compared to fly ash or slag, silica fume has gained rapid popularity. Silica fume is available in loose bulk form, densified form, slurry form, and in the form of blended silica fume portland cement.

The small size (0.1-0.12μm) and spherical shape of the silica fume particles allow them to fill the voids between the larger cement particles (10-12μm) which would have otherwise been filled with mix water. The entrapped water is consequently unable to contribute to the consistency of the mix. In spite of the better particle distribution, the larger specific area of silica fume particle increases its capacity to absorb water with the resulting need for more water in the mix. High range water reducers eliminate the need for any additional water. This is due to the extensive dispersal of the cement particles and silica fume with decreased contact between their particles. In addition, with high cementitious content, hence a low W/(C+SF) ratio, the cohesiveness of the paste increases considerably due to the reduction of internal bleeding in the

mixture. As a result, more water-reducing agents are needed (18). The change in the fresh concrete properties are as follows

- Reduces concrete segregation and increases its cohesiveness
- Decreases bleeding due to its high affinity to water
- Decreases concrete air-content due to its very high surface area
- Increases plastic shrinkage

Permeability and strength improvement are the two major reasons for the use of silica fume in concrete. If a large percentage of cement such as 20 percent is replaced by silica fume, the compressive strength of the concrete increases considerably. The addition of silica fume may produce concretes with a compressive strength in excess of 15000 psi. The improved (18) qualities of concrete with the addition of silica fume can be summarized as follows:

- Considerably reduced permeability
- High compressive, tensile and flexural strengths
- At similar water/cementitious materials ratio, drying shrinkage of silica fume is often lower than that of non-silica fume concrete
- Creep deformations are 40-70 percent of non silica fume type III cement concrete
- Reduced reinforcement corrosion
- Better freeze-thaw resistance comparable to properly air entrained non silica fume concrete
- Increases the fatigue life
- Improves concrete sulphate resistance
- Increases resistance to chemical attack

Long-term durability and strength development of silica fume concretes has been studied by Malhotra et al. (23). They used a W/(C+SF) ratio of 0.25 for non air entrained mixes and 0.3 and 0.4 for air-entrained mixes using a maximum aggregate size of 19.7 mm (3⁄4 in.). A superplasticizer was used to maintain a slump of 150-175 mm (6-7 in.). The following conclusions were made after 3 ½ years of study:

- Some retrogression is noticed in compressive strength between the ages of 91 days and 2 ½ years. It becomes more pronounced as the W/(C+SF) ratio is increased from 0.25 to 0.45. However this decrease in strength would not be of significance in structures.
- Silica fume concretes exhibit gain of flexural strength with age.

- Carbonation measured at the end of 3 ½ years does not seem to be of any significance with W/(C+SF) ratio not exceeding 0.25. As this ratio increases, carbonation penetration becomes significant. At 0.40 ratio, a carbonation depth of 8 mm (0.31 in.) was observed.

3.1.5 Chloride Permeability

The durability of concrete largely depends on its ability to resist the penetration of water and aggressive solutions. One of the major environmental distress in reinforced concrete is the corrosion of steel reinforcement. Significant damage to concrete results from the intrusion of corrosive solutions. Any treatment that effectively blocks the penetration of these solutions will greatly reduce this damage and lead to increased durability with the consequent economic benefits. Considerable research has been done in this area including the evaluation of special coatings, pore-blocking admixtures, and special concretes applied as overlays. One successful system for overlays has been latex-modified concrete (24). In addition to the added cost of materials for such overlays, special expertise and equipment are needed for field applications; consequently such concretes are considerably more expensive than commercially prepared ready-mixed concretes (27). A variety of materials have been developed which by virtue of their low permeability can retard the ingress of chloride ions into the concrete cover. All other factors being equal, low permeability concretes perform better in severe environment than ordinary Portland cement.

The AASHTO Test Method T277, “Rapid Determination of Chloride Permeability of Concrete” was adopted in 1983. Virtually the same test procedure was designated by the ASTM as C1202, “Electrical Indication of concrete’s ability to Resist Chloride Ion Penetration”. In this ASTM test, one surface of a water saturated concrete specimen is exposed to a sodium chloride solution, and the other surface to a sodium hydroxide solution. A 60-volt DC electrical potential is placed across the specimen for a six-hour period. The electrical charge (in coulombs) passed through the concrete specimen in that time represents its “rapid chloride permeability”. The ease and speed of this test method has made it more popular compared to the other methods (28).

The AASHTO T259 90-day ponding test was used to evaluate chloride penetration of concrete for many years prior to the adaptation of the rapid test (AASHTO T 277 or ASTM C1202). Permeability, diffusion and absorption are the important physical processes controlling chloride penetration into concrete during the 90-day ponding test, whereas electrical resistivity

appears to be the primary factor controlling charge passed through the rapid test. The sensitivity of the two methods to these different physical processes may cause significant variations in the ranking of permeabilities of various concretes. As stated in the scope of ASTM C1202, the rapid test procedure is applicable to types of concrete in which correlation has been established between this rapid test procedure and long-term chloride ponding procedures such as AASHTO T259.

The rapid test method ASTM C1202 is now commonly required by construction project specifications for both precast and cast-in-place concrete. An arbitrary value of less than 1000 coulombs is typically selected by the engineer or owner. This rating usually chosen from the scale shown below is characterized as “very low” chloride ion penetrability.

Charge Passed (Coulombs)	Chloride Permeability (ASTM C 1202)
> 4000	High
2000-4000	Moderate
1000-2000	Low
100-1000	Very Low
<100	Negligible

3.1.6 Effect of Curing Temperature on Strength and Permeability

Moist-curing greatly facilitates the gain in compressive strength. The 28-day compressive strength in air-dried silica fume concretes can be 20 % lower than moist-cured silica fume concretes, as continuous gain in strength is achieved with time.

Ozyildirim et.al. (29) conducted tests after subjecting concrete to various curing temperatures. Control concretes and concretes containing 15 % fly ash, 50 % slag, and 7 % silica fume were prepared. For each variable, two batches of concrete, one with Type II and another with Type III cement were prepared. Test specimens were prepared for chloride permeability and strength at room temperature. Within half an hour, they were placed in different curing environments at 4°C (40°F), 23°C (73°F) and 38°C (100°F) without removal of the moulds. Moulds were removed the following day and the specimens returned to different curing environments. Cylinders for the rapid chloride permeability test were kept moist for 2 weeks and air dried for 2 weeks. Those for the strength were moist cured until testing.

The results from the tests conducted at 28 days indicated that control concretes with either cement had comparable values for total charge passed through specimen (Q values) at 23°C (73°F) and 38°C (100°F); but the control concrete cured at 4°C (40°F) had significantly higher Q values. Strengths were comparable or significantly higher for concretes containing Type III cement. With either cements, the highest strengths were obtained when cured at 23°C (73°F) and the lowest when cured at 38°C (100°F). With either cement, the Q values of the specimens decreased significantly as the curing temperature increased. Specimens cured at 38°C (100°F) had Q values indicative of chloride permeabilities in or very close to the very low range. The results for the specimens cured at 23°C (73°F) indicated high chloride permeabilities, and those cured at 4°C (40°F) indicated even higher permeabilities.

Fly ash concretes with Type II cement had the lowest strength when cured at 4°C (40°F) and the highest strength when cured at 38°C (100°F). With Type III cement, fly ash specimens cured at 23°C (73°F) developed the highest strength.

The results for concrete containing silica fume indicated the lowest permeability of 580 coulombs when combined with Type III cement and cured at 38°C (100°F). The Q values for the concretes made with either cement and cured at 23°C (73°F) were approximately 1000 coulombs, indicating low chloride permeability. This was also true for those containing Type II cement cured at 38°C (100°F). Significantly higher Q values were obtained for concretes containing either cement when cured at 4°C (40°F). The highest strengths for concretes containing silica fume were obtained when specimens were cured at 23°C (73°F) for either cement (29).

Results of the 90-day ponding test on concretes with w/c of 0.40 and containing pozzolans, slag or latex had less chloride intrusion than the controls, but all the values were above the threshold value of 0.78 kg/m^3 (1.32 lb./cu.yd.) except for one batch of silica fume concrete. At the deeper depth of 6 to 19 mm (0.75 to 1.25 in.) the chloride intrusion for all the concretes was very low. The highest value was in the control concrete that had an average chloride content of 0.22 kg/m^3 (0.38 lb./cu.yd.). It appears likely that all the low w/c concretes in this study (0.40 or less) would have significant resistance to chloride penetration under actual service that may be expected from them.

3.1.7 Effect of Fundamental Properties of Concrete

Mobasher et. al. (30) conducted the AASHTO T277 test and reported that several fundamental properties affect chloride permeability of concrete:

- Chloride Permeability increases as water-cement ratio increases.
- Permeability varies with coarse aggregate selection.
- For a given aggregate source, permeability is lower for a dense-graded concrete than for a gap-graded concrete and, among dense-graded concretes, it decreases as the maximum size of the aggregate decreases.
- Permeability increases as the entrained air content in concrete increases.

A one- percent increase in air content has the same impact on the chloride permeability as a 0.03 increase in water-cement ratio.

3.1.8 Effect of Silica Fume

Permeability is reduced in the concrete element through the addition of silica fume to the mix as the permeability of the cement paste decreases. This is due to the great dispersion of the finer silica fume particles as discussed earlier, filling most of the voids previously occupied by the mixing water. The addition of silica fume at 10 percent of cement by weight reduces the water permeability coefficient from 1.6×10^{-7} to 4×10^{-10} m/sec (6.3×10^{-6} to 1.6×10^{-8} in./sec). If the silica fume replacement is increased to 20-25 percent, the permeability almost approaches zero. This great reduction in permeability improves the freeze-thaw resistance of the concrete since very little water can diffuse through the concrete surface (18).

Perraton et al (28) conducted the AASHTO T 277 test on control and silica fume concrete and reported that the current passing through control concretes with w/c ratios of 0.4 and 0.5 was consistently higher than the silica fume concretes. The values obtained in this series for control concretes with w/c ratios of 0.4 and 0.5 are in good agreement with those obtained by Whiting (27). The authors concluded that the results obtained “clearly indicate the beneficial influence of silica fume on chloride ion permeability” as previously shown by Ozyildirim (29). According to the permeability scale provided by Whiting (27), it can be seen that the silica fume concretes with w/c of 0.4 exhibit chloride-ion permeability equivalent to that of latex-modified concrete. In the case of silica fume concrete with w/c of 0.24, the total amount of electrical charge passed in 6 hours was equal to 150 coulombs. This level of chloride- ion permeability is only matched by

polymer impregnated concretes according to Whiting (27). Perraton et al (28) concluded that the concept of permeability of concrete is more complex than it appears on the surface. The permeability coefficient not only varies according to the type of fluid used to measure it but also with sample preparation. It has been found that concretes with w/c ratios of 0.5 or less are practically impervious to any water flow whether silica fume is admixed or not. If the chloride ions can pass through saturated non-silica fume concrete, the higher the w/c ratio, the higher the amount of chloride ions passing through concrete. This pattern remains true when concrete contains silica fume (31-33). The major effect of silica fume on chloride ion permeability, however, is a drastic decrease, so that silica fume concretes provide chloride-ion impermeability in the same range as latex concretes with w/c ratios of 0.4 to 0.5 or polymer impregnated concretes with a w/c of 0.24. The experiments conducted also show that dosages of silica fume greater than 7.5 percent by weight of cement do not decrease the permeability significantly. The same pattern was also found in compressive strength results.

For a comprehensive study of literature relevant to HPC's use for bridge decks and prestressed girders refer to references 56 through 184 in the bibliography.

3.1.9 HPC Application in Bridges

The use of HPC in highway structures, mainly bridges, has shown promise as a way of achieving long-term, cost effective results (34). HPC enhances the strength and durability of a bridge's beams, deck, and columns. With the higher strength, bridge spans can be increased and girders can be reduced in number or cross-section size, while improvement of durability lessens the deterioration of the structure over time. Even though HPC is more expensive to produce than normal concrete, cost savings may be incurred with a reduction of materials, improved capabilities, reduced maintenance costs, and by extending the service life for the structure (35).

This section presents the background information for HPC, with focused discussions on the use of concrete strength to estimate modulus of elasticity and time dependent behavior. A review of previous instrumentation methods used to monitor HPC bridges is also discussed.

3.1.10 Federal Highway Administration Showcase Projects

The Federal Highway Administration, in cooperation with state highway departments, has a current program to construct demonstration showcase bridges with HPC throughout the United States (5). The goal is to promote the implementation of HPC technology for use in

highways and highway structures. Using this program, states can share knowledge, benefits, and challenges with each other. Since several states across the U.S. have been involved, HPC bridges with various climatic conditions, traffic weights and volumes, locally available materials, and construction methods have been constructed. These factors, along with others, require different approaches to building with HPC (45).

3.1.11 Using Compressive Strength to Estimate Modulus of Elasticity of HPC

Compressive strength, specified at a certain number of days after placement, is the major design parameter for structural concrete. Secondary parameters such as the modulus of elasticity, shrinkage, tensile strength, etc. have all been empirically linked to, and can be estimated based on the compressive strength (37).

The increased compressive strengths in HPC raised the need to re-evaluate the established equations used to predict the modulus of elasticity. The current equations were based on concrete with much lower compressive strengths and simply extrapolating the equations did not produce adequate results. When extrapolated past approximately 34.5 MPa (5000 psi), the equation suggested by Pauw (38) produces estimates that are too large. Pauw' s equation is the long-standing equation that is currently recommended in the ACI 318 building code and in the current ASHTO specification. It is given below for reference.

$$E = 33 w_c^{1.5} (f_c^{'})^{0.5} \qquad \text{equ. 3-1}$$

E = Static modulus of elasticity, psi

$f_c^{'}$ = Compressive strength of the concrete, psi

w_c = Unit weight of concrete, lbs/ft^3

Research was initiated and conducted at Cornell University (39) in order to provide an equation for HSC. A series of experiments was conducted to develop an equation to predict the modulus of elasticity of high strength concrete (HSC). The equation (equ. 3-1) was developed using least squares regression techniques and was based on unit weight and compressive strength.

$$E = (40{,}000*(f'_c)^{0.5} + 1*10^6)*(w_c/145)^{1.5} \qquad \text{equ. 3-2}$$

E = Static modulus of elasticity, psi

f'_c = Compressive strength of the concrete at time of test, psi

w_c = unit weight of concrete, lbs/ft^3

In the 1984 State of the Art Report on HSC, ACI Committee 363 recognized equation 3-1 as the equation to use when estimating the modulus of elasticity of HSC. This equation is still recognized by the ACI Committee 363 (17) as the equation for estimating the modulus for HSC, though there is considerable research that disputes its accuracy and applicability.

The ACI Committee 363 equation follows directly from research by Pauw, utilizing the linear relationship between the experimental modulus of elasticity and the square root of the compressive strength. The resulting equation (equation 3-2) does not take into account that the material properties of the individual components affect the modulus of elasticity. Carrasquillo, et al. (39) admitted that the aggregate plays a significant role in the modulus of elasticity of the concrete mix. However, no consideration is given as to the effects of the use of different aggregates on the modulus

Iravani (40) conducted a study to accurately measure the effects of various parameters on the physical properties of HSC. The type of coarse aggregate used was found to be the largest influence on the modulus of elasticity. In light of this fact, Iravani developed the following suggested equation for normal weight HSC. The equation is presented below.

$$E = 56{,}600(C_{ca})(f'_c)^{0.5} \qquad \text{equ. 3-3}$$

E = Static modulus of elasticity, psi

C_{ca} = Coarse aggregate coefficient,

f'_c = Compressive strength of the concrete at time of test, psi

This equation takes into account the influence of different coarse aggregates on the modulus of elasticity.

3.1.12 Time Dependent Behavior of HPC

In order to account for the total strain occurring in concrete structures, three major components are considered, creep strain related to applied loads, shrinkage, and temperature. Determining each component's contribution to the total strain proves to be extremely difficult.

In order to fully understand the nature of the problem each of these time dependent phenomena must be analyzed.

3.1.13 Temperature Effects

Similar to other materials, the properties of concrete are affected by changes of temperature. Thermal expansion, heat of hydration, and temperature gradients are important mechanisms considered in concrete analysis. Except in extreme cases, concrete bridges will not lose structural capacity as a result of temperature variations. The primary detrimental effect from temperature variation is the formation of unacceptable cracks in concrete that could reduce the serviceability of the bridge (41).

When working with HPC heat of hydration is an important aspect to consider, especially in structures with large masses. Internal loads are induced by the heat of cement hydration in all concrete structures. In the case of HPC, where increased amounts of cement and silica are applied, these internal loads could become quite substantial. High temperatures in concrete during hydration could lead to cracking or could adversely affect the development of mechanical properties.

Since the expansion properties of the rock used in a concrete mix govern the expansion properties of the composite, HPC is found to expand and contract in a similar fashion to normal concrete. There might be a slight reduction in the expansion coefficient of HPC because the hardened paste is often stronger than the aggregate, which reduces the aggregate's overall effect.

3.1.14 Creep and Shrinkage of HPC

Creep and shrinkage are interrelated phenomena because there are a number of similarities between the two (42). Experimental parameters affect creep the same way as shrinkage because similar to shrinkage, creep is a paste property and the aggregate in the concrete serves as a restraint. The magnitudes of the strains are the same and they each include a considerable amount of irreversibility. Shrinkage plays an integral part in evaluating creep. Usually the amount of strain related to creep is determined by factoring out shrinkage strain, which only adds to the complexity of accounting for time dependent phenomena in concrete design.

3.1.15 Creep

Most research concerning creep looks at the effect of the increased compressive strength of HPC. In general, as the strength of concrete increases, the magnitude of the creep strain is reduced. The total load induced deformation, however, depends on the initial strain as well as the creep strain. It must be noted that the initial strain at any stress-strength ratio (f_c / f'_c) is always greater the higher the strength. As a result, the total load induced strain at early ages of loading is greater for higher strength concrete as compared to lower strength concrete. In addition, at the same stress-strength ratio, the initial recovery is greater for higher strength concrete while the amount of creep recovery is comparable (43).

3.1.16 Shrinkage

Since shrinkage cracking plays a major role in reducing the durability of concrete bridge decks, much emphasis has been placed on research related to this phenomenon. Even though HPC has lower w/c ratios than normal concrete, and therefore less water in the mix, the total shrinkage in HPC is usually greater. When comparing the drying shrinkage, HPC is very comparable to normal concrete. The problem lies with the plastic shrinkage. HPC often uses mineral additives as partial replacements for cement. These additives, namely fly ash and silica fume, increase the cohesiveness of the cement paste. This increased cohesiveness reduces the amount of bleeding in HPC. A reduction in bleed water causes the surface layers of a concrete element to dry out more quickly, which in turn increases the amount of plastic shrinkage. This problem has been shown to be more prevalent when silica fume is used in the mix. Knowing this, special curing procedures should be implemented for HPC using silica fume whenever possible.

3.1.17 Previous Instrumentation Methods Used to Monitor HPC Bridges

The instrumentation and monitoring of structures is crucial to the continuing development of HPC. In preparation for this research project, the document FHWA-SA-96-075, "Implementation Program on High Performance Concrete: Guidelines for Instrumentation of Bridges" was consulted. Along with this document, previous work related to the monitoring of HPC bridges was reviewed. The following is an overview of a few projects that implemented instrumentation methods similar to the ones used for this research project.

Lachemi et. al. (44) instrumented the Portneuf Bridge in Quebec with thermocouples and strain gages in the deck. The instrumentation was used to monitor the heat development during concrete hardening and to follow the mechanical behavior of the deck slab during the post-tensioning as well as during ambient temperature variations. Twenty-four thermocouples and twenty-four vibrating wire transducers were placed at various locations in the deck slab. The thermocouples were placed in stacks at five pre-determined locations while the vibrating wire transducers were placed over two of the beams in the longitudinal direction of the bridge. The analysis of the temperature and corresponding strain data dealt only with the thermal effects in concrete such as temperature differences and gradients. The CNT Super Bridge in Japan was instrumented by Yonezawa et. al. (45) and monitored to ensure safety and obtain technical data for future reference. The project was not large in scale but was significant in that it proposed several new bridge design concepts – most importantly the first application of 100 MPa (14,500 psi) ultra-high strength concrete. Similar to this research project, the long-term behavior was monitored using strain gages imbedded into the girder. Specimens for measuring drying shrinkage and creep were also fabricated in order to determine the magnitude of each of these phenomena on the total deformation.

For the Colorado Showcase on HPC Box-Girder Bridge, Shing et. al. (46) instrumented girders to determine, among other things, transfer lengths, camber, creep, shrinkage, and curing temperatures. The instrumented girders were scaled down versions of the actual box girders specified for use in the Yale Avenue Bridge in Denver, Colorado. High performance concrete was implemented because the four span bridge was being replaced with a two span bridge and a high span-to-depth ratio was needed. To evaluate transfer length, strain gages were attached to the side of the girder and readings were recorded before and after transfer of prestressing. The camber was determined by stretching a fishing line tight between two bolts attached at the center of gravity at each end of the girder. Shrinkage and creep strains in the concrete were determined from test specimens evaluated in laboratory conditions. Finally, thermocouples were placed in the girders at each third point to monitor curing temperatures.

3.2 Research Task 2: Meet with Technical panel to review the research topic and work plan.

Both P. I's participated in a RDTN conference on June 2, 1998 in which the SDDOT research personnel, bridge personnel and the contractors participated. The following topics were

discussed and satisfactory solutions were agreed upon: concrete mix design, instrumentation, sampling and testing, test slab, deck placement, curing, and constructions costs for the I-29 bridges. A technical panel meeting was held on October 23, 1998 in Pierre, Dr Ramakrishnan and Dr. Sigl attended. At this meeting details of the tasks that related to the construction portion of the project were discussed. Details concerning the field quality control tests, sampling, number of specimens, and test procedures were finalized.

3.3 Research Task 3: Determine the HPC mix design which best improves the desired properties for the bridge decks and prestressed girders by testing trial batches.

3.3.1 Bridge Deck Concrete:

The properties that will be improved are reduced permeability and low crack potential. The aim was to reduce the bridge deck permeability by a significant amount (50%) as compared to SDDOT standard bridge deck mix. Trial mixes were made incorporating fly ash, silica-fume, a combination of fly ash and silica-fume, limestone aggregates and quartzite aggregates. The following variables were investigated.

Type of Aggregate	-	Limestone and Quartzite
Silica Fume	-	Optimum amount of silica fume to be added to achieve the desired reduction in permeability without compromising strength was investigated.
Combination of Silica Fume and Fly ash	-	In order to achieve the desired improvement with minimum cost, optimum blending of silica fume and fly ash was investigated.

First the mix proportions were investigated without the addition of mid-range water reducer (MRWR) and not exceeding the SDDOT specified water to cement ratios and cement content. The selected mix proportions satisfied the strength and workability requirements of SDDOT Class A Concrete for bridge deck construction. The coarse aggregates conformed to the gradation requirements of Size Number 1.

The following trial mixes were tested:

- Control mix with no admixtures
- Cement replacement with fly ash at 15, 20, and 25%.

- Cement replacement with silica fume at 7, 10, and 12%.
- Cement replacement with a combination of silica fume and fly ash at the following percentages: 5% silica fume and 15% fly ash; 5% silica fume and 20% fly ash; 7% silica fume and 15% fly ash.

Ten mix proportions were tested for each aggregate type and the total trial mixes were 20. When some of the mixes did not have the required workability of 125 mm to 150 mm (5 to 6 inches) of slump, MRWR was added to achieve the required workability. The amount of MRWR added was recorded.

Tests were carried out to determine the following properties:

- Fresh concrete properties such as slump, air-content, unit weight and temperature of concrete.
- Hardened concrete properties such as compressive strength, static modulus, static flexural strength, and unit weight were found at 14 and 28 days using the appropriate ASTM test methods.

Chloride Permeability tests were carried out in accordance with the ASTM C1202 as follows:

- Tests were carried out for all mixes after subjecting the specimen to 7-day accelerated curing.
- Tests were carried out for all mixes at 90-days.

3.3.2 Concrete for Prestressed Girders

Trial mixes were conducted to achieve increased 28-day strength and early strength development to achieve the required strand release strength in 18 hours. The specified compressive strength and strand release strength were determined by the Office of Bridge Design, SDDOT.

High compressive strength and early strength development can be achieved with low water to cement ratios and the addition of silica fume. To achieve the required workability, High Range Water Reducer (HRWR) was used.

Mixture proportions were decided for twelve mixes varying the water to cementitious materials ratio (0.28, 0.30, and 0.32) as well as the percentage replacement of cement with silica fume (7%, 10%, and 12%). Tests were carried out to determine the following properties:

- Fresh concrete properties such as slump, air-content, unit weight and temperature of concrete.
- Compressive strength test was carried out at 1, 3, 7, 28 and 56 days and test for static modulus was carried out at 28 and 56 days.

After detailed analysis it was decided to repeat one mix (out of the 12 High Strength Concrete Mixes). This mix was selected based on the concrete strength requirement at release. The tests conducted on this mix were two fold:

- Specimens were subjected to accelerated curing and were tested for compressive strength and static modulus at the end of 6, 12, 18, 24 hrs and Rapid Chloride Permeability Test (RCPT) at the end of 24 hrs of accelerated curing.
- Specimens were subjected to normal continuos moist curing and were tested for compressive strength and static modulus at the age of 1, 2, 3, 7, 28 and 56 days, and Rapid Chloride Permeability Test at the age of 90 days.

3.3.3 Mixture and Specimen Designation

The basic mix proportions for the high performance bridge deck concrete mixes with the mixture designations are given in Tables A1, A2 and, A8 and A9, Appendix A. A total of twenty mixes were made. Mixes Q1CONTROLW0.4 through Q10F0S12W0.46 were made of quartzite aggregate and mixes L1CONTROLW0.4 through L10F0S12W0.46 were made of Limestone aggregate. The following mix designation scheme is used. The first letter refers to the type of aggregate used: Q-Quartzite, L-Limestone, H-High Strength Girder Concrete. The second letter indicates a number that indicates the mix number. The next letters indicate whether the mix contains fly ash and/or silica fume: F-Fly Ash, S- Silica Fume. The number following S or F indicates the percentage of cement replaced with fly ash and/or silica fume. A zero indicates no fly ash or silica fume. The last letter with W indicates the water to cement ratio. All control mixes are referred to as CONTROL followed by the water to cement ratio.

The mixture designations and mixture proportions for the high strength bridge girder concrete mixes are given in Tables B1 and B2, Appendix B. The mixture proportions for the corresponding quartzite and limestone aggregates remained the same.

Each mix was made in a batch of 0.08 m^3 (3.5 cu.ft.). All the mixing was done in a drum mixer of 0.25 m^3 (9 cu.ft.) capacity. The batching of the materials was done one day prior to the mixing and stored in the lab at constant humidity and temperature conditions. The moisture contents of fine and coarse aggregate were determined. The mixing water was adjusted to saturated surface dry (SSD) condition of the coarse and fine aggregate based on the calculated moisture contents of the aggregates. The fly ash and silica fume were mixed with the cement during batching. The mixing was done thoroughly ensuring uniform mixing. Mixing was done according to ASTM C192 in the following sequence:

First the coarse aggregate and then the fine aggregate were added. Two-thirds water mixed with the air-entraining agent was then added to the aggregate and mixed for one minute to allow the aggregate to absorb the water. Cement and the remaining one-third water were then added. All the ingredients were then mixed for three minutes, which was followed by a three-minute rest and a final mixing period of two minutes.

3.3.4 Test Specimens

The specimens cast for each bridge deck mix are as follows:

- Eight 100 mm x 100 mm x 350 mm (4 in. x 4 in. x14 in.) beams - Four to be tested at 14 and four at 28-day for static flexural strength.
- Six 150 mm x 300 mm (6 in. x 12 in.) cylinders – Three to be tested at 14 and three at 28-day for static modulus and compressive strength.
- Ten 100 mm x 200 mm (4in. x 8 in.) cylinders – To be used in chloride permeability tests.

The specimens cast for each bridge girder mix are as follows:

- Ten 100 mm x 200 mm (4in. x 8 in.) cylinders – To be used in compressive strength tests.

The specimens cast for the recommended girder mix are as follows:

- Twenty-two 100 mm x 200 mm (4in. x 8 in.) cylinders – To be used in chloride permeability tests and compressive strength tests.

All the beams were cast in wooden molds and all the cylinders in plastic molds. All the molds were oiled prior to the casting. The specimens were covered with plastic sheets for twenty-four hours after casting at room temperature. They were then demolded and placed in

lime saturated water tank for curing. The beams and cylinders remained in the curing tanks until testing at either 14 or 28-day.

Research Task 3A: Quality Control Tests for Fresh and Hardened Concrete for Bridge Deck Concrete

3.3.5 Fresh concrete Properties

The fresh concrete data for all the mixes showed good uniformity and a degree of consistency. The results of the tests for unit weight, air-content, slump, and concrete temperature are given in Tables A3 and A10, Appendix A, and Figures 3.1 through 3.3 and 3.5 through 3.7, for quartzite and limestone mixes respectively. The slump of concrete varied from 100 mm (4 inches) to 230 mm (9 inches) for quartzite aggregate concrete and it varied from 75 mm (3 inches) to 200 mm (8 inches) for limestone aggregate concrete. The air content varied from 4 percent to 8 percent for quartzite aggregate concrete and 5 percent to 9 percent for limestone aggregate concrete. There was no significant difference between the fresh concrete unit weights between the various mixes in either the quartzite or limestone aggregate concretes. And there was no appreciable difference in the unit weights of quartzite and limestone aggregate concretes with the same air content and slump. The room temperature, humidity and the concrete temperature were recorded and there was no appreciable difference in these values; the average room temperature was 22^0 C (72^0 F), the average humidity was 35%, and the average concrete temperature was 29^0 C (89^0 F).

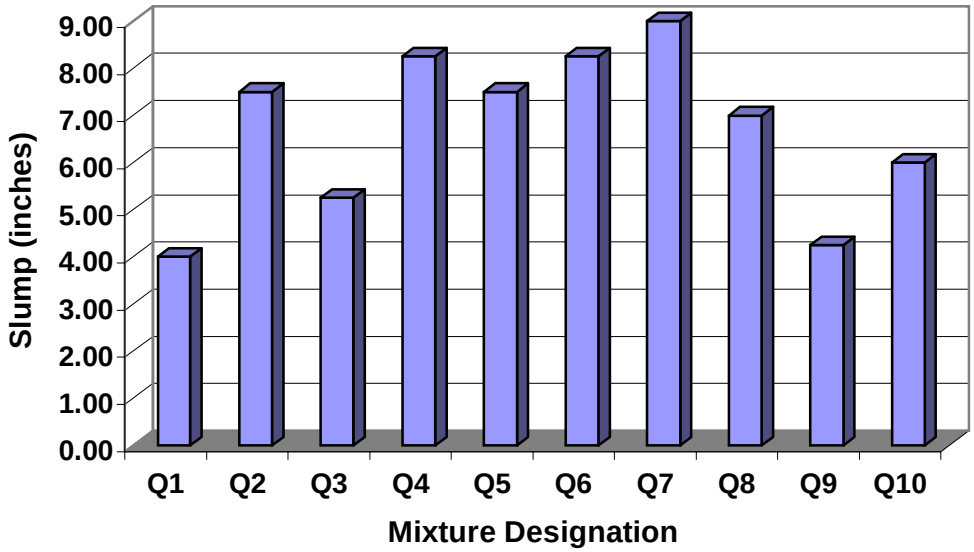

Fig. 3.1: Comparison of Slump (Quartzite Aggregate)

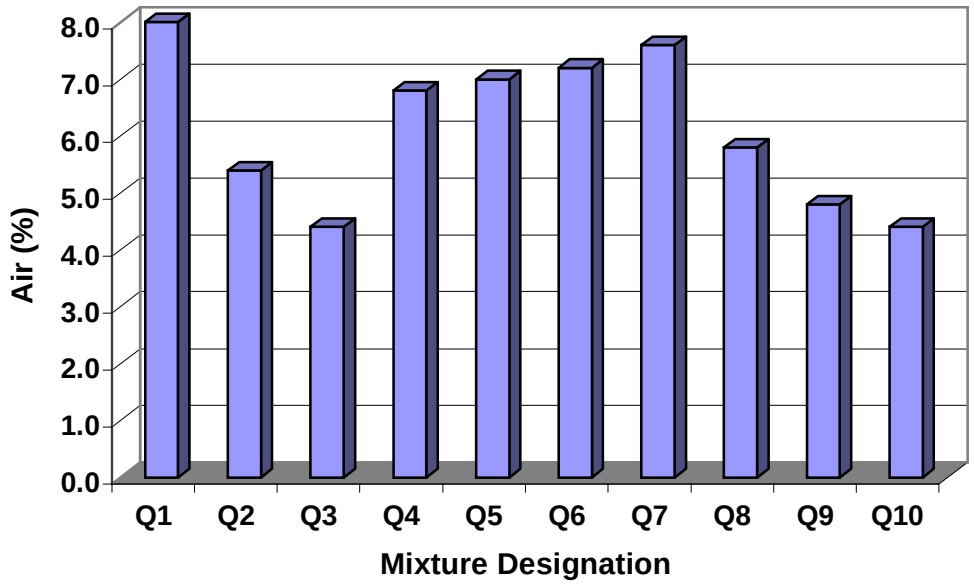

Fig. 3.2: Comparison of Air Content (Quartzite Aggregate)

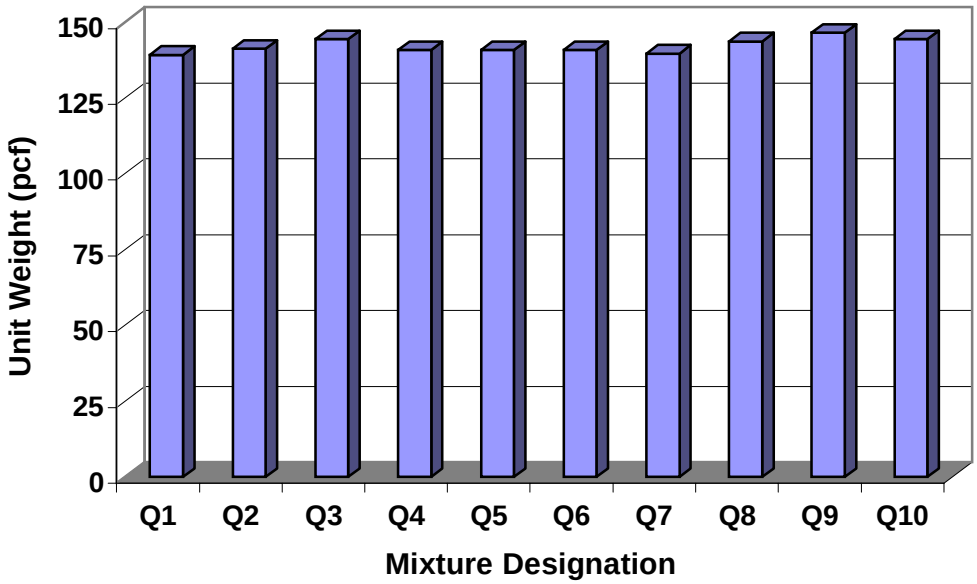

Fig. 3.3: Comparison of Unit Weight of Fresh Concrete (Quartzite Aggregate)

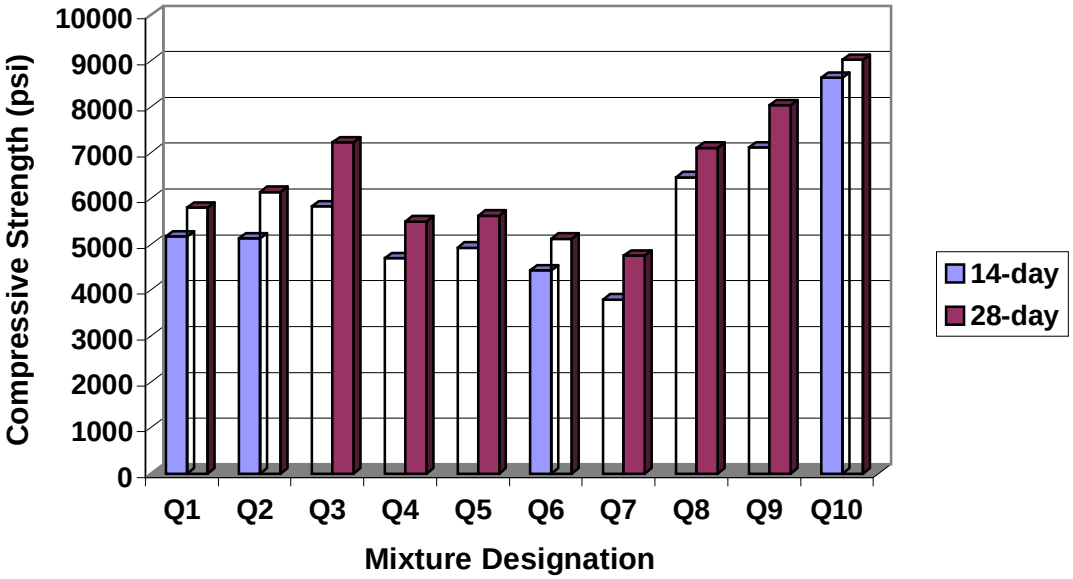

Fig. 3.4: Comparison of Compressive Strength at 14 and 28 day (Quartzite Aggregate)

3.3.6 Hardened Concrete Properties

3.3.6.1 Compressive Strength: The compressive strength results at 14 and 28-day are given in Tables A4 and A6 and A11 and A13, Appendix A, for the quartzite mixes and limestone mixes respectively. The corresponding bar charts are shown in Figures 3.4 and 3.8.

Among the mixes that contained both silica fume and fly ash and, quartzite aggregate, the mix Q3F15S5W0.5 (5% of cement by weight replaced with silica fume and 15% with fly ash) showed the highest compressive strength (14-day: 36.7 MPa [5830 psi]; 28-day: 49.9 MPa [7222 psi]). Among the mixes that had just fly ash as replacement, the mix Q5F15S0W0.47 (15% of cement by weight replaced with fly ash) showed the highest compressive strength (14-day: 34.1 MPa [4928 psi]; 28-day: 38.8 MPa [5622 psi]). In the mixes containing just silica fume as replacement, mix Q10F0S12W0.46 (12% of cement by weight replaced with silica fume) showed the highest compressive strength (14-day: 59.6 MPa [8632 psi]; 28-day: 62.4 MPa [9025 psi]). Mix Q7F25S0W0.54 (25% of cement by weight replaced with fly ash) showed the lowest compressive strength (14-day: 26.2 MPa [3797 psi]; 28-day: 32.9 MPa [4757 psi]), and mix Q10F0S12W0.46 (12% of cement by weight replaced with silica fume) showed the highest compressive strength (14-day: 59.6 MPa [8362 psi]; 28-day: 62.4 MPa [9025 psi]) values respectively. The same trends were followed at both 14 and 28-days.

Among mixes that contained both silica fume and fly ash and, limestone aggregate, the mix L2F15S7W0.52 (7% of cement by weight replaced with silica fume and 15% with fly ash) showed the highest compressive strength (14-day: 44.3 MPa [6408 psi]; 28-day: 57.2 MPa [8283 psi]). Among the mixes that had just fly ash as cement replacement the mix L6F20S0W0.50 (20% of cement by weight replaced with fly ash) showed the highest compressive strength (14-day: 34 MPa [4923 psi]; 28-day: 38 MPa [5495 psi]). In the mixes containing just silica fume as cement replacement, mix L10F0S12W0.46 (12% of cement by weight replaced with silica fume) showed the highest compressive strength (14-day: 52.2 MPa [7560 psi]; 28-day: 60.1 MPa [8697 psi]). Mix L5F15S0W0.47 (15% of cement by weight replaced with fly ash) showed the lowest compressive strength (14-day: 30.4 MPa [4393 psi]; 28-day: 36.4 MPa [5270 psi]), and mix L10F0S12W0.46 (12% of cement by weight replaced with silica fume) showed the highest compressive strength (14-day: 52.2 MPa [7560 psi]; 28-day: 60.1 MPa [8697 psi]) values respectively. The same trends were followed at both 14 and 28-days.

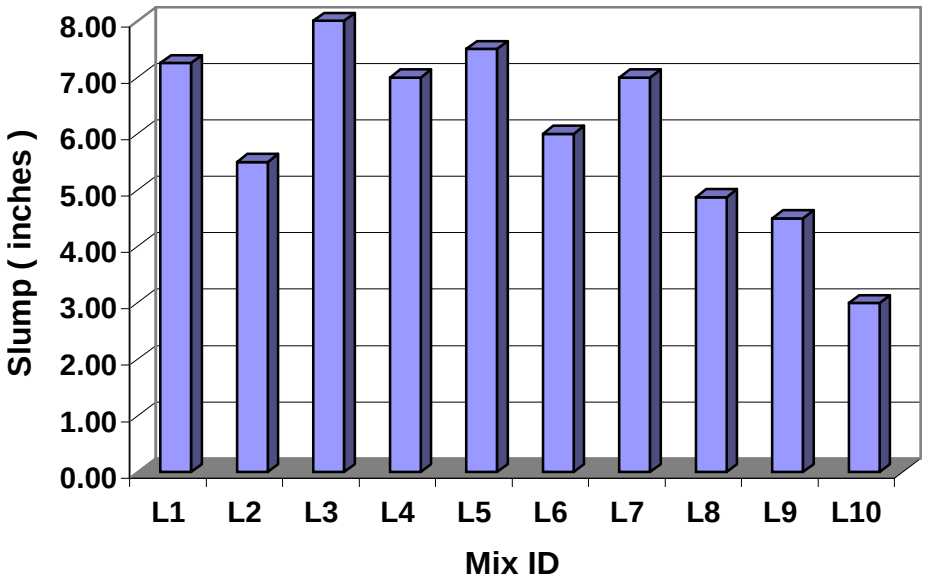

Fig. 3.5: Comparison of Slump (Limestone Aggregate)

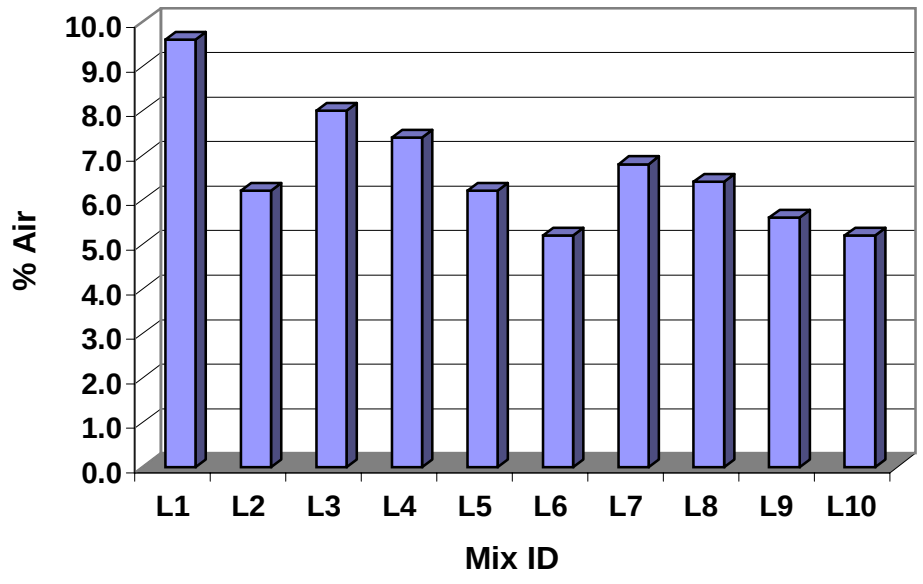

Fig. 3.6: Comparison of Air Content (Limestone Aggregate)

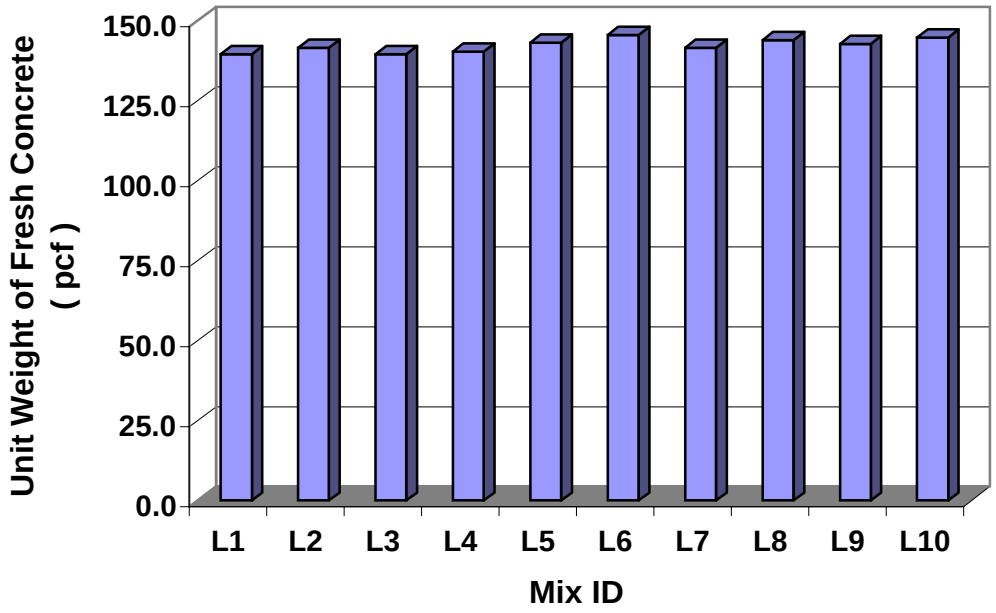

Fig. 3.7: Comparison of Unit Weight of Fresh Concrete (Limestone Aggregate)

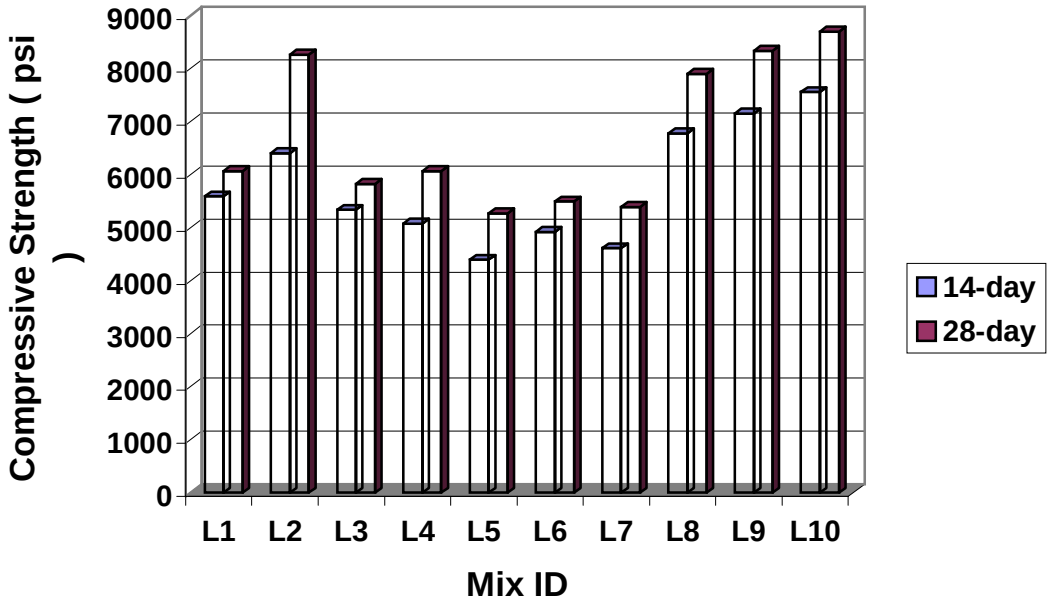

Fig. 3.8: Comparison of Compressive Strength at 14 and 28 day (Limestone Aggregate)

Figures 3.9 and 3.10 show a comparison of compressive strength of concretes containing limestone and quartzite aggregate. From the figures it can be concluded that there is no significant change in compressive strength due to variation in type of aggregate used.

3.3.6.2 Static Modulus: The static modulus results at 14 and 28-days are given in Tables A4 and A5 and A11 and A13 for the quartzite and limestone mixes respectively in Appendix A. The corresponding bar charts are shown in Figures 3.11 and 3.12.

The three quartzite mixes that contained both silica fume and fly ash (Q2F15S7W0.52, Q3F15S5W0.50 and Q4F20S5W0.54) showed approximately the same static modulus value ($2.9x10^4$ MPa [$4.2x10^6$ psi]) at 14-days and the mix with the highest strength [Q3F15S5W0.50], showed the highest static modulus value at 28-days ($3.7x10^4$ MPa [$5.3x10^6$ psi], as expected. Among the mixes containing just fly ash as a cement replacement material, the mix Q5F15S0W0.47 (15% of cement by weight replaced with fly ash) showed the highest 14 and 28 day static modulus values (14-day: $3.3x10^4$ MPa [$4.7x10^6$ psi]; 28-day: $3.2x10^4$ MPa [$4.7x10^6$ psi]). In the mixes containing just silica fume as a cement replacement material, mix Q10F0S12W0.46 (12% of cement by weight replaced with silica fume) showed the highest 14 and 28-day static modulus values (14-day: $3.4x10^4$ MPa [$5.0x10^6$ psi]; 28-day: $4.2x10^4$ MPa [$6.0x10^6$ psi]). Mix Q7F25S0W0.54 (25% of cement by weight replaced with fly ash) and mix Q10F0S12W0.46 (12% of cement by weight replaced with silica fume) showed the lowest static modulus (14-day: $2.4x10^4$ MPa [$3.5x10^6$ psi]; 28-day: $2.9x10^4$ MPa [$4.2x10^6$ psi]) and highest static modulus (14-day: $3.4x10^4$ MPa [$5.0x10^6$ psi]; 28-day: $4.2x10^4$ MPa [$6.0x10^6$ psi]) values respectively.

Among mixes that contained both silica fume and fly ash and limestone aggregate, the mix L2F15S7W0.52 (7% of cement by weight replaced by silica fume and 15% by fly ash) showed the highest 14 and 28 day static modulus values (14-day: $3.6x10^4$ MPa [$5.3x10^6$ psi]; 28-day: $3.6x10^4$ MPa [$5.3x10^6$ psi]). Among the mixes that had just fly ash as a replacement, the L6F20S0W0.50 (20% of cement by weight replaced with fly ash) showed the highest 14 and 28 day static modulus values (14-day: $3.2x10^4$ MPa [$4.7x10^6$ psi]; 28-day: $3.6x10^4$ MPa [$5.3x10^6$ psi]).

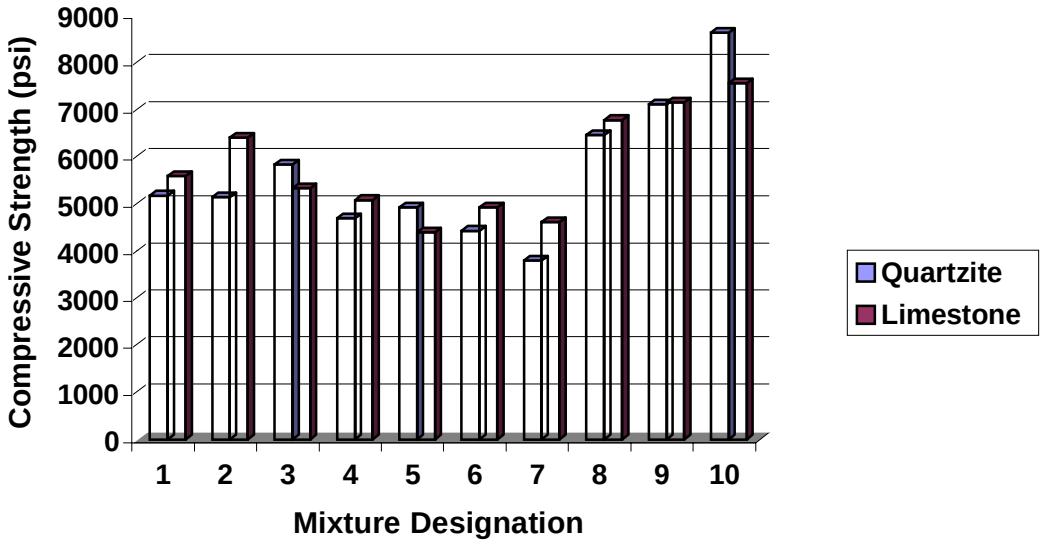

Fig. 3.9: Comparison of Compressive Strengths of Mixes Using Quartzite and Limestone Aggregate at 14- day

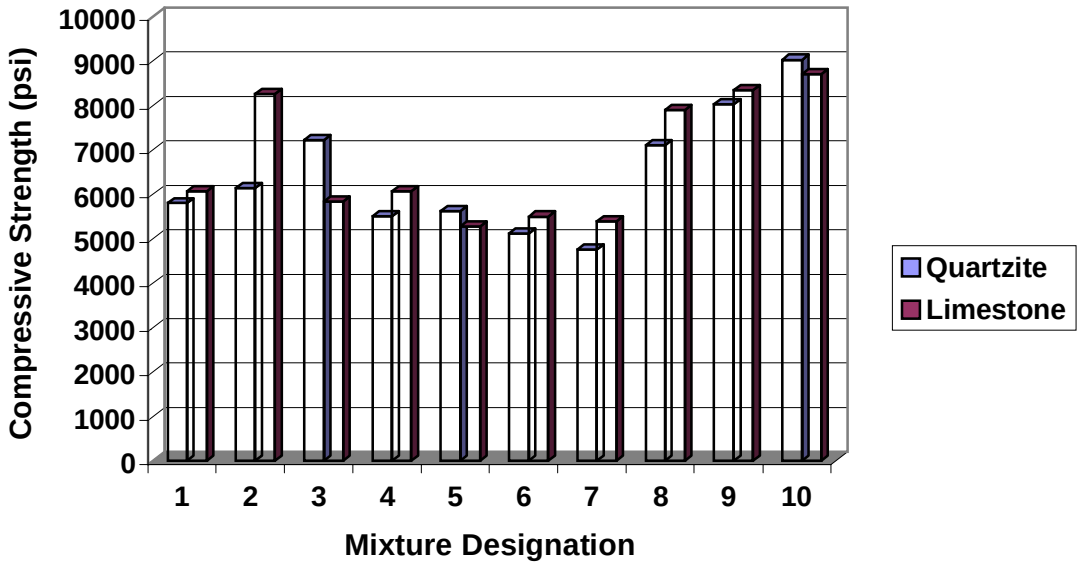

Fig. 3.10: Comparison of Compressive Strengths of Mixes Using Quartzite and Limestone Aggregate at 28- day

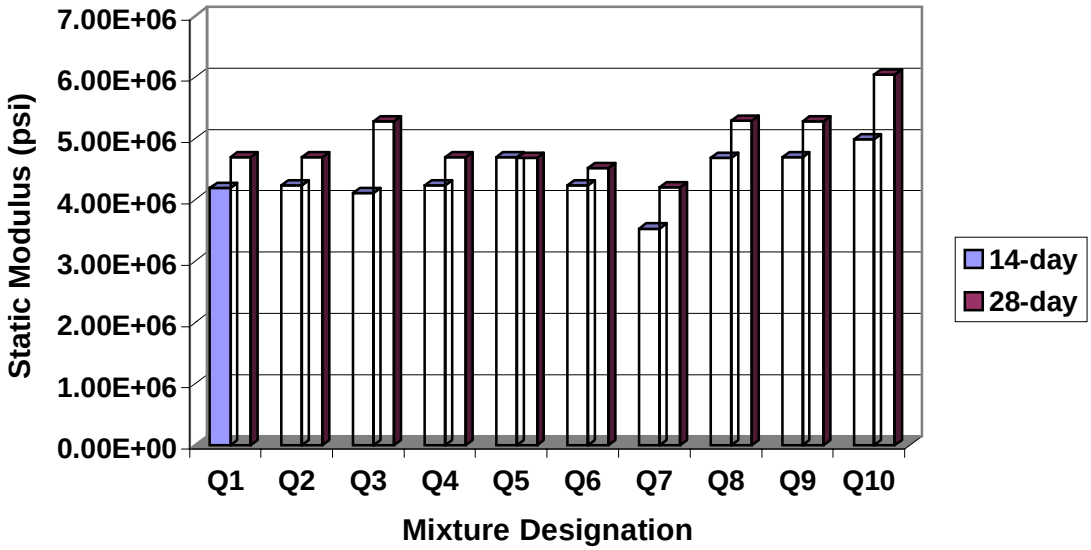

Fig. 3.11: Comparison of Static Modulus at 14 and 28 day (Quartzite Aggregate)

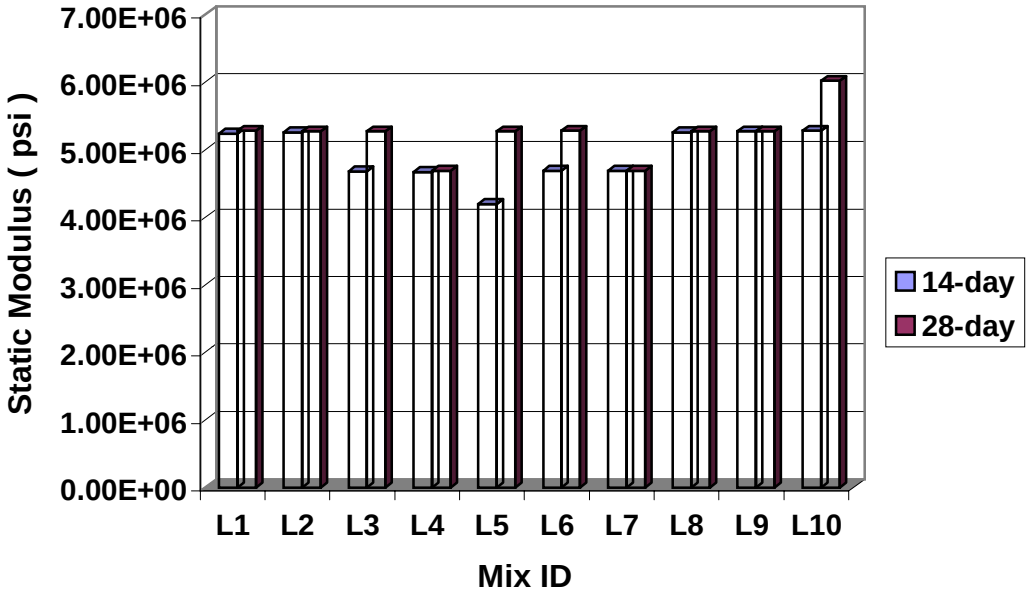

Fig. 3.12: Comparison of Static Modulus at 14 and 28 day (Limestone Aggregate)

In the mixes containing just silica fume as cement replacement, mix L10F0S12W0.46 (12% of cement by weight replaced with silica fume) showed the highest static modulus (14-day: $3.6x10^4$ MPa [$5.3x10^6$ psi]; 28-day: $4.2x10^4$ MPa [$6.0x10^6$ psi]). Mix L5F15S0W0.47 (15% of cement by weight replaced with fly ash) showed the lowest 14 and 28 day static modulus values (14-day: $2.9x10^4$ MPa ($4.2x10^6$ psi); 28-day: $3.6x10^4$ MPa [$5.3x10^6$ psi]) and mix L10F0S12W0.46 (12% of cement by weight replaced with silica fume) showed the highest 14 and 28 day static modulus values (14-day: $3.6x10^4$ MPa [$5.3x10^6$ psi]; 28-day: $4.2x10^4$ MPa [$6.0x10^6$ psi]).

3.3.6.3 Modulus of Rupture (Static Flexural Strength): The results of the modulus of rupture test at 14 and 28-day are given in Tables A5 and A7, and A12 and A14 for the quartzite and limestone mixes respectively in Appendix A. The corresponding bar charts are shown in Figures 3.13 and 3.14.

Quartzite: Among mixes that contained both silica fume and fly ash and quartzite aggregate, the mix Q3F15S5W0.50 (5% of cement by weight replaced with silica fume and 15% by fly ash) showed the highest static flexural strength (14-day: 5.1 MPa [740 psi]; 28-day: 5.7 MPa [825 psi]). Among the mixes that had just fly ash as replacement, the mix Q5F15S0W0.47 (15% of cement by weight replaced with fly ash) showed the highest static flexural strength (14-day: 5.0 MPa [725 psi]; 28-day: 6.1 MPa [885 psi]). In the mixes containing just silica fume as cement replacement, mix Q10F0S12W0.46 (12% of cement by weight replaced with silica fume) showed the highest static flexural strength (14-day: 6.2 MPa [903 psi]; 28-day: 7.0 MPa [1007 psi]). Mix Q7F25S0W0.54 (25% of cement by weight replaced with fly ash) showed the lowest 14 and 28 day static flexural strength values (14-day: 3.9 MPa [560 psi]; 28-day: 4.5 MPa [650 psi]) and mix Q10F0S12W0.46 (12% of cement by weight replaced with silica fume) showed the highest 14 and 28 day static flexural strength values (14-day: 6.2MPa [903 psi]; 28-day: 7.0 MPa [1007 psi]). The same trends were followed at both 14 and 28-days.

Limestone: Among mixes that contained both silica fume and fly ash, and limestone aggregate, the mix L2F15S7W0.52 (7% of cement by weight replaced with silica fume and 15% by fly ash) showed the highest 14 and 28 day static flexural strength values (14-day: 5.7 MPa [827 psi]; 28-day: 6.6 MPa [953 psi]). Among the mixes that had just fly ash as cement replacement, mix

L6F20S0W0.50 (20% of cement by weight replaced with fly ash) showed the highest 14 and 28 day static flexural strength values (14-day: 5.7 MPa [825 psi]; 28-day: 6.2 MPa [895 psi]).

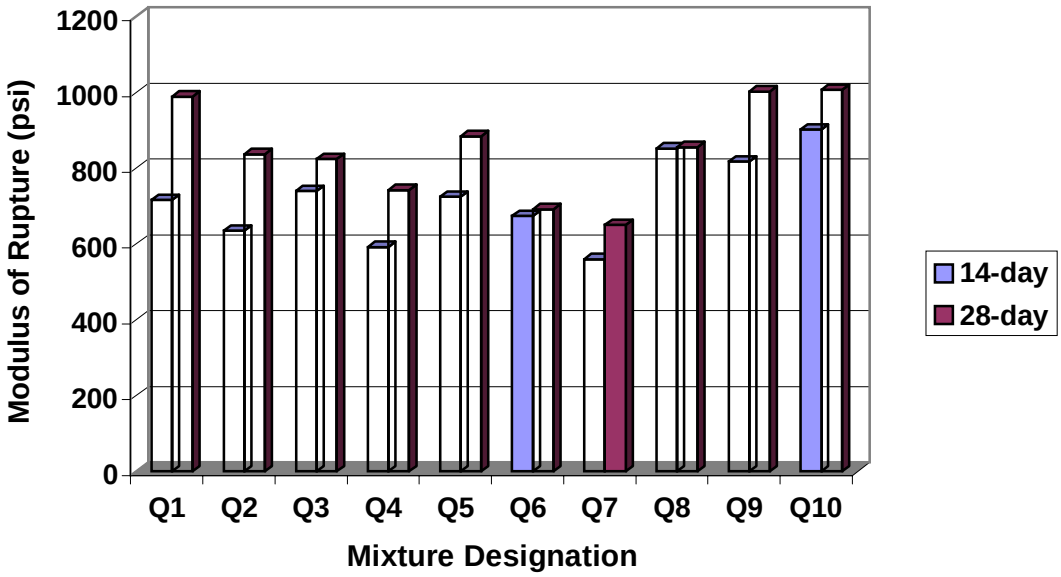

Fig. 3.13 : Comparison of Modulus of Rupture at 14 and 28 day (Quartzite Aggregate)

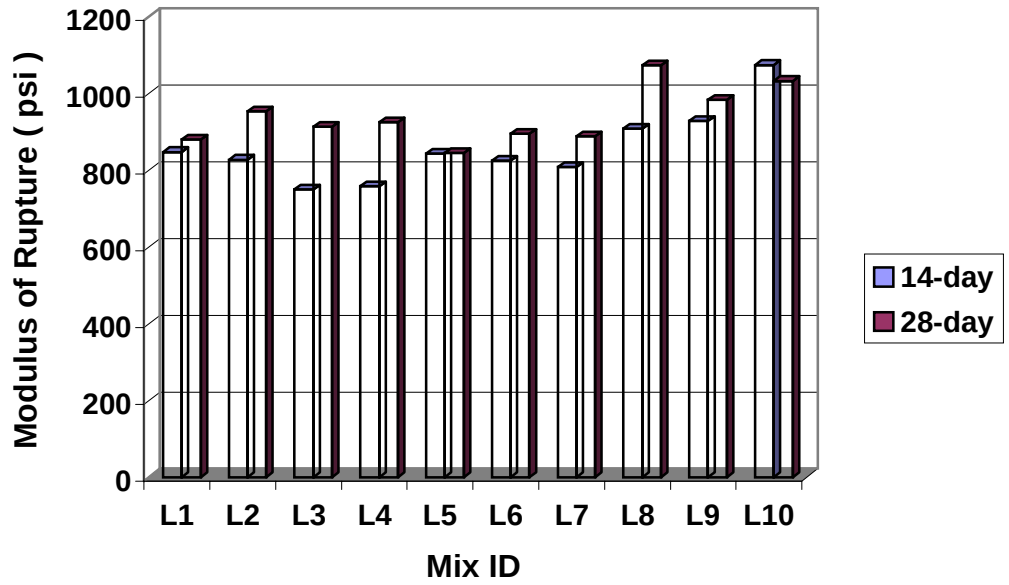

Fig. 3.14: Comparison of Modulus of Rupture at 14 and 28 day (Limestone Aggregate)

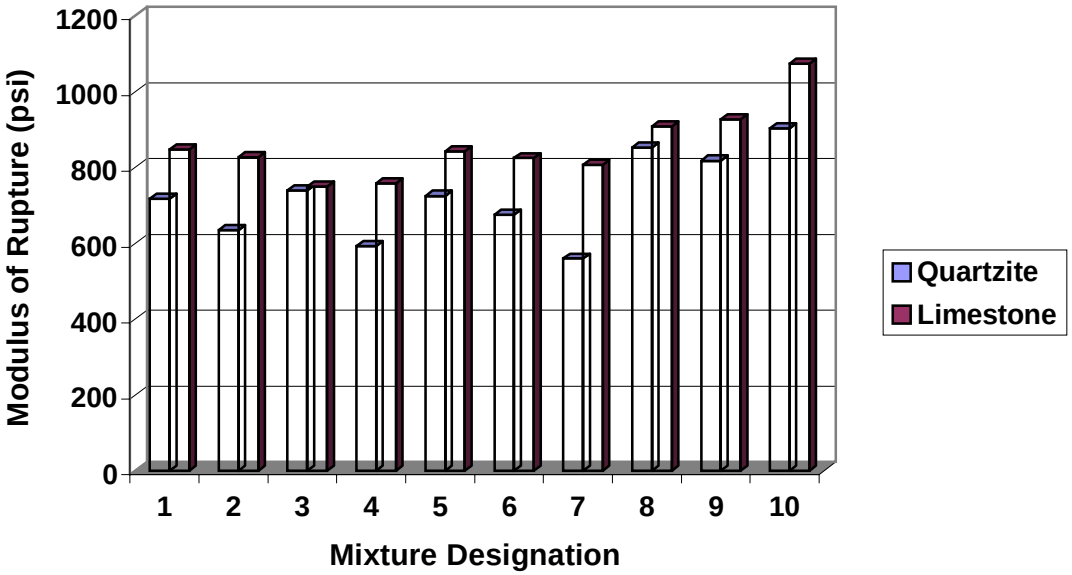

Fig. 3.15: Comparison of Modulus of Rupture of Mixes Using Quartzite and Limestone Aggregate at 14-day

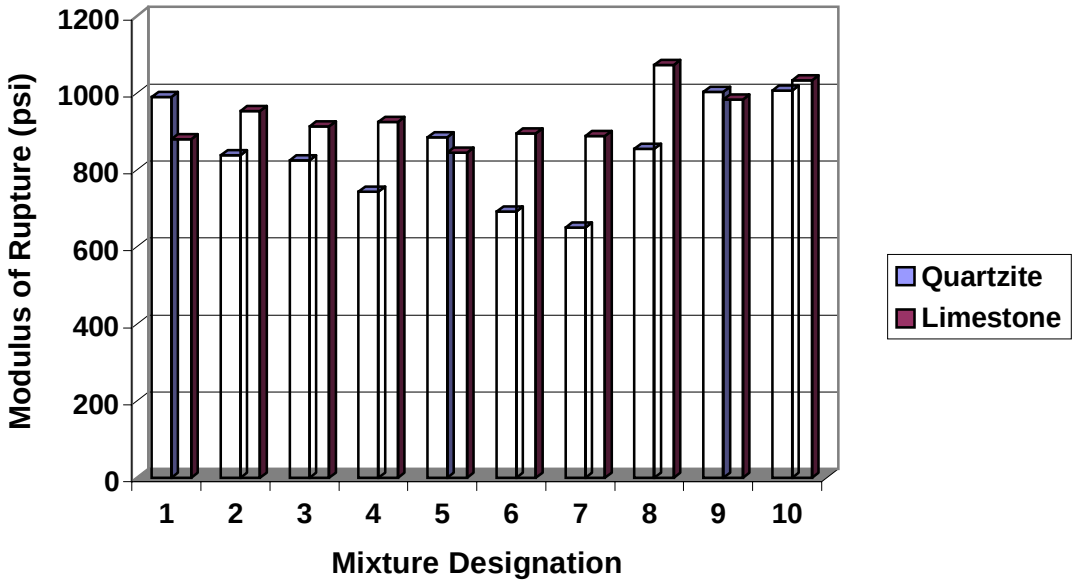

Fig. 3.16: Comparison of Modulus of Rupture of Mixes Using Quartzite and Limestone Aggregate at 28-day

In the mixes containing just silica fume as cement replacement, mix L10F0S12W0.46 (12% of cement by weight replaced with silica fume) showed the highest static flexural strength (14-day: 7.4 MPa [1074 psi]; 28-day: 7.5 MPa [1085 psi]). Mix L5F15S0W0.47 (15% of cement by weight replaced with fly ash) showed the lowest 14 and 28 day static flexural strength values (14-day: 5.8 MPa [843 psi]; 28-day: 5.8 MPa [845 psi]) and mix L10F0S12W0.46 (12% of cement by weight replaced with silica fume) showed the highest 14 and 28 day static flexural strength (14-day: 7.4 MPa [1074 psi]; 28-day: 7.5 MPa [1085 psi]) values respectively.

Figures 3.15 and 3.16 show comparative bar charts of concretes containing limestone and quartzite aggregates. From the figures it can be concluded that the limestone mixes show higher modulus of rupture when compared to quartzite mixes.

3.3.6.4 Dry Unit Weight: The dry unit weight results at 14 and 28-day are given in Tables A4 and A6 and A11 and A13 for the quartzite and limestone mixes respectively in Appendix A. The comparative bar charts are shown in Figures 3.17 and 3.18. The highest value for dry unit weight (2357.0 kg/m^3 [147.2 lb./ft^3] at 28-day) was obtained for mix Q3F15S5W0.50 (5% of cement by weight replaced with silica fume and 15% with fly ash) and the lowest value for dry unit weight (2228.0 kg/m^3 [139.1 lb./ft^3] at 28-day) was obtained for mix Q7F25S0W0.54 (25% of cement by weight replaced with fly ash). Among the mixes using limestone aggregate, mix L6F20S0W0.50 (20% of cement by weight replaced with fly ash) showed the highest value for dry unit weight (2350.1 kg/m^3 [146.7 lb./ft^3] at 28-day) and mix L4F20S5W0.54 (5% of cement by weight replaced with silica fume and 20% by fly ash) showed the lowest value for dry unit weight (2273.4 kg/m^3 [141.9 lb./ft^3] at 28-day).

The trends shown in the results are the same as that followed by compressive strength, modulus of rupture and static modulus except in a few specimens, which could be considered as outliers.

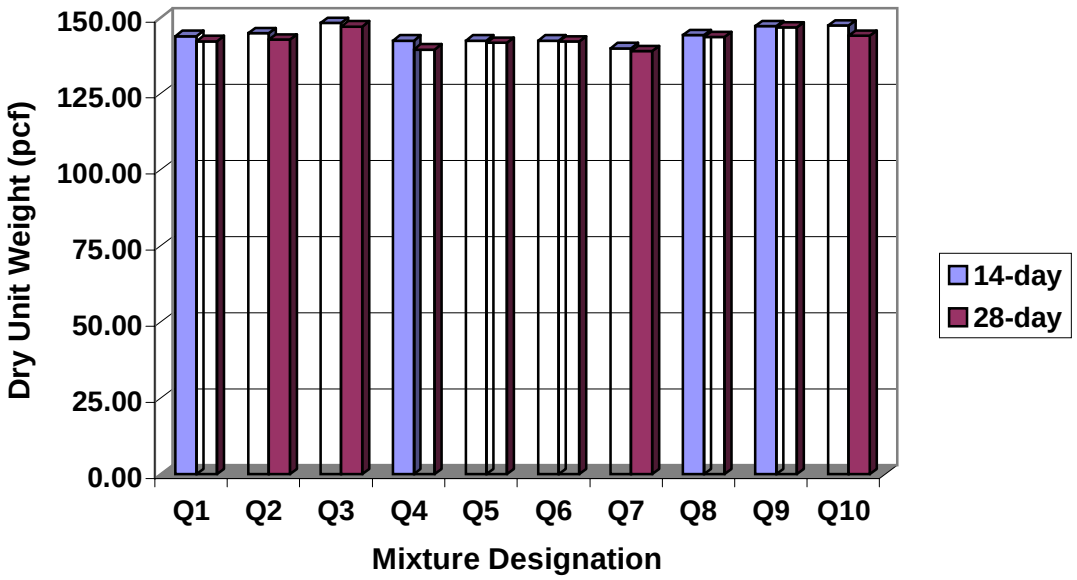

Fig. 3.17 : Comparison of Dry Unit Weight at 14 and 28 day (Quartzite Aggregate)

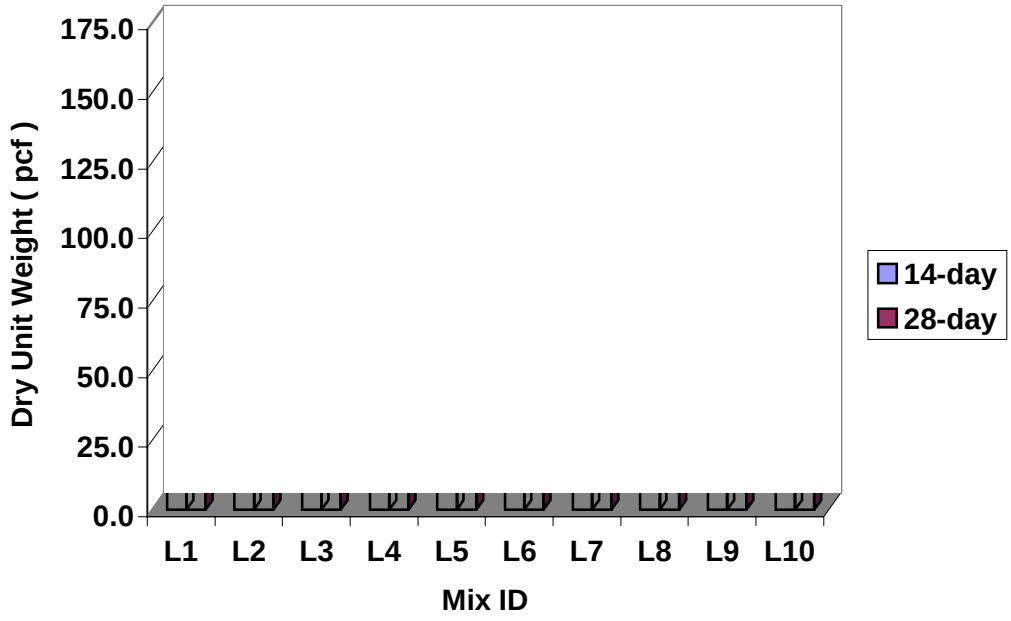

Fig. 3.18: Comparison of Dry Unit Weight at 14 and 28 day (Limestone Aggregate)

3.3.6.5 Chloride Permeability: The results of all tests conducted for chloride permeability are tabulated in Tables A15 through A18 in Appendix A and bar charts are shown in Figures 3.19 through 3.22.

Initially it was expected that a significant reduction in chloride permeability would occur between the ages of 14 and 28-days. Mixes Q1CONTROLW0.4 through Q7F25S0W0.54 were tested after being subjected to 14 days of normal moist curing in cold water and mix Q1CONTROLW0.4 was also subjected to 28-day testing under the same conditions of curing. As can be followed from the results of the tests on mix Q1CONTROLW0.4 (Table A15, Appendix A) which showed 7941 and 5719 coulombs at 14 and 28-day (both high values), reliance on age alone was not enough to differentiate between the mixtures. Therefore it was decided to subject the specimens to accelerated curing. In this type of curing the specimens after being demolded are placed in a curing tank containing water, maintained at a constant temperature of 38^{o}C (100^{o}F). The first batch (Q1CONTROLW0.4) was subjected to 1 day of accelerated curing and mix Q2F15S7W0.52 was subjected to 12 days of accelerated curing. Based on the results of these tests it was decided to subject the specimens to a constant accelerated curing period of seven days before testing. The tests were then carried out and the results tabulated (Table A15, Appendix A).

Quartzite: Among mixes that contained both silica fume and fly ash and, quartzite aggregate, the mix Q2F15S7W0.52 (7% of cement by weight replaced with silica fume and 15% by fly ash) showed the lowest permeability (Charge Passed: 533 Coulombs; ASTM Category: Very Low). Among the mixes that had just fly ash as cement replacement the mixes Q5F15S0W0.47 and Q7F25S0W0.54 (with 15% and 25% of cement by weight replaced with fly ash respectively) showed lower permeabilities (Charge Passed: 4088 and 4059 Coulombs respectively) as compared to mix Q6F20S0W0.50 (with 20% of cement by weight replaced with fly ash), which showed a higher value (4548 Coulombs).

In the mixes containing just silica fume as cement replacement, mix Q10F0S12W0.46 (12% of cement by weight replaced with silica fume) showed the lowest permeability (Charge Passed: 132 Coulombs; ASTM Category: Very Low) and mix Q1CONTROLW0.40 (plain concrete with no mineral admixtures) showed the highest chloride permeability (Charge Passed: 5566 Coulombs; ASTM Category: High) values.

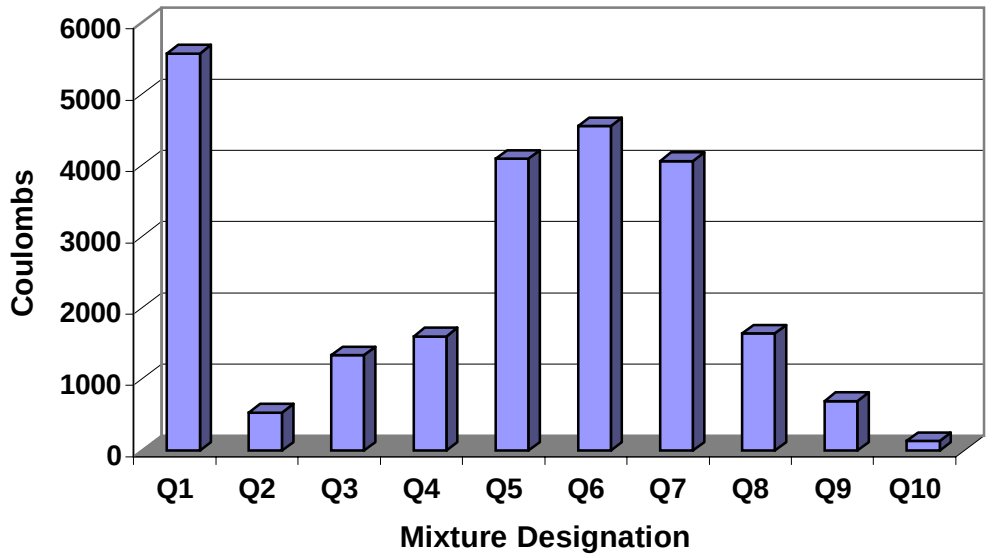

Fig. 3.19: Chloride Permeability of Quartzite Mixes - Accelerated Curing

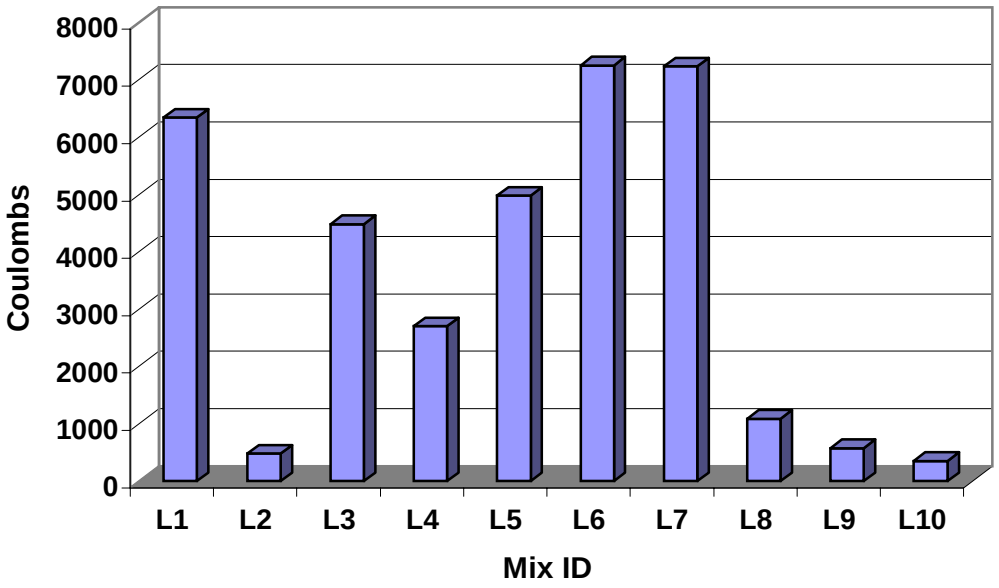

Fig. 3.20: Chloride Permeability of Limestone Mixes - Accelerated Curing

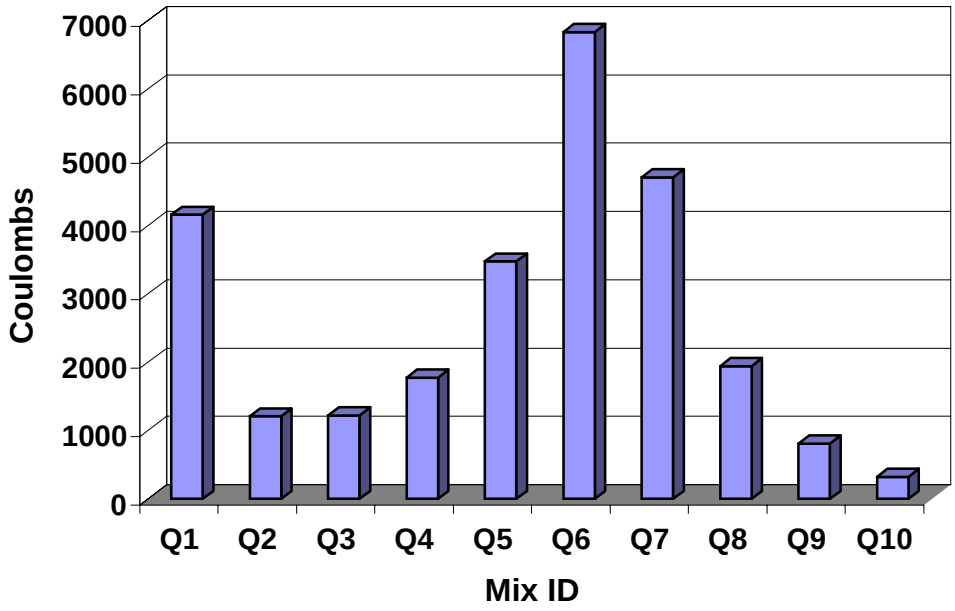

Fig. 3.21: Chloride Permeability of Quartzite Mixes at 90-day

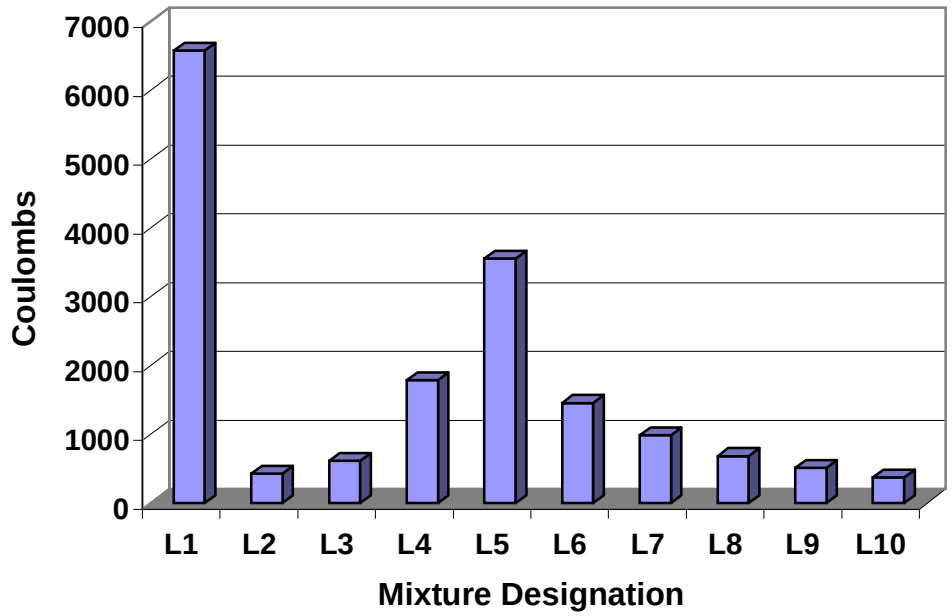

Fig. 3.22: Chloride Permeability of Limestone Mixes at 90-day

Limestone: For the mixes with limestone aggregate it was decided to subject the specimens to 3 days of accelerated curing (immediately after demolding the specimens at 24 hrs) before testing for chloride permeability. The results of the tests carried out are tabulated in Table A16 and a comparative bar chart is shown in Figure 3.20.

Among mixes that contained both silica fume and fly ash, and limestone aggregate, the mix L2F15S7W0.52 (7% of cement by weight replaced with silica fume and 15% by fly ash) showed the lowest chloride permeability (Charge Passed: 481 Coulombs; ASTM Category: Very Low). Among the mixes that had just fly ash as cement replacement the mix L5F15S0W0.47 (15% of cement by weight replaced with fly ash) showed lower chloride permeability (Charge Passed: 4979 Coulombs; ASTM Category: High) as compared to the other two mixes, L6F20S0W0.50 and L7F25S0W0.54 (20% and 25% of cement by weight replaced with fly ash, respectively) which showed almost equal values (Charge Passed: 7249 and 7232 Coulombs, respectively). In the mixes containing just silica fume as cement replacement, mix L10F0S12W0.46 (12% of cement by weight replaced with silica fume) showed the lowest chloride permeability (Charge Passed: 354 Coulombs; ASTM Category: Very Low).

The mixes were subjected to rapid chloride permeability tests again after 90-days. The results of these tests are tabulated in Tables A17 and A18, Appendix A. The comparative bar charts are shown in Figures 3.21 and 3.22. The specimens were subjected to an average of 28 days of continuous moist curing and then air-dried till they reached an age of 90-days. They were then tested for chloride permeability. A comparative analysis of the results of the accelerated curing and 90-day test results shows a good correlation for 12 mixes (Q2F15S7W0.52, Q3F15S5W0.50, Q4F20S5W0.54, Q8F0S7W0.43, Q9F0S10W0.45, Q10F0S12W0.46, L1CONTROLW0.4, L2F15S7W0.52, L3F15S5W0.50, L8F0S7W0.43, L9F0S10W0.45 and L10F0S12W0.46). The comparative bar charts are shown in Figures R5 and R6.

Among mixes that contained both silica fume and fly ash and quartzite aggregate, mix Q2F15S7W0.52 (7% of cement by weight replaced with silica fume and 15% by fly ash) showed the lowest chloride permeability (Charge Passed: 1207 Coulombs; ASTM Category: Low). Among mixes that had just fly ash as cement replacement, mixes Q5F15S0W0.47 and Q7F25S0W0.54 (with 15% and 25% of cement by weight replaced with fly ash respectively) showed lower chloride permeabilities (Charge Passed: 3475 and 4704 Coulombs respectively) as

compared to mix Q6F20S0W0.50 (with 20% replacement by fly ash), which showed a higher value (6831 Coulombs).

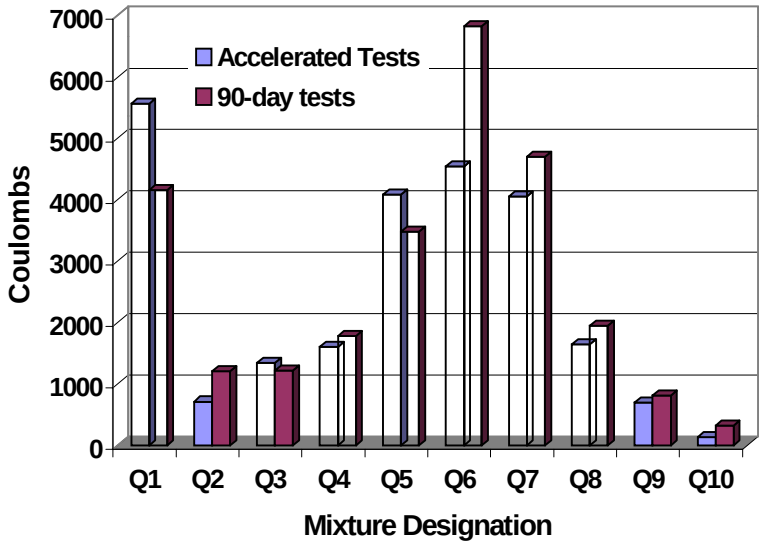

Fig. 3.23: Comparison of Chloride Permeability of Quartzite Mixes

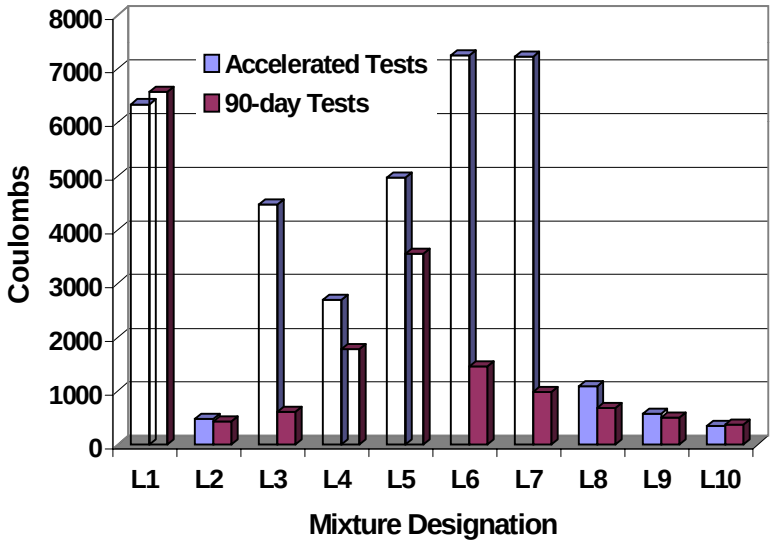

Fig. 3.24: Comparison of Chloride Permeability of Limestone Mixes

In the mixes containing just silica fume as cement replacement, mix Q10F0S12W0.46 (12% of cement by weight replaced with silica fume) showed the lowest chloride permeability (Charge Passed: 323 Coulombs; ASTM Category: Very Low). Mix Q1CONTROLW0.4 (plain concrete with no mineral admixtures) and mix Q10F0S12W0.46 (12% of cement by weight replaced with silica fume) showed the highest chloride permeability (Charge Passed: 4158 Coulombs; ASTM Category: High) and lowest chloride permeability (Charge Passed: 323 Coulombs; ASTM Category: Very Low) values respectively.

Among mixes that contained both silica fume and fly ash and, limestone aggregate, the mix L2F15S7W0.52 (7% of cement by weight replaced with silica fume and 15% by fly ash) showed the lowest chloride permeability (Charge Passed: 430 Coulombs; ASTM Category: Very Low). Among the mixes that had just fly ash as cement replacement mix L7F25S0W0.54 (25% of cement by weight replaced with fly ash) showed lower chloride permeability (Charge Passed: 986 Coulombs; ASTM Category: Low) as compared to the other two mixes, L5F15S0W0.47 and L6F20S0W0.50 (15 and 20% of cement by weight replaced with fly ash, respectively) which indicated higher chloride permeabilities (Charge Passed: 3553 and 1455 Coulombs, respectively). In the mixes containing just silica fume as cement replacement material, mix L10F0S12W0.46 (12% of cement by weight replaced with silica fume) showed the lowest chloride permeability (Charge Passed: 373 Coulombs; ASTM Category: Very Low).

3.3.7 High Strength Concrete for Prestressed Girders

3.3.7.1 Fresh Concrete Properties: The fresh concrete data for all the mixes showed good uniformity. The results of the tests for unit weight, air-content, and slump, are given in Table B3, Appendix B. The measured slumps for various mixes are shown in Fig. 3.25 and the recorded air contents and fresh concrete unit weights are shown in Fig. 3.26 and 3.27 respectively. The slump varied from 88.9 mm (3.5 inches) to 215.9 mm (8.5 inches) and the air content varied from 2.5% to 7%. The fresh Concrete unit weights were nearly the same for all mixes and it had an average value of 2286.2 kg/m^3 (142.7 lb./ft^3). The room temperature, the humidity and the concrete temperature were nearly the same for all mixes. The average value of the room temperature was 24^{o}C [75^{o}F]), the average value of humidity was 35 % and the average concrete temperature was 28^{o}C [82.4^{o}F].

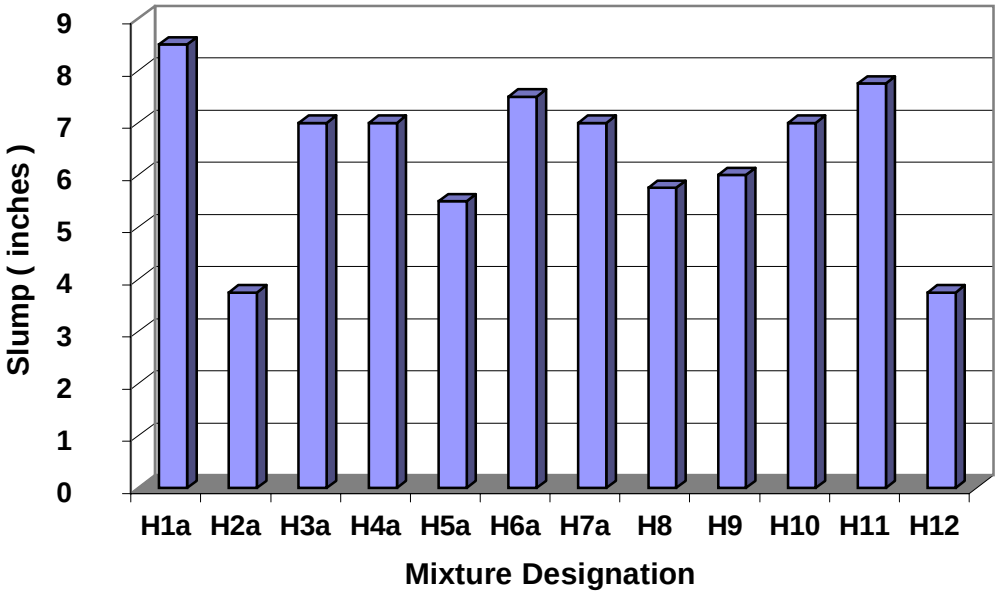

Fig. 3.25: Comparison of Slump for Bridge Girder Concretes

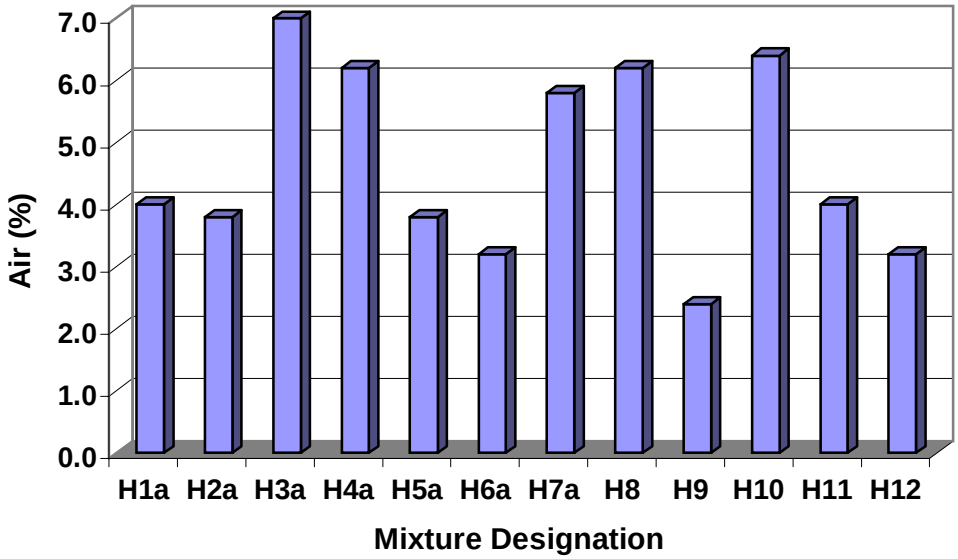

Fig. 3.26: Air Content of Fresh Concrete for Bridge Girder Concretes

3.3.7.2 Hardened Concrete Properties

Compressive Strength

Testing for compressive strength was carried at 1, 3, 5, 7, 28, and 56 days. The results of these tests are given in Tables B4 through B8 in Appendix B. The compressive strength test results at various ages can be summarized as follows (refer Tables B4 through B8 in Appendix B and Figures 3.28 through 3.33)

At 1 day

- Plain Concrete specimens showed the regular trend i.e. The mix H1CONTROLW0.28 with the lowest w/c ratio (0.28) showed highest compressive strength (45.2 MPa [6548 psi]) and mix H3CONTROLW0.32 with the highest w/c ratio (0.32) showed lowest compressive strength (25.3 MPa [3665 psi]).
- In mixes with 7% of cement by weight replaced with silica fume, the mix with w/c ratio of 0.30 (H7F0S7W0.30) showed highest compressive strength (43.1 MPa [6235 psi]) as compared to the other two mixes (H4F0S7W0.28 and H10F0S7W0.32) with w/c ratios of 0.28 and 0.32.
- In mixes with 10% of cement by weight replaced with silica fume the mix with w/c ratio 0.30 (H8F0S10W0.30) showed the highest compressive strength (46.8 MPa [6775 psi]) as compared to the other two mixes (H5F0S10W0.28 and H11F0S10W0.32) with w/c ratios of 0.28 and 0.32.
- In mixes with 12% of cement by weight replaced with silica fume the mix with the highest w/c ratio of 0.32 (H12F0S12W0.32) showed the highest compressive strength (42.9 MPa [6205 psi]).

At 3-day

- Plain Concrete specimens showed the same trend as at 1-day with mix H1CONTROLW0.28 showing the highest compressive strength (53.5 MPa [7743 psi]).
- In mixes with 7% of cement by weight replaced with silica fume the mix with w/c ratio 0.32 (H10F0S7W0.32) showed the highest compressive strength (43.4 MPa [6283 psi]) as compared to the other two mixes H7F0S7W0.30 and H4F0S7W0.28 with w/c ratios of 0.28 and 0.30.

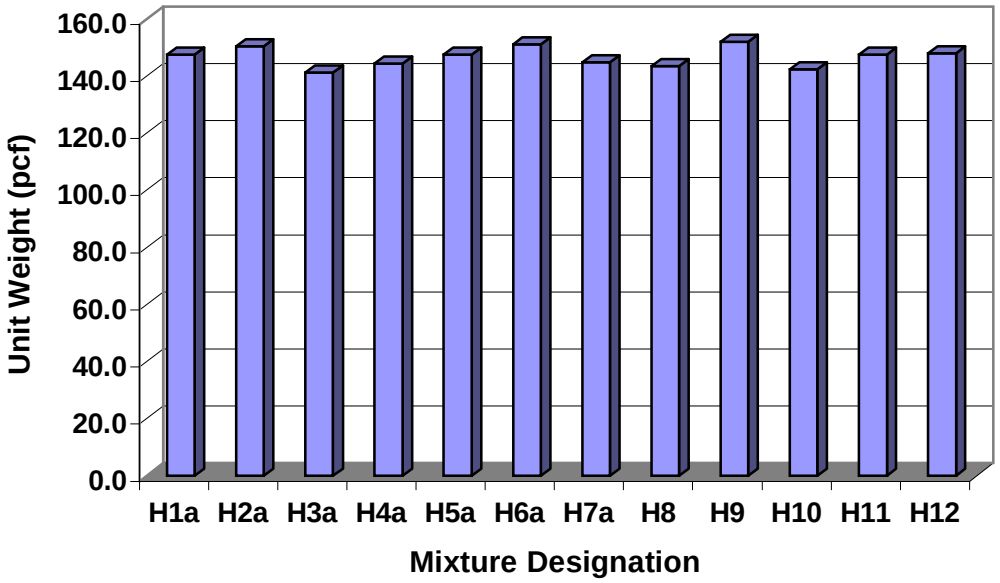

Fig. 3.27: Unit Weight of Fresh Concretes for Bridge Girder

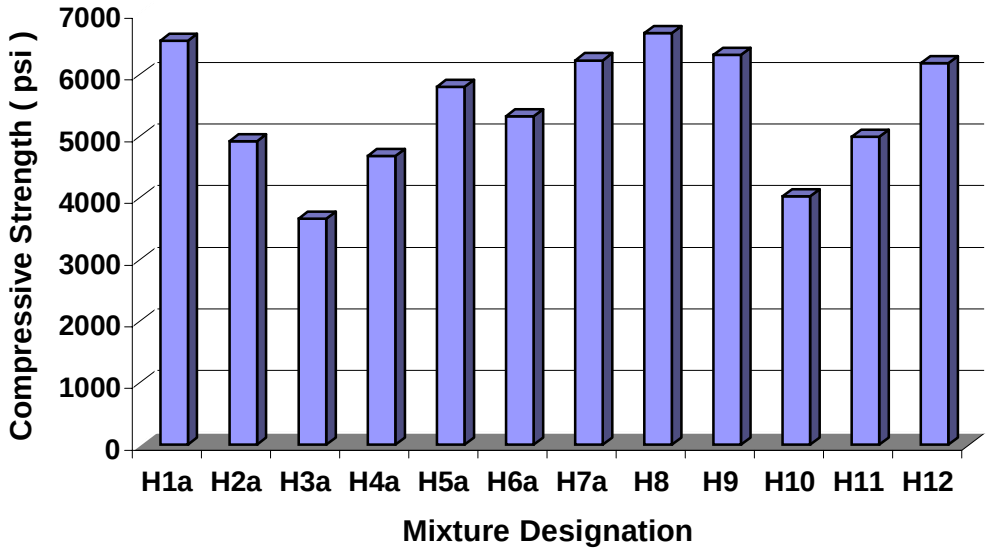

Fig. 3.28: Compressive Strength at 1-day for Bridge Girder Concretes

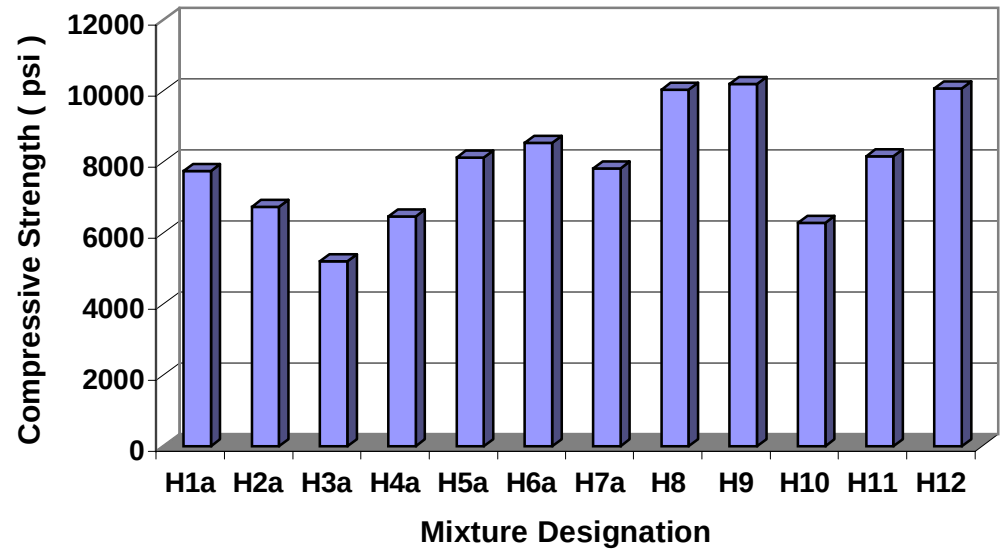

Fig. 3.29: Compressive Strength at 3-day for Bridge Girder Concretes

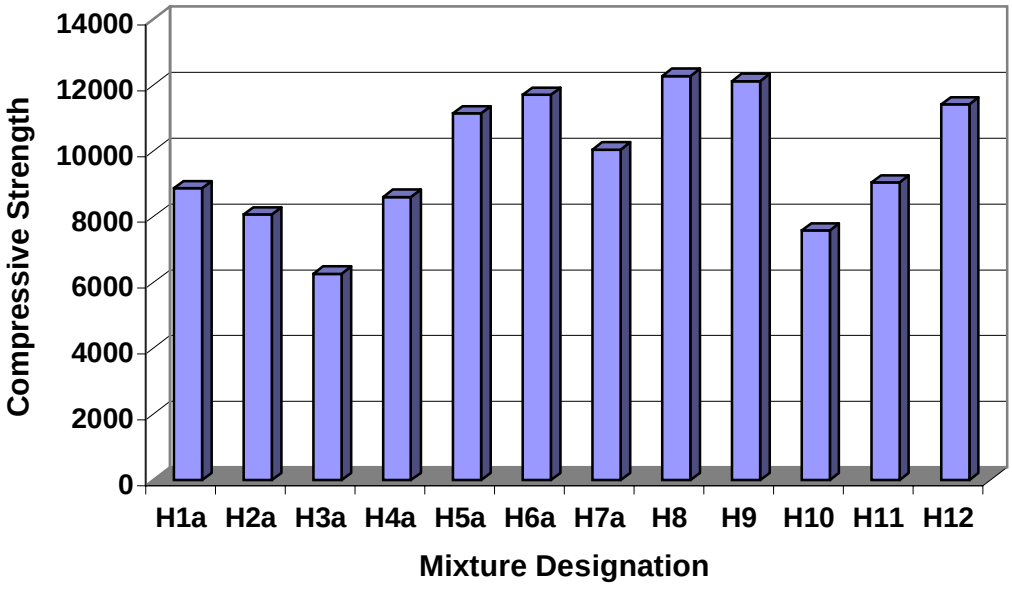

Fig. 3.30: Compressive Strength at 7-day for Bridge Girder Concretes

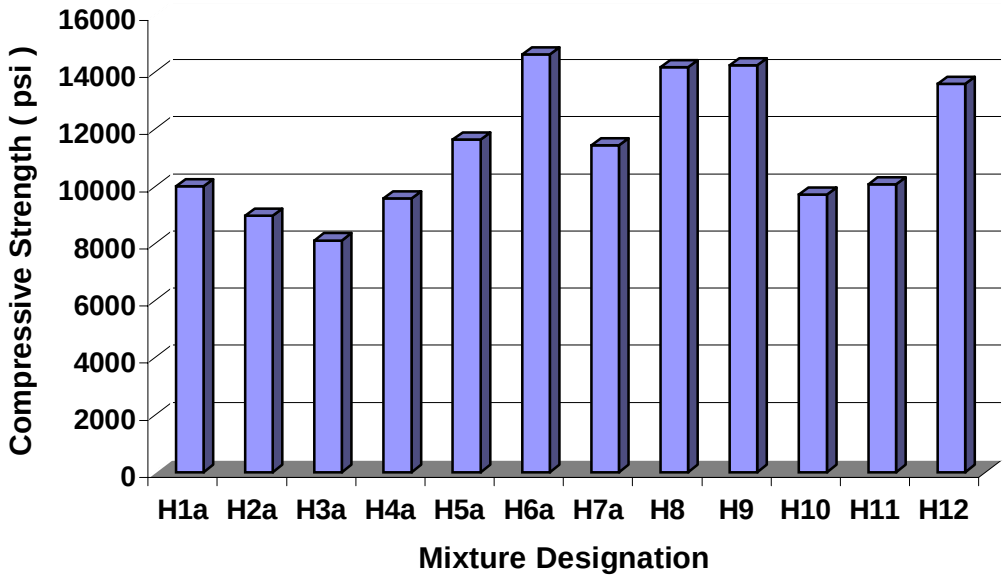

Fig. 3.31: Compressive Strength at 28-day for Bridge Girder Concretes

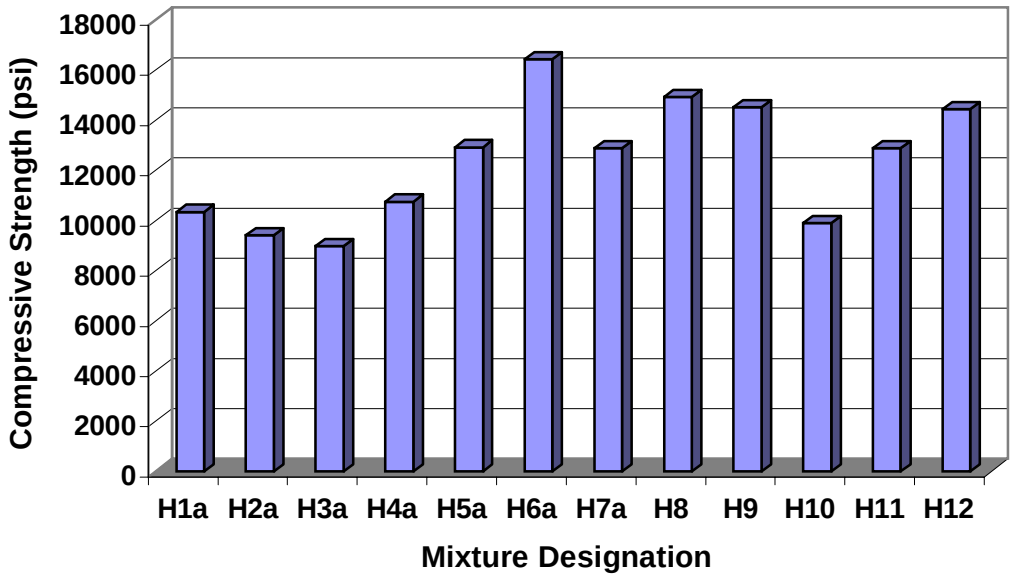

Fig. 3.32: Compressive Strength at 56-day for Bridge Girder Concretes

- In mixes with 10% of cement by weight replaced with silica fume the mix with w/c ratio 0.32 (H11F0S10W0.32) showed the highest compressive strength (56.5 MPa [8170 psi]) as compared to the other two mixes (H5F0S10W0.28 and H8F0S10W0.30) with w/c ratios of 0.28 and 0.30.
- Mixes with 12% of cement by weight replaced with silica fume showed the same trend as at 1-day with the mix H12F0S12W0.32 showing the highest compressive strength of 69.6 MPa (10,075 psi).

At 7-day

- Plain concrete specimens showed the same trend as at 1-day and 3-day with the mix H1CONTROLW0.28 showing the highest compressive strength (61.3 MPa [8865 psi]).
- Mixes with 7% of cement by weight replaced with silica fume showed the same trend as at 3-day with the highest value being 52.4 MPa (7585 psi) for mix H10F0S7W0.32.
- In mixes with 10% of cement by weight replaced with silica fume, the mix with w/c ratio 0.30 (H8F0S10W0.30) showed the highest compressive strength (84.9 MPa [12,283 psi]) as compared to the other two mixes with w/c ratios of 0.28 and 0.32.
- Mixes with 12% of cement by weight replaced with silica fume showed the same trend as at 1-day and 3-day with the mix H12F0S12W0.32 showing the highest compressive strength of 78.9 MPa (11,423 psi).

At 28-day

- Plain concrete specimens showed the same trend as at 1,3,7-day with the mix H1CONTROLW0.28 showing the highest compressive strength (69.2 MPa [10,008 psi]).
- Mixes with 7% of cement by weight replaced with silica fume showed the same trend as at 3,7-day with the highest value being 67.1 MPa (9705 psi) for mix H10F0S7W0.32.
- In mixes with 10% of cement by weight replaced with silica fume the mix with w/c ratio 0.32 (H11F0S10W0.32) showed the highest compressive strength (69.6 MPa [10,078 psi]) as compared to the other two mixes (H10F0S7W0.32 and H12F0S12W0.32) with w/c ratios of 0.28 and 0.30 (same trend as at 3-day).

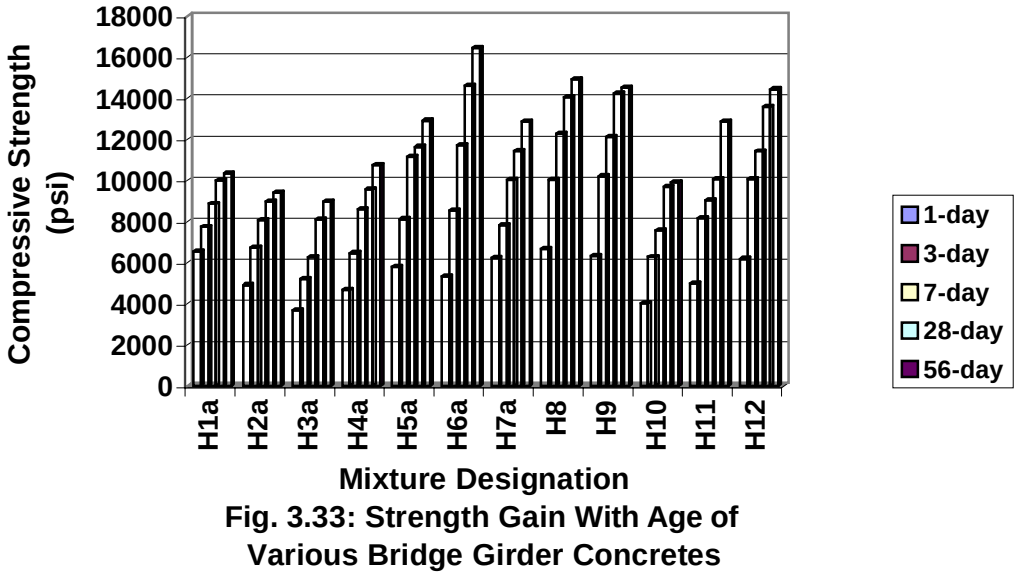

Fig. 3.33: Strength Gain With Age of Various Bridge Girder Concretes

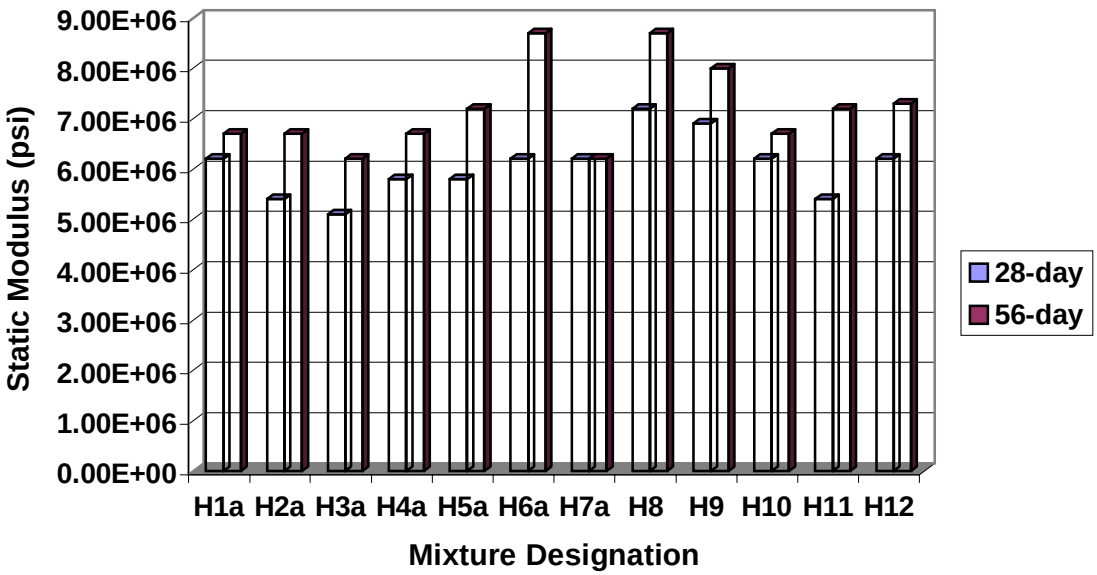

Fig. 3.34: Comparison of Static Modulus for Bridge Girder Concretes

- Mixes with 12% of cement by weight replaced with silica fume showed the same trend as at 1,3,7-day with the mix H12F0S12W0.32 showing the highest compressive strength of 93.9 MPa (13,593 psi).

At 56-day

- Plain concrete specimens showed the same trend as at 1,3,7,28-day with the mix H1CONTROLW0.28 showing the highest compressive strength (71.5 MPa [10,343 psi]).
- Mixes with 7% of cement by weight replaced with silica fume showed the same trend as at 3,7,28-day with the highest value being 68.4 MPa (9900 psi) for mix H10F0S7W0.32.
- In mixes with 10% of cement by weight replaced with silica fume the mix with w/c ratio 0.30 (H8F0S10W0.30) showed the highest compressive strength of 103.2 MPa (14,935 psi) as compared to the other two mixes (H7F0S7W0.30 and H9F0S12W0.30) with w/c ratios of 0.28 and 0.32.
- Mixes with 12% of cement by weight replaced with silica fume showed the same trend as at 1,3,7,28-day with the mix H12F0S12W0.32 showing the highest compressive strength of 99.8 MPa (14,443 psi).

Among all the mixes, the mixes with a w/c ratio of 0.3 showed the maximum compressive strength at all ages. Among the mixes with w/c of 0.30 the mix H8F0S10W0.30 (with 10% of cement by weight replaced with silica fume) showed the highest compressive strength at all the ages at which the mix was tested. Figures 3.40 and 3.41 show comparative bar charts of compressive strength at 56 day with variation of the percentage replacement of cement and w/c ratio. From Figure 3.40 we can see that a water to cement ratio of 0.30 and a percentage replacement of 10% seems to be the best combination. The same is confirmed from Figure 3.41.

Static Modulus

The specimens were tested for static modulus at 28 and 56 days and the results are tabulated in Tables B7 and B8, in Appendix B. The comparative bar chart is shown in Figure H10F0S7W0.32.

Static Modulus followed the same trend as the compressive strength i.e.; the mix, which showed the highest strength also, showed the highest static modulus at that particular age. The static modulus values :

- For plain concrete varied between 4.1 x 10^4 MPa (6.0 x 10^6 psi) and 4.5 x 10^4 MPa (6.5 x 10^6 psi) at 28 days and between 4.5 x 10^4 MPa (6.5 x 10^6 psi) and 4.8 x 10^4 MPa (7.0 x 10^6 psi) at 56 days.
- For mixes with 7% of cement by weight replaced by silica fume varied between 3.8 x 10^4 MPa (5.5 x 10^6 psi) and 4.5 x 10^4 MPa (6.5 x 10^6 psi) at 28 days and between 4.1 x 10^4 MPa (6.0 x 10^6 psi) and 4.8 x 10^4 MPa (7.0 x 10^6 psi) at 56-days.
- For mixes with 10% of cement by weight replaced by silica fume varied between 3.4 x 10^4 MPa (5.0 x 10^6 psi) and 5.2 x 10^4 MPa (7.5 x 10^6 psi) at 28 days and between 4.8 x 10^4 MPa (7.0 x 10^6 psi) and 6.2 x 10^4 MPa (9.0 x 10^6 psi) at 56-days.
- For mixes with 12% of cement by weight replaced by silica fume varied between 4.1 x 10^4 MPa (6.0 x 10^6 psi) and 4.8 x 10^4 MPa (7.0 x 10^6 psi) at 28 days and between 4.8 x 10^4 MPa (7.0 x 10^6 psi) and 6.2 x 10^4 MPa (9.0 x 10^6 psi) at 56-days

Dry Unit Weight

The trends shown in the results are the same as that followed by compressive strength, modulus of rupture and static modulus except in a few specimens, which can be considered as outliers. The dry unit weight results at 1, 3, 7, 28, 56 days are given in Tables B4 through B8, in Appendix B. Also comparative bar charts are shown in Figures 3.35 through 3.39. The average value of dry unit weight was found to be 2319.6 kg/m^3 (144.8 lb./ft^3) at 56-day. The highest value 2399.7 kg/m^3 (149.8 lb./ft^3) was obtained for mix H8F0S10W0.30 (10% of cement by weight replaced with silica fume and w/c ratio of 0.30) and the lowest value 2182.7 kg/m^3 (136.3 lb./ft^3) was obtained for mix H5F0S10W0.28 (10% of cement by weight replaced with silica fume and w/c ratio of 0.32) at 56-day. The trends followed by the results are the same as that followed by compressive strength and static modulus except in a few specimens, which can be considered as outliers.

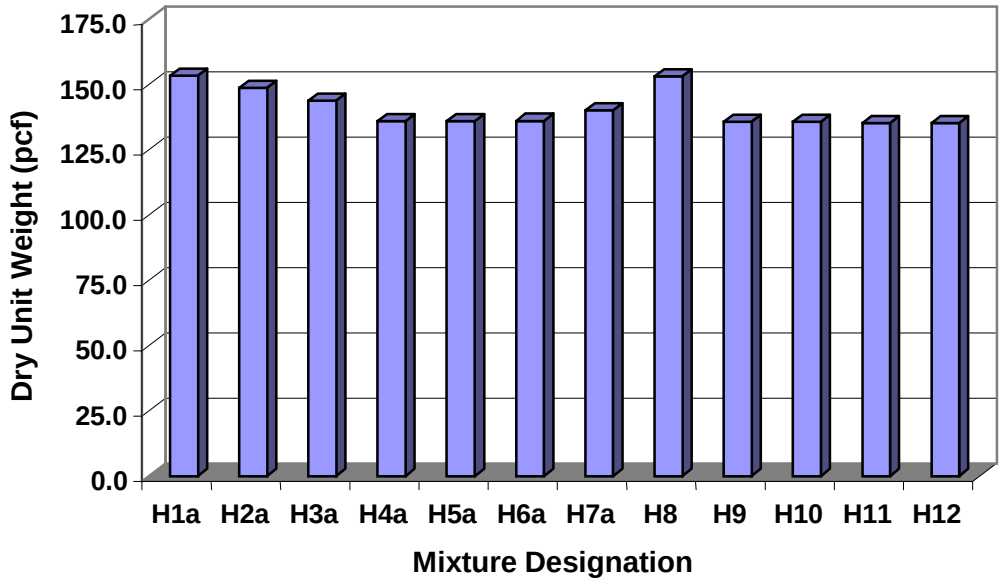

Fig. 3.35: Dry Unit Weight at 1 day for Bridge Girder Concretes

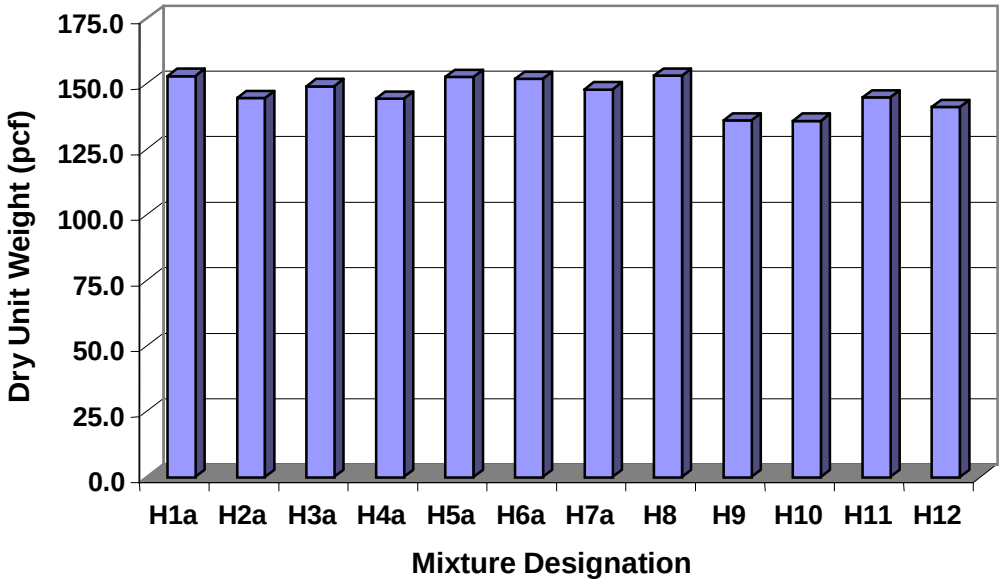

Fig. 3.36: Dry Unit Weight at 3 day for Bridge Girder Concretes

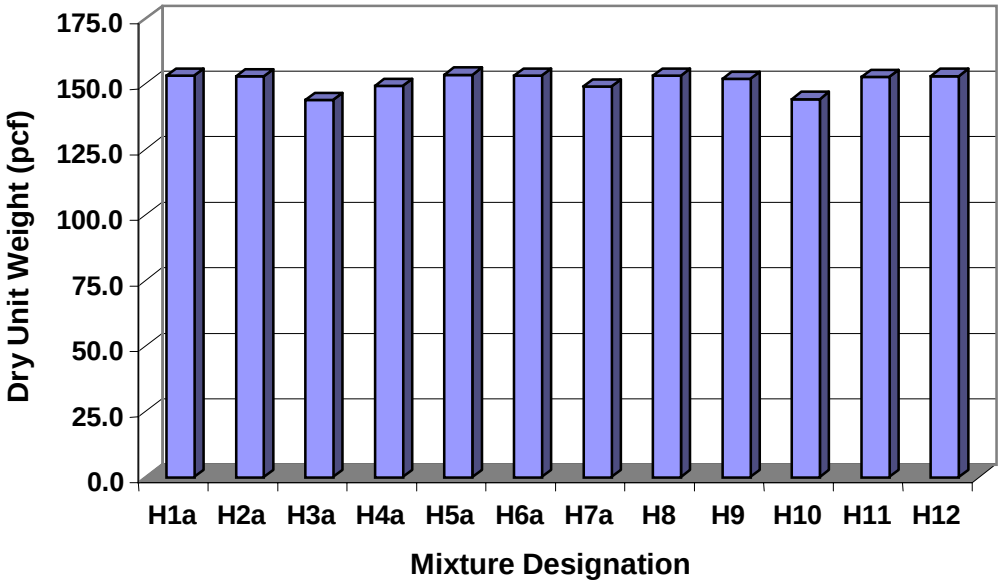

Fig. 3.37: Dry Unit Weight at 7 day for Bridge Girder Concretes

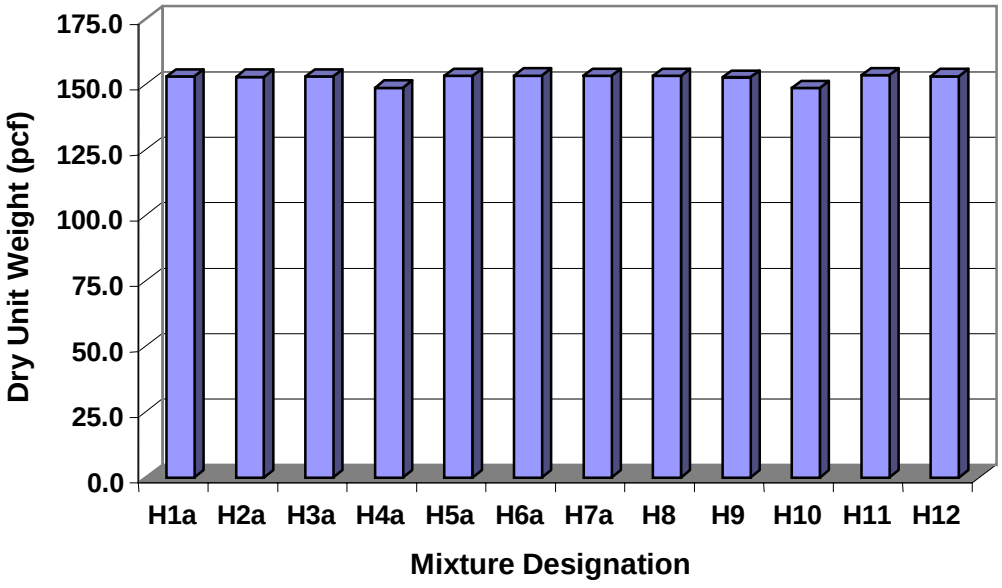

Fig. 3.38: Dry Unit Weight at 28 day for Bridge Girder Concretes

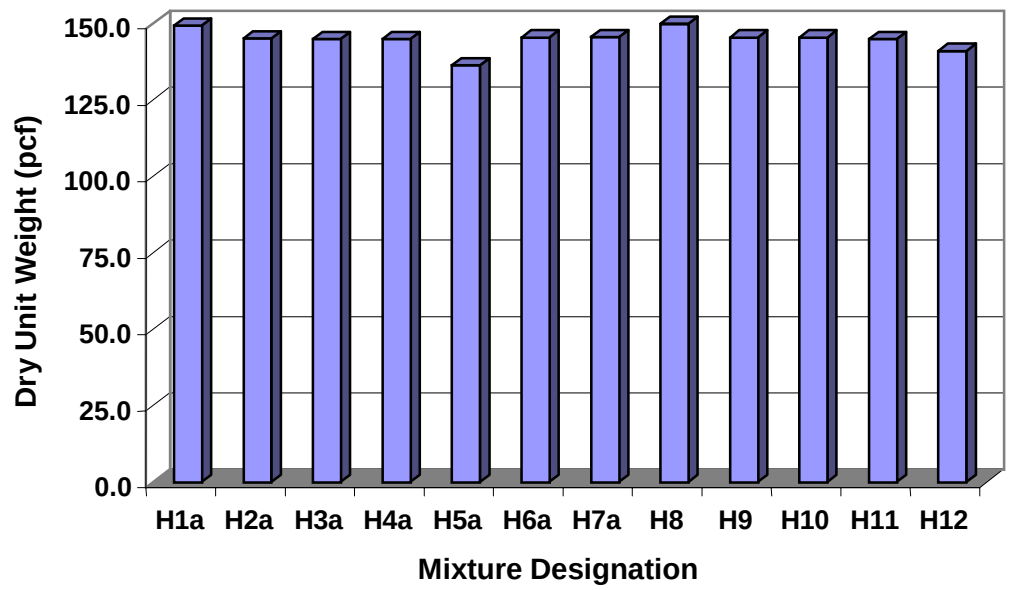

Fig. 3.39: Dry Unit Weight at 56 days for Bridge Girder Concretes

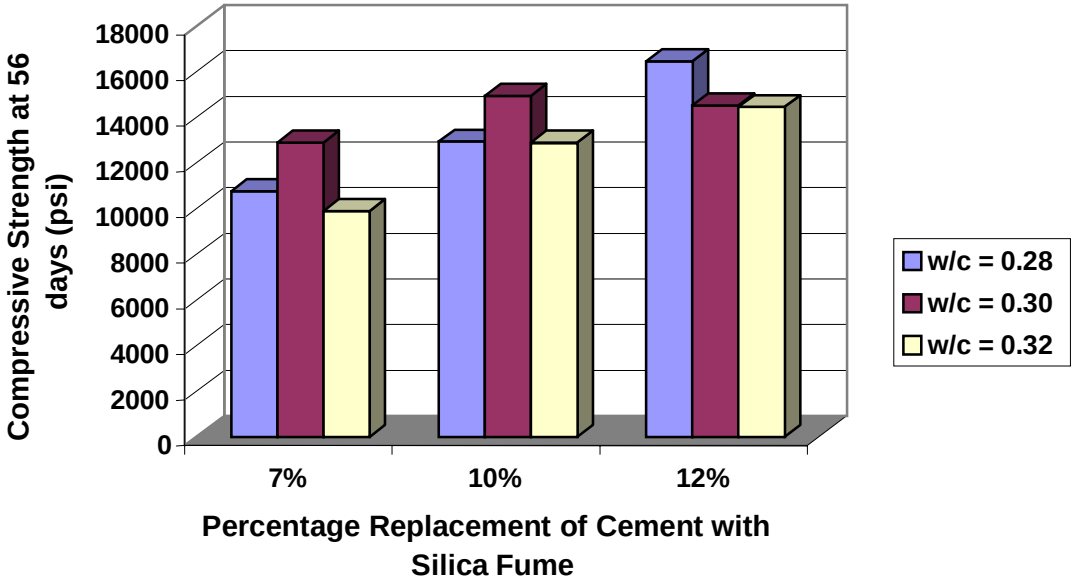

Fig. 3.40: Comparison of Compressive Strength at 56 days of Mixes with different percentage replacements of cement for Bridge Girder Concretes

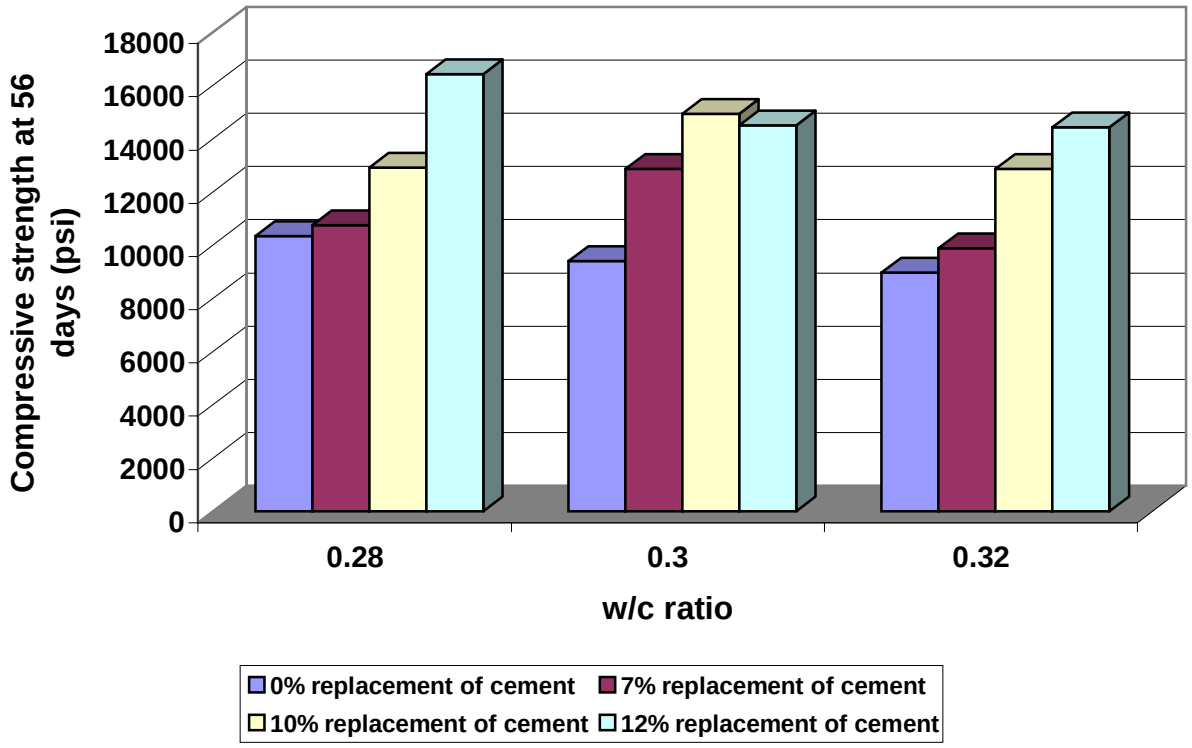

Fig. 3.41: Comparison of Compressive Strength at 56 day of Mixes with different w/c ratios for Bridge Girder Concretes

3.3.8 Tests Carried out on Recommended Mix (H8RF0S10W0.30)

3.3.8.1 Fresh Concrete Properties: The fresh concrete data for the mix showed satisfactory results. It showed a slump of 146.1 mm (5.75 inches), air content of 6.2% and a unit weight of 2300 kg/m^3 (143.6 lb/ft^3).

3.3.8.2 Hardened Concrete Properties

Compressive Strength: All the results are given in Table B9, Appendix B.

The testing that was carried out on this mix for compressive strength was two fold:

- Tests carried out after the specimen was subjected to accelerated curing of 6, 12, 18 and 24 hours.

  The results from these tests indicated the strength gain of this particular mix over a period of 24 hours when subjected to accelerated curing. The maximum strength of this concrete at the end of 24 hours was 90.3 MPa (13,073 psi).

- Tests carried out after the specimens were normally cured in cold water at 1, 2, 3, 7, 28 and 56 days.

  The results from these tests indicated the strength gain of this concrete over a period of 56 days. This particular concrete showed a compressive strength of 46.8 MPa (6775 psi) at the end of one day and 62.8 MPa (9085 psi) at the end of 2 days. This strength is enough for release. The maximum strength of the concrete at the end of 56 days was 103.2 MPa (14,935 psi).

Static Modulus: The specimens were tested for static modulus at 1, 2, 3, 7, 28 and 56 days after normal curing and the results are tabulated in Table B9, Appendix B. Static modulus followed the same trend as the compressive strength i.e. the mix, which showed the highest strength also, showed the highest static modulus at that particular age. The static modulus varied with the age of the concrete and curing conditions. The maximum static modulus value was shown by the mix at 56-days (6×10^4 MPa [8.7×10^6 psi]). The specimens subjected to accelerated curing were also tested for static modulus and the results from these tests are given in Table B9, Appendix B.

Dry Unit Weight: The dry unit weight results at 1, 2, 3, 7, 28, 56 days are given in Table H8. The average value of dry unit weight was found to be 2443.7 kg/m^3 (152.55 lb./ft^3)

The trends shown by these results are the same as that followed by compressive strength and static modulus except in a few specimens, which could be considered as outliers.

Chloride Permeability: The rapid chloride permeability test was conducted on a total of four specimens; two after 24 hours of accelerated curing and two after 90-days of normal curing (28 days continuos moist curing and then air dried for 62 days). The specimens, which were tested after being subjected to, accelerated curing showed an average value of charge passed as 158 coulombs and the 90-day test showed a value of 515 coulombs. Both the test results indicate that this concrete comes under the ASTM C1202 Category of "Very Low" chloride permeability.

3.4 Task 4: Prepare and submit a field sampling and testing program for determining the deck and girder HPC fresh and hardened concrete properties to the technical panel for approval.

3.4.1 Field Sampling and Testing for Cylinder Concrete

Wheel-barrows were used to obtain fresh concrete for testing and sample preparation. The slump, air content, temperature, and unit weight standard tests were performed on the plastic concrete. Once these tests were completed, the field samples were fabricated.

The compression testing machine at SDSU has a maximum capacity of 300,000 lbs. Because very high compressive strengths were expected, the 15.24×30.48 cm (6×12 inch) standard cylinder could not be used. To permit the testing of cylinders exhibiting these high strengths it was decided that all cylinder tests would be conducted on 10.16×20.32 cm (4×8 inch) cylinders.

To obtain some measure of the variance in the process, it was decided that a compression test result would be the average of the results of testing three cylinders. A strength time series was defined as a sequence of tests conducted at predetermined ages. A full strength time series provided tests at concrete ages of 1, 3, 7, 14, 28, 56 (or 90), 180 days, and 1 year. If a full series were planned for a specific girder this required 24 cylinders. In addition, cylinders were needed for the rapid chloride test. Typically, the rapid chloride test required 2 to 4 additional cylinders.

A series results from each girder that is cast. A full or shortened series was utilized for all concrete that was cast. A summary of the chronology of the concrete placement for the girders and the deck for each of the two bridges is provided in Table 3.1. A summary of the cylinders cast and tested for each series is also presented in the table. It should be noted that at each fabrication, two girders were cast and, as has been stated, two series for testing were generated.

The instrumented girders required additional field samples. For these girders, it was decided to produce two series for each girder. The first series was cured overnight at the fabrication yard and subsequently transported to the laboratory and moist cured for the entire testing period. This series is defined as a laboratory cure. The second series was called a companion cure, and these cylinders were cured with the girders. The companion-cured cylinders were retrieved and brought to the laboratory just before they were to be tested.

The preceding discussion presents the general philosophy of the testing program. There were some variations from this standard format. With the first trial mix (April 28, 1999) nine 15.24×30.48 cm (6×12 inch) cylinders were cast and tested along with the 10.16×20.32 cm (4×8 inch) cylinders. It was observed that there was little if any difference between the tests on the 4×8 cylinders and the tests on the 6×12 cylinders and thereafter no additional 6×12 cylinders were cast.

3.4.2 Field Sampling and Testing for Bridge Deck Concrete

The testing of the concrete for the deck placement proceeded a little differently. The routine tests of slump, air content, fresh unit weight, and temperature were also carried out on the deck concrete. It was decided to collect cylinders for five testing series. The need for five series was arrived at by considering the configuration of the decks. Both bridges included in the study were three-span structures. It was decided to obtain a series near the middle of each span and one series each at the bents, this requires five series. The one-day test was not run, thus a series consisted of 21 cylinders. Four cylinders were needed for rapid chloride testing so the total number of cylinders came to 25 cylinders. From this, it is observed that 125 cylinders were cast for each deck. The first year (bridge1) 12 beams (6 x 6 x 22 inch) were cast and tested at age 28 days to determine the modulus of rupture. No beams were cast for the second year (bridge 2).

Table 3.1 Casting Chronology and summary of field tests, both bridges.

Casting/date	Rapid Chloride Cylinders	Total Cyl.	Type of Cure[1]	Projected testing age (Days)								
				1	3	7	14	28	56	90	180	1 yr.
Bridge no. 1 (B1)												
Trial mix no. 1 April 28, 1999	yes	49	Laboratory	x	x	x	x	x	x		x	
Trial mix no. 2 May 4, 1999	yes	40	Laboratory Companion	x x	x x	x x	x x	x x	x x			
Girder Casting (G1) May 21, 1999	yes	40	Laboratory	x	x	x	x	x	x			
Girder Casting (G2) May 24, 1999	yes	40	Laboratory	x	x	x	x	x	x			
Girder Casting (G3) June 3, 1999	yes	100	Laboratory Companion	x x	x x	x x	x x	x x	x x		x x	x x
Girder Casting (G4) June 4, 1999	yes	22	Laboratory			x	-	x	x			
Girder Casting (G5) June 11, 1999	yes	22	Laboratory			x	-	x	x			
Girder Casting (G6) June 14, 1999	yes	22	Laboratory			x	-	x	x			
Deck Trial Mix July 9, 1999	yes	19	Laboratory		x	x	x	x	x			
Deck Placement August 16, 1999	yes	125	Laboratory		x	x	x	x		x	x	x
Bridge no. 2 (B2)												
Girder Casting (G2) April 28, 2000	yes	46	Laboratory		x	x	x	x		x	x	x
Girder Casting (G3) May 9, 2000	yes	46	Laboratory		x	x	x	x		x	x	x
Girder Casting (G5) May 18, 2000	yes	100	Laboratory Companion	x x	x x	x x	x x	x x		x x	x x	x x
Deck Placement July 20, 2000	yes	125	Laboratory		x	x	x	x		x	x	x

Note 1: A laboratory cure is a standard moist cure. A Companion cure defines a series that was cured with the girder for which the series is representative.

3.4.3 Girder Fabrication

The fabrication sequence at the precasting yard began with the prestressing steel being tensioned on the prestressing bed. The prestressing bed was large enough to accommodate up to four girders. Standard reinforcing steel for two girders was tied in position on the bed. The forms for these two girders were set and the girders were fabricated. Due to the amount of concrete required for the two beams, two concrete trucks were needed to deliver the concrete. Following the placement of two of the girders, steel was tied for two additional girders, forms were set for these second two girders, and concrete was placed. This second placement was normally on the following day after the first fabrication. The full complement of four girders was cured on the bed until sufficient strength was obtained so that prestress could be transferred to the girders. This typically was three days. Prestress was then transferred to the girders and the bed was cleared. The cycle then repeats. Each bridge required 12 girders, therefore, 6 girder fabrications were required.

3.5 Task 5: Prepare and submit instrumentation and evaluation plans for the HPC decks and girders to the technical panel for approval by September 15, 1998.

The instrumentation plan was prepared and submitted to the SDDOT on September 28, 1999. The same instrumentation layout and monitoring was used for both bridges. Strains were measured by using Geokon model VCE 4200 vibrating wire (VW) strain transducers. These devices measure strain over a gage length of 15.24 cm (6.0 inches). In addition to measuring strain, each vibrating wire transducer carries a thermistor that provides the function of measuring temperature in addition to strain. Several thermistors were embedded at selected locations in the bridge decks in order to supplement the temperature readings that were being obtained from the vibrating wire transducers. The general layout of the bridge showing the location of the instrumented girders and the layout of the deck instrumentation are provided in Figures 3.44 and 3.45.

3.5.1 The Girder instrumentation:

The bridges included in this study carried four girder lines of AASHTO type II girders on three spans. Two girders in the end span of these structures were selected to receive

instrumentation. In each bridge the instrumented girders were located in the north end-span and are the west side edge girder and the adjacent interior girder.

The girders were instrumented at their mid-span cross sections with four vibrating wire transducers distributed through the depth of the girder. The typical locations of these transducer locations are shown in Figure 3.44. The lowest transducer was located a few inches from the bottom of the girder. The top transducer was located at the approximate centroid of the top flange element of the girder. The remaining two were located approximately at equal spacing between the top and bottom transducer. Two companion shrinkage blocks, one for each girder, 152×152×304 mm (6×6×12 inches) in size were cast, each containing a vibrating wire transducer. These permitted the tracking of shrinkage strains.

3.5.2 The Deck instrumentation:

Eight deck locations were selected to receive vibrating wire instrumentation. The general positions of these transducer locations are provided in Figure 3.43. Four of these were located at the mid-span of the north end span of the bridge. The remaining four were located over the bent centerline. Of the four locations at mid-span, two are located directly above the set of transducers in the girders. The other two are located midway between the girder lines perpendicular to the longitudinal axis of the girders. At the bent, the two locations are positioned over the gap between the girders and thus directly above the stacked set in the bent; the remaining two are located midway between the girder lines.

The instrumentation in a deck location consists of two vibrating wire transducers one positioned in the plane of the top mat of steel and the lower transducer in the plane of the bottom mat of steel. A thermistor located midway between the two vibrating wire transducers completes this instrumentation. See Figure 3.45 for the general details showing typical transducer layouts at the deck locations. To permit the tracking of shrinkage strains in the deck concrete, two shrinkage blocks were fabricated. Each block contained a vibrating wire transducer.

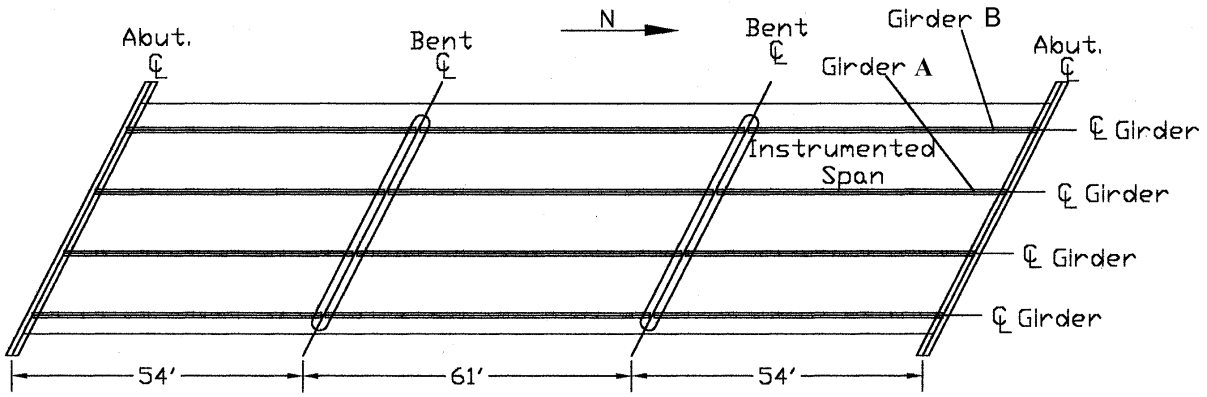

Figure 3.42 Plan view of the bridge indicating instrumented girder locations.

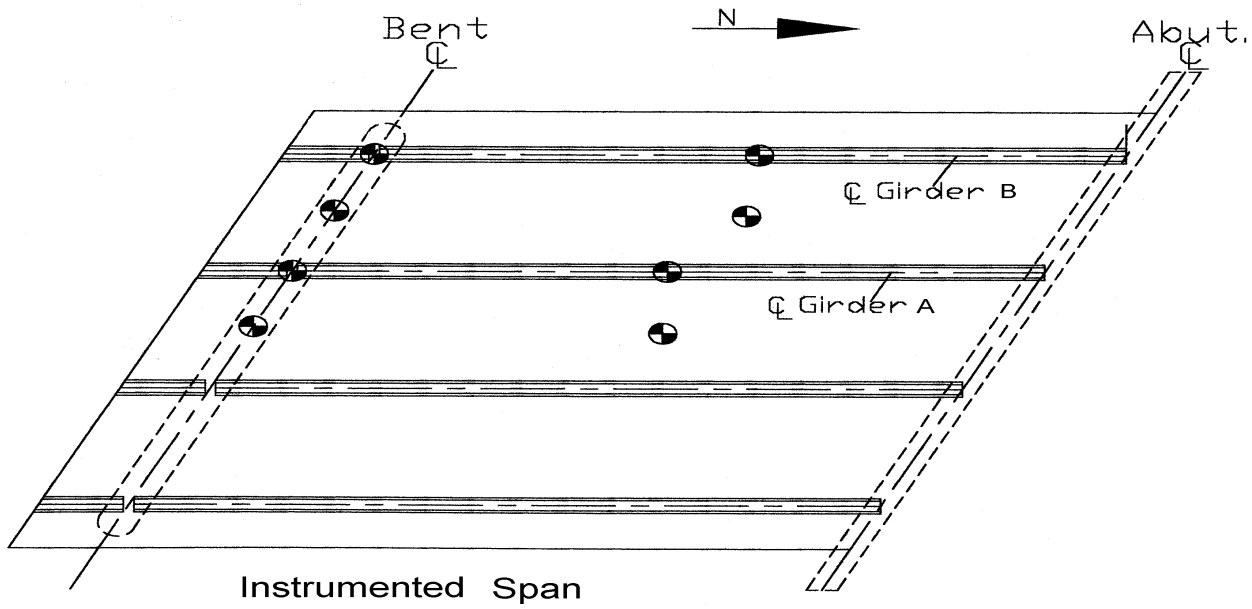

Figure 3.43 Plan view of the north end-span indicating the deck instrumentation locations.

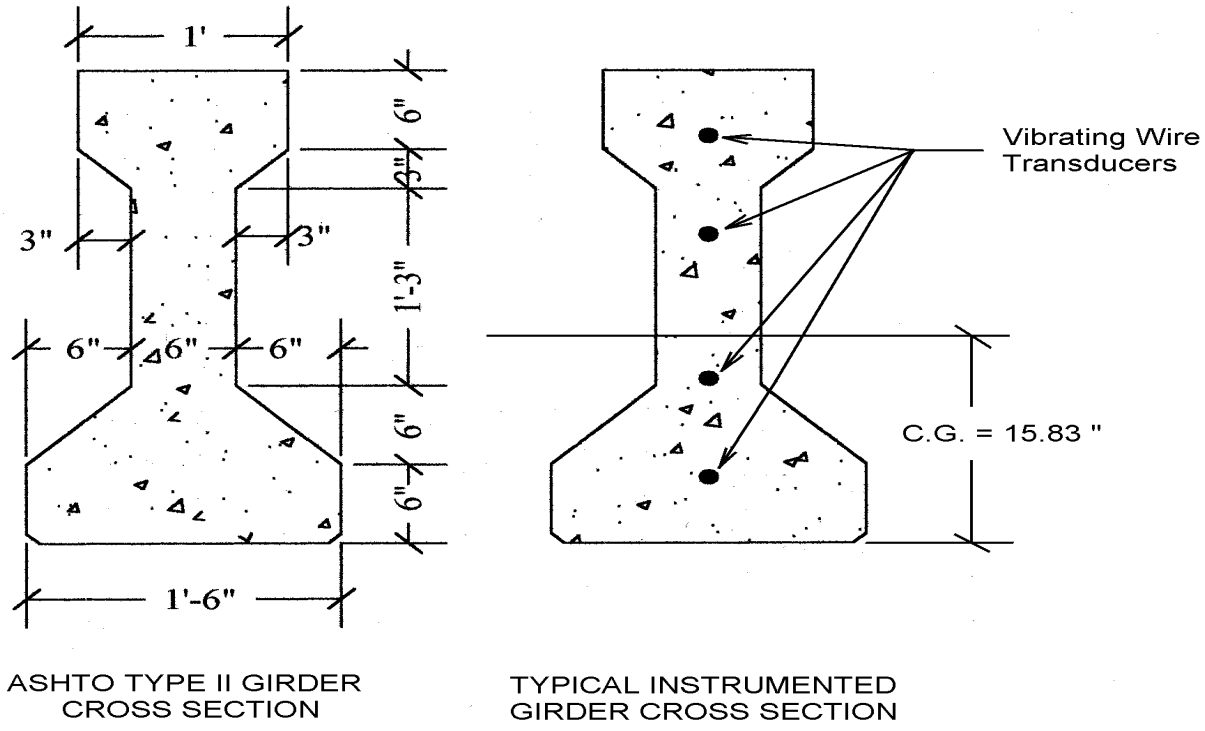

Figure 3.44 Girder cross section indicating the typical transducer locations.

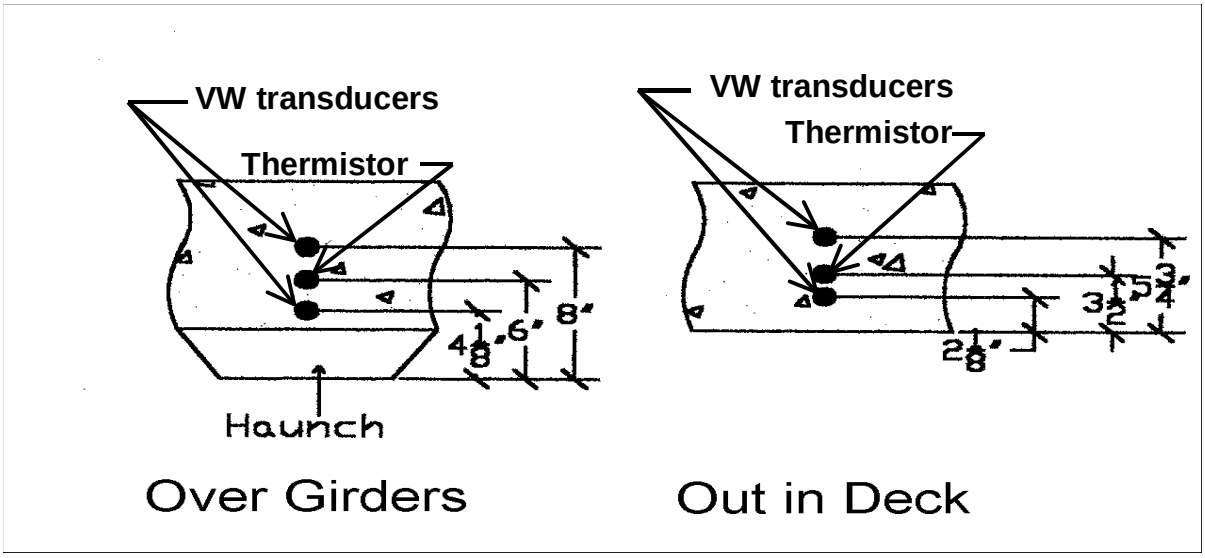

Figure 3.45 Typical sections in the deck illustrating the instrumentation details.

3.5.3 The bent instrumentation:

A stacked set of three transducers was placed in the gap between the west exterior girders at bent number one. A second stacked set of three transducers was placed in the corresponding location at the adjacent interior girder line of the same bent. In each stack, the lowest transducer was located near the bottom of the girder, the top transducer was located near the top of the girder and the middle transducer was located about midway between the top and bottom transducers.

3.5.4 The Deflection measurements:

In order to track the camber and deflection of the instrumented girders, reference points for monitoring deflection were established on each of the instrumented girders. In the girders for bridge 1 five full depth rods were placed in the girder forms and cast into the girder. The end rods were placed at the support points of the girder. The remaining three rods were located one at mid-span and other two at the quarter points of the span. The lengths of these rods were recorded so that deflection measurements could be transferred to the underside of the girders. A three wire leveling technique was used to obtain relative elevations of these reference points. Initial readings were taken on these rods prior to casting the beams. Readings were taken immediately after prestress transfer both on the bed and after the girders were removed from the bed. Thereafter, readings were taken at close but increasing time intervals until, at the current time, readings are being taken monthly.

After the deck was cast the elevations were taken from the underside of the girders. At that time the reference points at the support point of the beams were no longer available. (The ends of the girders had been cast in the abutment and in the bent and thus were integral parts of these components.) Prior to the deck being cast a permanent reference point was established on the abutment. Essentially this established the dimension between the reference point and the support points of the girder.

With one modification, the same procedure was followed for the second set of instrumented girders for the second bridge. The change that was made was instead of five rods being cast into these girders seven rods were used. The additional two rods were positioned just interior to the rods that were located at the beam seat locations. These rods were positioned so that their lower ends would just clear the face of the abutment or bent when the girders were set

in place on the bridge. This made the lower ends of these rods available for under-side elevation readings.

3.5.5 The Impedance measurements:

Devices were fabricated that permitted the measurement of impedance of the concrete in the deck. These devices were patterned after a device that the SDDOT had developed and used in a previous bridge structure. Each impedance device consisted of two stainless steel parallel plates spaced 50.4 mm (2.0 inches) apart. Wires that permitted the energizing of the circuit were attached to each plate. The plates are 25 mm (1.0 in.) wide by 50 mm (2.0 in.) long. The spacing between the plates was maintained by using two blocks of polyethylene attached to two pieces of acrylic plastic. The stainless steel plates were in turn attached to the acrylic plastic plates.

A total of six devices were embedded in the deck of each bridge. Of the six devices, three were located in the east half and three were located in the west half of the north span of each bridge. Device one and two were stacked vertically with the number one device being located in the plane of the bottom mat of steel and device number two being located in the plane of the top mat of steel. The third device was located in the plane of the top mat of steel but several feet from the other two devices. This same pattern was used to locate the other three devices, i.e. two devices were stacked vertically and the third device was located several feet from the first device.

3.6 Task 6: Attend preconstruction meeting(s) to ensure the HPC mixes, sampling and testing instrumentation, curing methods, and monitoring are understood by all.

Both Investigators and graduate students from SDSM&T and SDSU attended the prestressed girder trial mixes and bridge deck trial mix in which SDDOT engineers, the concrete supplier and the prestressed girder supplier participated. The first girder trial mix was done on April 28, 1999 and the second trial mix was done on May 4, 1999. Additional trial mixes were performed until the appropriate mix was selected to the satisfaction of all concerned. This final trial mix had the required fresh and hardened concrete properties and there were very minor variations from the original recommended mix. In the trial mixes and the actual mix used for the twelve bridge girders a silica fume slurry was used instead of the condensed silica fume powder used in the laboratory trial mixes.

The research team from SDSMT reached the site at 9:00 AM and met the engineers from SDDOT, W.R.Grace, Concrete Materials, Gage Brothers and the research team of the South Dakota State University (SDSU), at the concrete materials plant. The storage tanks containing the silica fume slurry were inspected. The silica fume slurry was being stirred for 15 minutes per hour in the tank. The mix proportion was agreed upon and 5 cu.yd. of concrete was mixed in the mixing plant of Concrete Materials and then transported to Gage Brothers by transit mixer.

The concrete was tested by the Gage Brothers personnel. The air-content was found to be 12% and the slump was found to be 140 mm (5.5 inches). To increase the slump to 178 mm (7 inches), 140 ounces of high range waster reducer was added into the truck, thoroughly mixed for 2 minutes. A sample of concrete was taken again and tested for air content and was found to be 12%. Therefore the mix was rejected.

The second mix reached the Gage Brothers plant at 11:20 AM and was tested for air-content and slump. The slump was found to be 121 mm (4.75 inches) and the air-content was 7%. To increase the slump, 140 ounces of extra high range water reducer was added into the truck and was thoroughly mixed for 2 minutes. A sample of concrete was taken again and tested for slump and air content. The slump was found to be 178 mm (7 inches) and air-content was found to be 6.5%. The sampling of the concrete was done by research teams from SDSM&T, SDSU, Gage Brothers and SDDOT. The slump and air-content were tested by the SDSU research team and was found to be 178 mm (7 inches) and 6.5% respectively. The SDSM&T research team casted 16 cylinders to be tested for compressive strength and chloride permeability. Two girders were cast. The concrete was vibrated using a spud vibrator and covered with wet burlap. The girders were covered with burlap and moisture was supplied through soaker hoses to maintain 100% humidity. The humidity-temperature sensors were placed under the burlap next to the concrete to monitor the humidity conditions continuously.

During the trial mixing, the same field quality control testing, as it would be done for the final girder manufacturing, and bridge placement, was done. The sampling, testing, curing methods, instrumentation and monitoring were discussed and all concerned agreed on these procedures to be followed. The bridge deck trial mix was done on July 9, 1999.

Dr. Ramakrishnan attended the pre-pour construction check for the second bridge deck on Wednesday July 19, 2000. The SDDOT engineers were checking the reinforcement details, the potential depths of deck slab when finished, and the potential crown in the deck slab. It was

found that they had to get different chairs. The mix proportions were changed for this deck. Silica fume was omitted and flyash was added as a replacement for cement. The actual mix proportions to be used were discussed and finalized. The mix design used for this deck is given below:

Mix Proportions	**for 1 Cubic Meter**	**for 1 Cubic Yard**
Cement (Lehigh Type II)	349.87 kg	590 lbs.
Fly ash (CoalCreek, ND)	74.53 kg	124 lbs.
Water	151.22 kg	255 lbs.
Fine aggregate (sand)	724.65 kg	1222 lbs.
Coarse aggregate (rock)	968.96 kg	1634 lbs.
Percent air	6.5	6.5
Water reducer (WR-91)	8510 milliliters	220 oz
Water/C+FA ratio	0.357	0.357

3.7 Task 7: Purchase and install the approved bridge deck and prestressed girder instrumentation for the trial as well as actual HPC Placements.

The two instrumented girders for bridge 1 were fabricated on June 3, 1999. The instrumentation for these girders was installed over a couple of days preceding the fabrication of the girders. The deck for bridge 1 was placed on August 16, 1999. The instrumentation for the deck was installed over a three-day period from August 10 through August 13.

The instrumented girders for bridge 2 were cast on May 18, 2000. The instrumentation for these two girders was installed starting a couple of days ahead of the actual fabrication. The deck for this second bridge was cast on July 20, 2000. The instrumentation for the deck was installed over a period of several days just preceding the placement of the deck on July 20, 1999.

3.8 Task 8: Attend the contruction of a trial slab on grade utilizing the recommended HPC mix for the bridge decks. Conduct the sampling and testing for the trial placement as approved in Tasks 4 and 5 above. As a result of the trial, recommend necessary HPC mix design alterations.

The construction of the trial slab on grade utilizing the recommended HPC mix for the bridge decks was carried out on July 9, 1999. Both Dr. Ramakrishnan and Dr. Sigl were present during the trial slab construction. The objective was to test the performance of the mix and to

observe the effectiveness of the proposed fogging and finishing equipment. A short section of the trial slab concrete was placed on the existing interstate pavement approximately one-half mile south of the bridge construction site. It was determined that the plastic properties of the mix were satisfactory. The finishing equipment was determined to be satisfactory but the fogging equipment was not quite performing as expected. Modifications were suggested and it was expected that with modifications the fogging equipment would perform satisfactorily. The SDSU research sampled and tested the plastic concrete as approved in Tasks 4 and 5. Based on the satisfactory performance of the mix during the trial placement, the final mix design was approved. No changes or alterations were recommended for the mix.

Dr. Ramakrishnan visited the slab site and inspected the trial slab on July 22, 1999. There were no plastic shrinkage cracks. There was a longitudinal crack over the entire length of the slab. This crack was about 7 mm wide. It was immediately above the centerline joint in the slab below. This looked like a reflection crack, which was due to the thermal stress and might have been due to the drying shrinkage.

3.9 Task 9: Attend the construction of the HPC bridge decks and prestressed girders. Conduct sampling and testing as approved in Tasks 4 and 5 above. In addition, record weather conditions, evaporation rates (on the decks) and observe and record construction methods.

The girders for bridge 1 were fabricated two at a time with the first set fabricated on April 28, 1999 and the last set on June 14, 1999. Concrete placement was by crane and concrete bucket. A photo of this activity is provided in Figure 3.46. The concrete was sampled and tested as approved in Tasks 4 and 5. The details of the cylinders cast and tested are provided in Table 3.1. The deck placement for bridge 1 was conducted on August 16, 1999. The weather was about as good as could be expected during the placement. The high temperatures for the day were in the middle 80' s. There was little or no wind during the time that the deck was placed. Several measurements were made of relative humidity with the average value during placement being around 60 percent.

The placement began about 5:00 p.m. at the north end of the bridge (This is the end of the bridge that carried instrumentation.). A picture of the deck placement activity as it approached

Figure 3.46 Casting one of the girders for bridge 1.

the instrumentation section of the deck is give in Figure 3.47. The work was finished between 8:00 and 9:00 p.m. (An exact time was not recorded.).

A conveyor system was used to place the deck concrete. The fogging system was used. The work proceeded smoothly and without incident. One note should be made. As the work approached completion near the south end of the bridge, it was determined that the slump was too high, this raised concern about maintaining the pavement crown. Because of this concern, a couple of loads of concrete were rejected. Cylinders were prepared from the deck concrete as detailed in Table 3.1.

Curing consisted of wet burlap topped with a plastic cover to prevent evaporation of water from the deck. Some of the burlap that was placed on the deck was not fully saturated prior to being placed on the deck. A soaker hose was used under the burlap in order to keep the deck continuously wet.

Figure 3.47 Deck placement on bridge 1.

Further comment needs to be made concerning the fogging equipment. The fogging nozzles were too high above the deck to be completely effective. If the nozzles had been 1 to 1.5 feet lower they would have been more effective. There was a delay in getting the fogging machine operational. All in all, it is hard to say how effective or ineffective the fogging operation was.

It should be noted that considerable effort was expended on the development of the fogging equipment, not only by the contractors personnel, but also by the personnel of the SDDOT. The equipment just did not work exactly as expected.

The girders for bridge two were fabricated over the period between April 28, 2000, and the end of May 2000. The SDSU research personnel attended half of the girder fabrications for the second bridge. The dates of the fabrications attended and the number of cylinders taken are listed in Table 3.1.

The deck for bridge 2 was placed on July 20, 2000. The weather for this placement was very good. The high temperatures for the day were in the high 70' s. The wind was blowing but it was no more than a breeze. The relative humidity was not recorded.

The concrete for this deck was placed by concrete pump. The work began at 10:45 a.m. with the arrival of the first truck. The work proceeded from the south end of the bridge to the north end (The transducers are located in the north span.). It progressed slowly at times, but the minimum rate of deck placement was met. No significant problems developed during the deck placement. The last concrete was placed at 3:50 p.m.

The curing conditions were the same as used in the first bridge. Concrete cylinders were cast as detailed in Table 3.1.

3.10 Task 10: Review and evaluate two curing methods on the two bridges in I-29. One deck will use SDDOT' s standard method of curing and the second will utilize a soaked 1" cotton blanket backed with polyurethane in lieu of the burlap. Based on the findings from the curing methods, recommend a curing method to be used which is believed to give the best product.

A supplier could not be located for the polyurethane cotton blanket which was planned as an alternative curing method. For this reason the SDDOT' s standard method of curing was used for both bridge decks. This standard curing method utilizes wet burlap covered with plastic. Soaker hoses are used under the burlap to supply water to the burlap and keep it moist.

3.11 Task 11: Conduct performance tests of hardened concrete on the collected field samples for the bridge deck and the prestressed girders as approved in Task 4.

In total for the two bridges, 796 cylinders were cast. Four hundred seventy-nine were cast for the first bridge, while 317 cylinders were cast for the second bridge. The different number between the two years is primarily due to the fact that two trial mixes and a trial deck placement were completed the first year, but these tasks were not part of the work the second year. Samples were taken from each girder fabrication the first year, but in the second year samples were taken from only half of the girder fabrications. Of the total cylinders (796), about 92 cylinders were assigned to the rapid chloride test. In total, 701 cylinders were tested in compression. To document the modulus of elasticity, 102 tests were performed, 49 the first year and 53 the second year.

3.11.1 The Rapid Chloride Permeability Test

The rapid chloride permeability test was done at the SDSM&T Civil Engineering Laboratory on all the samples supplied by SDSU and the results are given in Table 3.2. The test was conducted as per ASTM C 1202. A total of 60 specimens from the construction of first bridge in 1999 were tested.

Table 3.2: Individual 90- day Permeabilities of the Specimens Obtained from SDSU

Source	Specimen #	Total Charge Passed (Coulombs)	Remarks
Trial Mix 1	TM 1-38	146	One Truck
	TM 1-39	178	
	TM 1-40	160	
	Average	161	
Trial Mix 2	TM 2-21	109	One Truck
	TM 2-22	105	
	TM 2-23	112	
	TM 2-39	100	
	TM 2-40	117	
	Average	109	
Girder Fabrication 1	G 1-19	43	First Truck
	G1-20	41	
	G1-39	41	Second Truck
	G1-40	42	
	Average	42	
Girder Fabrication 2	G2-21	66	First Truck
	G2-38	76	Second Truck
	G2-39	74	
	G2-40	82	
	Average	75	
Girder Fabrication 3	G3-49	72	First Truck
	G3-50	68	
	G3-99	64	Second Truck
	G3-100	70	
	Average	69	
Girder Fabrication 4	G4-10	57	First Truck
	G4-11	57	
	G4-21	74	Second Truck
	G4-22	56	
	Average	61	
Girder Fabrication 5	G5-10	108	First Truck
	G5-12	64	
	G5-21	71	Second Truck
	G5-22	79	
	Average	81	

Source	Specimen #	Total Charge Passed (Coulombs)	Remarks
Girder Fabrication 6	G6-10	58	First Truck
	G6-11	51	
	G6-21	71	Second Truck
	G6-22	65	
	Average	61	
Deck Trial Placement	DT-16	543	One Truck
	DT-17	553	
	DT-18	629	
	DT-19	508	
	Average	558	
Deck Placement	D1-22	281	Sample # 31
	D1-25	323	
	D1-23	323	Sample # 33
	D1-24	342	
	Average	317	
Deck Placement	D2-22	359	Sample # 34
	D2-23	414	
	D2-24	535	
	D2-25	534	
	Average	461	
Deck Placement	D4-22	625	Sample # 35
	D4-23	654	
	D4-24	581	
	D4-25	622	
	Average	621	
Deck Placement	D5-22	300	Sample # 35
	D5-23	484	
	D5-24	432	
	D5-25	355	
	Average	393	
Deck Placement	D3-22	439	Extra
	D3-23	582	
	D3-24	482	
	D3-25	560	
	Average	516	

The girders for the second bridge were fabricated on April 28, May 9, and May 18, 2000. The bridge deck was constructed on July 20, 2000. Specimens made from the actual concretes used in the six-girder fabrication and the bridge deck, a total 32 specimens were tested and the results are given in Table 3.3

3.12 Task 12: Periodically collect the data from the instrumentation and conduct visual condition surveys of the constructed HPC bridge girders and decks as approved in Task 5.

The instrumented girders for bridge 1 have been continuously monitored except for two interruptions since they were cast on June 3, 1999. The first interruption occurred while they were transported from the prestressing yard and set in place at the bridge site. The second interruption occurred when the data-logging computer failed in September of 1999. The instrumented girders from the second bridge experienced only one interruption, that interruption coinciding with the time that the girders were transported and erected into location at the bridge site.

The interval at which the sensors have been read has varied. Generally, a close interval of 5 to 10 minutes was used during periods when detail was desired, and a longer time interval between readings, when long-term information was desired. The time interval for obtaining long-term information was selected as 30 minutes.

The interval between the times that the data was downloaded from the computer has also varied. Early in the life of the girders, the data was downloaded every few days. This coincided with retrieving companion cylinders or taking deflection readings on the girders. As the girders aged, the interval between the down loading of data was increased. Once the bridges were complete, the data was downloaded once a month. At these monthly visits, in addition to downloading data, deflection and impedance readings were recorded.

The fundamental control in the logging of the data is the clock in the data logger. At the selected increment of time the computer polls the transducer array and records the data. At the conclusion of the polling of the transducers, the computer records the clock time at which the data was taken. This clock time corresponds to the total days since the computer clock was set and the hour minute and second into the current, 24-hour period. The records contain temperatures in Celsius degrees and the square of the natural frequencies of the wires in the vibrating wire transducers. This is the data that is downloaded from the computer.

TABLE 3.3: 90-day Rapid Chloride Permeability Test Results as per ASTM C1202 (Second Bridge)

Source	Date Cast	Comment	Sp.no	Permeability	Remarks
Girder Fabrication 2	April 28,2000	First Truck	Y2-G2-22	100	Very Low
Girder Fabrication 2	April 28,2000	First Truck	Y2-G2-23	110	Very Low
			AVG	105	Very Low
Girder Fabrication 2	April 28,2000	Second Truck	Y2-G2-45	80	Negligible
Girder Fabrication 2	April 28,2000	Second Truck	Y2-G2-46	95	Negligible
			AVG	88	Negligible
Girder Fabrication 3	May 9,2000	First Truck	Y2-G3-22	71	Negligible
Girder Fabrication 3	May 9,2000	First Truck	Y2-G3-23	68	Negligible
			AVG	70	Negligible
Girder Fabrication 3	May 9,2000	Second Truck	Y2-G3-45	93	Negligible
Girder Fabrication 3	May 9,2000	Second Truck	Y2-G3-46	76	Negligible
			AVG	85	Negligible
Girder Fabrication 5	May 18,2000	First Truck,Moist Cure	G5A-25	86	Negligible
Girder Fabrication 5	May 18,2000	First Truck, Companion Cure	G5A-50	93	Negligible
			AVG	90	Negligible
Girder Fabrication 5	May 18,2000	Second Truck	G5B-25	90	Negligible
Girder Fabrication 5	May 18,2000	Second Truck	G5B-50	87	Negligible
			AVG	89	Negligible
Deck Placement	July 20,2000	Center of South Span	D1-22	844	Very Low
Deck Placement	July 20,2000	Center of South Span	D1-23	654	Very Low
Deck Placement	July 20,2000	Center of South Span	D1-24	827	Very Low
Deck Placement	July 20,2000	Center of South Span	D1-25	804	Very Low
			AVG	782	Very Low

Source	Date Cast	Comment	Sp.no	Permeability	Remarks
Deck Placement	July 20,2000	South Bent	D2-22	676	Very Low
Deck Placement	July 20,2000	South Bent	D2-23	620	Very Low
Deck Placement	July 20,2000	South Bent	D2-24	941	Very Low
Deck Placement	July 20,2000	South Bent	D2-25	593	Very Low
			AVG	708	Very Low
Deck Placement	July 20,2000	Center of Middle Span	D3-22	1548	Low
Deck Placement	July 20,2000	Center of Middle Span	D3-23	1396	Low
Deck Placement	July 20,2000	Center of Middle Span	D3-24	1279	Low
Deck Placement	July 20,2000	Center of Middle Span	D3-25	1394	Low
			AVG	1404	Low
Deck Placement	July 20,2000	North Bent	D4-22	1219	Low
Deck Placement	July 20,2000	North Bent	D4-23	1157	Low
Deck Placement	July 20,2000	North Bent	D4-24	1417	Low
Deck Placement	July 20,2000	North Bent	D4-25	1436	Low
			AVG	1307	Low
Deck Placement	July 20,2000	Center of North Span	D5-22	877	Very Low
Deck Placement	July 20,2000	Center of North Span	D5-23	944	Very Low
Deck Placement	July 20,2000	Center of North Span	D5-24	1052	Low
Deck Placement	July 20,2000	Center of North Span	D5-25	1079	Low
			AVG	988	Very Low

After the raw data was downloaded, it was processed through two programs to produce a standard record containing a calendar date, a clock time, strains, and temperatures. To this standard record, in addition to these elements, is added a time variables that records the age, in days, of the girders and the deck. These records produce a time series that was subjected to several cycles of analysis.

In order to provide a general idea of the amount of data being gathered and catalogued, consider the following. In a complete bridge there are 32 vibrating wire transducers and 10 temperature sensors. Each vibrating wire transducer yields temperature and the natural frequency of the wire in the transducer. In total 74 pieces of information are recorded at each time interval. In addition, it takes five pieces of information to provide calendar information and the clock time for the record. It requires two variables to log the age of the girders and the deck. In total 81 pieces of information are logged in each record with a record being logged every 30 minutes. The total amount of data catalogued per bridge per year is obtained by multiplying 81 pieces of information per record, times 48 records per day, times 365 days per year which results in more than 1,400,000 pieces of information. Actually, this is the minimum since there were times for both the girders and the deck when closer spaced readings were taken. Though this may not be considered to be a huge amount of data, it is significant.

To date the transducers have performed very well. In bridge one we have lost the temperature sensor on one vibrating wire transducer. In bridge two one vibrating wire strain transducer has quit working. The temperature sensor associated with this transducer is still functioning. As this indicates, the transducer arrays are performing very well.

On July 20, 2000, just prior to the deck placement for bridge 2, Dr. Ramakrishnan and project monitor Mr. Dan Strand conducted a visual inspection of the deck for bridge 1. Both the underside and the top of the bridge deck were inspected. A few photographs were taken.

There were a considerable number of cracks on bottom side of the slab. These cracks were transverse cracks extending nearly the entire width of the slab. The crack spacing was approximately 3 to 5 m (10 to 15 ft) apart in the end spans. In the middle span the crack spacings were much closer. In nearly every corner created by the girder meeting the abutment diagonal cracks extended from the girder to the abutment. In some cases multiple cracks of this type existed. These cracks were restrained shrinkage cracks.

On the top of the deck, there were a few thin transverse cracks. These were not clearly visible. There were a number of cracks on the Jersey Barrier. These cracks are considered to be restrained shrinkage cracks. Some cracks observed on the barrier had extended to the edge of the deck slab. These were thinner cracks.

Visual condition surveys of the decks were completed on both bridges shortly before they were opened to traffic. These surveys noted a good number of fine cracks extending transverse to the longitudinal axes of the bridges. They were more easily observed close to the Jersey Barrier but because of the tining, difficult to trace into the interior of the deck.

Significant cracks were noted on the underside of bridge 1 in January of 2000. These cracks were observed to be weeping moisture indicating that water was seeping out of the concrete. In January of 2001, a similar condition, though with fewer total cracks, was noted on bridge 2. Due to the heavy traffic on these bridges, no top-side inspection has been carried out on these bridges since the two surveys that were conducted just before the bridges were opened to traffic (except as noted above). A visual survey of the under side of both bridges was conducted in August of 2001. These results will be discussed later in this report.

3.13 Task 13: Based on the data collected from the instrumentation as well as the condition surveys, evaluate the performance of the HPC bridge girders and decks.

3.13.1 The Girders:

The reader is referred to chapter 4 for the complete results and conclusions, but selected summary information will be presented here. In order to evaluate the girders one must look at several parameters.

The first is compressive strength. For a prestressed application high strength is of primary interest. The instrumented girders exhibited a 28-day compressive strength ranging from a low of 91.0 MPa (13,200 psi) to a high of 108.2 MPa (15,690 psi). If one computes the statistics on the 28-day compressive strengths, the results yield a mean of 99.3 MPa (14,400 psi) and a standard deviation of 6.83 MPa (990 psi). The ratio of the standard deviation to the mean defines the coefficient of variation which, in this case, is 6.9 percent. This indicates a well-controlled process.

It appears that these strength results can be achieved with reasonable expectation. If one assumes that acceptance tests were, as is the case in this report, made up of three cylinders averaged to produce a single result, one can arrive at the design strength as follows. Taking the

position that one expects 95 percent of the 28 day test results to be above the specified design strength, the design strength of this mix could be set at 88.3 MPa (12,800 psi), or conservatively at 82.7 MPa (12,000 psi). This assumes that the test results are normally distributed.

A second parameter is the modulus of elasticity. It is important that the modulus of elasticity be able to be predicted with reasonable accuracy during the early age of the concrete, normally within the first 28 days. It was found in this research that the modulus could be predicted with acceptable results by the ACI 363 equation if one change is made. (This equation is given earlier in this chapter as equation 3-2 under task 3.) This change is in the constant 6890 MPa (1,000,000 psi). It is recommended that this constant be replaced with 13,800 MPa (2,000,000 psi).

The girder concrete demonstrated a 28-day average modulus (all tests) result of 49,600 MPa (7.20×10^6 psi). A high modulus for the girder concrete results in increased girder stiffness, which helps control short-term as well as long-term deflections. Both the short term and long term deflection, based on the data to date, are considered acceptable.

A third parameter is the deflections exhibited by the girders. This includes the immediate deflection produced at transfer and the additional deflection that developes with time. The maximum camber reached by girder G5-A, bridge 2, was 31.8 mm (1.25 inches). The camber exhibited by its sister girder, G5-B, was 30.0 mm (1.18 inches). The two girders from bridge 1 exhibited maximum cambers of 25.4 mm and 23.6 mm (1.00 and 0.93 inches).

If one makes use of the sometimes-referenced L/360 parameter as a limit of serviceability, this calculation yields a maximum deflection of 45.7 mm (1.80 inches). The L in that expression is the span length. With the deck in place, these girders are not exhibiting any tendency to develop significant additional long-term deflections.

A fourth parameter is shrinkage. The early age shrinkage, first 100 days, was observed to be about 150 με for the girders of bridge 1, and about 200 με for the second set of girders that went into bridge 2. The standard equations that are recommended by the ACI would yield estimates of shrinkage at 100 days of about 400 με. Thus, it is observed that this is below the so-called standard concrete. It is known that silica fume increases the tendency for the concrete to shrink. The data shows that there is interaction with the environment and after the early shrinkage occurs the shrinkage does not continue to increase. It appears that there may be a long-period cycle that is affecting the later-age shrinkage. The reader is referred to Figures 4.9

through 4.12 in Chapter 4. The shrinkage exhibited by the concrete in these girders is considered to be well within design limits.

The last parameter that is important in assessing the performance of these girders is the time-dependent loss of initial prestress. The initial prestress resulted in an average compressive strain of 425 με in the two girders for bridge 1, and a value of 525 με in the girders for bridge 2. The losses, over the time that the girders were stored in the prestressing yard, were about 5.9 percent for the girders in bridge 1, and about 14.0 percent for the girders in bridge 2. Additional long-term change after the deck was placed is not noted in bridge 1. In bridge two an additional 5 percent loss occurred from the time that the deck was placed until the bridge was one year old. No additional data is available for this bridge. Adding these values results in a loss of 5.9 percent out to two year for bridge 1, and a loss of 19 percent in bridge two for the first year. These values do not include the effect of shrinkage, but do include the combined effect of creep and relaxation. Low relaxation strand was used, so the loss due to relaxation is small.

Overall, the performance of the girders is judged to be excellent.

3.13.2 The Decks

Two different types of concrete mixes were used in the decks for these two bridges. A silica fume mix was used in the deck of the first bridge and a fly ash mix was used in the deck for the second bridge. The achievement of high concrete strengths was not the major objective when selecting the mixes for these two decks. Nevertheless, fairly high compressive strengths resulted from the mixes that were employed. An average 28-day compressive strength of about 48.8 MPa (7,070 psi) was attained in the silica fume mix, and a 28-day compressive strength of 46.6 MPa (6760 psi) was attained with the fly ash mix. At 90 days, the silica fume mix had attained a compressive strength of 53.4 MPa (7750 psi) while the fly ash mix reached the same strength exhibiting a value of 53.57 MPa (7770 psi). Thus, the strengths were very comparable in these two decks.

Of major interest, is the shrinkage potential of these mixes. Two shrinkage blocks were cast from each mix. The two blocks of the same concrete essentially exhibited the same shrinkage history. If one arbitrarily defines the shrinkage that takes place in the first 100 days as the early period shrinkage, the silica fume mix exhibited a maximum strain of 240 με, while the fly ash concrete exhibited a maximum strain of 150 με. From this it is observed that the silica

fume mix exhibited 1.6 times more shrinkage in the first 100 days as the fly ash concrete. This is very significant as it reflects the relative tendency for shrinkage cracks to occur.

Deck surveys were conducted in August 2001 to assess the crack development that had occurred in these bridges. These surveys were conducted on the underside of the bridges. Summary data is presented in Table 4.12 in chapter 4. The result of this survey yielded an average crack spacing of 1.37 m (4.5 feet) in the silica fume deck and a spacing of 2.32 m (7.6 feet) in the fly ash deck. The ratio of 2.32 to 1.37 is 1.7 and is essentially the same as the ratio of the shrinkage that has been cited. This may be a coincidence, but it can be argued that the crack spacing is indicative of the shrinkage strains. Nevertheless, the crack spacing data support the shrinkage data.

A significant number of strain transducers were embedded in each of these decks (Thirty-two). Half of the transducers were embedded at the middle of the north span of these bridges. The other half were embedded at the first bent from the north end of the bridges. If one factors out the shrinkage strain and simply considers an overall average, the silica fume mix yields an average tensile strain of about 160 με at mid-span and an average tensile strain of 420 με at the bent. Parallel values for the fly ash mix are 60 με at mid-span and 250 με over the bent. The actual data from which these figures have been taken is presented in Figures 4.20 and 4.21 in Chapter 4. These numbers support the general observation that more cracking is likely to show up in the silica fume deck when compared to the fly ash deck.

Based on this data, the fly ash mix is deemed better for deck use than the silica fume mix. There is apparently no economical way to effectively control the shrinkage, and thus the tendency to produce cracks in the silica fume mix.

3.14 Task 14: Determine the cost difference for the HPC decks and girders as compared to costs for SDDOT present design.

The information about the cost of the HPC girders and bridge decks, and the normal girders and bridge decks was supplied by Mr. Hadly Eisenbeisz, Office of Bridge Design, SDDOT. In the HPC bridges constructed as part of this research 4 prestressed girders (AASHTO Type II) were used per span instead of 5 as is done for similar bridges in SDDOT. In HPC bridges the girders were spaced at 3.48 m (11 ft-5 inches) and the deck thickness was 22.9 cm (9 inches) whereas in the SDDOT present design, the girder spacing would be 2.72 m (8ft-11

inches) and the deck thickness would be 21 cm (8.25 inches). For the HPC girders, the design compressive strength was 68.3 MPa (9900 psi) with a strength of 56.9 MPa (8250 psi) required before strand release. The use of HPC allowed designers to reduce the number of girders in each span from five to four, however there was an increase in the thickness of the deck and therefore an increased quantity of HPC deck concrete. A comparison of the costs for the girders and decks for the HPC in the year 1999 and 2000, and the present SDDOT design prestressed girders and decks is given in Table 3.4

Table 3.4 Cost Comparison

	Conventional Concrete	High Performance Concrete (1999)	High Performance Concrete (2000)
Girders	$94, 778.75	$50, 459.2	$91, 660
Deck	$72, 587. 27	$81, 972	$85, 536

In the first year, the prestressed girders were purchased by SDDOT directly from the fabricator (Gage Brothers) and the second year the contractor purchased the girder from the same fabricator (Gage Brothers) and installed at almost twice the cost. The cost of the girders were less for bridge 1 because the bid items were set up to remove any risk to the contractor. The fact that the contractor had no risk possibly was the cause for the reduction in girder cost. Therefore it is difficult to compare the actual unit cost of the HPC girders with that of the standard girders. It can be fairly assumed that the unit cost of the HPC girders and the standard concrete girders would be the same in the future as the fabricator and contractor gain enough experience in the

Table 3.5 Total Cost Comparison

	1999-First Year Bid Cost	2000-Second Year Bid Cost
Conventional Concrete Bridge		
Girders	$94, 778.75	
Deck	$72, 587. 27	
Total	**$167366.0**	
HPC Bridge		
Girders	$50, 459.2	$ 91, 660
Deck	$81, 972	$ 85, 536
Total	**$132431.0**	**$177196**

use of HPC girders. The HPC for the 1999 bride deck consisted of both silica fume and fly ash, whereas the HPC for the 2000 bridge had only fly ash as partial replacement for cement. HPC for both decks gave an average compressive strength higher than 48.3 MPa (7000 psi). The required compressive strength for the deck was 31 MPa (4500 psi). If this higher compressive strength is used in design, the HPC deck thickness could be reduced. The cost of the 1999 HPC deck was $345/cu.yd and the 2000 HPC deck was $360/cu.yd even though silica fume was not included in the mix. There was a 4.3 percent increase in the unit cost between the 1999 and 2000 deck concretes, which can be considered as inflation cost. Therefore it can be stated that both HPC with and without silica fume would cost the same. The cost of normal concrete in 1999 was around $312/cu.yd. In the long run the HPC cost may come down when the concrete contractor gains enough experience in the production and use of HPC. The total cement cost in HPC is less than for the normal concrete. The total cost comparison of the HPC bridges in 1999 and 2000, with a typical SDDOT prestressed girder bridge constructed in 1999 is shown in Table 3.5

In the year 1999, the girder cost was well below the average (normal concrete) and the total bridge cost was also below average because of the reasons stated above. The cost of the girders were less for bridge 1 because the bid items were set up to remove any risk to the contractor. The fact that the contractor had no risk possibly was the cause for the reduction in girder cost. When comparing the HPC superstructure with 4 lines of girders to a more conventional bridge with 5 lines of girders, the HPC superstructure cost was about $ 5700 more. The thicker deck due to the wider girder spacing had a higher cost of around $5800 and the deck grooving added additional $ 5400. The one less girder saved about $ 12,500 but the higher priced thicker deck negated those savings. Therefore for this particular bridge, the cost of the superstructure was the same on a first cost basis for both the HPC bridge and the normal concrete SDDOT present design bridge. However the life cycle cost might be cheaper for the HPC bridge because of the anticipated longer life and reduced maintenance cost.

3.15 Task 15: Recommend mix design, testing, and construction guidelines for using HPC in prestressed girder and bridge deck applications base on results observed from this study.

3.15.1 Recommended Mix Design

Based on extensive testing of trial mixes and analysis of the results as given in Task 3, the following mixture proportions were recommended for the high strength HPC for prestressed girders and HPC mix for the bridge deck using silica fume.

3.15.1.1 Recommended Mixture Proportions for Bridge Deck Concrete: (for Quartzite Aggregates)

Cement Type 1/11	303 kg/m^3 (511 lb/cu.yd.)	0.073 m^3 (2.58 cu.ft.)
Fine Aggregate	652 kg/m^3 (1100 lb/cu.yd.)	0.190 m^3 (6.70 cu.ft.)
Coarse Aggregate	1023 kg/m^3 (1725 lb/cu.yd.)	0.297 m^3 (10.51cu.ft.)
Water	157 kg/m^3 (264 lb/cu.yd.)	0.120 m^3 (4.23 cu.ft.)
Fly Ash	70 kg/m^3 (118 lb/cu.yd.)	0.022 m^3 (0.76 cu.ft.)
Silica Fume	33 kg/m^3 (55 lb/cu.yd.)	0.012 m^3 (0.42 cu.ft.)
Air	6.5% $\pm$ 1.0%	0.050 m^3 (1.76 cu. ft.)
		0.764 m^3 (26.96 cu.ft.)

Note:
A mid range water reducer (Polyheed-997 Master Builders) was used at 8 oz/cwt of cement. The Air-entraining agent MB-VR Standard (Master Builders) shall be used. An appropriate amount of air-entraining agent should be used to obtain an air content of 6.5 + 1%.
The recommended slump is 127 to 178 mm (5 to 7 inches). An appropriate amount of approved superplasticizer (High Range water reducer) can be used if needed to obtain the specified slump.
The following properties were obtained from the trial mixes done at the SDSM&T Laboratory:

Plastic Properties:

Slump:	190 mm (7.5 in.)
Air Content:	5.40%
Unit Weight:	2258.85 kg/m^3 (141.2 Ib/ft^3)

Hardened Properties:

	14-day	**28-day**
Compressive Strength:	35.41 Mpa (5135 psi)	42 Mpa (6140 psi)
Static Modulus:	2.92x10^4 Mpa (4.24x10^6 psi)	3.24x10^4 Mpa (4. 7x10^6 psi)
Modulus of Rupture:	4.55 Mpa (660 psi)	5.5 Mpa (800 psi)
Chloride Permeability: (at 90 days)	1207 Coulombs (Category: Low)	

3.15.1.2 Recommended Mixture Proportions for High Strength Concrete for Prestressed Girders:

Cement Type I/II	374 kg/ m^3 (630 lb/cu.yd.)	0.089 m^3 (3.18 cu.ft.)
Fine Aggregate	712 kg/ m^3 (1200 lb/cu.yd.)	0.204 m^3 (7.31 cu.ft.)

Coarse Aggregate	1082 kg/ m^3 (1825 lb/cu.yd.)	0.311 m^3 (11.12 cu.ft.)
Water	112 kg/ m^3 (189 lb/cu.yd.)	0.085 m^3 (3.03 cu.ft.)
Silica Fume	42 kg/ m^3 (70 lb/cu.yd.)	0.015 m^3 (0.53 cu.ft.)
Air	4.0% $\pm$ 1.5%	0.050 m^3 (1.76 cu.ft.)
		0.754 m^3 (26.93 cu.ft.)

Note:
A High Range Water Reducer (RHEOBUILD 1000 Master Builders) was used at 26.7 oz/cwt of cementitious material (1739 ml/100 kg). The Air-entraining agent MB-VR Standard (Master Builders) shall be used. Appropriate amount of air-entraining agent should be used to obtain an air content of 6.5 ± 1.5 %.
The recommended slump is 127 to 178 mm (5 to 7 inches). An appropriate amount of approved superplasticizer (High Range water reducer) should be used to obtain the specified slump.
The following properties were obtained from the trial mixes done at the SDSM&T Laboratory:

Plastic Properties:

Slump:	146 mm (5.75 in.)
Air Content:	6.20%
Unit Weight:	2300.04 kg/m^3 (143.6 lb/ft^3)

Hardened Properties:

	7 -day	**28-day**
Compressive Strength:	85 Mpa (12280 psi)	97 Mpa (14065 psi)
Static Modulus:	4.28x10^4 Mpa	4.97x10^4 Mpa
	(6.2x10^6 psi)	(7 .2x10^6 psi)
Chloride Permeability:	158 Coulombs (Category:Very Low)	
(at 2 days after accelerated curing)		

Note:
1. Required fc' = 68.95 MPa (10,000 psi)
According to ACI 214, the target strength for the mixture should be fc' x1.2=82.74 MPa (12,000 psi). We used 101.6x203.2 mm (4"x8") cylinders for the compression tests. We can assume that the compressive strength indicated by the smaller cylinders 101.6x203.2 mm (4"x8") will be slightly higher than that indicated by standard cylinders 152.4x304.8 mm (6"xI2"). This may be approximately about 8 to 10%. Therefore the target strength should be slightly higher than 82.74 MPa (12,000 psi).
2. The trial mix for which the properties are given below contained 49.8 kg/m^3 (84 lbs./cu.yd of silica fume, which is 12% replacement of cement by weight. The suggested mixture proportions which has 10% replacement of cement by weight will have very similar properties as the trial mix H8F0S10W0.30. We have used Rheobuild 1000 as the superplasticizer but any equivalent, approved superplasticizer can be used.

The silica fume used should satisfy ASTM C1240, which covers both densified silica fume and liquid form. Class F fly ash was recommended. The same aggregates (both fine and coarse) currently used in the SDDOT projects in the Sioux Falls area, without any change in the aggregate gradation could be used. The recommended slump of 127 to 177.8 mm (5 to 7 inches) was based on the experience of other states (particularly Virginia). They did not have any problems when the finishing machine was used. Because of the inclusion of silica fume and fly ash, no segregation was anticipated. The reason for recommending high slump was to ensure proper distribution of silica fume and good consolidation. With this slump, the rate of

development of heat of hydration would be reduced and the potential for microcracking in the concrete would be reduced, which would be essential for reduced permeability. No change in the setting time compared the standard concrete in the summer time was anticipated based on the laboratory trial mixes and in discussions with others who have used similar mixes. Of course, the set properties might vary, within reasonable limits, with a change in the ambient temperature and humidity conditions. No special finishing requirements were recommended. It was strongly recommend that, whenever silica fume was used, a proper 100% humid curing 5 to 7 days was essential. This could be achieved with continuous water sprays or misting and/or fogging devices.

In the laboratory trial mixes dry densified silica fume was used. However, the concrete supplier on the project had requested to use the slurry form of silica fume in the HPC mixes, eventhough the specifications for this project did not allow slurry. After considerable discussions and research, the concrete supplier was allowed to use the slurry form of silica fume. However certain conditions were specified, such as sampling of the slurry before and during addition of the slurry to the mix. Because the silica fume is suspended in water (not dissolved), there is an inevitable tendency for the silicafume to settle to the bottom. To avoid this, a continuous agitation of the liquid with proper instruments was recommended. The standard vibration used for plain concrete was suggested because from our experience and experience of others (Virginia, Texas and other states) the entrapped air in silica fume concrete was not a problem. Therefore excessive vibration was not necessary and the standard air test was recommended to measure the air content in fresh concrete.

Trial mixes were done at the Concrete Materials Plant (concrete supplier) and transported to the prestressing plant (Gage Brothers). The slump, air, and unit weight tests were conducted. The compressive strength tests indicated the specified early strength (prestress release strength) was not obtained eventhough the 28 day design strength was satisfactory. This might have been due to the addition of silica fume in the slurry form instead of the condensed silica fume powder used in the laboratory trial mixes. Therefore, to obtain the required early strength, the cement quantity was increased by 29.65 kg/m^3 (50lbs.cu.yd) with the approval of SDDOT engineers and the admixture water was considered. However the water to cement ratio was kept the same at 0.28. Two mixes of 4.59 m^3 (6 cubic yards) of concrete were mixed at the concrete materials plant and transported to the casting yard (Gage Brothers) by transit mixer. 652 milliliters of

superplasticizer per 100 kgs (10 ounces per 100 lbs.) of cement was added during the mixing at Concrete Materials and a slump of 101.6 mm (4 inch) was obtained. Another 652 milliliters of superplasticizer per 100 kgs (10 ounces per 100 lbs.) of cement was added at the prestressing yard and a slump of 215.9 mm (8.5 inches) was obtained. The air was found to be 4.1 percent. Inspection of the fresh concrete had shown that the materials had mixed well with no segregation. The compressive strength tests indicated that the specified early strengths were obtained. Because of the satisfactory performance of this mix both at the fresh and hardened states this mix was recommended for all further girder fabrication. However the air content specification was changed to 4±1% because the HPC concrete for the girders will be more dense and less permeable than normal girder concretes, less entrained air can be tolerated without affecting the durability of the concrete girders. The reduced air content also helped to increase the strength slightly. The following was the final mix design recommended for high strength HPC mix for prestressed girders.

Mix Proportions	**for 1 Cubic Meter**	**for 1 Cubic Yard**
Cement (Type II)	403.24 kg	680 lbs.
Water included from silica fume slurry and HRWR	112.67 kg	190 lbs.
Coarse aggregate (3/4" quartzite)	1082.23 kg	1825 lbs.
Fine aggregate (S.S.D)	683.16 kg	1200 lbs.
Silica fume	49.81 kg	84 lbs.
Air Content	4.0±1.0%	4.0±1.0%
Water to Cement ratio	0.28	0.28
Water/C+S.F. ratio	0.25	0.25

Note: The recommended slump was 127 to 178 mm (5 to 7 inches). The dosage of High Range Water Reducer (HRWR) and/or water reducer should be adjusted according to the field conditions to achieve the specified slump. The 19mm (3/4 inch) quartzite aggregate used in this project conformed to the standard specifications for Roads and Bridges, Section 820 for Size No. 1 (SDDOT).

The approximate admixture dosages used in this project are given below:

Air entraining agent - Master Builders/ Pavair 232 milliliter/m^3 (6 oz per cubic yard)

HRWR- W.R.Grace/ Daracem 19-	2217 milliliters/100 kgs (34 oz per 100 lbs.) of cementitious material.
Water Reducer-	
Master Builders/ MB 997 -	391 milliliters/100 kg (6 oz per 100 lbs.) of cementitious material.
Silica fume slurry -	
W.R.Grace / Force 10,000-	69.15 liters/m^3 (13.97 gallons per cubic yard).

The cement used was produced at the South Dakota Cement Plant.

3.15.2 Recommended mix proportions for Bridge Deck

For bridge no 1, the recommended HPC mix with silica fume based on the laboratory trial mixes performed satisfactorily in the field in both fresh and hardened states. However highly controlled curing was required to eliminate plastic shrinkage cracking. These were a number of cracks at bottom surfaces of the deck due to the high restraint caused by the deck reinforcement. It seemed that silica fume addition caused higher shrinkage cracking. Therefore, for the second bridge, silica fume was omitted and only fly ash was included as a cement replacement. This mix performed well both in fresh and hardened states. There was also less cracking at the bottom surface of the slab. Therefore this mix is recommended for all future bridge deck construction. The recommended mix proportions are given in Task 6.

3.15.3 Recommended Quality Control Testing

When silica fume is used in the slurry form, it is recommended that the slurry must be sampled and tested before use and at specified intervals during concrete production. The amount of silica fume in the slurry can be determined by a hydrometer test. It is suggested that a curve can be generated by taking a sample and running the hydrometer testing on the slurry. For a given sample hydrometer tests could be run with different water contents to generate a curve. Also, from a sample, the slurry could be carefully dried to determine the amount of silica fume in the sample. Based on this information and the curve, the silica fume content could be easily and quickly determined when the slurry consists of water and silica fume only.

When HPC mixes are used, it is recommended that the following quality control tests should be conducted in the field using ASTM test procedures for the fresh concrete: slump, unit

weight, air content, and the concrete temperature. The ambient temperature, humidity, and the wind velocity be recorded during placing of the concrete in the bridge deck or fabricating the prestressed girders. The following hardened concrete control tests should be conducted on the field samples collected and cured according to the ASTM standard procedures at 28 days: compressive strength and static modulus. When HPC is used for fabricating prestressed girders, it is recommended that companion cylinders (preferably 102 mm × 204 mm (4" × 8")) be placed near the girder and cured under identical conditions as the girders, to determine when the prestress can be released as per specifications.

The specifications for bridge deck concrete and also for the high strength concrete used for prestressed girders should include a required Chloride Permeability value as measured by the ASTM C 1202. When chloride permeability is specified, the hardened concrete samples made from the actual concrete placed should be tested for rapid chloride permeability as per ASTM C 1202.

The standard ASTM test procedures to be followed are given in Chapter 2.

3.15.4 Construction Guidelines

When silica fume concrete is used for the bridge deck, the curing specifications (as mentioned earlier) should be strictly followed. The same construction procedures for mixing, transporting, placing, consolidating, finishing and tinning used for construction with standard concrete, be followed. The same construction techniques and equipment without major modification could be used for the construction of HPC bridge decks.

3.16 Task 16: Submit a final report summarizing relevant literature, research methodology, test results, specifications, design standards, conclusions, and recommendations.

With the acceptance of this draft final report the revised final report will be submitted before December 30, 2001.

3.17 Task 17: Make an executive presentation to the SDDOT Research Board summarizing the findings and conclusions.

A presentation to the SDDOT Research Board will be given on November 28, 2001.

CHAPTER 4.0

FINDINGS AND CONCLUSIONS

4.1 Compressive strength results:

Summaries of the extensive tests that were conducted in order to assess the strength and strength development with time are provided in Tables 4.1 through 4.6. Tables 4.1 through 4.4 provide information on the concrete used in the prestressed girders while Tables 4.5 and 4.6 provide strength information for the deck concretes. Note that a single result in a table is the average of three separate cylinder tests. The exception to this is trial mix one where more cylinders were tested. In some instances, both companion cured cylinders as well as moist cured cylinders were used. Companion cured cylinders were cured with the girder for which they were representative up until the cylinders were retrieved for testing. Table 4.1 contains the information

Table 4.1: Trial Mixes, Bridge no. 1 (B1), Compressive strength results.

Concrete Age Days	Trial Mix no. 1 Cast: April 28, 1999		Trial Mix no. 2 Cast: May 4, 1999		Deck Trial Mix Cast: July 9, 1999
	Moist cure		Moist cure	Companion cure	Moist cure
	No. of cylinders	f_c' (psi)	f_c' (psi)	f_c' (psi)	f_c' (psi)
1	6	3,430	5,500[2]	5,500[2]	-
3	9	6,400[3]	7,290	7,090	5,840
7	8	7,590	8,550	9,220	7,230
14	6	9,670	9,820[4]	9,450	8,070
28	6	10,720	11,660	11,840[5]	8,910
56	6	11,520	12,760	13,170[5]	9,020
180	3	11,880	-	-	-

Unit Conversions: 1 psi = 0.006895 MPa

Note 1: All compressive strength results are the average of three cylinders except as specified for Trial mix no. 1.

Note 2: No difference between the companion cure and the moist cure at one day. Only three cylinders were tested.

Note 3: Tests were conducted at four days instead of three days.

Note 4: Tests were conducted at thirteen days instead of fourteen days.

Note 5: Companion cured the first fourteen days, moist cured thereafter.

Table 4.2 Bridge no. 1 (B1) Girder Fabrications, Compressive strength results[1].

Conc. Age Days	Fabrication 1 May 21, 1999		Fabrication 2 May 24, 1999		Fabrication 4 June 4, 1999		Fabrication 5 June 11, 1999		Fabrication 6 June 14, 1999	
	Girder no. 1 f_c' (psi)	Girder no. 2 f_c' (psi)	Girder no. 1 f_c' (psi)	Girder no. 2 f_c' (psi)	Girder no. 1 f_c' (psi)	Girder no. 2 f_c' (psi)	Girder no. 1 f_c' (psi)	Girder no. 2 f_c' (psi)	Girder no. 1 f_c' (psi)	Girder no. 2 f_c' (psi)
1	7,200	-	6,120	-	-	-	-	-	-	-
3	9,830	-	8,670	8,950	-	-	-	-	-	-
7	11,880	12,140	10,740	11,350	12,630	13,170	11,710	11,720	12,410	11,900
14	13,800	14,200	12,960	13,300	15,560	15,930	14,070	14,810	16,500	15,950
28	15,350	15,950	14,100	14,860	15,740	16,540	14,480	15,360	16,690	17,300
56	16,180	16,780	14,700	15,400	-	-	-	-	-	-
180	-	18,100[2]	-	-	-	-	-	-	-	-

Unit Conversions: 1 psi = 0.006895 MPa
Note 1: All compressive strength results are the average of three cylinders.
Note 2: One cylinder broke significantly higher than the other two. The test cylinder results were as follows: 17,600, 17,330 and 19,100.

for the various trial mixes that were conducted. They do not provide information on the specific mixes that were employed but they are included here for completeness. Trial mixes no. 1 and 2, were conducted on April 28, and May 4, 1999. The specified strength for the girder mix was 68.26 MPa (9,900 psi) at 28 days. The stress at prestress transfer was required to be 58.6 MPa (8,520 psi). Upon reflection, it is clear that the governing requirement is the stress at transfer. In order to meet the production schedule the prestress supplier wanted to transfer prestress at three days or less. By inspecting the trial mix results, it is seen that neither of these mixes met this requirement.

The deck trial mix employing silica fume was conducted on the interstate near the bridge site and was conducted on June 14, 1999. This mix employed silica fume and the trial mix was conducted to provide experience with handling the production mix and to test the fogging equipment that the contractor was required to use with this concrete. Strength was not the main concern for the deck concrete. The major emphasis was to produce concrete of very low permeability so that the decks would have superior resistance to the migration of chlorides to the

level of the reinforcing steel. As stated, the trial mix results are simply reproduced here for completeness.

The results from the production girder mixes are presented in Tables 4.2 through 4.4. Table 4.2 contains the compressive strength results for the five girder fabrication sequences for bridge B1. Initially, the plan was to test cylinders from the concrete from the instrumented girders only. A change was made and during the first year all girder fabrications were attended with cylinders being prepared and tested from each sequence. The time series for these girders employed tests at 7, 14 and 28 days. The second year, only half the girder fabrications were attended but a more complete time history was developed. These results appear in Table 4.3. In general these concretes achieved sufficient strength at three days 58.7 MPa (8,520 psi) in order to permit the transfer of prestress to the girders.

Table 4.3: Bridge no. 2 (B2) Girder Fabrications, Compressive strength results[1].

Conc. Age Days	Fabrication 2 April 28, 2000		Fabrication 3 May 9, 2000	
	Girder no. 1 $f_c^{'}$ (psi)	Girder no. 2 $f_c^{'}$ (psi)	Girder no. 1 $f_c^{'}$ (psi)	Girder no. 2 $f_c^{'}$ (psi)
3	6,770	7,310	8,000	8,380
7	9,050	10,020	10,200	10,140
14	11,050	12,670	12,350	11,650
28	12,340	13,880	13,780	14,080
90	13,190	15,190	15,010	14,950
180	13,410	15,190	14,810	15,350
1 year	14,090	15,690	15,470	16,150

Unit Conversions: 1 psi = 0.006895 MPa
Note 1: Each compressive strength is the average of three cylinders.

When reviewing these results it should be noted that the ready-mix supplier was trying to produce the same mix with the expectation that the strengths would be the same. By perusing the row an estimate of the variation from mix to mix can be noted. Two separate trucks were used to produce each girder. An interesting phenomenon that was noted throughout the project was that the cylinder strengths from the second truck were always higher than the strengths from the first truck.

In each year, two girders were selected to receive instrumentation. The instrumentation permitted the measurement of strain and temperature at mid-span of each girder. In addition, reference points were established on the girder to permit the measurement of deflections. These two girders were always the two girders that were to be placed in the end span at the north end of the bridge. These girders occupied the west exterior and the next adjacent interior girder positions. The first year these two girders were fabricated third in the sequence. The second year the instrumented girders were fabricated fifth in the sequence. The compressive strength results for these four instrumented girders are listed in Table 4.4.

The instrumented girders exhibited a 28-day compressive strength ranging from a low of 91.0 MPa (13,200 psi) to a high of 108.2 MPa (15,690 psi). If one computes the statistics on the 28-day compressive strengths, the results yield a mean of 99.3 MPa (14,400 psi) and a standard deviation of 6.82 MPa (990 psi). The ratio of the standard deviation to the mean defines the coefficient of variation and this is 6.9 percent. This indicates a well-controlled process. It appears that these strength results can be achieved with reasonable expectation.

Assuming the acceptance tests were, as is the case in this report, made up of three cylinders averaged to produce a single result. Then— if one expects 95 percent of these results to be above the specified design strength at 28 days, the design strength of this mix could be set at 88.2 MPa (12,800 psi), or conservatively at 82.7 MPa (12,000 psi). This assumes that the test results are normally distributed. An instrumented girder time series begin at one day and was defined as ages of 3, 7, 14, 28, 56 or 90, and 180 days with the final test being conducted at one year. Note that in the second year the 56-day test of the first year was not carried out, but that a 90-day test was substituted. This, it is believed, permits a better plot.

These time series are presented graphically in Figure 4.1. Also presented in this figure is a line that represents the results from the standard equation that is used to predict strength vs. time for a moist cured Type I cement concrete. In this figure, the line for each bridge is the average of the results from the two instrumented girders for that bridge. Though difficult to discern in the figure, the maximum early period difference between these two curves (The first 28 days) is about 11.0 percent. At later ages, they are essentially identical.

The deck compressive strength results are provided in Tables 4.5 and 4.6. For each deck five time series were developed. The time histories in the tables were defined by testing three cylinders at each age. The concrete for each series was taken at one time and the time selected

depended upon where in the deck placement the contractor was. Concrete was sampled at the center of the first span, at the first bent, at the middle of the center span, at the second bent and at the middle of the last span. In the case of bridge one, the deck placement proceeded from north to south. Therefore, series one is representative of the concrete at the middle of the north span and at the location of the deck instrumentation.

Table 4.4: Instrumented Girders, Bridges 1 and 2, Compressive strength results[1].

Conc. Age Days	Bridge no 1 Casting date: June 3, 1999				Bridge no. 2 Casting date: May 18, 2000			
	Girder no. 1 (G3B)		Girder no. 2 (G3A)		Girder no. 1 (G5A)		Girder no. 2 (G5B)	
	Moist Cure	Comp. Cure	Moist Cure	Comp. Cure	Moist Cure	Comp. Cure	Moist Cure	Comp. Cure
	f_c' (psi))	f_c' (psi)	f_c' (psi)	f_c' (psi)	f_c' (psi)	f_c' (psi)	f_c' (psi)	f_c' (psi)
1	6,430	6,430	6,060	6,060	5,240	5,408	6,103	6,198
4	9,510	10,600	10,400	11,330	7,810	8,790	9,540	10,030
7	11,020	12,140	11,770	13,000	9,520	10,690	11,470	12,110
14	12,800	12,940	13,790	14,070	10,880	12,020	13,310	13,605
28	13,200	13,840	14,630	15,320	13,230	13,950	15,410	15,690
56	14,200	14,230	15,660	14,990	-	-	-	-
90	-	-	-	-	14,180	14,270	16,540	15,940
180	14,300	15,140	16,530	16,240	14,860	13,900	16,820	16,270
1 year	15,680	15,100	17,200	16,450	15,390	15,000	16,900	16,650

Unit Conversions: 1 psi = 0.006895 MPa
Note 1: Each compressive strength is the average of three cylinders.

Series two was taken from concrete placed at the first bent and coincided with a location at which instrumentation is located. Table 4.6 presents the parallel information for bridge 2. In this case, the placement was from south to north so series four and five represent the concrete at the locations of the instrumentation in the second bridge. The two deck concretes were not the same. In bridge 1, a silica fume mix was used while in bridge 2 a fly ash mix was employed. Figure 4.2 provides a time history plot of the average strength from all series for each bridge.

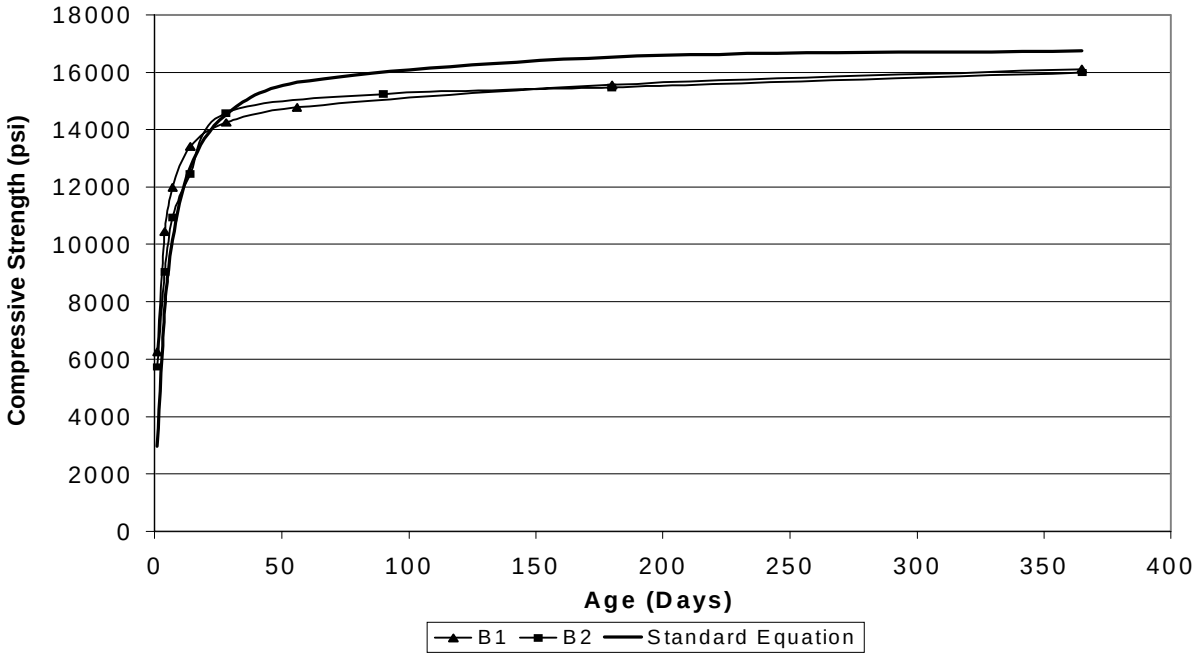

Figure 4.1: Compressive strength history for the instrumented girders of Bridges 1 and 2.

Table 4.5: Bridge 1, Deck placement (August 16, 1999) compressive strength summary.

Concrete Age	Series (All entries lbs/in^2, value listed, result from 3 cylinders)					Row Average
	No. 1	No. 2	No. 3	No. 4	No. 5	
3	4030	3740	3720	3640	3990	3830
7	5300	5020	5040	4960	5290	5120
14	6730	6100	5960	5970	6490	6250
28	7530	6830	6960	6750	7290	7070
90	8260	7560	7520	7430	8000	7750
191	8140	7820	7900	7890	8410	8030
1 year	8510	8080	8290	8280	8570	8350

Unit Conversions: 1 psi = 0.006895 MPa

Table 4.6: Bridge 2, Deck placement (July 20, 2000) compressive strength summary.

Concrete Age	Series (All entries lbs/in^2, value listed, result from 3 cylinders)					Row Average
	No. 1	No. 2	No. 3	No. 4	No. 5	
3	4450	3990	4420	4270	4420	4310
7	5030	4440	5000	4970	5150	4920
14	5840	5400	5870	5610	6070	5760
28	6860	6330	6950	6530	7110	6760
90	8120	7030	7930	7520	8360	7770
180	9090	7690	8110	8100	8720	8340
1 year	9590	8655	8705	8850	9420	9040

Unit Conversions: 1 psi = 0.006895 MPa

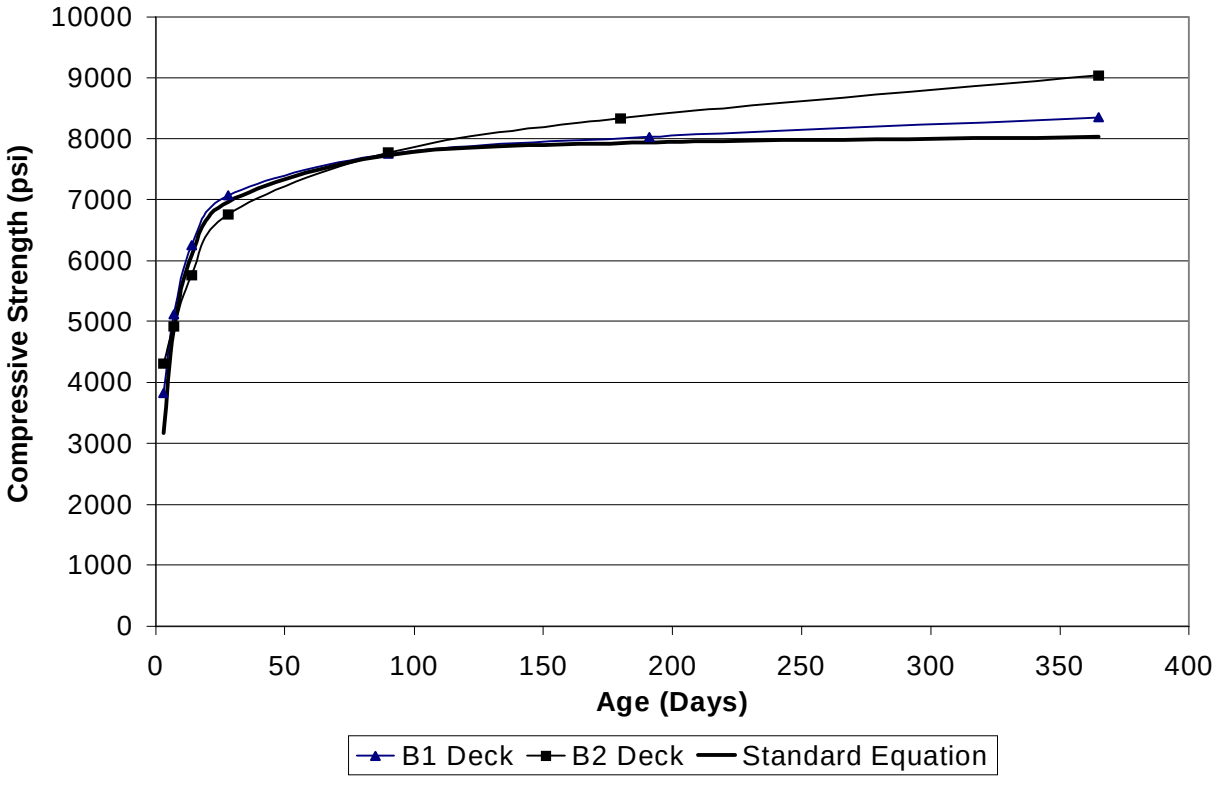

Figure 4.2: Compressive strength history of the deck concrete of Bridges 1 and 2.

The compressive strength results from these two mixes are rather comparable. One notes from Figure 4.2 that the fly ash mix produced slightly higher long term strength than the silica fume mix. It is well established that fly ash tends to hydrate slower than silica fume, and thus contributes more significantly to later strength gain. The previously mentioned standard equation is also presented in Figure 4.2. This standard curve is calibrated to the average of the two mixes at 28 days. It provides relatively good strength prediction with time for both of the mixes.

4.2 Modulus of Elasticity Results:

In order to design prestressed structures or even regular concrete structures utilizing HPC or HSC one needs an equation that is capable of providing a reasonably accurate estimate of the modulus of elasticity of the concrete at various ages. As has been noted earlier in this report, several equations have been used for this purpose. Equation 4-1 given below is the long-standing equation used in both the AASHTO and ACI 318 design specifications. The ACI 363 equation is the one currently recommended for high strength concrete.

AASHTO and ACI 318 equation:

$$E_c = 33 w_c^{1.5} \sqrt{f_c'} \qquad \text{eq. 4-1}$$

ACI equation 363:

$$E_c = \left(40{,}000\sqrt{f_c'} + 1{,}000{,}000 \right) \left(\frac{w_c}{145} \right)^{1.5} \qquad \text{eq. 4-2}$$

E_c = Modulus of Elasticity (psi units).

w_c = Unit weight of the concrete (lbs/ft^3).

f_c' = Compressive strength of the concrete (psi units.)

The equation 4-1 is the one that has long been used to estimate the modulus of elasticity of normal strength concrete. It is considered to yield results that are too high for HSC. The ACI 363 equation is recommended for HSC concrete, i.e. concrete with a 28-day compressive strength greater than 6,000 psi. This equation was based on concrete utilizing limestone aggregates.

The results from all the modulus of elasticity tests conducted on the concrete from the instrumented girders are presented in Table 4.7. The table includes data from both bridges. In

Table 4.7: Bridges 1 and 2, Modulus of Elasticity results for the instrumented girders[1].

Conc. Age Days	Bridge 1				Bridge 2			
	f_c'		Mod of Elast.		f_c'		Mod of Elast.	
	Av. (psi)	st. dev. (psi)	Av. ($x10^{-6}$) (psi)	st. dev. ($x10^{-6}$) (psi)	Av. (psi)	st. dev. (psi)	Av. ($x10^{-6}$) (psi)	st. dev. ($x10^{-6}$) (psi)
1	-	-	-	-	5,740	462	4.98	0.213
4	10,460	1,120	6.27	0.289	9,010	951	5.62	0.351
7	12,090	775	6.60	0.269	11,090	1260	6.26	0.363
14	13,390	882	6.89	0.261	12,450	1290	6.82	0.340
28	14,320	984	7.28	0.148	14,460	1080	7.13	0.332
56	14,750	671	7.18	0.387	-	-	-	-
90	-	-	-	-	15,450	1410	7.03	0.366
180	15,600	1060	7.01	0.387	15,600	1124	7.06	0.268
1 year	16,230	589	7.02	0.230	15,920	863	7.20	0.318

Unit Conversions: 1 psi = 0.006895 MPa
Note 1: The results at each age are from four individual cylinders.

total, this data represents 60 tests. These tests were conducted according to the procedure outlined in ASTM C-469, "Standard test method for static modulus of elasticity and poisson' s ratio of concrete in compression". The unit weight of the test concrete was obtained from the individual cylinders used in the test. These results are plotted in Figure 4.3. The square symbols in Figure 4.3 represent all of the data from the instrumented girders. The data from the two sets of girders from the two bridges were tested statistically with the conclusion that the two sets of modulus data were not significantly different. Proceeding from the left side of the figure, the regression line on the experimental data is the upper line. Two thirds of the way along its length it passes under the line that represents the long-standing equation that has been in the ACI code for many years, the ACI 318 equation. Included in this figure is the ACI 363 equation and the equation by Iravani. The regression results on the data yielded a line essentially parallel to the

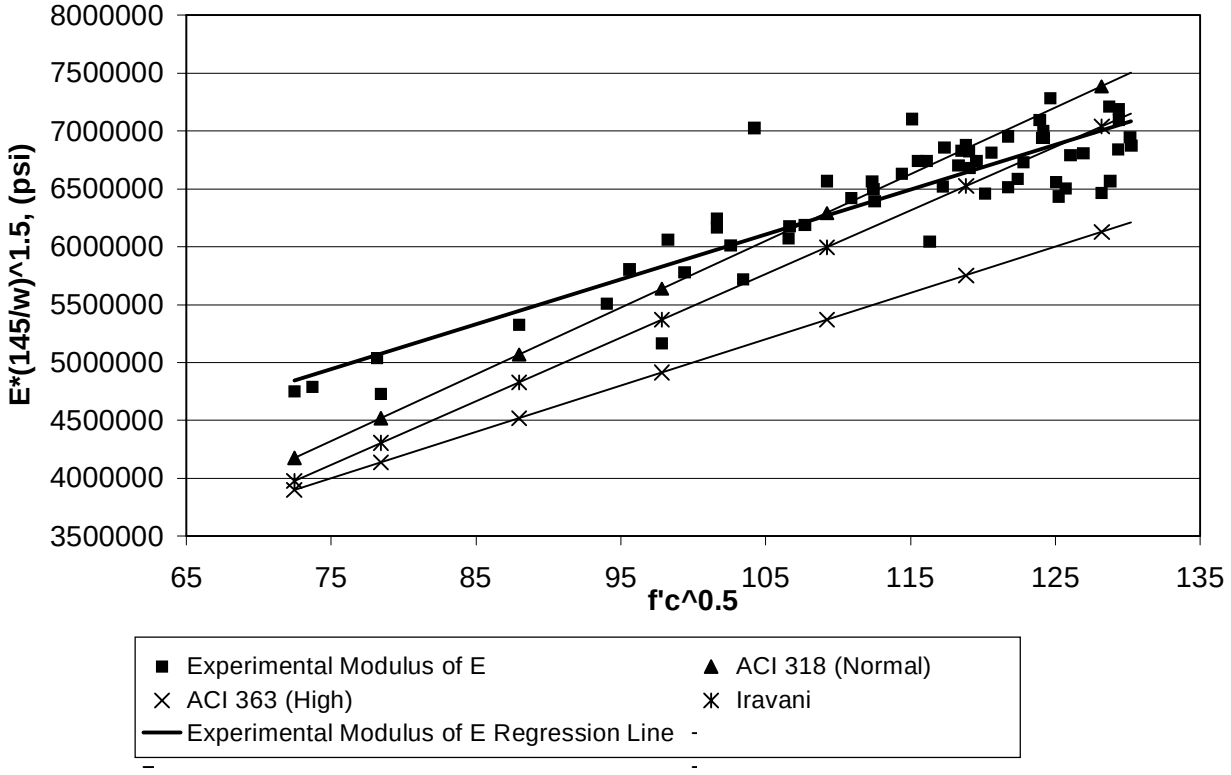

Figure 4.3 Modulus of elasticity regression analysis, all instrumented girders and both bridges.

ACI 363 equation. The specific form is –

$$E_c = \left(38{,}900\sqrt{f_c'} + 2{,}000{,}000\right)\left(\frac{w_c}{145}\right)^{1.5} \qquad \text{eq. 4-3 .}$$

The terms in this equation are as previously defined. The constant multiplying the $\sqrt{f_c'}$ term in the ACI 363 equation was determined to be 38,900 in the present work. This is not viewed as significantly different than the value, 40,000 in the ACI 363 equation. The constant of 1,000,000 psi in the ACI 363 equation was determined from the project data to be 2,000,000 psi. This is viewed as a significant difference.

This difference can be partially explained by noting that the work that was done to develop the ACI 363 equation was conducted on concrete that utilized limestone aggregates. As is known, the quartzite aggregate which was used in the mixes developed in this project, is a

much harder rock and expected to exhibit a higher modulus. It is interesting to note that the standard equation that is considered to yield results that are too high for HSC, produces

Table 4.8: Bridges 1 and 2, Modulus of Elasticity results for the deck concrete[1].

Conc. Age Days	Bridge no. 1				Bridge no. 2			
	f_c'		Mod. of Elast.		f_c'		Mod. of Elast.	
	Av. (psi)	st. dev. (psi)	Av. ($x10^{-6}$) (psi)	st. dev. ($x10^{-6}$) (psi)	Av. (psi)	st. dev. (psi)	Av. ($x10^{-6}$) (psi)	st. dev. ($x10^{-6}$) (psi)
3	3,750	202	3.84	0.028	4,230	271	4.40	0.211
7	5,170	240	4.51	0.243	4,800	267	4.55	0.152
14	6,090	303	4.90	0.163	5,840	220	5.23	0.338
28	7,120	465	5.22	0.231	6,640	421	5.62	0.217
90	7,840	262	5.14	0.276	7,480	817	5.67	0.079
180[2]	7,820	67	5.34	0.182	8,400	472	5.96	0.133
1 year	8,150	278	5.37	0.079	9,280	464	6.19	0.372

Unit Conversions: 1 psi = 0.006895 MPa
Note 1: The results at each age are from three individual cylinders.
Note 2: The cylinders for bridge no. 1 were tested at 191 days instead of 180 days.

reasonable results for the mixes used in this project. Iravani' s equation is also seen to produce acceptable results. He includes a factor in his equation for the type of aggregate used in the mix. underside of the girders.

Forty-two modulus of elasticity tests were conducted on the deck concrete from the two bridges. The basic test results are summarized in Table 4.8 and presented in graphical form in Figure 4.4. In Figure 4.4 two regression lines are presented, one for each bridge. These data sets have not been tested statistically in order to determine if they are significantly different, but it is believed that they will test as one set of data. Included in this figure as was done in the previous figure, are the ACI 318 and 363 equations. By inspection it is observed that the two regression lines for bridges 1 and 2 are reasonably parallel to the ACI 363 equation. The offset between these two is also about the same. The conclusion is that the previous equation 4.3 obtained from the girder tests will yield reasonable results for this data as well.

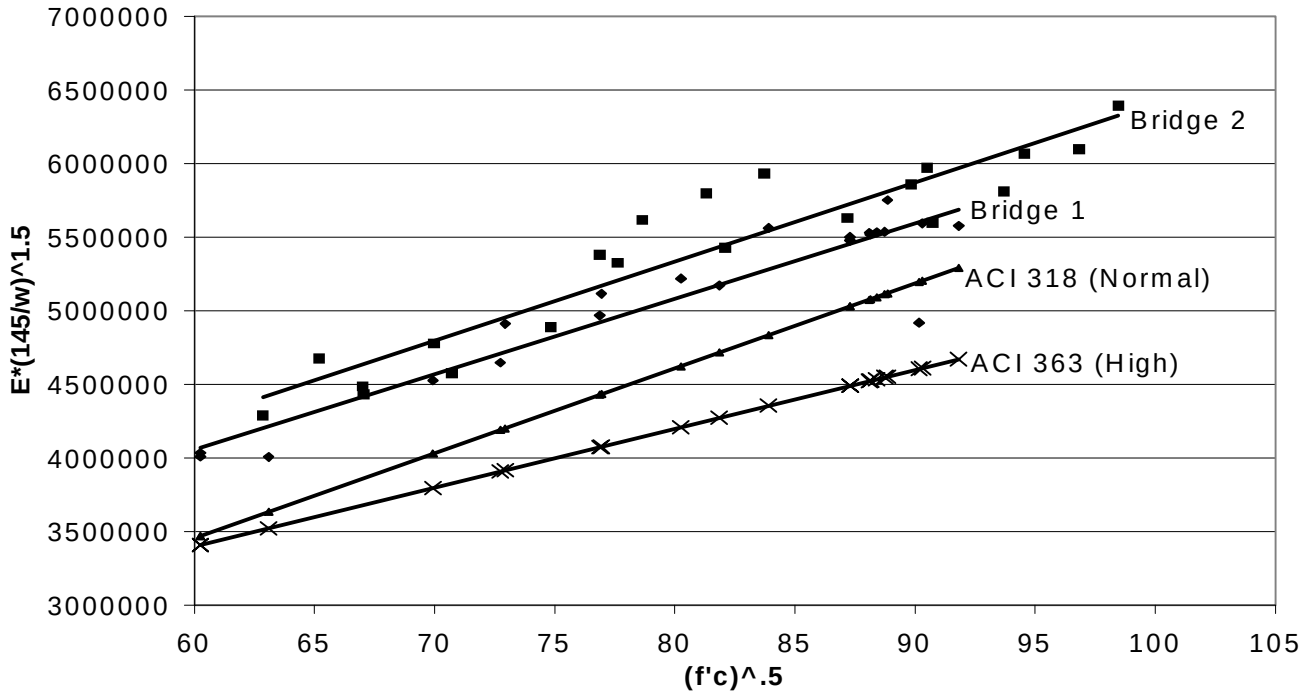

Figure 4.4: Modulus of elasticity regression analysis of the deck concrete, both bridges.

4.3 Girder and Bridge Deflections.

Initial girder deflections were taken immediately after the transfer of prestress. Observations continued to be taken at close, but increasing time intervals out to one month, thereafter readings were taken approximately monthly. After the concrete decks was placed readings had to be taken from the underside of the girders. The three wire leveling technique employed is expected to yield results within ±0.46 mm (± 0.0015 ft)

Deflection summaries are provided in Table 4.9. Note that the girders from bridge 2 exhibited more early camber, more deflection due to the deck loading, and maintained a greater camber under long term loading. In both cases, prestress was transferred over the period of about a half-day, and the girders were removed from the bed the next day. Deflection readings were taken just at the conclusion of prestress transfer, on the bed the next day prior to removing the girders from the bed, and immediately after the beams were removed from the prestressing bed.

The girders from bridge number two increased their camber about 0.4064 mm (0.016 inches) during the time they were lifted from the bed. Both girders exhibited the same deflection increase. This increase did not occur with the girders from bridge 1.

Table 4.9 Mid-span deflection data, both bridges.

	Bridge 1		Bridge 2	
	G3-A (in.)	G3-B (in.)	G5-A (in.)	G5-B (in.)
Instantaneous Camber	0.74	0.67	0.72	0.60
Maximum Camber	1.00	0.93	1.25	1.18
Deck Placement Deflection	-0.33	-0.36	-0.45	-0.42
Average deflections:				
Winter 1999	0.25	0.21	-	-
Summer 2000	0.29	0.25	-	-
Winter 2000	0.23	0.20	0.48	0.44
Summer 2001	0.29	0.24	0.54	0.49

Unit Conversions: 1 psi = 0.006895 MPa
Note 1: Positive values indicate an upward deflection.
Note 2: The deflections have not been corrected for temperature.
Note 3: Girders G3-A and G5-A are inside girders while Girders G3-B and G5-B are exterior girders.

The averages for the winters and summers indicate that the girder deflections have not changed very much over the monitoring period. The graph of the deflection history for the instrumented girders in bridge 1, specifically, G3A and G3B, is provided in Figure 4.5. A parallel graph for the girders G5A and G5B in bridge 2 is provided in Figure 4.6.

The change in camber that was previously noted as the G5A and G5B girders were removed from the bed is easily seen in Figure 4.6. The two graphs clearly show the development of camber with time. This camber being due to the creep and shrinkage occurring in the girders. Careful inspection notes the onset of the downward deflection due to the placement of the deck formwork. Clearly visible is the instantaneous deflection due to the placement of the deck. In both bridges, the outside girder tends to deflect more than the inside girder. The slight tendency for the deflections to decrease during the winter months and increase slightly during the summer months can be observed. In general, the girder deflections are not changing significantly. The separate deflections of the two instrumented girder for each bridge were averaged and plotted on

a time scale having zero as the time at which prestress was transferred to the girder, these results are provided in Figure 4.7.

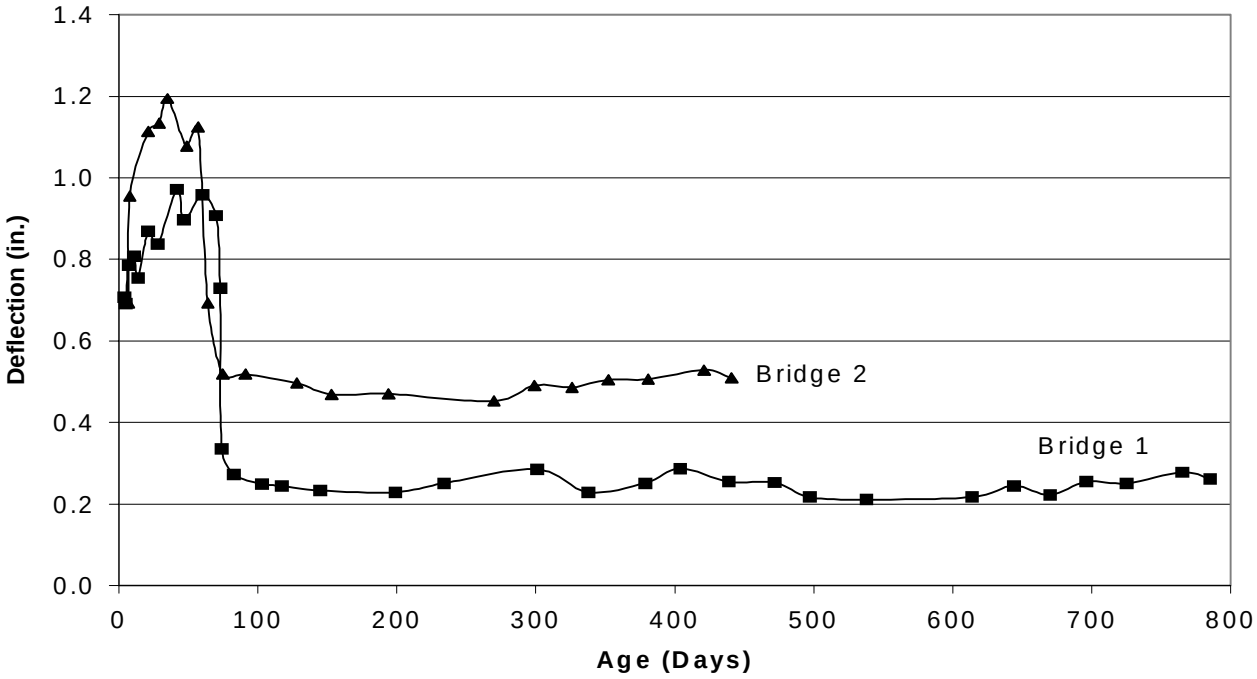

Figure 4.5: Bridge no. 1, mid-span deflection history of both instrumented girders.

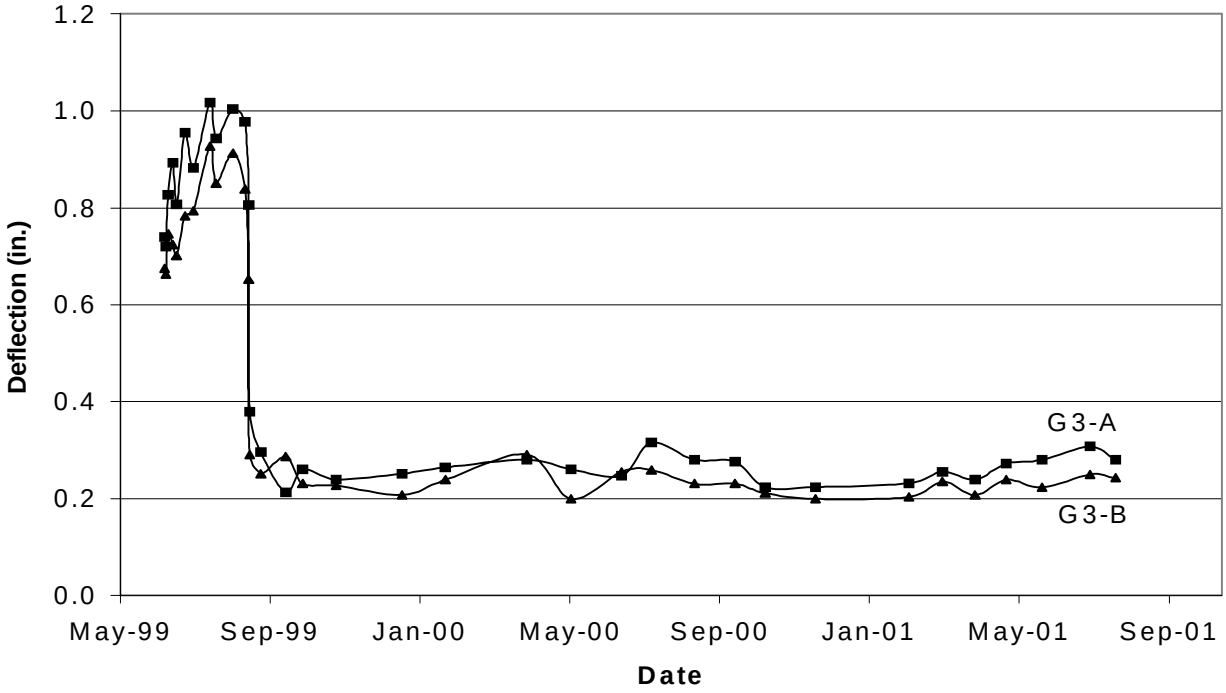

Figure 4.6: Bridge no. 2, mid-span deflection history of both instrumented girders.

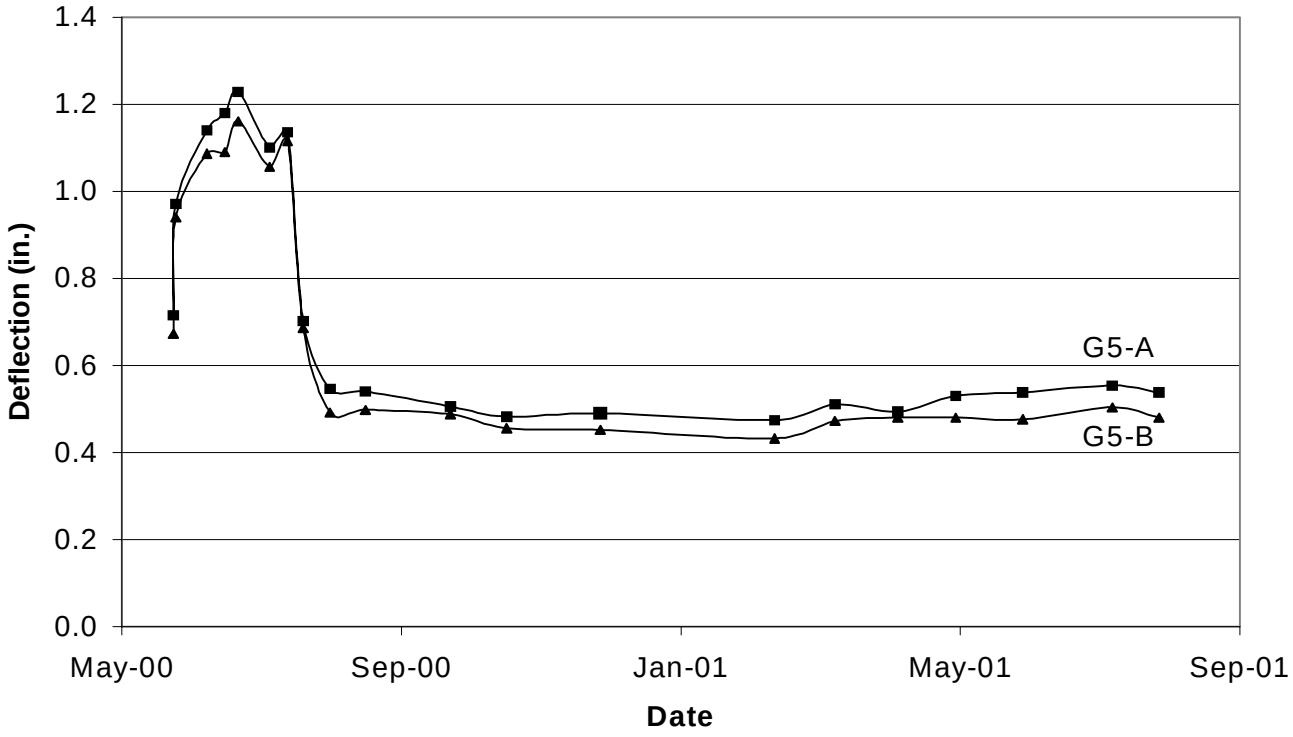

Figure 4.7: Bridges 1 and 2, average mid-span deflection for each bridge.

The elapsed time in this case represents concrete age. By placing both sets of girders on this scale one can inspect what is happening in each bridge relative to the age of the concrete. The camber differences are easily observed as well as the greater long-term deflection differences in the two bridges.

4.4 Impedance Measurements:

As was detailed in chapter 3, six devices were embedded in the deck concrete of each bridge that permitted the measurement of the electrical resistance in the concrete. The electrical resistance of the concrete was measured using these parallel plate devices. There is some belief that high values of electrical resistance are indicative of relatively impermeable concrete. Also, a sudden change in resistance may indicate the presence of chloride ions and thus the potential for corrosion to be initiated in the steel.

The deck on bridge 1 was placed on August 16, 1999. Due to the slow pace at which the formwork was removed, the first electrical resistance measurements were not made until

September 23, 1999. Since that time, measurements have been taken at approximately monthly intervals. The deck for the second bridge was placed on July 20, 2000. The first readings from this deck were recorded on September 18, 2000. This was only about one month after the deck was placed.

The measurements from the silica fume concrete of the first bridge have tended to exhibit a great deal of variability. While the measurements from the fly ash concrete in the second deck have not shown nearly as much variability. The detailed readings are not presented in this report (They are given in the quarterly reports.) but a summary of the measurements is presented in Figure 4.8. Each point that is plotted in the figure is the average of the six readings from the individual devices embedded in the deck. A great deal of variability is evident in the silica fume concrete over a one-year period. In general, the winter period results are much higher readings than the summer. It was noted that a transducer could give very different readings from month to month.

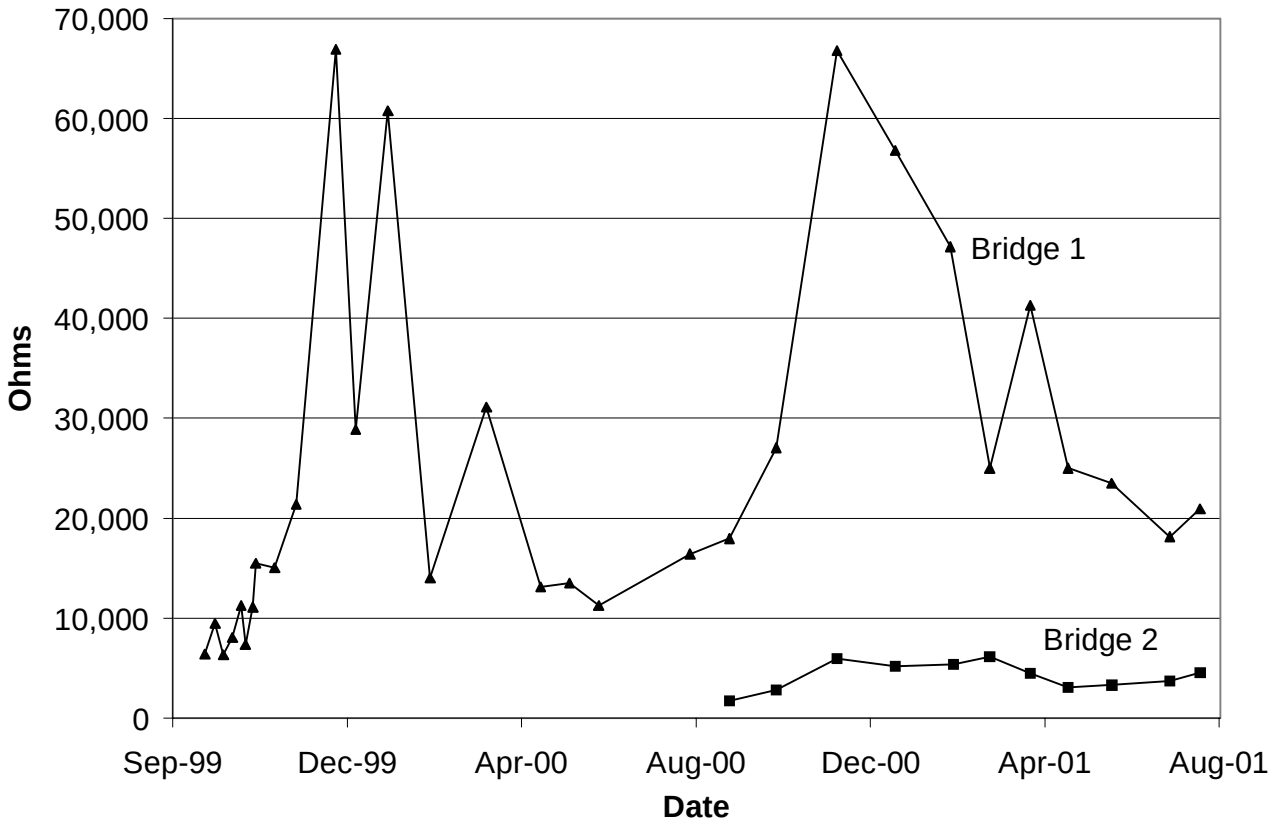

Figure 4.8: Deck impedance readings.

To provide a partial diagnosis of the reason for these readings, the instrument was checked by measuring the resistance of a high precision known resistance. This indicated that the instrument was working correctly. The next diagnostic test that was conducted involved taking multiple readings from the array of devices by disconnecting and reconnecting the leads to the instrument. This procedure of disconnecting and reconnecting the device was followed if the device being read yielded greatly different readings, either from the time before, or quite different from the others in the array. This procedure was followed to determine the change in resistance that could be attributed to simply making the connection to the measuring instrument. This provided no explanation as to the variability of the readings. The only remaining conclusion is that the readings in the silica fume concrete have a high degree of variability and border on being erratic.

This tendency is not observed in the fly-ash concrete deck. These readings have been relatively stable. As with the silica-fume concrete, the fly-ash concrete also tends to exhibit higher values in the cold months and lower values in the warmer months.

4.5 Thermal Strains:

Shrinkage and temperature related strains were evaluated with the use of shrinkage blocks. These blocks were fabricated along with the bridge girders and decks and subjected to the same environmental conditions. The shrinkage blocks have dimensions 152.4×152.4×304.8 mm (6×6×12 in) and contain vibrating wire gages that are embedded in the approximate center of each block. In total, eight blocks were cast, a companion block for each instrumented girder and two companion blocks for each deck.

The blocks experience both temperature and shrinkage strains. In order to be able to evaluate the shrinkage strains, one must first filter out the thermal strains. To accomplish this, the coefficient of thermal expansion for the concrete must be determined.

Early in the history of the shrinkage blocks, the shrinkage strains and the thermal strains are approximately of the same order of magnitude. For this reason, a significant time must elapse so that the shrinkage strains that occur during a half diurnal cycle are small with respect to the thermal strains. After analysis of the time variation of shrinkage strains, it was determined that this condition would be met approximately 90 days after the concrete was cast.

The equation for evaluating the coefficient of thermal expansion is

$$\alpha_c = \frac{(\varepsilon_1 - \varepsilon_0)B}{(T_1 - T_0)} + \alpha_g \qquad \text{Eq. 4.4}$$

α_c = Coefficient of thermal expansion for the concrete.
α_g = Coefficient of thermal expansion for the vibrating wire gage. (6.78×10^{-6} 1/°F)
ε_0, ε_1 = Strains measured at times t_0 and t_1 respectively.
T_0, T_1 = Temperatures measured at times t_0 and t_1 respectively.
B = Calibration factor for the gage (0.980).

Each day's cycle gives an opportunity to calculate two estimates of the coefficient of thermal expansion. After inspecting the daily temperature effects, it was determined the best results correlated with cycles showing reasonably large temperature changes. Therefore, the calculation of the estimate of the coefficients of thermal expansion was restricted to time-periods with temperature changes greater than 10.0 °C (18 °F). The original plan was to group the data into months and evaluate the results for the entire data logging time-frame. A curious problem developed during the analysis. It appeared that during the cold months the coefficient of thermal expansion was significantly less than during the summer months. It seemed that the blocks were frozen, or, perhaps, frozen to the supports and were not responding without restraint to the temperature change. Therefore, data was analyzed for the summer months only, this included May, June, July, and August of 2000 and 2001.

The means and variances for each month were computed. These means were tested to see if they were significantly different statistically. For this analysis it was determined that the monthly means of the coefficient of thermal expansion were statistically different. The difference in the coefficient of thermal expansion from month to month could be attributed to seasonal thermohygrometric cycles. In previous research it has been hypothesized that the coefficient of thermal expansion in concrete is not constant, where hygrometric exchanges with the atmosphere causes fluctuations in the value. The next step was to compare the average values from block to block to determine if they differed significantly from each other. From this analysis it was determined that there is a small but statistically significant difference among the means for the coefficient of thermal expansion for the blocks. Because the difference is small, it was decided

to ignore this difference and use a single average value for the coefficient of thermal expansion. Results on the average values for each block during each month are shown in Tables 4.10 for bridge 1 and 4.11 for bridge 2.

It is noted that analysis of coefficients of thermal expansion during year 2001 produced a slightly larger value than in year 2000. This could be due to the improved field support conditions of the shrinkage blocks for the year 2001. In year 2000 the blocks were simply set on a flat piece of wood. In 2001 the blocks were set on a frame and supported by rollers. This set up was better suited for the analysis of temperature effects because air was allowed to circulate underneath the blocks and the rollers provided less friction against movement.

Table 4.10 Bridge no. 1, coefficient of thermal expansion, summary results.

Month Year 2000	Girder G3-A Shrinkage block		Girder G3-B Shrinkage Block		Deck Shrinkage Block no. 1		Deck Shrinkage Block no. 2	
	Average $1/^oF$	n^1	Average $1/^oF$	n^1	Average $1/^oF$	n^1	Average $1/^oF$	n^1
May, 2000	7.283	39	7.172	43	7.333	33	7.289	37
June, 2000	7.406	37	7.183	44	7.400	32	7.417	37
July, 2000	7.761	48	7.761	44	7.628	43	7.661	45
Aug., 2000	7.606	38	7.506	38	7.567	41	7.478	38
Summary Preceding Four Months	7.528	162	7.406	169	7.500	149	7.472	157
May, 2001	7.761	45	7.350	47	7.656	40	7.472	34
June, 2001	7.561	38	7.517	40	7.756	49	7.628	44
July, 2001	7.628	49	7.600	53	7.611	55	7.633	54
Summary Preceding Three Months	7.556	132	7.494	140	7.678	144	7.589	132

Note 1: The 'n ' v alue in the table indicates how many separate coefficients were in the sample for which the average is quoted in the table.
Note 2: All coefficients of thermal expansion in the table have been multiplied by 10^6.

Table 4.11 Bridge no. 2, coefficient of thermal expansion, summary results.

Month Year 2001	Girder G5-A Shrinkage Block		Girder G5-B Shrinkage Block		Deck Shrinkage Block no. 1		Deck Shrinkage Block no. 2	
	Average $1/^oF$	n^1	Average $1/^oF$	n^1	Average $1/^oF$	n^1	Average $1/^oF$	n^1
May, 2001	7.628	43	7.611	37	7.450	41	7.455	42
June, 2001	7.817	51	7.850	46	7.639	47	7.555	47
July, 2001	7.739	55	7.744	55	7.717	55	7.628	556
Summary Preceding Three Months	7.739	149	7.744	138	7.644	143	7.578	145

Note 1: The 'n ' v alue in the table indicates how many separate coefficients were in the sample for which the average is quoted in the table.
Note 2: All coefficients of thermal expansion in the table have been multiplied by 10^6.

It had been decided, based on some of the year 2000 results and before all of the data was available, that a coefficient of thermal expansion equal to 7.50 x $10^{-6}/^oF$ would be used for the project. As it turned out this value may have been a little low, but, in any case, it was used. The strain analysis is not that sensitive to the exact value of the coefficient of thermal expansion. The value selected for use does fit within the range of values that are quoted for quartzite aggregate concrete in ACI Publication 209R-92, 11.76 x 10^{-6} / ^oC to 14.6 x 10^{-6} / ^oC (6.50 x 10^{-6} / ^oF – 8.11 x 10^{-6} / ^oF).

4.6 Shrinkage strains.

Having a value for the coefficient of thermal expansion, the thermal strains were filtered from the shrinkage block strain histories. This isolates the shrinkage strain and permits the analysis of the time variation of the shrinkage strains. The resulting strain histories for all eight blocks are provided in Figures 4.9 through 4.12. All four figures illustrate the classical increase in shrinkage strain with time during the early age of the concrete. After this more rapid development of shrinkage strains the development of shrinkage strains levels off and, in theory, asymptotically approaches a limiting maximum value.

In the results from all eight blocks there appears to be a significant seasonal effect after the initial shrinkage occurs. The shrinkage decreases over the winter months and then rises to a maximum value during the summer months. The reason for this phenomenon is not fully

understood. It is likely that the concrete actually gains back a portion of the initial shrinkage when water from rain or melted snow permeates into the blocks. A further complicating factor in the behavior of the blocks is the effect of freezing and subsequent thawing, or the occurrence of several freeze-thaw cycles. In addition, the support conditions may have been an issue. It will be interesting to see if the seasonal effects continue.

Further monitoring of the bridges is needed in order to determine whether it is a seasonal phenomenon due to the interaction of the blocks with the environment, or something different. The daily and weekly undulations of the plots represent the influence of seasonal and daily variations in relative atmospheric humidity and the fact that the temperature related strains may not be completely removed.

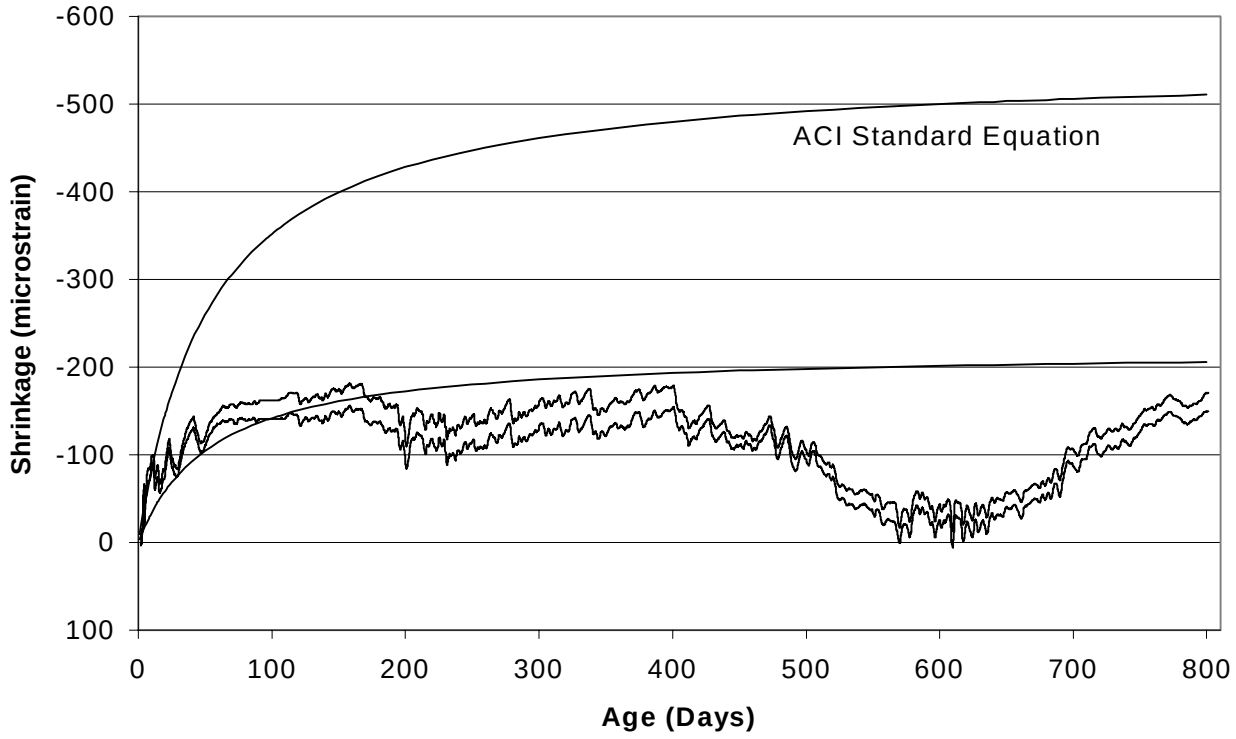

Figure 4.9: Bridge 1, girder shrinkage strains, both blocks.

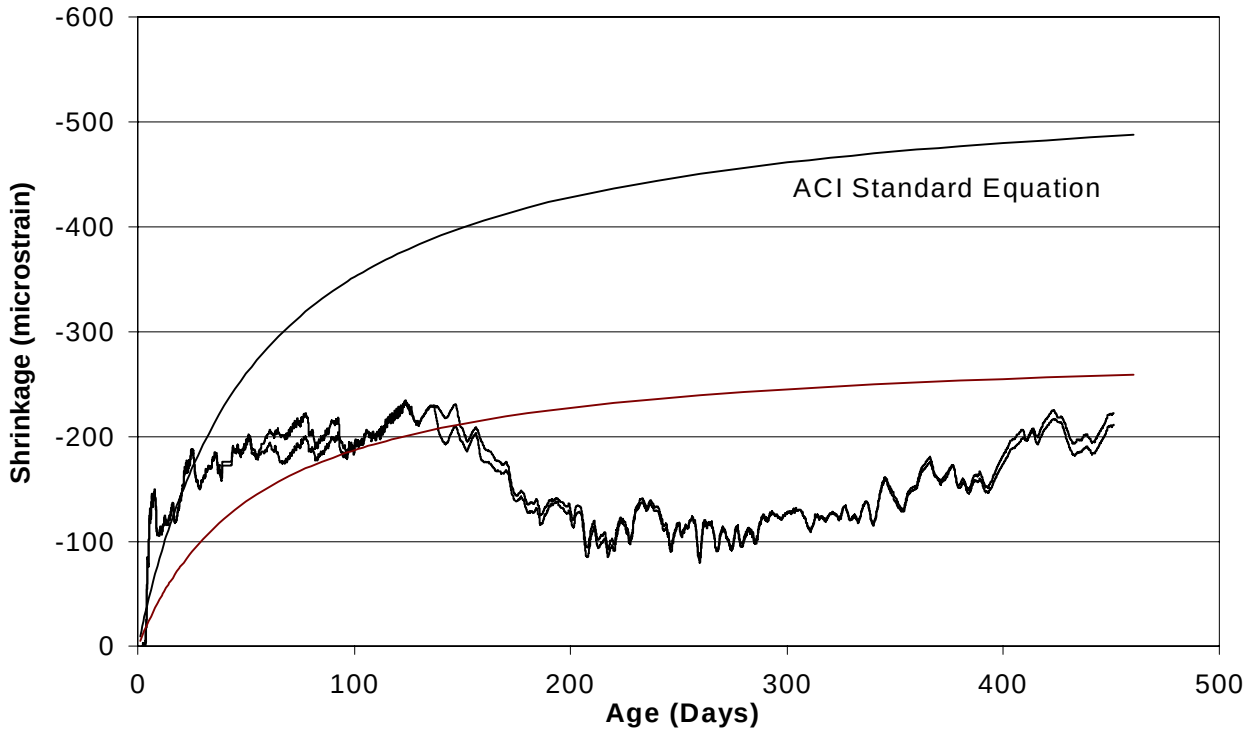

Figure 4.10: Bridge 2, girder shrinkage strains, both blocks.

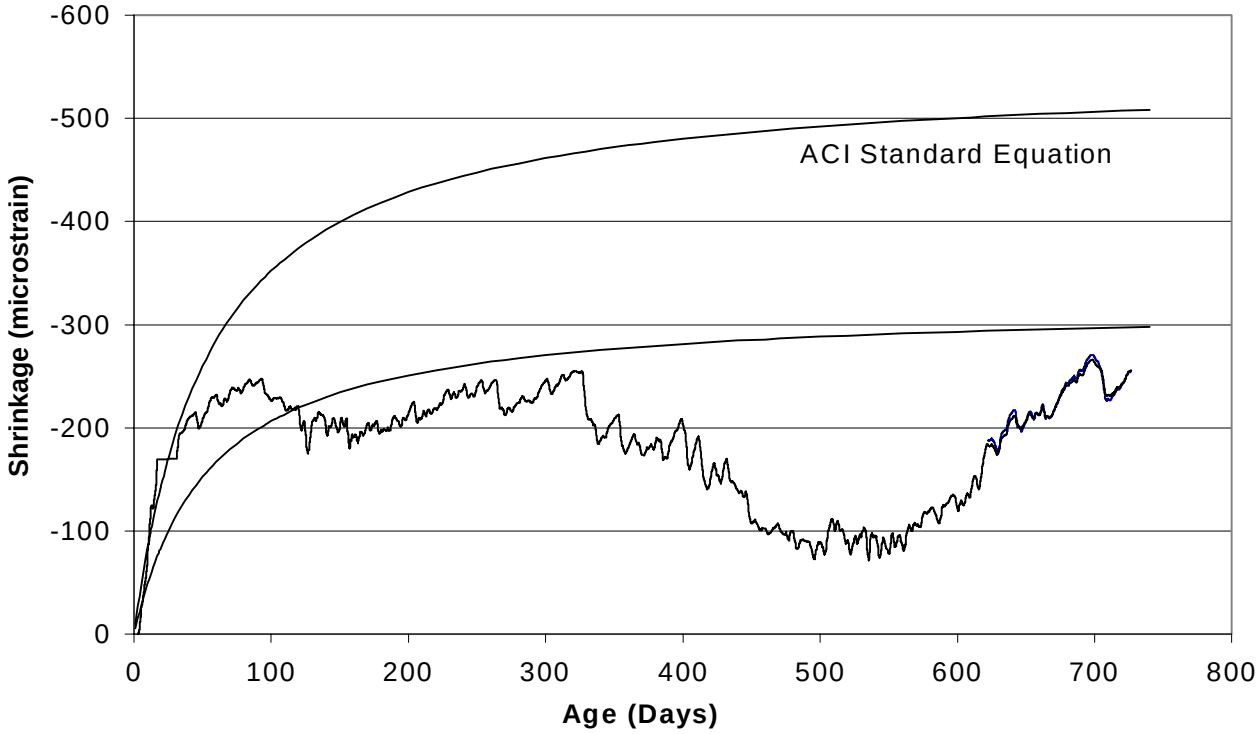

Figure 4.11: Bridge 1, deck shrinkage strains (silica fume), both blocks.

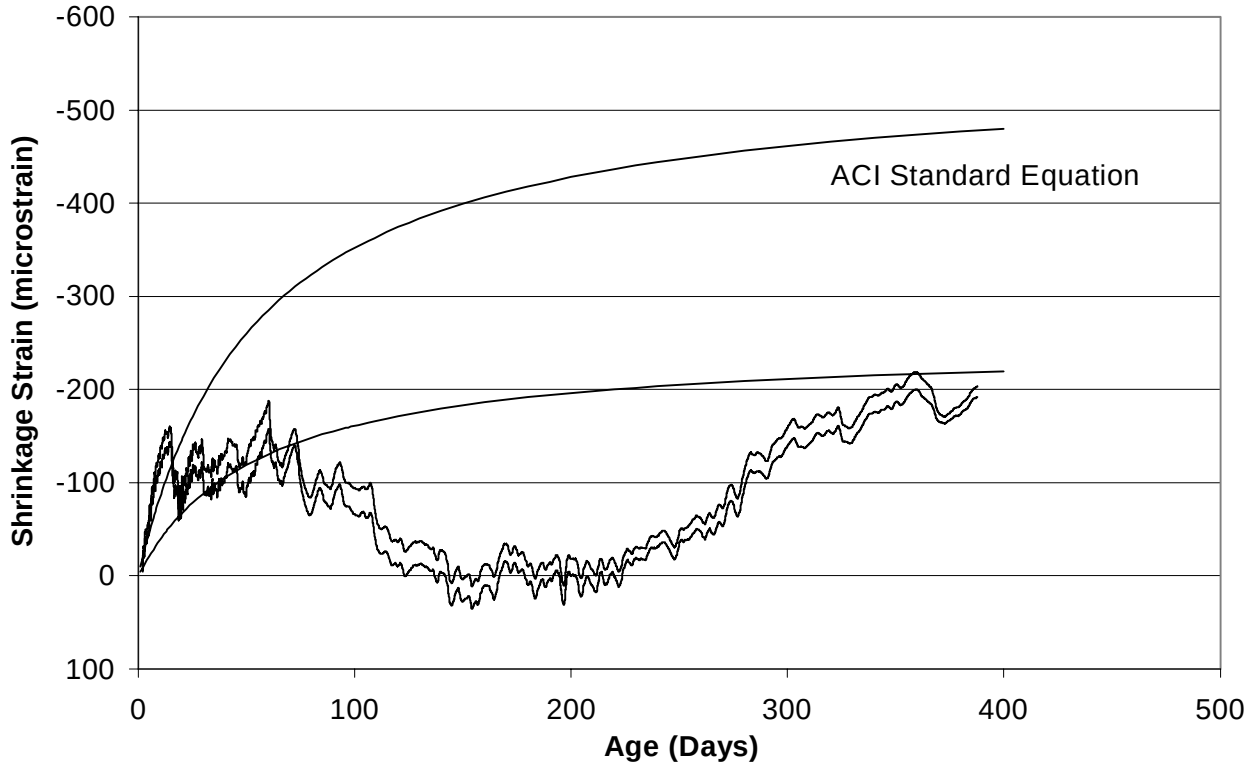

Figure 4.12: Bridge 2, deck shrinkage strains (fly ash), both blocks.

A logarithmic trend-line has been fitted for each set of data to show the general development of shrinkage strain. Another trend-line is shown on the plots illustrating the predicted value for shrinkage using the standard shrinkage equation listed in ACI Publication 209R-92. The form of this equation is (moist cured concrete)-

$$\varepsilon_{sh,t} = \frac{t}{35+t}\varepsilon_{sh,u} \qquad \text{equ. 4.5}$$

$\xi_{sh,t}$ = Shrinkage strain at age t, days.
t = Age of the concrete in days
$\xi_{sh,u}$ = Ultimate shrinkage strain as t goes to infinity.

If no better information is available, this publication recommends an ultimate shrinkage strain value of 780 με. The symbol 'μ' , represents a multiplier equal to 10^{-6}. The term 'ε' stands for strain. To this ultimate shrinkage value, a correction for humidity is recommended. Eastern South Dakota has an annual average relative humidity of 70 percent. The coefficient for this humidity is 0.70. With this modification the ultimate shrinkage strain estimate is 550 με.

The AASHTO specification does not have an equation of this exact form. The approach in the AASHTO specification is to predict the stress loss due to ultimate shrinkage directly in one calculation. In addition, the correction for humidity is incorporated in the equation. The AASHTO equation can be put in a strain form by dividing the referenced equation by the modulus of elasticity of prestressing strand, which is 186.1 MPa (27,000,000 psi). The resulting equation is given below-

$$\xi_{sh,u} = (630 - 5.56\ H)\ 10^{-6} \qquad \text{equ. 4.6}$$

$\xi_{sh,u}$ = Ultimate shrinkage strain.

H = Relative humidity in percent

Substituting the average relative humidity of 70 percent for Eastern South Dakota one obtains an estimate of the ultimate shrinkage of 240 με.

If one considers the early shrinkage to be that that occurs within the first 100 days, the following observations can be made. The girder concrete for bridge 1 demonstrated a maximum early age shrinkage of about 150 με the corresponding value for the girders in bridge 2 is 200 με. This difference is about 25 to 30 percent depending on how one elects to express the difference. The average of these two strains is about 180 με. What is interesting is that there is not nearly this variation between the respective shrinkage blocks from the same bridge. It may be indicative of the variation inherent in dealing with a silica fume mix. This difference in shrinkage is a factor in the increased camber that developed in the girders for bridge 2.

Turning to the point of predicting ultimate shrinkage and computing the ratio of the 180 με average to the ultimate shrinkage as recommended by the ACI 209 Committee (590 με) the results is 0.30. In general one could use a conservative estimate of about half of 590 με to estimate the ultimate shrinkage for the concrete used in the girders in these bridges. If one next compares this value to the ultimate shrinkage as predicted from the current AASHTO equation, one must note that a modifying coefficient is required that reflects the surface area to volume ratio of the element for which the ultimate shrinkage is being estimated. This coefficient is about 0.76 for the girders used in these bridges. Applying this coefficient to the 590 με one ends up with an estimated ultimate shrinkage strain for the girders of about 450 με. Applying this coefficient to the average of the maximum 100-day shrinkage strain from the blocks one obtains approximately, 135 με. This is less than the value predicted from the current AASHTO

equation, 240 με. The conclusion is that the shrinkage strains in the silica fume girder mix appear to be less than what one would predict for normal concrete. One must be careful about generalizing this result.

The deck concretes present a little different picture. The early period shrinkage for the silica fume concrete making up the deck is about 240 to 250 με. The corresponding fly ash concrete early period (first 100 days) shrinkage is about 150 με. This difference is significant. The silica fume concrete exhibited about 1.6 times as much early period shrinkage as the fly ash concrete. This difference holds true for the late shrinkage as well.

4.7 Development of the strain time series and selection of the initial time (t_0):

The data from the vibrating wire strain transducers is initially converted to raw strains. These strains are subsequently converted to a base temperature so that the series can be analyzed without the temperature effects. The base temperature that was selected was 22.2 ^{o}C (72.0 ^{o}F). The conversion of the strain to the base temperature requires a correction for expansion of the gage as well as a correction for the thermal expansion of the concrete. This produced a series that can be considered to have been taken at a common temperature. The next step was to define a zero time so that the difference in strain relative to this time-zero could be determined.

This equation is given as

$$\Delta\varepsilon_{t_i} = \varepsilon_{t_i} - \varepsilon_{t_0} \qquad \text{equ. 4.7}$$

$\Delta\varepsilon_{t_i}$ = Change in strain since t_0

ε_{t_i} = Strain at time t_i

ε_{t_0} = Strain at time t_0

These differences in strain are the values that are of interest in the time history analysis of strain. Time zero was selected by inspecting the data over the first few days after the concrete was placed. One seeks a time close to the time that the concrete has set, yet at a time at which the temperature has settled down a little bit. In all four cases, the two girder placements and the two deck placements, a time zero was selected about 2 days after the concrete was initially placed in the forms. The selection of time zero does influence the subsequent time histories, but a half day one way or the other will not have a large influence on the strain time histories that are calculated.

Once the time histories were generated, the shrinkage block time histories were used to remove the shrinkage strains. This was done according to the following equation-

$$\Delta\varepsilon'_{t_i} = \Delta\varepsilon_{t_i} - \Delta\varepsilon_{sh,ti} \qquad \text{equ. 4.8}$$

$\Delta\varepsilon'_{t_i}$ = Strain increment at time t_i, with the shrinkage strain removed.
$\Delta\varepsilon_{t_i}$ = Strain at time t_i.
$\Delta_{sh,ti}$ = Shrinkage strain at time t_i.

The strain time series that result from the application of equation 4.6 are then subjected to further analysis.

4.8 Analysis of the girder strain time histories:

As has been noted earlier in this report, each prestressed girder had four vibrating wire strain transducers located at mid-span. These transducers were distributed uniformly through the depth of the girder. A program was developed that permitted the linear regression analysis on these four readings. After the regression analysis was performed, the resulting regression results were used to compute strains on the top, bottom and at the centroid of the AASHTO Type II girders. This exercise was repeated at each 30-minute interval throughout a 24-hour period.

After this was completed, the readings were averaged through the day. This averaging tends to remove the remaining cyclical daily variations in the data. Once this was completed on all of the data, the results for each girder were plotted. These two separate plots are similar to each other. The next step was to average the results from the two separate girders. The result of this operation is provided in Figure 4.13 for the instrumented girders from bridge 1, and in Figure 4.14 for the girders from bridge 2. Inspection of these two graphs provides interesting insights into the behavior of these girders.

By inspecting Figures 4.13 and 4.14, the strains introduced into the prestressed girders due to transferring prestress is readily observed. The average compressive strain at the centroid of the girders from bridge 1 is about 425 με. Since this strain is at the centroid of the section it is an indicator of the initial prestress force, P_i. Inspecting the graph for bridge 2, it is observed that the initial compressive strain at the centroid is about 525 με. The difference between these two values is about 19 percent. This difference seems a little large considering the agreement in

the initial deflections. (Table 4.9). The changes in strain associated with the early camber development are noted in the figures.

The change in strains associated with the placing of the decks is clearly observed in the figures by focusing on the lines that represent the strains at the top and bottom fibers of the beam. The plot of the strain at the centroid should not show any effect from the placement of the deck. The fact that it does show a small increment of strain indicates that the actual centroid is not located exactly as predicted.

The change in the strain with time at the centroid of the cross section is indicative of the effect of creep. It would include shrinkage strains but these have been removed. It does include the effect of relaxation in the steel, but low-relaxation strand was specified, so the relaxation effect is not very large. The time variation change in the strain due to creep from the time the girder was cast until the deck was placed is about 25 με in bridge 1 and about 75 με in bridge 2. These values represent a change of about 5.9 percent in the initial prestress in the girders for bridge 1 and about a 14.0 percent change in the initial prestress for bridge 2. This change in strain occurs over an approximate two-month period

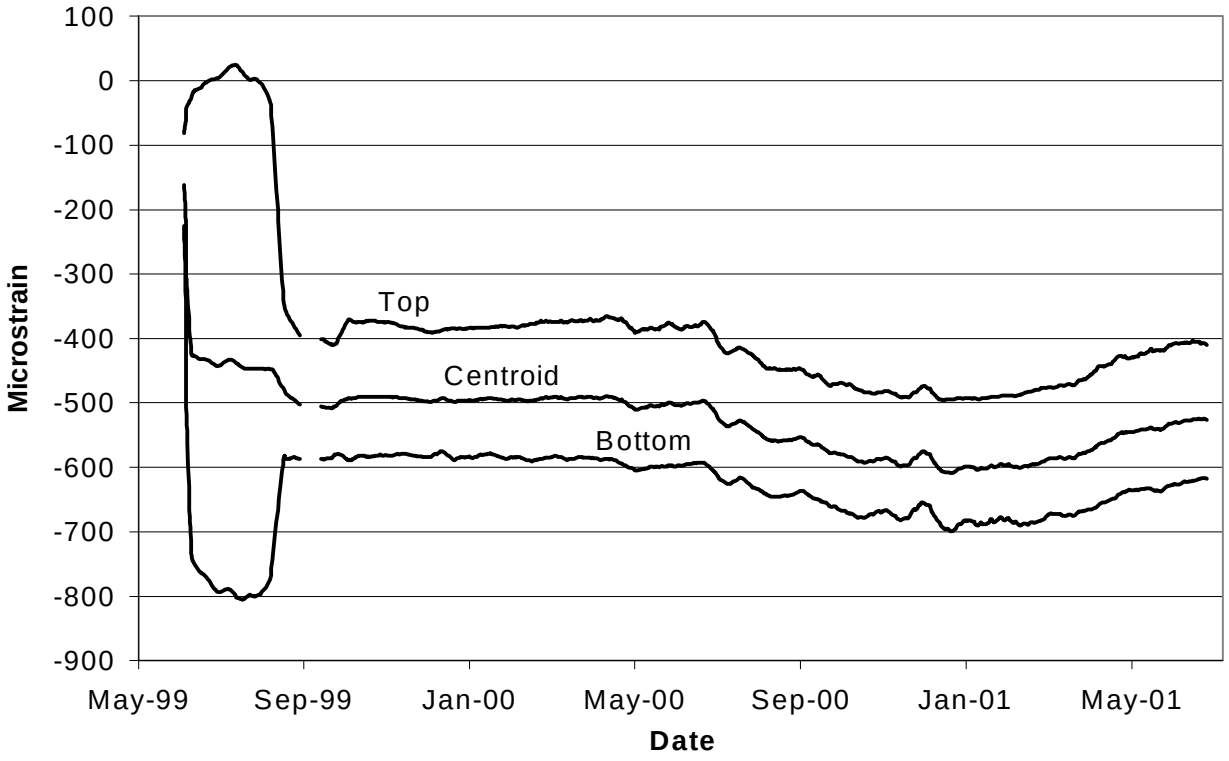

Figure 4.13: Bridge no. 1, girder daily average strain histories.

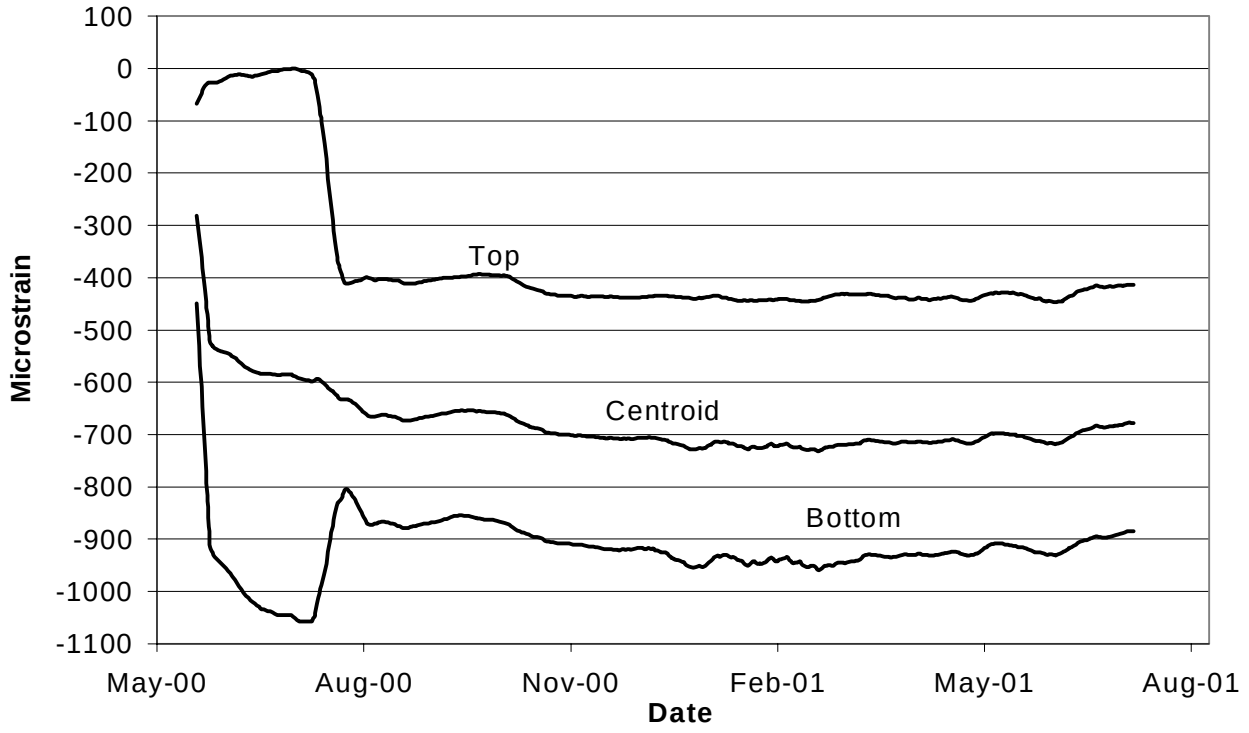

Figure 4.14: Bridge 2, Girder daily average strain histories.

After the deck is in place, the neutral axis shifts upward to a location near the top fiber of the girder. The top line in the figure can be traced to determine the time dependent changes that take place after the deck is placed. There is no significant long-term change in the graph for Bridge 1 from August 1999, through March 2000. After March 2000, it appears that a seasonal effect begins. If it is not seasonal, it is at least a long period change. It will be interesting to see if these trends are indeed long period seasonal changes, or simply a nonrecurring change. Note, that all three lines remain separated by an equal amount. This indicates the system is responding in a linear manner. Since the strains moved in a compressive direction, it indicates the beams are coming under a uniform compressive force. This behavior is interesting.

Inspecting Figure 4.14 (bridge 2 data) for this same long-term change, it is noted that the strains at the top edge of the girder do indicate a long-term change. It is noted to be about 20 to 30 με. This strain developing over an 11-month period. This indicates a further 4 to 5 percent loss in the initial prestress force. It appears that this trend tends to reverse at the end of this 11-month period. More data is needed to see if this continues; if it continues, it is the same behavior as observed in bridge 1.

There is one curious event in the strain history of bridge 1. Note the gap in the data during September 1999. A little to the right of this gap is a small but noticeable inflection in the strain registered by all three transducers. The gap itself is due to the failure of the computer sometime after Labor Day in September 1999. The computer was put back on-line in late September. The location in time of this inflection corresponds approximately to the time that the traffic was routed over the bridge. The inflection takes place over several days, perhaps ten days. The change on the top fiber of the beam is tensile which corresponds to a small increase in camber (upward deflection). In any case, it is interesting. In later analysis, it will be noted that this inflection only occurred in the outer girder.

4.9 Girder curvature analysis:

The curvature of a beam is an indicator of the radius to which the beam is bent. Specifically the curvature is the reciprocal of the radius to which the beam is flexed. In general, it changes in a continuous manner along the beam. It is defined by the following equations-

$$\phi = \frac{1}{\rho} = \frac{(\varepsilon_2 - \varepsilon_1)}{h} \qquad \text{Equ. 4.9}$$

ϕ = curvature

ρ = radius to which the beam is bent

ε_1, ε_2 = strain at the top and bottom fiber of the beam respectively.

h = the depth of the beam.

From the strain measurements, the strains at the top and bottom fiber of the beam are known. These equations are simply equations of kinematics and do not require elastic behavior of the material. A program was developed that computed the curvature in the girders from the transducer readings. There are four transducers at the center of the girder, and, as has been stated, a regression line was computed from these four readings. From this regression line the strain was computed on the top and bottom fibers of the beam. From these two values of strain, the curvatures are computed. The curvatures for the two girders (G3-A and G3-B) in bridge 1 are provided in Figure 4.15. The curvatures for the instrumented girders (G5-A and G5-B) in Bridge 2 are provided in Figure 4.16. Larger positive values of curvature indicate a tendency for

the beam to exhibit upward camber (upward deflection). A decrease in positive curvature indicates the beam is tending to exhibit downward deflection.

This positive change in curvature is noted in all four girders over the period that they were stored in the prestressing yard. In addition, the instantaneous and maximum camber are in general agreement with the deflections that were measured on these girders. From Table 4.9 it is noted that girder G3-A exhibited a maximum camber of 25.4 mm (1.00 inches) and girder G3-B exhibited a maximum camber of 23.62 mm (0.93 inches). The difference in these two values is about 3 percent. The curvature for these two girders is about 22.0 and 24.0 respectively. This is a difference of about 8 percent. This is relatively good agreement. The maximum camber noted in girders G5-A and G5-B was 31.8 mm (1.25 in.) and 30.0 mm (1.18 inches) respectively. Their two curvatures are nearly identical, as are the deflections. In both figures, the effect of the deck placement is noted by a sharp drop in curvature. The deck placement occurring in August 1999 for bridge 1 and in July 2000 for Bridge 2.

There is a sharp positive curvature change in Girder G5-B (Bridge 2) immediately after the deck was placed. This change is not mirrored in Girder G5-A. This is puzzling. If it were an elastic change, it would reflect a change of about 4.8 mm (0.19 inches) in deflection. This is not noted on the graph of deflections. This could indicate that the response was inelastic. Thereafter the two girders exhibit nearly identical curvatures.

Creep should show up as a positive or negative drift in the curvature with time. The trends in these figures reflect the observations made on the strain at the centroid of the girders. The difficulty is that it is not as easy to observe small changes in this figure due to the scale employed. For example if the curvature were about 6, then a 10 percent change would change this value by 0.6. This change not being obvious due to the scale of the graph.

The inflection that was previously noted on Figure 4.13 on Bridge 1 can be observed as a change in the curvature of Girder G3B in Figure 4.15. There may be a small corresponding change on the graph of Girder G3A, but it is very slight. This inflection results in an increase in the camber of the beam.

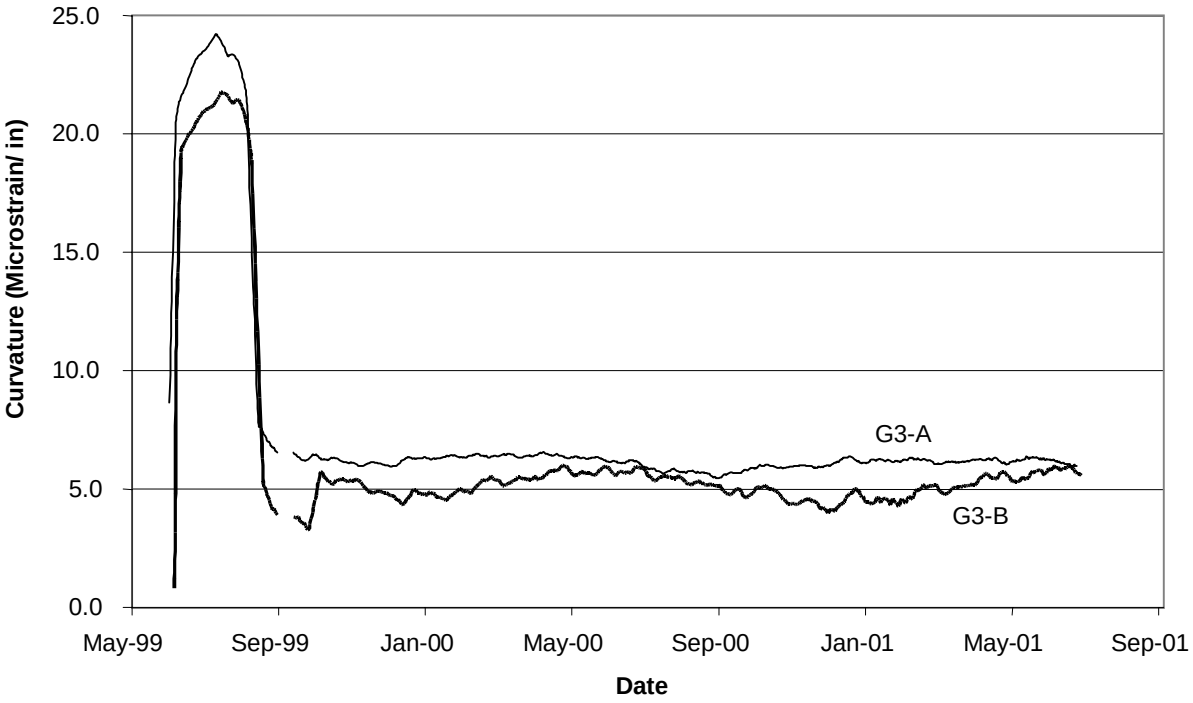

Figure 4.15: Bridge no. 1, individual girder curvature at mid-span.

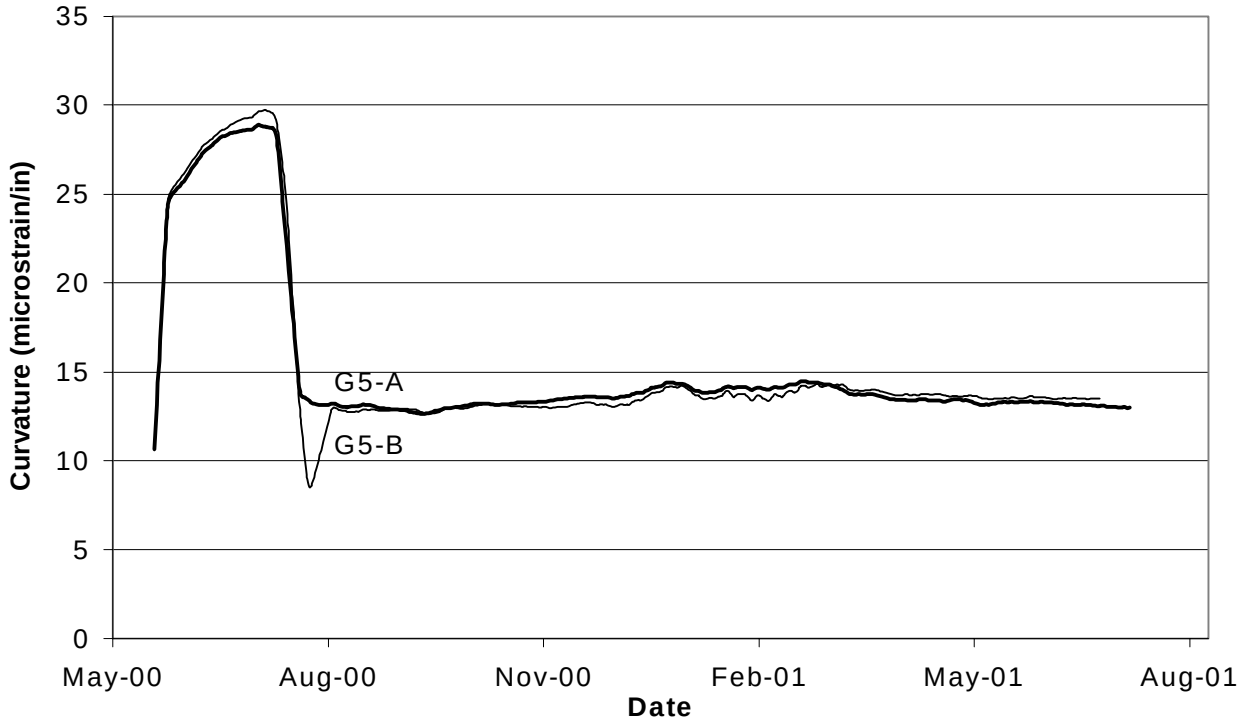

Figure 4.16: Bridge no. 2, individual girder curvature at mid-span.

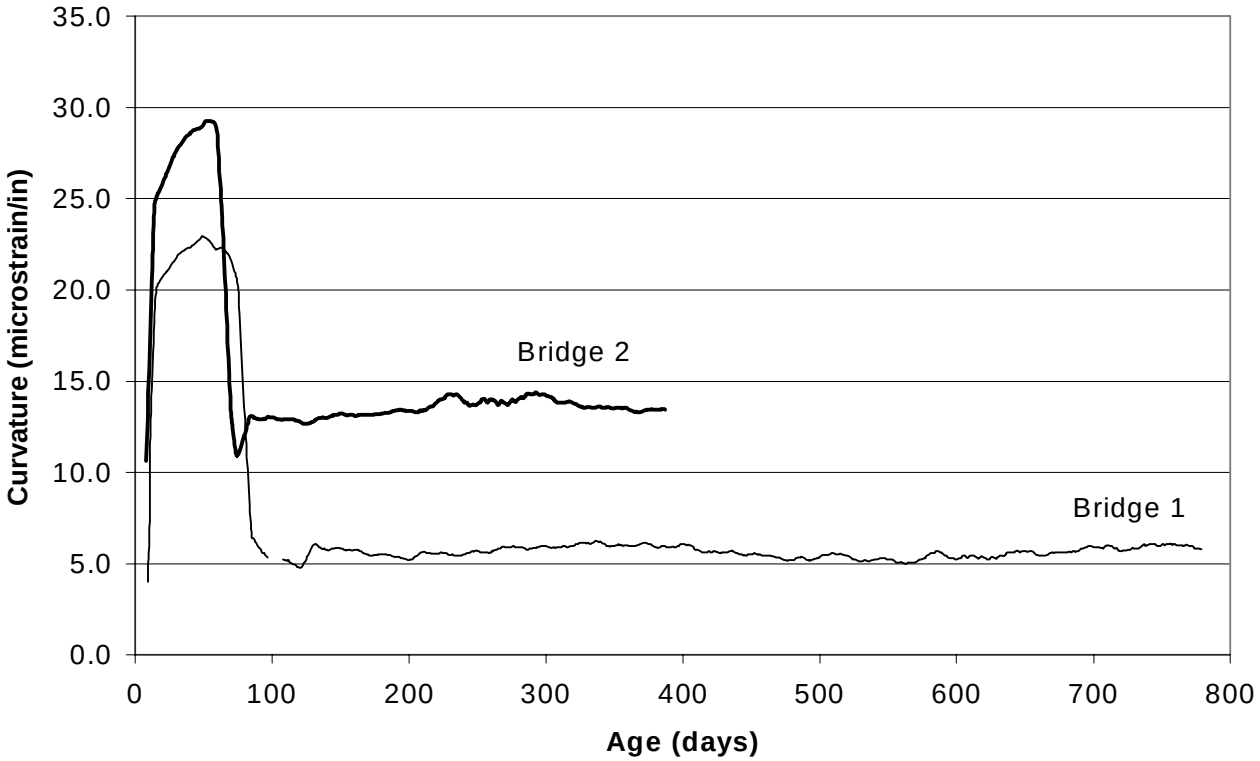

Figure 4.17: Bridges 1 and 2, average girder mid-span curvature.

The curvatures for the two separate girders in each bridge were averaged. The results of this exercise are presented in Figure 4.17. In this figure, the time scale is just days from time zero, time zero being the time of the casting of the girders. The difference between the two girder averages is easier to view in this figure. As noted previously, the camber and thus the prestress, was greater in the girders cast for bridge 2. Not only this, but the long term curvature is about double in this second set of girders as compared to the girders from bridge 1. These trends can be verified by inspecting the change in the deflections back in Figure 4.7. These also are in the same ratio.

4.10 Bent curvature analysis:

A uniformly spaced stacked set of three vibrating wire transducers was placed at the bent in the gap between the prestressed girders. As the deck is placed this region between the girders is filled with fresh concrete. This forms an integral bent diaphragm. In each bridge two sets of transducers were placed at the bent. One set was placed in the gap between the two girders located on the outside girder line. The second set was placed in the gap between the girders at

the adjacent interior girder line. The bent transducers in bridge 1 are all providing, what appears to be useable readings. In bridge 2 one of the bottom bent transducers was apparently ruined during the placement of the deck. This reduced the set of three to two transducers. The remaining two do not appear to be giving good readings. Because of these apparent poor readings, this group was not used to develop the information for the following discussion. The second set in bridge 2 is believed to be providing useable results and has been employed to develop the following results.

The bent curvatures were computed employing the same method that was used for the girder curvatures. The results are provided in Figure 4.18. The plot for bridge 1 is the most interesting. It is observed that the curvature has steadily decreased over the two years that the bridge has been monitored. This graph is the average of two locations, but both locations show this same general trend. It is possible that this curvature change is due to the higher deck shrinkage that has been noted in bridge 1. The girders are tending to come together at their tops and tending to separate at their bottom fibers. This same trend may be showing up in the second bridge, but there has not been sufficient data gathered to indicate that it is definitely taking place.

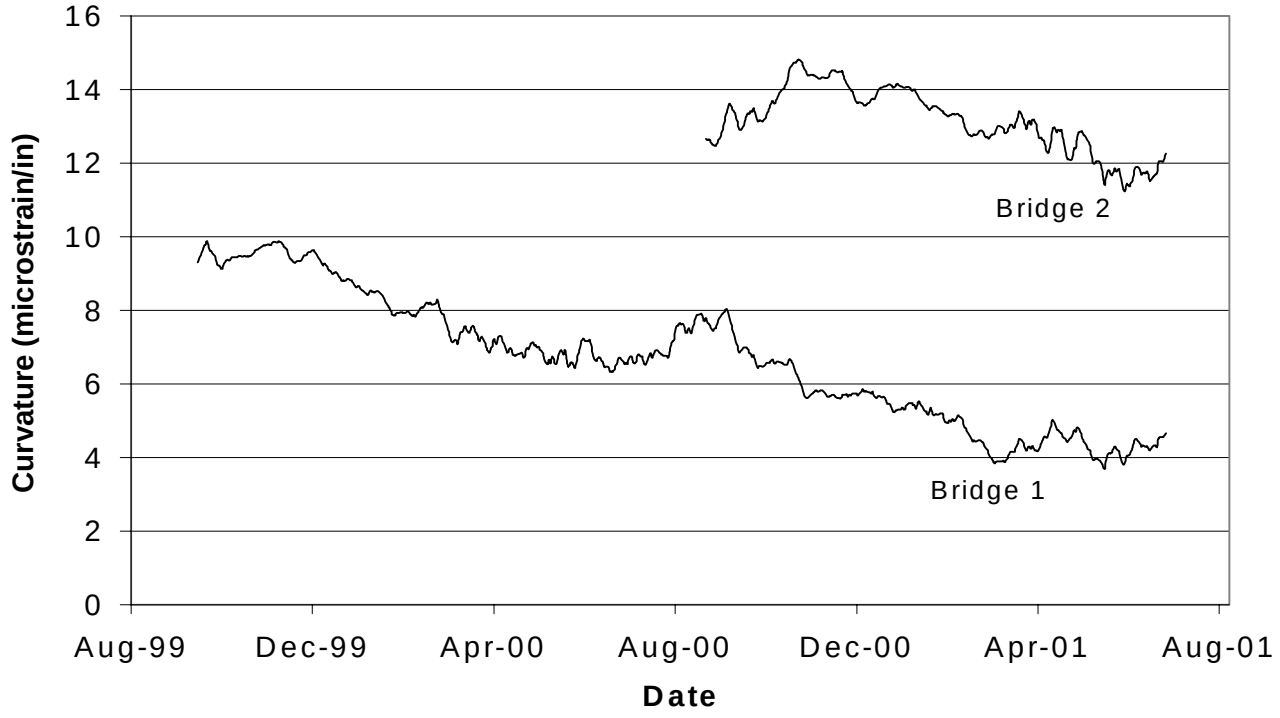

Figure 4.18: Bridges 1 and 2, curvature between the girders at the bent.

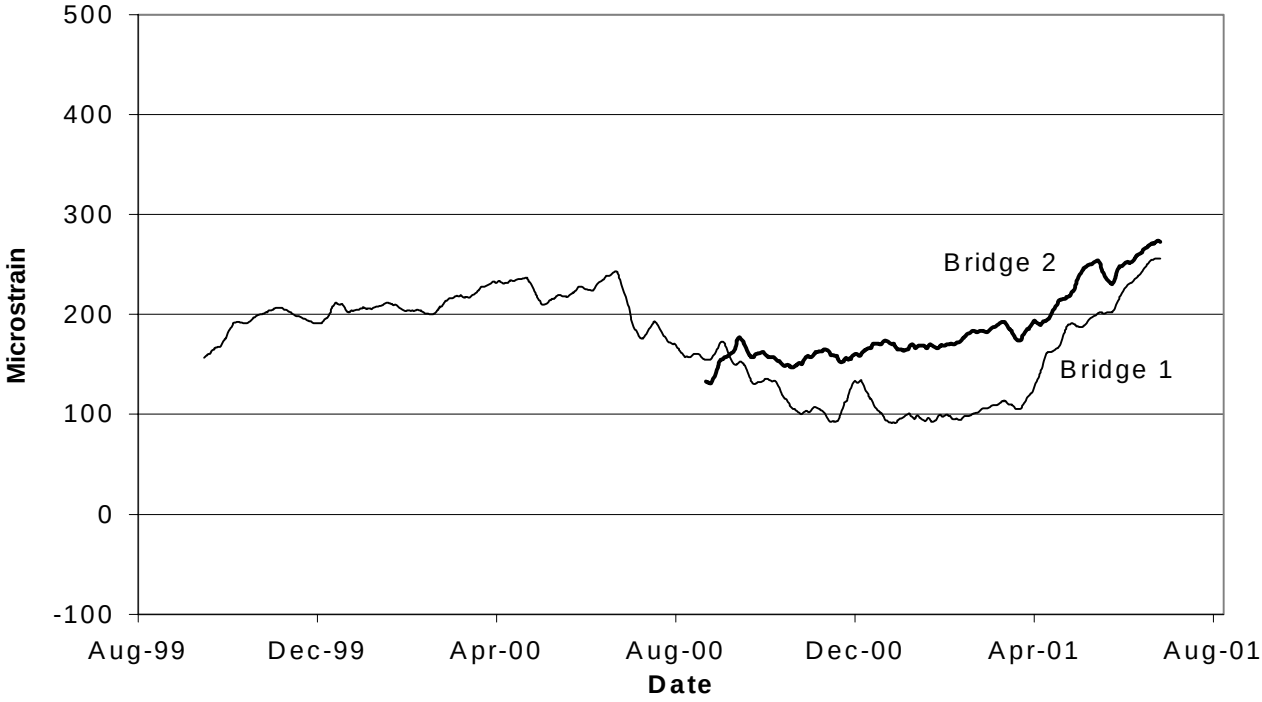

Figure 4.19: Bridges 1 and 2, centroidal strains between the girders at the bent.

One could argue that during the first year the change in curvature was about 2. Over the first year in bridge1, this change was about 2.5. More data is needed to see if this trend continues. Strain between the girders at the level of the girder centroids is plotted in Figure 4.19. This strain is relatively insensitive to the curvature. These strains demonstrate that tensile strains are developing between the girder ends at the level of the girder centroids. In this case, the two bridges are comparable. As stated, the strains between the girder ends are tensile, and vary cyclically about a value of about 175 με. More data records and further analysis are needed before one can make further comments on the behavior of the bridge at the bent locations

4.11 Deck Strains:

There are four sets of two strain transducers positioned at mid-span with a second similar array over the bent. Utilizing the two transducers that are stacked vertically in the deck, regression analysis was employed to compute the constants for an equation that would permit the computation of strain through the thickness of the deck. The strain was then computed at the

mid-depth of the deck. After the separate values were computed they were then averaged. Figure 4.20 presents the results from both bridges for the mid-span location. Figure 4.21 provides similar results over the bent.

The results before the shrinkage strains are removed are presented along with the results after the shrinkage strains are subtracted. Since the shrinkage strains are negative, subtracting them from the record results in a shift in the tensile, or positive, direction. Here as in other results, there is a long period cyclical change indicated. This cyclical change is demonstrated in both figures and is occurring in both bridges. Focusing on the net strains, after subtracting out the shrinkage strains, it is observed that overall the tensile strains are significantly higher in bridge 1 as compare to bridge 2. Bridge one has an average tensile strain of about 160 με at mid-span. The corresponding value over the bent is about 420 με. Similar results for Bridge 2 are 60 με at mid-span and 250 με over the bent. If one ratios the numbers for each bridge, the results are 2.6 for Bridge no. one and 4.2 for bridge 2. The ratios are not comparable.

The strains in the deck are interesting, but difficult to explain. They are consistent with the developing data that indicates that the silica fume deck exhibited a greater tendency to shrink and thus develop tensile stresses. On the other hand, as will be seen, there are about twice as many transverse cracks in the silica fume deck as compared to the fly ash deck, thus with cracking the tensile stresses should be reduced.

The data is consistent with a highly restrained element, which the deck seems to be. Not much is known about the creep of concrete in tension except that it certainly takes place. Additional data and further detailed analysis is needed before additional comments can be made.

4.12 Underside deck crack surveys:

Significant transverse deck cracking was noted in bridge 1 during the first winter (Early January 2000) after it was constructed. Transverse deck cracking was also noted in bridge 2 during this bridge' s first winter. In August of 2001, underside deck surveys were conducted on these two bridges. These surveys were conducted from the ground. The number of cracks was counted between each girder and along the overhangs. In some cases, a significant distance occurred between the end of the span and the first crack. When this was observed the distance to the first crack was estimated and this dimension to the first crack was taken into consideration when computing the crack spacing in that span. In general, within a span the spacing between

cracks was relatively uniform. Reasonable estimates of dimensions could be made due to the imprint of the 4x8 plywood form-sheets on the underside of the deck concrete. Nearly all of these cracks are exhibiting calcium carbonate precipitate and under appropriate winter conditions exhibit moisture seepage. This was readily observed during the winter months and was the reason that the cracks were first noted in January 2000. The results of the surveys on the two bridges are summarized in Table 4.12.

A couple of points must be noted. Consider the first bridge. The crack spacing in the end spans is about double the spacing in the center span. This same relative spacing is true as well for bridge 2. This indicates, which makes sense, that there is more restraint in the center span which contributes to greater cracking. Overall, the average crack spacing in bridge 1 is about 1.37 m (4.5 feet). The corresponding value for bridge 2 is about 2.32 m (7.6 feet). The ratio of the crack spacing in bridge 2 to the crack spacing in bridge 1 is 1.7. This is in general agreement with the shrinkage data from the two bridges. This ratio, as previously cited, is 1.6. The basic point is that there is significantly more cracking in the silica fume deck as compared to the fly ash deck and this is supported by the data that has been taken.

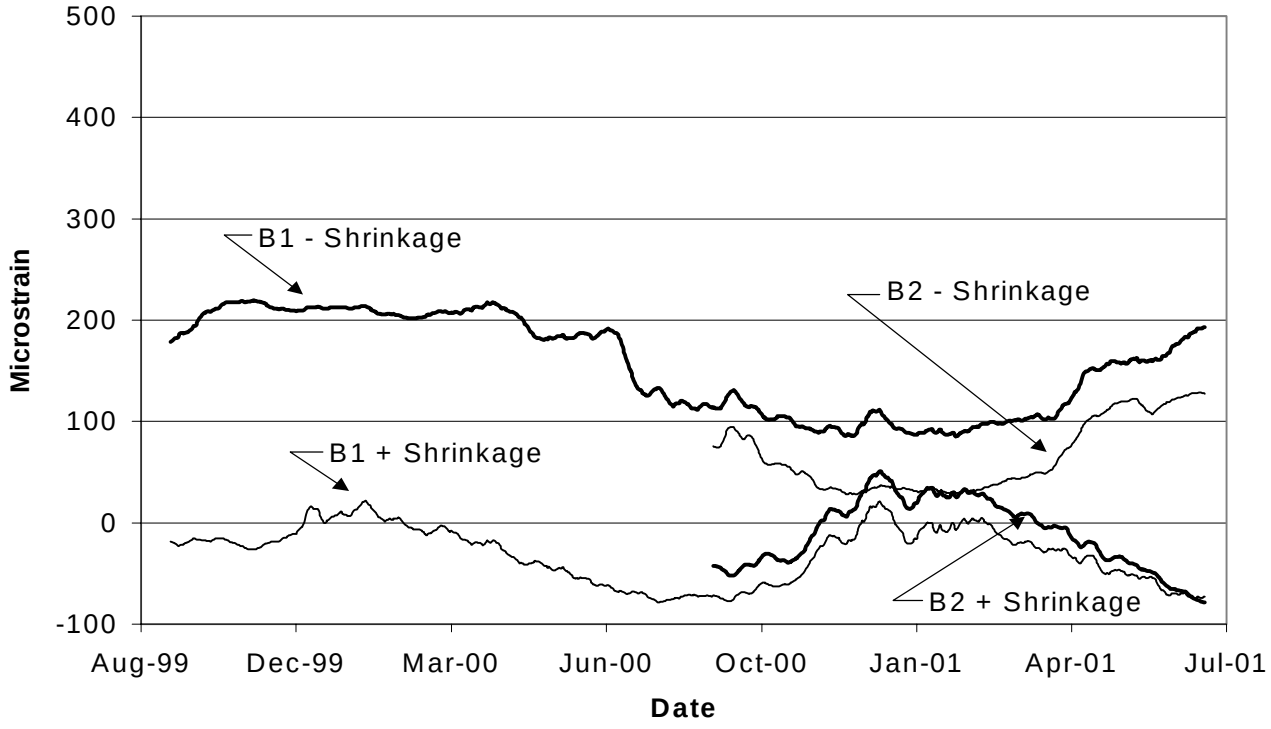

Figure 4.20: Bridges 1 and 2, mid-thickness deck strain at mid-span.

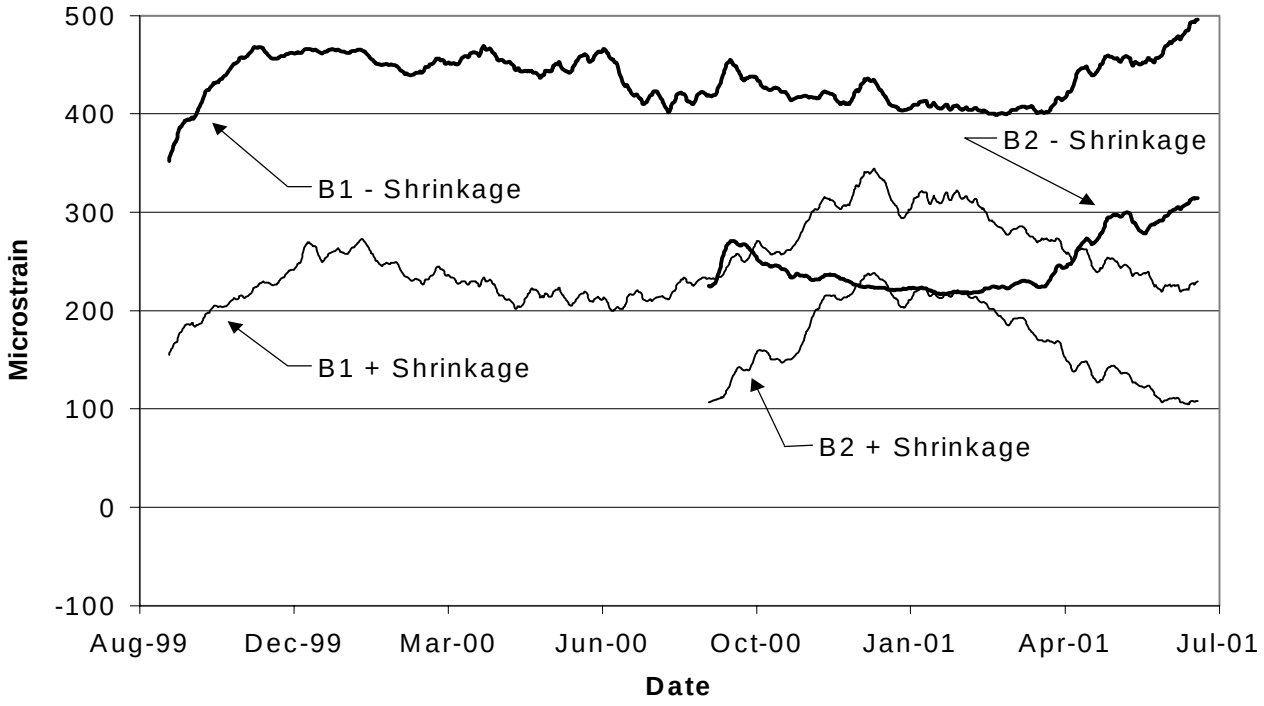

Figure 4.21: Bridges 1 and 2, mid-thickness deck strain at the bent.

Table 4.12 Bridge no 1 and 2, Summary crack data (Surveys of August 2001).

	Bridge no. 1		Bridge no. 2	
	No. of Cracks	Spacing (ft.)	No. of Cracks	Spacing (ft.)
North Span	38	6.0	17	12.9
Middle Span	82	3.3	49	5.4
South Span	43	5.5	27	8.1
Overall Data	163	4.5	93	7.6

Unit Conversions: 1 ft = 0.3048 m

4.13 Temperature analysis:

There are a large number of temperature sensors in each of these two bridges. Only summary information is presented here because detailed analyses have not been completed. The maximum temperature that was observed in the instrumented girders during the initial hydration of the concrete was essentially the same for each girder and was about 60 ^{o}C (140 ^{o}F). This peak

temperature was achieved about 16 hours after the concrete was placed. The fabricator applied supplementary heat in the form of hot water that was circulated through pipes that are directly under the beam forms. Insulating blankets were used to retain the heat in the girders.

The highest temperature that was observed during the curing of the decks was about 52.8 ^{o}C (127 ^{o}F) in the silica fume deck and about 46.1 ^{o}C (115 ^{o}F) in the fly ash deck. The high temperature in the silica fume deck was achieved about 23 hours after concrete placement. The high temperature in the fly ash deck was achieved about 27 hours after the deck was initially placed. Since silica fume hydrates very rapidly and contributes significantly to early strength gain, one would expect the silica fume mix to exhibit a higher peak temperature than the fly ash mix.

The average girder and deck temperature for bridge 1 during the summer and winter of 2000 are provided in Figures 4.22 and 4.23, respectively. Averaging all temperature transducers in the deck and performing a similar average for the girders generates these curves. The individual values are daily averages, for this reason they do not reflect the diurnal variation over the day. In addition to the data, a trend line has been imposed. As would be expected the girders are cooler than the deck.

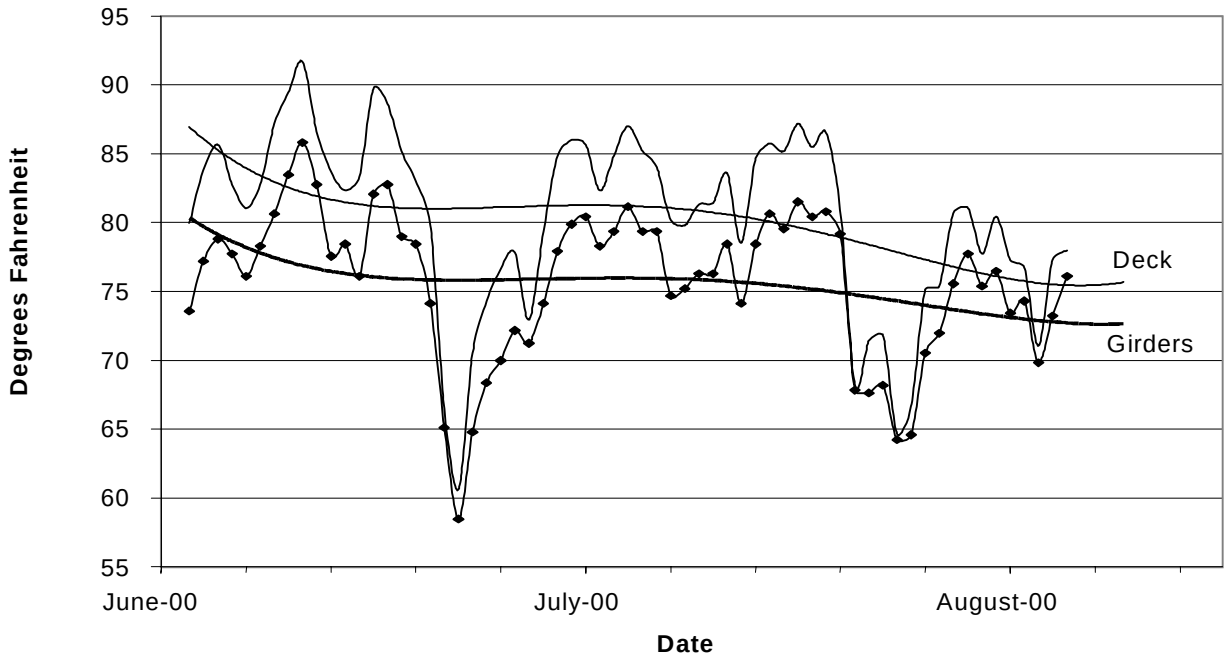

Figure 4.22: Bridge 1, average daily deck and girder temperatures during the summer of 2000.

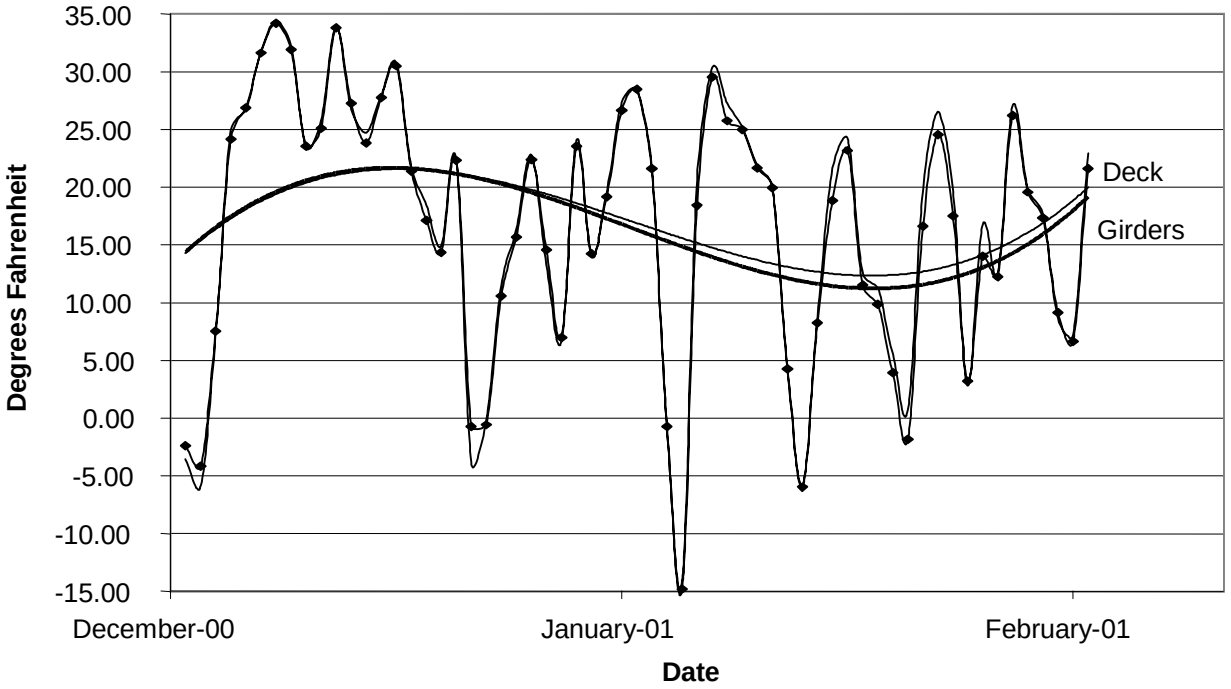

Figure 4.23: Bridge 1, average daily deck and girder temperatures during the winter of 2000.

By examining the trend line, it can be seen that in the summer the girders are about 9 ^{o}C (5 ^{o}F) cooler than the deck. This difference causes thermal gradients and will give rise to thermal stresses.

A similar graph is presented for the winter of 2000. Winter 2000 was a significant winter. It was very long and a record duration of continuous snow cover was recorded. The winter was not extremely cold, though significant stretches of cold weather occurred. As was the case in the summer, the girders are cooler than the deck. The difference though is not very much, being on the order of 1 ^{o}C (2 ^{o}F) degrees. What can not be seen in the data is the diurnal effect. This would be expected to be more significant in the deck than in the girders. The data does show that on an average basis the girders are not too much different in temperature than the deck.

4.14 Rapid Chloride Permeability

Durability of the concrete in bridge decks has a major impact on maintenance costs and the material design is of utmost importance. One of the most severe problems is the corrosion of the bridge deck reinforcing steel, aggravated by chloride ions. Penetration of the chloride ions

into and through the deck concrete, to the reinforcing steel, is a critical parameter to be controlled. The major purpose of this project is to develop the concrete mixture proportions to minimize the transport of chloride ions.

The specimens fabricated from the actual concretes used in the bridge decks, prestressed girders and trial mixes were tested for rapid chloride permeability as per ASTM C 1202. The individual test results are given in Tables 3.2 and 3.3 in Task 11. A total of 92 specimens were tested and the average values of rapid chloride permeability for the trial mix concrete, the girder concrete and bridge deck concrete are given in Table 4.13 for bridge 1 constructed in the summer of 1999 and the corresponding values obtained for bridge 2 constructed during the summer of 2000 are given in Table 4.14.

4.14.1 Bridge Deck Concrete

The comparison of the permeabilities measured for various batches of the concrete used in the construction of bridge 1 in the summer of 1999 is shown in Fig. 4.24. For this deck silica fume HPC mix was used. The values ranged from 393 to 621 coulombs. This is a very low variation, which is due to the better quality control used in the production of concrete. A similar comparison for the various batches of deck concrete used for the construction of the bridge 2 during the summer of 2000 is shown in Fig. 4.25. For this deck silica fume was omitted and fly ash was added as partial replacement for cement. The permeabilities varied from 708 to 1404 coulombs, which is again a low variability for field concrete. It shows that the same quality control was also maintained for the construction of this bridge.

The main objective of developing a HPC mix for the bridge deck construction was to reduce the chloride permeability of the concrete so that the corrosion potential of the steel reinforcement is reduced. The project' s requirement stated that "The bridge deck permeability should be reduced by a significant amount (50%) as compared to the SDDOT' S standard bridge deck mix. The average values of permeabilities for all the concretes used during the construction of both bridges are compared in Fig. 4.26. The rapid chloride permeability (average of 24 specimens) for the HPC silica fume concrete used in bridge 1 is 462 coulombs whereas the permeability of SDDOT' s standard bridge deck mix was 4158 coulombs. According to ASTM C1202, the chloride ion penetrability is "High" for SDDOT' s standard concrete and it is "Very Low" for HPC bridge concrete. This is a 88.9% reduction which has far exceeded the required 50% reduction. The chloride permeability (an average of 24 specimens) of the concrete

used for the second bridge is 1038 coulombs.

Table 4.13: Bridge 1 (Summer 1999) - Average Chloride Permeabilities of Samples taken at different times

Girder Fabrication		
Source	No. of Specimens	Total Charge Passed (Coulombs) - Average
Trial Mix 1	3	161
Trial Mix 2	5	109
Average of 8 specimens		135
Girder Fabrication 1	4	42
Girder Fabrication 2	4	75
Girder Fabrication 3	4	69
Girder Fabrication 4	4	61
Girder Fabrication 5	4	81
Girder Fabrication 6	4	61
Average of 24 specimens		65

Bridge Deck Concrete		
Source	No. of Specimens	Total Charge Passed (Coulombs) - Average
Deck Trial Placement	4	558
Deck Placement 1	4	317
Deck Placement 2	4	461
Deck Placement 3	4	621
Deck Placement 4	4	393
Deck Placement 5	4	516
Average of 24 specimens		462

There was a reduction of 75% in the chloride permeability, which is again greater than suggested. However the permeability of this fly ash mix was 123 % higher than that of the HPC mix that contained 7 percent silica fume.

Table 4.14: Bridge 2 (Summer 2000) - Average Chloride Permeabilities of Samples taken at different times

Girder Fabrication		
Source	No. of Specimens	Total Charge Passed (Coulombs) - Average
Girder Fabrication 2	4	96
Girder Fabrication 3	4	77
Girder Fabrication 5	4	89
Average of 12 specimens		87

Bridge Deck Concrete		
Source	No. of Specimens	Total Charge Passed (Coulombs) - Average
Deck Placement 1	4	782
Deck Placement 2	4	708
Deck Placement 3	4	1404
Deck Placement 4	4	1307
Deck Placement 5	4	988
Average of 24 specimens		1038

According to ASTM C1202, the chloride ion penetrability is "low" for the fly ash HPC mix used in Bridge 2. Therefore, it can be assumed that the potential for the rebar corrosion is very low for bridge 1 and low in bridge 2.

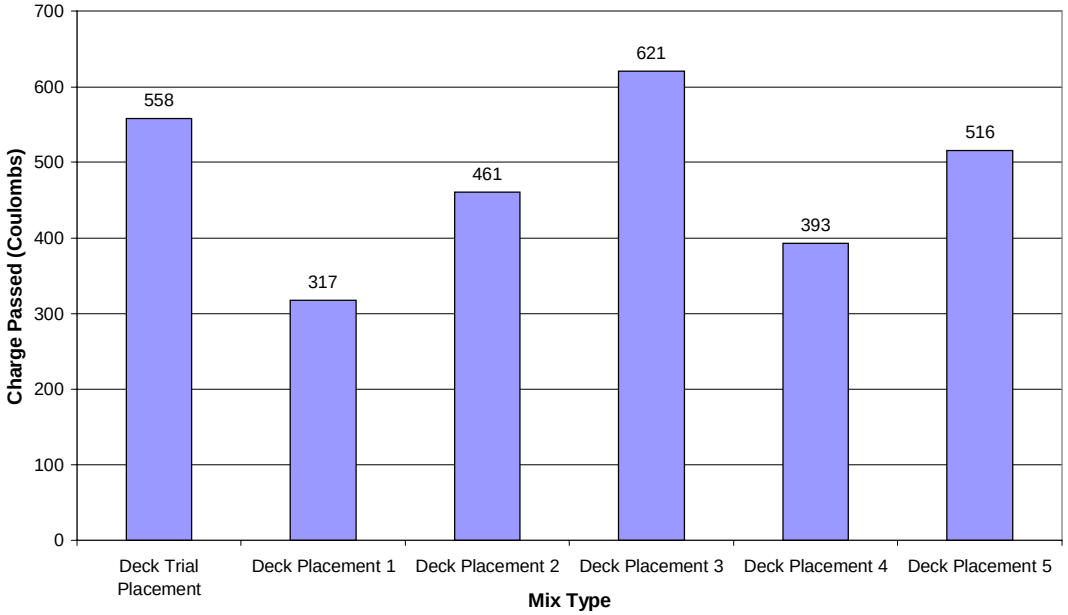

Fig 4.24: Comparison of Permeabilities for various Batches of Silica Fume Bridge Deck Concrete - Bridge 1 (Summer 1999)

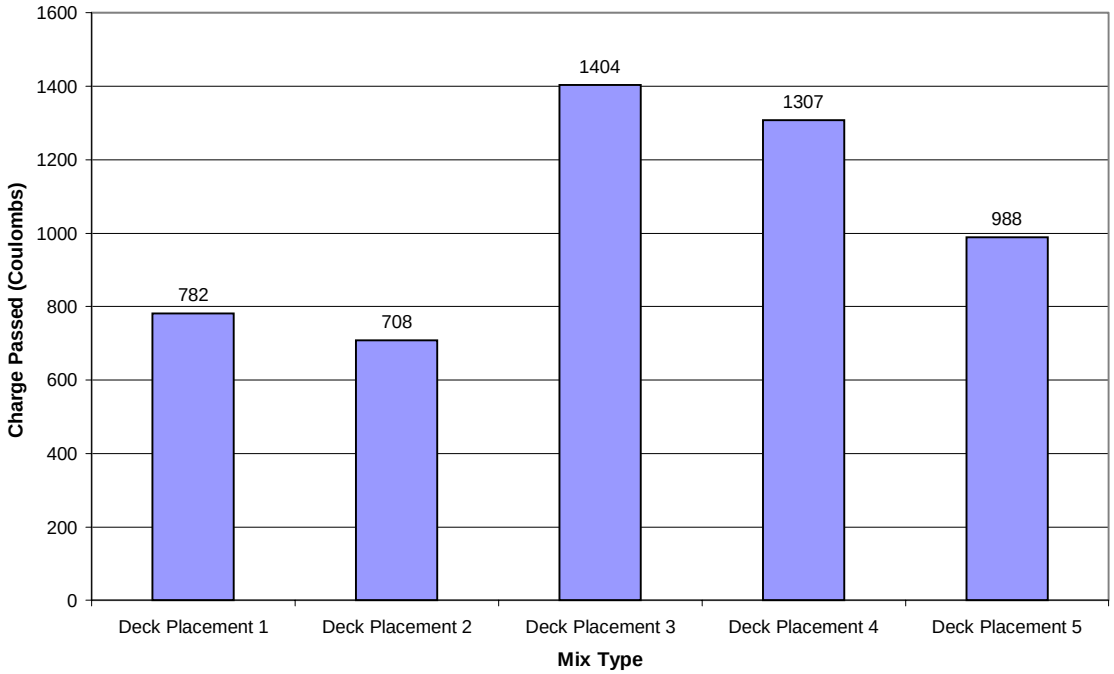

Fig. 4.25: Comparison of Permeabilities for Various Batches of Fly Ash Bridge Deck Concrete for Deck No. 2 (Summer 2000)

4.14.2 Bridge Girder Concrete

The average values of the permeabilities of concretes used in the fabrication of prestressed girders for bridge 1 and 2 are compared in Fig. 4.27 and 4.28 respectively. The permeabilities varied from 42 to 81 in bridge 1 and 77 to 96 in bridge 2. This variation can be considered reasonable for field concrete and it can be assumed that the silica fume distributed properly in the concrete. The quality control obtained in the production of HPC was good. The permeability (average of 24 specimens) for bridge 1 is 65 coulombs and the permeability (average of 12 specimens) for bridge 2 is 87 coulombs. According to ASTM C 1202 the chloride ion penetrability is classified as "Negligible". Therefore the high strength HPC could be considered as impermeable and the corrosion potential of the prestressed steel tendons is negligible.

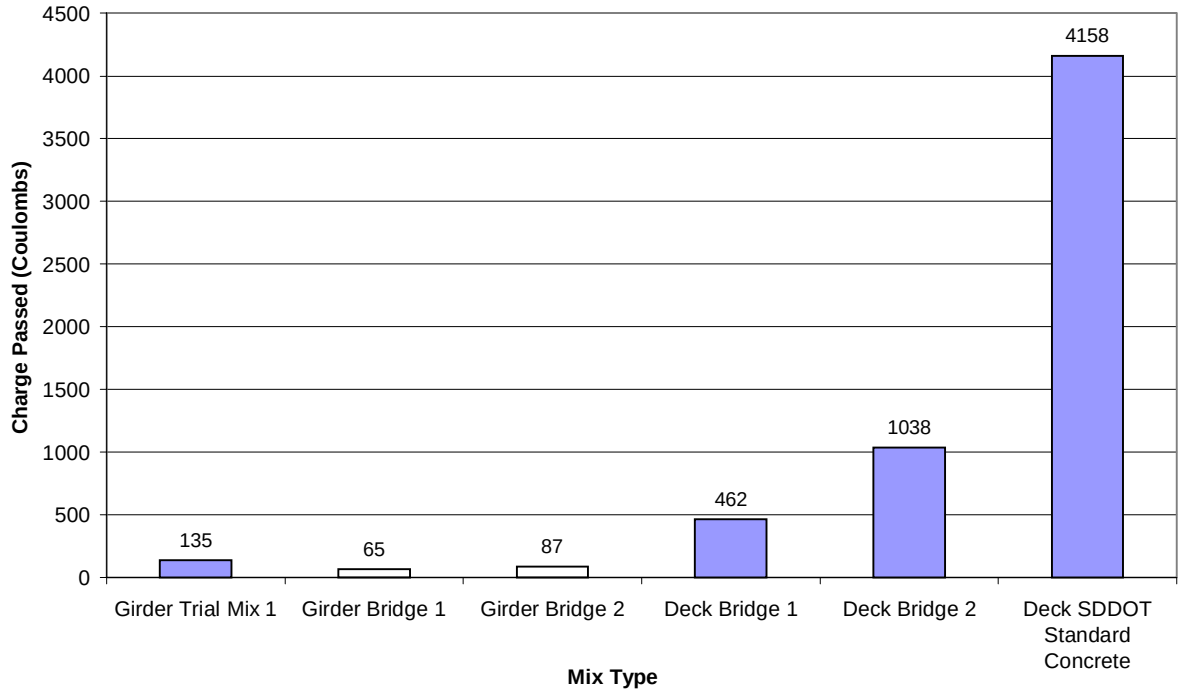

Fig. 4.26: Average Permeabilities of Bridge Deck and Girder Concrete for Bridges 1 & 2

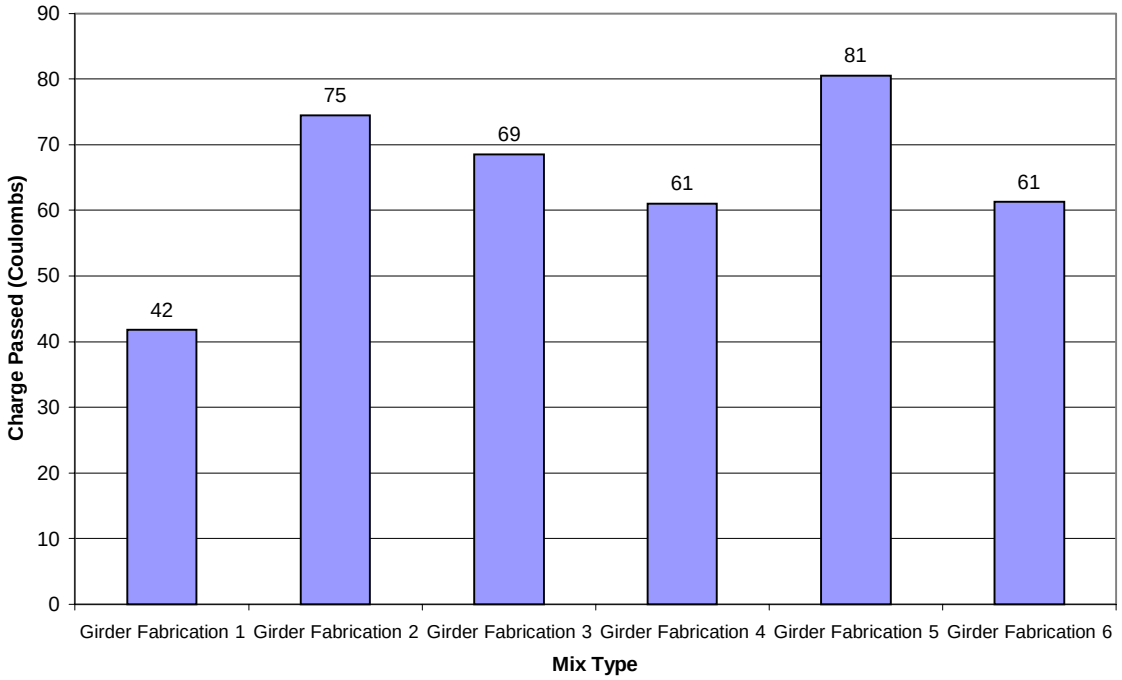

Fig. 4.27: Comparison of Permeabilities for various Batches of HPC Girder Concrete (Bridge 1 - Summer 1999)

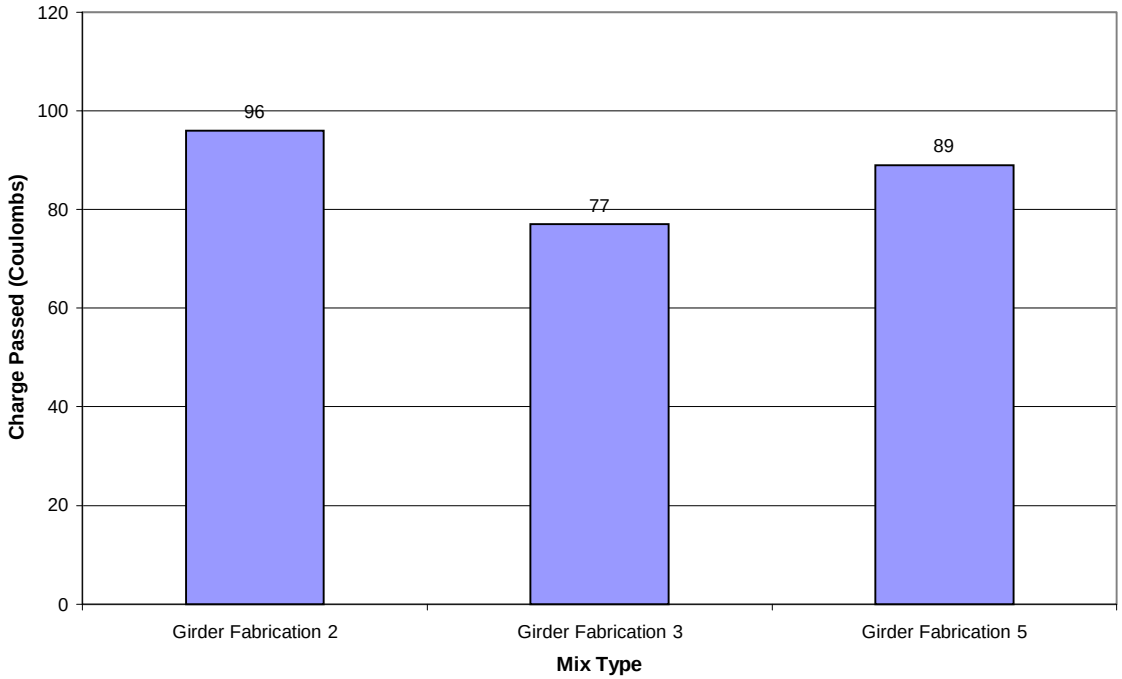

Fig. 4.28: Comparison of Permeabilities for Various Batches of HPC Girder Concrete (Bridge 2-Summer 2000)

4.14.3 Accelerated Rapid Chloride Test

Currently the 90 day rapid chloride permeability (ASTM C 1202) results are specified for bridge deck concretes by various DOT' s (14). This is too long a period to wait to know the results. Therefore accelerated curing of the specimens at a higher temperature and then testing them within a few days to determine the permeability is quicker way to get the same result. This procedure had been suggested by the Virginia DOT (14) and Malhotra (21). In this project, a comprehensive testing program was conducted to prove that it is possible to predict the 90-day rapid chloride permeability at a 7 day testing by using the accelerated curing of concrete specimens before testing for permeability. The following procedure was used for accelerated curing. The specimens were demolded after 24 hours following the ASTM specification and they were placed in an accelerated curing tank containing water maintained at a constant temperature of 38^0 C (100^0 F) for 3 days. Then they were tested for the rapid chloride permeability using the ASTM C 1202 test procedure.

4.14.4 Test Program and Regression Model: Ten mixes with quartzite aggregate with various quantities of silica fume and fly ash were made and eight specimens from each mix were fabricated from these mixes. Four specimens were subjected to accelerated curing mentioned above and tested after 7 days for rapid chloride permeability. The remaining four specimens were standard cured for 90 days and were then tested for rapid chloride permeability. The test results are given in Table 4.15.

A log-log linear model for predicting the relationship between the accelerated permeability (Y), a dependent variable, and the 90-day permeability value (X), an independent variable is presented.

$$\text{Log}(Y) = b_0 + b_1 \text{Log}(X)$$

In the above equation the constants b_0 and b_1 are evaluated by regression analysis and they are equal to -0.8307 and 1.2245 respectively. Hypothesis testing was also done to determine whether a strong and significant relation existed between Y and X. Adequacy of the regression model was assessed using the values of coefficient of correlation, conditional estimation of standard deviation and the significance-F (p-value) of the hypothesis test. Complete details of the analysis are given in Appendix C.

Table 4.15: Predicted 90 Day Permeability Values using Log-Log Linear Model

Proposed Logarithmic Model: Log Y= b_0+b_1Log X						
90 Days Coulombs (X)	**Accelerated Coulombs (Y)**	**Log X**	**Log Y**	**Pred Log Y**	**Standard Residuals**	**Pred Y**
323	132	2.51	2.12	2.24	-0.84	174.51
812	692	2.91	2.84	2.73	0.75	539.56
1207	533	3.08	2.73	2.94	-1.50	876.67
1219	1337	3.09	3.13	2.95	1.24	887.35
1774	1559	3.25	3.19	3.15	0.31	1404.85
1943	1642	3.29	3.22	3.20	0.13	1570.44
3475	4088	3.54	3.61	3.51	0.74	3200.25
4158	5566	3.62	3.75	3.60	1.01	3986.66
4704	4059	3.67	3.61	3.67	-0.40	4636.83
6831	4548	3.83	3.66	3.86	-1.44	7321.69

Table 4.16: Regression Statistics of Model for Predicting 90 Day Permeability

Proposed Logarithmic Model: Log Y= b_0+b_1Log X						
Std Deviation Sy/x	b_0 (Intercept)	b_1 (X Variable)	Coef of Correlation r	R Square	Significance F-P value	f
0.15	-0.83	1.22	0.96	0.92	1.07E-05	93.95

Table 4.16 gives the regression statistics of the developed model. The normal probability plot of the residuals is shown in Figure 4.29. The logarithmic line fit plot of permeability in coulombs due to accelerated curing (Y) with permeability in coulombs due to standard 90-day curing (X) is shown in Fig. 4.30.

This equation can be used to predict the 90-day permeability for the quartzite aggregate concretes used in this project for any compressive strength, if the accelerated permeability value is known for that concrete. This is highly advantageous because we need not wait for 90 days to know the permeability of concrete used. Some preliminary tests done with limestone aggregate seemed to agree with the suggested equation, however further extensive testing is needed to develop a universal equation applicable to all aggregates.

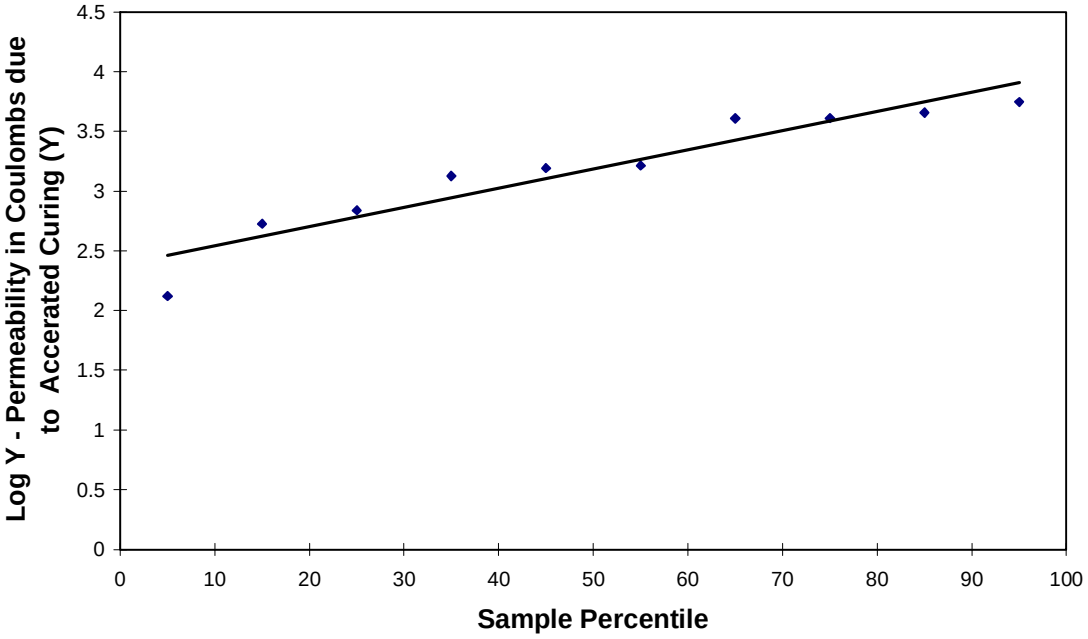

Fig 4.29: Normal Probability Plot

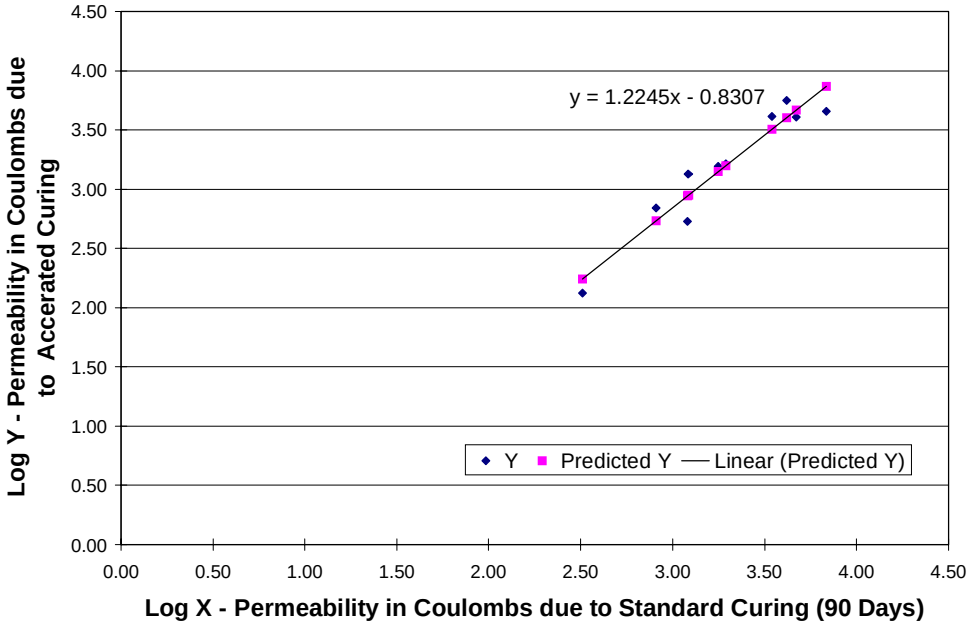

Fig. 4.30: Logarithmic Line Fit Plot of Permeability in Coulombs due to Accelerated Coulombs (Y) with Permeability in Coulombs due to Standard Curing (X)

4.15 Conclusions

Based on the test results and the observations made during the course of this investigation, the following conclusions are offered.

4.15.1 High Strength HPC Mix and Performance of Prestressed Girders

- The silica fume high strength HPC mix developed by the laboratory trial mixes and slightly modified for the field conditions and used in the fabrication of prestressed girders performed well both in the fresh and hardened states. The selected mix had 403.24 kg/m^3 (680 lb/cu.yd) cement and 49.81 kg/m^3 (84 lb/cu.yd) of silica fume with a water to cement ratio of 0.28 and water to cement + silica fume ratio of 0.25. This mix gave the required 127 to 178 mm (5 to 7 inches) slump and 4.0±1.0 % air. The coarse aggregates consisted of 19 mm (3/4 inch) Sioux falls quartzite aggregate. There was a significant increase in the compressive strength due to the addition of silica fume. This mix exceeded the specified design strength requirements of 56.9 MPa (8520 psi) at release of the strands and 68.3 MPa (9900 psi) at 28 days. This mix developed a range in stress at 28 days of 89.64 MPa (13, 000 psi) to 108.25 MPa (15,700 psi). Based on the results obtained from the field concrete used in the fabrication of the girders this high strength HPC mix could be used with design strength (28 days) conservatively set at 82.7 MPa (12,000 psi). This predicts that 95 percent of the results would break at, or higher than the design strength. This statement assumes that three cylinders be used and averaged to produce one test result, and that the test results are normally distributed.
- The modulus of elasticity of the high strength HPC mix with quartzite aggregate was higher than the SDDOT standard mixes used for prestressed girders. The modulus of elasticity for this mix can be estimated by the recommended ACI 363 equation with the substitution in this equation of 13790 MPa (2,000,000 psi) for the 6895 MPa (1,000,000 psi) constant.
- The modulus of elasticity of the high strength HPC mix with quartzite aggregate was higher than the SDDOT standard mixes used for prestressed girders. The current equation that is recommended for evaluating the modulus of elasticity of HSC is the ACI 363 equation. It has the form-

ACI equation 363:

$$E_C = \left(40{,}000\sqrt{f_c'} + 1{,}000{,}000\right)\left(\frac{w_C}{145}\right)^{1.5} \qquad \text{eq. 4-2}$$

An equation to predict the modulus of elasticity for HSC is not provided in either the current AASHTO or ACI 318 specifications. Based on the tests conducted as part of this research, and limited to mixes containing Sioux Quartzite aggregate, it is concluded that the above equation be used with the modification that the 1,000,000 constant be changed to 2,000,000. The resulting form is –

$$E_c = \left(40{,}000\sqrt{f_c'} + 2{,}000{,}000\right)\left(\frac{w_c}{145}\right)^{1.5} \qquad \text{eq. 4-3 .}$$

- The girders in bridge 1 exhibited a maximum early age (first 100 days) shrinkage of 150 με, the corresponding value for the girders of bridge 2 was 200 με. This is a variation of 25 to 30 percent. It is likely to be indicative of the variation in shrinkage that can be expected in silica fume high strength HPC. This was observed to be about half of that predicted for "so-called", standard concrete (Using the recommendations as suggested by the ACI 209 committee.)
- The loss in initial prestress for the girders due to the combined effect of creep and relaxation up to the time the deck was cast, was about 6 percent for the girders in bridge 1, and about 14 percent for the girders in bridge 2. The girders in bridge 2 exhibited an additional 4.8 percent loss from the time that the deck was placed up to the time that the girders were one year of age. Due to the form of the data record for bridge 1 it is not possible to estimate the losses in bridge 1 after the deck placement (More data is needed as the record is developing a possible periodic component). It is expected that additional losses (It is believed that their magnitude is not large.) have occurred, but their magnitude cannot be estimated at this time. Additional data and further analysis will be needed to determine a more reliable estimate of the time-dependent losses in these girders.
- The long-term curvature in bridge 2 is about double the curvature exhibited in bridge 1. This conclusion is consistent with the measured deflections. With the decks in place, these structures have not shown a tendency to develop increasing long-term deflections. It can be

concluded that this is due to the shrinkage that is occurring in the deck, which counteracts the tendency for the girders to exhibit increased camber. This conclusion is based on limited data.

- The measured curvatures taken in the gap between the girders at the bent demonstrate significant reduction over time. In bridge 1 it has been reduced from 9.5 to 4.0 (Curvature units in^{-1}, the values have been multiplied by 10^6.) over a two year time period. The results for bridge 2 show a similar trend but it is not as dramatic. The problem is that only one year of data is available from bridge 2 and more data will be needed to assess this behavior. The trend in the curvatures at the bents is difficult to explain.
- The average chloride permeability for the girders in bridges 1 and 2 were 65 and 87 coulombs respectively. According to ASTM C 1202, the chloride ion penetrability for both bridge girders is "Negligible". Therefore the high strength HPC could be considered as impermeable and the corrosion potential of the prestressed steel tendons is negligible.

4.15.2 Bridge Deck Concrete and Performance of the Decks

Based on the analysis of the trial mixes the following conclusions are made:

- The compressive strengths of concretes containing silica fume and fly ash were significantly higher when compared to plain concretes at the same w/c ratio and age. The increase in strength due to the addition of mineral admixtures was more prominent at later ages (28 day).
- There was no significant change in the modulus of rupture values for concretes containing silica fume and fly ash when compared to plain concretes at the same w/c ratio.
- The increase in static modulus values was more prominent in concretes containing just silica fume when compared with plain concrete at the same w/c ratios.
- There was no significant change in the compressive strength due to variation in the type of coarse aggregate used. Almost all the mixes containing limestone aggregate showed higher modulus of rupture values when compared to the same mixes containing quartzite aggregate.
- There was a significant reduction in the chloride permeability values in concretes containing silica fume when compared to plain concretes at the same w/c ratios. The reduction was more prominent in the concretes containing just silica fume than the concretes containing a combination of silica fume and fly ash. Concretes containing just fly ash showed higher

chloride permeabilities when compared to concretes with silica fume but lower chloride permeabilities when compared to plain concretes.

- The results of the rapid chloride permeability tests carried out on specimens, subjected to accelerated curing showed a good correlation with the results obtained from the tests carried out at 90-days.
- All mixes containing mineral admixtures showed low workability and hence water reducers were used to obtain the required workability. The addition of the water reducers did not affect the strength.

Based on the test results of the field concrete used in bridge 1 and 2, the following conclusions are offered:

- The 28 day compressive strengths obtained were, silica fume trial mix 61.5 MPa (8910 psi), silica fume mix for bridge 1- 48.8 MPa (7070 psi), fly ash mix for bridge 2 - 46.6 MPa (6760 psi). At 90 days, both concretes had the same compressive strength 53.5 MPa (7760 psi). The 1-year compressive strengths were silica fume mix for bridge 1-57.6 MPa (8350 psi), fly ash mix for bridge 2- 62.4 MPa (9040 psi). Both mixes had much higher strength than the design 28-day strength 31 MPa (4500 psi). This is about 50% higher strength than the required strength. At 28 days, the silica fume mix used in the bridge deck yielded a 5 percent greater strength than the fly ash mix used in bridge deck no. 2. At one year the fly ash mix yielded compressive strength results 7 percent higher than the silica fume mix. This was as expected.
- The silica fume deck concrete exhibited 1.6 times more early age shrinkage strain than the fly ash concrete mix. This contributed to the greater deck cracking than was observed in the fly ash deck concrete.
- Both decks tended to develop significant tensile strains. On average the silica fume deck developed average tensile strains 1.9 times greater than the average tensile strains that were measured in the fly ash deck.
- There was a higher heat of hydration and higher temperatures during the early curing period in silica fume concrete as compared to the fly ash concrete.
- A coefficient of thermal expansion of $13.5 \times 10^{-6}\ ^{o}C^{-1}$ ($7.5 \times 10^{-6}\ ^{o}F^{-1}$) can be used with confidence for silica fume and fly ash mixes representative of those studied in this research.

- The crack survey data demonstrate that there was 1.7 times more cracking in the silica fume deck as compared to the fly ash deck. This is in general agreement with the deck tensile strain data.
- The fly ash mix is considered to be better for deck use than the silica fume mix because of the fly ash concrete' s tendency to develop lower shrinkage strains and thus develop fewer cracks. A further negative for the silica fume mix is that it requires much more care during the placing and curing of the concrete. For this reason, silica fume concrete is likely to cost more than fly ash concrete.
- The rapid chloride permeabilities as measured from the ASTM C 1202 test for the silica fume bridge deck concrete ranged from 393 to 621 coulombs and for fly ash concrete used in bridge deck 2 varied from 708 to 1404 coulombs. The average permeability (24 specimens) for silica fume concrete was 462 coulombs whereas the permeability of SDDOT' s standard bridge deck concrete was 4158 coulombs. This is 88.9 % reduction which had far exceeded the required 50% reduction. The average permeability (24 specimens) for the fly ash concrete was 1038 coulombs which was a reduction of 75%. The permeability of fly ash concrete was 123 % higher than that of the silica fume concrete containing 7 percent silica fume.
- According to ASTM C1202, the chloride ion penetrability is "very low" for the silica fume concrete and "low" for the fly ash concrete. It is concluded that the potential for rebar corrosion is low for both silica fume and fly ash concretes.

4.15.3 Cost

- The cost of the superstructure for the bridges was the same on a first cost basis for both the HPC bridge and the normal concrete SDDOT present design bridge. However the life cycle cost might be cheaper for the HPC bridge because of the anticipated longer life and reduced maintenance cost.
- The use of HPC allowed designers to reduce the number of girders in each span from five to four. However the thicker deck needed due to the wider girder spacing negated the savings realized in the girders.

4.16 Recommendations

Prestressed Girders:

1. For the fabrication of prestressed girders, when compressive strengths greater than 62 MPa (9000 psi) are required, the high strength silica fume HPC should be specified. The 28-day design compressive strength could be specified as high as 82.7 MPa (12,000 psi), but the fabricator would want the concrete to reach the release strength in a few days for production purposes. Therefore the mix should be designed to reach the fabricator' s required release strength in the specified number of days.

   The feasibility of producing and using high strength silica fume HPC mix had been successfully demonstrated in this project. The concrete was almost impermeable and hence the corrosion potential was eliminated. The anticipated benefits are less number of girders, less deflection, less prestress loss due to creep and shrinkage.

2. Based on extensive testing of trial mixes and analysis, the following mix proportions are recommended for high strength girder concrete. This mix was used for a design strength (f_c') of 68.3 MPa (9900 psi) and the average strength obtained was 99.3 MPa (14,400 psi). The fabricator wanted to achieve the specified strand release strength of 56.9 MPa (8250 psi) in 3 days.

Cement (Type II)	403.24 kg/m^3	680 lbs./pcy
Water included from Silica fume slurry and HRWR	112.67 kg/m^3	190 lbs./pcy
Coarse aggregate (3/4" quartzite)	1082.23 kg/m^3	1825 lbs./pcy
Fine aggregate (S.S.D)	683.16 kg/m^3	1200 lbs./pcy
Silica fume	49.81 kg/m^3	84 lbs./pcy
Air Content	4.0±1.0%	4.0±1.0%
Water to Cement ratio	0.28	0.28
Water/C+S.F. ratio	0.25	0.25

Note: The recommended slump was 127 to 178 mm (5 to 7 inches). The dosage of High Range Water Reducer (HRWR) and/or water reducer should be adjusted according to the field conditions to achieve the specified slump. The 19mm (3/4 inch) quartzite aggregate used in this project conformed to the standard specifications for Roads and Bridges, Section 820 for Size No. 1 (SDDOT). The mixing water should be adjusted taking into account the excess water present in the silica fume slurry and the high range and mid range water reducers.

3. The equation currently recommended for calculation of modulus of elasticity (E_c) for HSC is the ACI 363 equation:

$$E_c = \left(40{,}000\sqrt{f_c'} + 1{,}000{,}000 \right)\left(\frac{w_c}{145} \right)^{1.5}$$

Based on the modulus of elasticity (ASTM C469) tests conducted as part of this research and limited to mixes containing Sioux Quartzite aggregate, it is recommended that the above equation be modified by changing the 1,000,000 constant to 2,000,000. Therefore the recommended formula becomes:

$$E_c = \left(40{,}000\sqrt{f_c'} + 2{,}000{,}000\right)\left(\frac{w_c}{145}\right)^{1.5}$$

It is recommended that the ACI 363 equation be used without modification for mixes containing limestone aggregates since the research was not conducted on mixes containing limestone aggregate.

Bridge Deck:

4. For the construction of bridge decks, the Class F fly ash concrete which was successfully used in the construction of bridge deck 2, should be specified for future deck concrete. Compared to plain deck concrete, the benefits of using fly ash deck concrete as demonstrated in this project, are substantial reduction in the chloride ion penetrability (a "low" value as per ASTM C1202), reduced corrosion potential, higher modulus concrete, reduced plastic shrinkage, reduced drying shrinkage, reduced restrained shrinkage cracking in the underside of the deck slabs, reduced early temperature rise due to the hydration activity, less micro-cracking, higher durability, better workability, and good finishability. This fly ash concrete developed smaller tensile stress in the deck than the silica fume concrete. All these benefits could be realized without an increase in cost.
5. The recommended bridge deck concrete mix proportions are given below.

Cement (Type I/II)	349.87 kg/m^3	590 lbs./cu.yd.
Fly ash (Class F)	74.53 kg/m^3	124 lbs./cu.yd.
Water	151.22 kg/m^3	255 lbs./cu.yd.
Fine aggregate (sand)	724.65 kg/m^3	1222 lbs./cu.yd.
Coarse aggregate (rock)	968.96 kg/m^3	1634 lbs./cu.yd.
Percent air	6.5%±1.0%	6.5%±1.0%
Water/C ratio	0.432	0.432
Water/C+FA ratio	0.357	0.357

Note: Appropriate quantity of water reducer either mid range or high range should be used to obtain the specified slump. The mixing water should be adjusted taking into account the excess water in the water reducer used. An appropriate amount of air entraining agent should be used to obtain an air content of 6.5±1 %.

The 28-day design compressive strength could be specified as 37.9 MPa (5500 psi) because this mix gave an average compressive strength of 46.2 MPa (6700 psi) at 28 days. According to ACI 318, for a design strength (f_c') of 37.9MPa (5500 psi), the required average strength

would be (5500+1200) 6700 psi. This higher design strength could be used in the design of the deck slab to reduce the thickness. Based on the performance of the bridge decks in bridges 1 and 2, the fly ash mix is deemed better for deck use than silica fume mix. There is apparently no economical way to efficiently control the shrinkage, and thus the tendency to produce cracks in the silica fume mix.

6. Where higher strength concrete is not needed and when the design compressive strength of 31 MPa (4500 psi) is required then the following Class F fly ash concrete could be used for both limestone and quartzite aggregate. This recommendation is based on the ongoing research "Determination of Optimized Fly Ash Content in Bridge Deck and Bridge Deck Overlay Concrete: SD00-06". When this mix is used the chloride ion permeability at 90 days (ASTM C1202) would be reduced more than 50 percent compared to Class A bridge deck concrete currently used.

Cement Type I/II	291 kg/m^3	491 lbs./cu.yd.
Fine Aggregate	652 kg/m^3	1100 lbs./cu.yd.
Coarse Aggregate	1023 kg/m^3	1725 lbs./cu.yd.
Water	155 kg/m^3	262 lbs./cu.yd.
Fly Ash	97 kg/m^3	164 lbs./cu.yd.
Percent air	6.5%±1.0%	6.5%±1.0%
Water to Cement ratio	0.53	0.53
Water/C+S.F. ratio	0.40	0.40

Note: The appropriate amount of air entraining agent should be used by the contractor to obtain the specified air content.

7. For bridge deck concrete, the rapid chloride permeability at 90 days, as determined by the ASTM C 1202 test, should be specified for accepting the concrete. The specification should require that the charge passed should be less than 2000 coulombs at 90 days testing, which ensures the "low" chloride ion penetrability. The major objective of this project was to develop a mix proportion to reduce the chloride permeability by 50 percent. The fly ash deck concrete used in the project achieved a 75% reduction in the chloride permeability.
8. In cases where the w/c ratios are very low (in the range of 0.28 to 0.32) and mineral admixtures such as silica fume and fly ash are in use, high range water reducers are recommended. In cases where the w/c ratio is around 0.40, mid range water reducers may be sufficient. Addition of large quantities of mid range water reducers lowers the rate of strength gain.
9. It is strongly recommended that, whenever silica fume is used in bridge deck concrete, a proper 100% humid curing for 5 to 7 days is necessary to minimize shrinkage cracking. This

could be achieved with continuous water sprays or misting and/or fogging devices. The same construction procedures for mixing, transporting, placing, consolidating, finishing and tining used for construction with standard concrete should be followed. The same construction techniques and equipment without major modification could be used for the construction of HPC bridge decks.

General:

10. When silica fume is used in a slurry form, the slurry should be sampled and tested while being continuously agitated, before use and at specified intervals during the concrete production. The amount of silica fume in the slurry could be determined by the hydrometer test. Because the silica fume is suspended in water (not dissolved), there is an inevitable tendency for the silica fume to settle to the bottom. To avoid this a continuous agitation of the liquid with proper instruments is recommended. The water in the slurry should be accounted for and the mix water should be adjusted.
11. When HPC mixes are used, it is recommended that the following quality control tests should be conducted in the field using ASTM test procedures for the fresh concrete: slump, unit weight, air content, and the concrete temperature. The ambient temperature, humidity, and the wind velocity should be recorded during the bridge deck concrete placement or the fabrication of the prestressed girders. The compressive strength and static modulus tests should be conducted on the field samples collected and cured according to the ASTM standard procedures at 28 days. When HPC is used for fabricating prestressed girders, it is recommended that companion cylinders (preferably 102 mm × 204 mm (4" × 8")) should be placed near the girder and cured under identical conditions as the girders, to determine when the prestressed strands can be released as per specifications. When chloride permeability is specified, the hardened concrete samples made from the actual concrete placed should be tested for rapid chloride permeability at 90 days as per ASTM C 1202. The cylinder samples can be made in the field and cured as per standard ASTM procedures for 28 days.
12. These two bridges should continue to be monitored by using the already installed instrumentation and by visual observation. Only limited data, (one-year for bridge 2, and two years for bridge 1) have been gathered. To determine the long term behavior, several years of monitoring is required.

References

1. Edward G. Nawy., “Fundamentals of High-Performance Concrete”, Second Edition., John Wiley & sons, Inc , 2001
2. Zia, Paul., Leming, M.L., Ahmad, S., H., “High Performance Concrete, A State – of – the – Art Report”, SHRP-C/FR-91-103.
3. Ramakrishnan, V., “Evaluation of Non-Metallic Fiber Reinforced Concrete in PCC Pavements and Structures”, Interim Report SD94-04, submitted to SDDOT, September 1995.
4. Russell, H.G., "ACI Defines High-Performance Concrete", From the Technical Activities Committee, Concrete International, *ACI Journal*, V.21, No.2, Feb. 1999, pp.56-57.
5. Russell, H.G., "High strength Concretes in Bridges- History And Challenges", Proceedings of the PCI/FHWA, *International Symposium on High Performance Concrete*, New Orleans, Luisiana, October 20-22, 1997, pp.27-38.
6. Aiticin, P., C., Baalbaki, M., "Candian Experience in Producing and Testing HPC", International Workshop on High Performance Concrete, Publication SP-159, ACI Bangkok, Thailand, November 1994, pp. 295-308.
7. Leming, M.L., Ahmad, S.H.;Zia,P.; Schemmel, J.J,; Elliot, R.P., and Naaman, A.E.,. "High Performance Concretes: An Annotated Bibliography 1974-1989" SHRP-C307, Strategic Highway Research Program, National Research Council, Washington, D.C. 1990.
8. Russell,H.G., “High Performance concrete Applications in North America”, International Conference on High Performance High Strength Concrete: Material Properties, Structural Behaviour and Field Applications, Perth, Australia, 1998.
9. Zia, P, Leming, M.L., Ahmad, S.H.; "Research on High Performance Concrete", Proceedings of Conference on the United States Strategic Highway Research Program. The Institution of Civil Engineers, London, October 29-31, 1990, pp.63-75.
10. Aiticin, P.-C., and Nivelle, A., "High Performance Concrete Demystified", Concrete International, *ACI Journal*, V.15, No.1, Jan. 1993, pp.21-26.
11. Ozyildirim, C., "HPC Bridge Decks in Virginia", Concrete International, *ACI Journal*, V.21, No.2, Feb. 1999, pp.58.
12. Waszczuk, M.C., and Juliano, M.L.,"Application of HPC in a New Hampshire Bridge", Concrete International, *ACI Journal*, V.21, No.2, Feb. 1999, pp.60.
13. Beacham,M., "HPC Bridge Deck in Nebraska", *University and government join forces*, Concrete International, *ACI Journal*, V.21, No.2, Feb. 1999, pp.66.
14. Ozyildirim, C., "Permeability Specification for High Performance Concrete Bridge Deck", A Report Virginia Transportation Research Council
15. Ralls,M.L, "Texas HPC Bridge Decks ”, New durable mix specification used", Concrete International, *ACI Journal*, V.21, No.2, Feb. 1999, pp.63.
16. Russell, H.G., “Long-term Properties of High-strength concretes,” Concrete Technology today, Portland Cement Association, Vol.14, No.3, November 1993, pp. 1-3.
17. ACI Committee 363, “State-of-the-art Report on High-strength Concrete” (ACI 363 R-84), American Concrete Institute, Detroit, 48 pp.
18. Nawy,E.G., “Fundamentals of High Strength High Performance Concrete”, Longman Group Limited,1996
19. ACI Committee 226, " Use of Fly Ash in concrete", *ACI Report 226.3R-87* American Concrete Institute, Detroit, 1990, pp. 1-29.
20. Berry, E.E., and Malhotra,V.M.,"Fly Ash for use in Concrete-A critical Review", *Proceedings, ACI Journal*, Vol.77 No.2, American Concrete Institute, Detroit, pp.59-73.
21. Sivasundaram, V.,Carette,G.G., and Malhotra, V.M.,"Mechanical Properties, Creep, and Resistance to Diffusion of chloride Ions of concrete Incorporating High Volumes of ASTM Class F Fly Ash From Different Sources", *MSL Diviision Report 89-126 (J)*, Energy, Mines, Resources Canada, Ottawa,1989.
22. Sivasundaram, V.,Carette,G.G., and Malhotra, V.M., "Properties of Concrete Incorporating Low quantity of Cement and High Volumes of Low-Calcium Fly Ash", *ACI SP114* Vol.1, ed. V.M.Malhotra, ACI Detroit, pp.45-71.
23. Carette,C.G., and Malhotra,V.M., "Long-Term strength Development of silica Fume Concrete", *Proceedings CANMET/ACI 4th International Conference on Fly Ash, silica Fume, Slag and Natural Pozzolans in Concrete*, Istanbul. ACI SP-132 Vol.2, ed. V.M.Malhotra, ACI, Detroit, pp.1017-1044.

24. Ramakrishnan, V., "Properties and Applications of Latex Modified Concrete", *Proceedings CANMET International Conference on Advances in Concrete Technology*, ed. V.M.Malhotra, Ottawa, Ontario, 1992, pp.839-890.
25. ASTM C 1202-94, "Standard Test Method for Electrical Indication of Concrete's Ability to Resist Chloride Ion Penetration", *ASTM Standards*, June 1994, pp.622-627.
26. Proove it, " Instruction and Maintenance Manual, PR-1090, Version 1.2", Germann Instruments, Inc.
27. Whiting, D., "Permeability of Selected Concretes," Permeability of Concrete, SP-108, American concrete Institute, Detroit, 1988, pp.195-222.
28. Perraton, D.,Aiticin, P.C., and Vezina, D.,"Permeabilities of Silica Fume Concrete," Permeability of Concrete, SP-108, American concrete Institute, Detroit, 1988, pp.63-84.
29. Ozyildirim, C., Halstead, W., "Resistance to Chloride Ion Penetration of Concretes containing Fly Ash, Silica Fume or Slag," Permeability of Concrete, SP-108, American concrete Institute, Detroit, 1988, pp.35-62.
30. Mobasher, B., Mitchell, T.,M., "Laboratory Experience with The Rapid Chloride Permeability Test," Permeability of Concrete, SP-108, American concrete Institute, Detroit, 1988, pp.117-144.
31. Marusin, S.,L.," Influence of Superplasticizers, Polymer Admixtures, and Silica Fume in Concrete on Chloride Ion Permeability", Permeability of Concrete, SP-108, American concrete Institute, Detroit, 1988, pp.19-34.
32. Janssen, D.,J., "Laboratory Permeability Measurement," Permeability of Concrete, SP-108, American concrete Institute, Detroit, 1988, pp.145-158.
33. NCHRP Report 410,"Silica fume Concrete for Bridge Decks", National Cooperative Highway Research Program, TRB, Washington, D.C.,1998
34. Smith, D. C. "The Promise of High-Performance Concrete." Business Insurance, 31 (14), 1997, pp. 31-39.
35. Adelman, D., and Cousins, T.E. "Evaluation of the Use of High Strength Concrete Bridge Girders in Louisiana." PCI Journal, (2), 1990, pp. 70-78.
36. Goodspeed, C. H., Vanikar, S., and Cook, R.A. "High Performance Concrete Defined for Highway Structures." Concrete International, 18 (2), 1996, pp. 62-67.
37. Mehta, P.K. and Monteiro, P.J.M., Concrete: Structure, Properties, and Materials 2nd Ed. (Prentice-Hall, Englewood Cliffs, New Jersey, 1993, pp. 154-159.
38. Pauw, A. "Static Modulus of Elasticity of Concrete as Affected by Density." ACI Journal, 57 (6), 1960, pp. 679-687.
39. Carrasquillo, R., Nilson, A., and Slate, F. "Properties of High Strength Concrete Subject to Short-Term Loads." ACI Journal, 78 (3), 1981, pp. 171-178.
40. Iravani, S. "Mechanical Properties of High-Performance Concrete." ACI Materials Journal, 93 (5), 1996, pp. 416-426.
41. Imbsen, R.A. "Thermal Effects in Concrete Bridge Superstructures", Transportation Research Board, National Research Council, Washington, D.C., 1985.
42. Mindess, S., and Young, F.J., Concrete, Prentice-Hall, Inc., Englewood Cliffs, NJ, 1981, 671 PP.
43. Smadi, M. M., Slate, F. O., and Nilson, A. H., "Shrinkage and Creep of High-, Medium-, and Low-Strength Concretes, Including Overloads." ACI Materials Journal, 84 (3), 1987, pp. 224-234.
44. Lachemi, M., Bois, A., Miao, B. Lessard, M., and Aitcin, P. "First Year Monitoring of the First Air-Entrained High-Performance Bridge in North America." ACI Structural Journal, 93 (4), 1996, pp. 379-386.
45. Yonezawa T., Mitsui K., Tezuka M., and Kinoshita M. "Application of 100 MPa High-Strength, High-Fluidity Concrete for a Prestressed Concrete Bridge with Span-Depth Ratio of 40." PCI/FHWA International Symposium on High Performance Concrete, New Orleans, Louisiana; Ed. by Johal, L. S., Precast/Prestressed Concrete Institute, Chicago, Illinois, 1997.
46. Shing, P. B., Cooke, D., Frangopol, D. M., Leonard, M. A., McMullen, M.L., and Hutter, W. "Colorado Showcase on HPC Box-Girder Bridge: Development and Transfer Length Tests." PCI/FHWA International Symposium on High Performance Concrete, New Orleans, Louisiana; Ed. by Johal, L. S., Precast/Prestressed Concrete Institute, Chicago, Illinois, 1997.
47. Nabil Bouzoubaa and Mohan Malhotra. V., "Performance of Lab-Produced HVFA-Blended Cements in Concrete", Volume 23, No.4, Concrete International, April 2001, pp. 29.
48. Nabil Bouzoubaa.; Zhang, M.H.; Bilodeau, A.; and Malhotra. M. V., "Effect of the grinding on the Physical Properties of Fly Ashes", Cement and Concrete Research, V. 27, No.12, Dec. 1997, pp. 1861-1874.
49. Bilodeau, A.; and Malhotra. M. V., "High Performance Concrete Incorporating Large Volumes of ASTM Class F Fly Ash", High Performance Concrete: Proceedings, ACI International Conference, Singapore, SP-149, V. M. Malhotra, ed., American Concrete Institute, Farmington Hills, Mich., Nov. 1994, pp. 177-193.

50. Nabil Bouzoubaa.; Zhang, M.H.; Bilodeau, A.; and Malhotra. M. V., "High-Volume Fly Ash-Blended Cement: Status Report", EPRI Report TE-114025, Electric Power Research Institute, Palo Alto, Calif., Oct. 1999, pp. 25.
51. Nabil Bouzoubaa.; Zhang, M.H.; Bilodeau, A.; and Malhotra. M. V., "Mechanical Properties and Durability of Concrete made with High-Volume FlyAsh-Blended Cement Using a Coarse Fly Ash", CANMET Report MTL 99-19(J), NATURAL Resources Canada, Ottawa, July 1999, pp. 25.
52. A. Peled; M. F. Cyr; and S. P. Shah., "High Content of Fly Ash (Class F) in Extruded Cementitious Composites", ACI Materials Journal, Vol. 97 No. 5, Sept-Oct 2000, pp. 509.
53. V. M. Malhotra; M. H. Zhang; P. H. Read; and J. Ryell., "Long Term Mechanical Properties and Durability Characteristics of High Strength/High Performance Concrete Incorporating Supplementary Cementing Materials under Outdoor Exposure Conditions", ACI Materials Journal, Vol. 97 No. 5, Sept-Oct 2000, pp. 518.
54. Khayat. K. H., "Optimization and Performance of Air-Entrained, Self Consolidating Concrete" ACI Materials Journal, Vol. 97 No.5, Sept-Oct 2000, pp. 526-535.
55. Malhotra V. M., and Ramezaniapour A.A., "Fly Ash in Concrete, Second Edition", Applications and Case Histories, CANMET, September 1994, pp 236-237.

ADDITIONAL BIBLIOGRAPHY

56. Aiticin, P.C., and Mehta, P.K., "Effect of Coarse Aggregates Characteristics on Mechanical Properties of High-strength Concrete", *ACI Materials Journal,* V.87, No.2, Mar.-Apr. 1990,pp.103-107.
57. Aiticin, P.-C., and Lessard, M., "Canadian Experience with Air-entrained, High Performance Concerte", *ACI Concrete International,* V.16, No.10, October 1994, pp.35-38.
58. Beacham,M.,"High Performance Concrete Lead state Team Activities- An Overview", Presented at the 1999 Spring Convention, ACI, Chicago Illinois, March 14-19, 1999.
59. Bush,T.D.,Russell,B.W.,Freyne,S.F.,"High Performance Concretes Using Oklahoma Aggregates", Proceedings of the PCI/FHWA ,*International Symposium on High Performance Concrete,* New Orleans, Luisiana, October 20-22, 1997, pp.84-95.
60. Evans, E.P.," High Perfromance Concrete from Laboratory to Construction Site", International Conference on High Performance High Strength Concrete: Material Properties, Structural Behaviour and Field Applications, Perth, Australia, 1998.
61. Fidjestol, P., Kojundic,T.," High-Performance Prefabricated Silica Fume Concrete for Infrastruture", Proceedings of the PCI/FHWA, *International Symposium on High Performance Concrete,* New Orleans, Luisiana, October 20-22, 1997, pp.159-171.
62. Hoff, G.C.,"The Hibernia Offshore Platform – A major application of High-Performance Concrete", International Conference on High Performance High Strength Concrete: Material Properties, Structural Behaviour and Field Applications, Perth, Australia, 1998.
63. Lwin,M.M.,"Use of High Performance Concrete in Highway Bridges in Washington State", Proceedings of the PCI/FHWA,*International Symposium on High Performance Concrete,* New Orleans, Luisiana, October 20-22, 1997, pp.657-668.
64. Malhotra,V.M.,"High-Performance High-Volume Fly Ash Concrete", International Conference on High Performance High Strength Concrete: Material Properties, Structural Behaviour and Field Applications, Perth, Australia, 1998.
65. Mather, B.,"Concrete in Transportation: Desired Performance and Specifications",Transactions No. 1382, Transportation Research Board, National Research Council, Washington, D.C., 1993, pp.5-10.
66. Mitchell,D., Aiticin,P.C., Bickley,J.A.," High-Performance Concrete Bridges: The Canadian Experience", Proceedings of the PCI/FHWA,*International Symposium on High Performance Concrete,* New Orleans, Luisiana, October 20-22, 1997, pp.355-367.
67. Moore, J.A.,"High-Performance Concrete for Bridge Decks", *Introduction: HPC Lead State Teams share data,* Concrete International, *ACI Journal,* V.21, No.2, Feb. 1999, pp.58.
68. Myers,J.J., Touma, W.E., Carrasquillo, R.L.," Permeability of High Performance Concrete: Rapid Chloride Ion Test Versus Chloride Ponding Test", Proceedings of the PCI/FHWA,*International Symposium on High Performance Concrete,* New Orleans, Luisiana, October 20-22, 1997, pp.268-282.
69. Navalurkar, R.K., and Ansari, F.,"Tensile Properties of High-Performance Concrete", International Workshop on High Performance Concrete, Publication SP-159, ACI Bangkok, Thailand, November 1994, pp. 283-294.

70. Ramakrishnan. V.,"Flexural Fatigue Performance Characteristics of High Performance Lightweight Concrete", International Conference on High Performance High Strength Concrete: Material Properties, Structural Behaviour and Field Applications, Perth, Australia, 1998.
71. Rangan,B.V.,"High-Performance High-Strength Concrete: Design Recommendations", *State-of-the-Art in HPHSC,* Concrete International, *ACI Journal,* V.20, No.11, Nov. 1998, pp.63-68.
72. Zia, P.,"State-Of-The-Art Of HPC: An International Perspective", Proceedings of the PCI/FHWA, *International Symposium on High Performance Concrete,* New Orleans, Luisiana, October 20-22, 1997, pp.49-59.
73. Zia, P, Leming, M.L.; Ahmad, S.H.; "Mechanical Behaviour of High Performance Concretes, Volume I, Summary Report", SHRP C-361, Strategic Highway Research Program, National Research Council, Washington D.C. 1993.
74. Adam Neville.; "Standard Test Methods: Avoid the Free-For-All", Volume 23, No.5, Concrete International, May 2001, pp 60.
75. Neville, A.M.; *Properties of Concrete*, 4th Edition John Wiley and Addison Wesley Longman, 1996.
76. "Fly Ash – Types and Benefits',Url. http://www.flyash.com/I_flyash.htm.
77. "Fly Ash in Ready Mix Concrete", Url. http://www.irmca.com/tipofthe/tipofo4.htm.
78. "Fly Ash Concrete", Sustainable Building Source Book, Url. http://www.greenbuilder.com/sourcebook/flyash.html11#CSI.
79. "Concrete, Fly Ash, and the Environment", Environmental Building News, Url. www.buildinggreen.com/features/flyash/shell.html.
80. Russell, H.G., " High-Strength Concrete Research for Buildings and Bridges," International Workshop on High Performance Concrete, Publication SP-159, ACI Bangkok, Thailand, November 1994, pp. 375-383.
81. Ahmad, S., H., and Zia, Paul, "High Performance Concretes for Highway Applications," International Workshop on High Performance Concrete, Publication SP-159, ACI Bangkok, Thailand, November 1994, pp. 335-350.
82. Davis, R. E., Carlson, R.W., Kelly, J.W., and Davis, H.E. 1937 "Properties of cements and concretes containing fly ash" Journal of the American Concrete Institute, 33: 577-612.
83. Stanton, T. E. "Expansion of concrete through reaction between cement and aggregate", Transactions of the American Society of Civil Engineers, Part 2, 1942, pp.68-85.
84. Bloem, D.L. "Effect of fly ash in concrete", National Ready Mixed Concrete Association, Silver Springs, MD, Bulletin 48, 1954.
85. Davis, R.E. "Pozzolanic material- With special reference to their use in concrete pipe", American Concrete Pipe Association, Technical Memo, 1954.
86. Brink, R.H., and Halstead, W.J. "Studies relating to the testing of fly ash for use in concrete", Proceedings of the American Society for Testing and Materials, 1956, pp. 56: 1161-1206.
87. Welsh, G.B., and Burton, J. R. "Sydney fly ash in concrete" Commonwealth Engineer (Jan.), 1958, pp. 62-67.
88. Pepper, L., and Mather, B. "Effectiveness of mineral admixtures in preventing excessive expansion of concrete due to alkali- aggregate reaction", Proceedings of American Society of Testing and Materials, 1959, pp. 59: 1178-1202.
89. Campbell, L. "Aggregate and fly ash in concrete for Barkley Lock", Proceedings of American Society for Civil Engineers, 1961, pp. 87: 1-16.
90. Grieb, W.E., and Woolf, D.O. "Concrete containing fly ash as a replacement for portland blast furnace slag cement", Proceedings of American Society of the American Society for Testing and Materials, 1961, pp. 1143-1153.
91. ASTM Committee m-H. "Co-operative tests of fly ash as an admixture in portland cement concrete", Proceedings of American Society of the American Society for Testing and Materials, 1962, pp. 314-348.
92. Tynes, W .0 "Fly ash and water reducing admixtures for articulated concrete mattress" U .S Army Corps of Engineers, Waterways Experiment Station, Vicksburg, MS, Miscellaneous Paper, 1962, pp. 6-473
93. ACI Committee 201. "Durability of concrete in service" Journal of the American Concrete Institute, 1962, pp. 59: 1771-1784.
94. Larson, T.D. "Air entrainment and durability aspects of fly ash concrete", Proceedings of American Society of the American Society for Testing and Materials, 1964, pp. 866-886.
95. Daniels, F., and Alberty, R., Physical Chemistry, 3rd Edition, Chapter 11, pp. 394-397, Wiley, New York, 1967.
96. Dikeou, J.T. "Fly ash increases resistance of concrete to sulphate attack", Bureau of Reclamation, Denver, Co, Water Resources Technical Publication, Research Report 23, 1970.
97. Lovewell, C.E. and Hyland, E. J. "Effects of combining two or more admixtures in concrete", 50th Annual Meeting of the Highway Research Board, Washington, DC, Jan.1971, Ctte. A2-E5.

98. Rehsi, S.S. "Studies on Indian fly ashes and their use in structural concrete", Proceedings 3rd lnternational Ash Utilization Symposium, Pittsburgh, PA, Mar. 13-14, 1973, Bureau of Mines, Washington, DC, Information Circular IC 8640,pp. 231-245.
99. Elfert, R.J. "Bureau of Reclamation experiences with fly ash and other pozzolans in concrete" Proceedings, 3rd International Ash Utilization Symposium, Pittsburgh, PA, Mar. 13-14, 1973, Bureau of Mines, Washington, DC, Information Circular IC 8640,pp. 80-93.
100. Samarin, A., and Ryan, W.G.J. "Experience in use of admixtures in concrete containing cement and fly ash" Proceedings, Workshop on the Use of Chemical Admixtures in Concrete, University of New South Wales, Sydney, Australia, Dec.1975, pp.91-112.
101. Gebler, S and Klieger, P. "Effect of fly ash on the air-void stability of concrete" In Proceedings, 1st International Conference on the Use of Fly Ash, Silica Fume,Slag, and Other Mineral By- products in Concrete, Montebello, PQ, July 31- Aug.5, 1983. Edited by V.M. Malhotra. American Concrete Institute, Detroit, MI, Special Publication SP-79, pp.103-142.
102. Dunstan, E. R. "Performance of lignite and sub-bituminous fly ash in concrete" - A progress report, Bureau of Reclamation, Denver, Co, Report REC- ERC -76-1, 1976.
103. Clear, K.C., "Time-to-Corrosion of Reinforcing Steel in Concrete Slabs", Report No.FHWA-RD-76-70, April, 1976.
104. Slater, I., Lankard, D., and Moreland, P.I., "Electro-Chemical Removal of Chlorides from Concrete Bridge Decks", Materials Performance, Vol. 15, No.11, 1976, pp. 21-26.
105. Morrison, G.L., Virmani, Y.P., Stratten, F.W., and Gilliand, W.I., "Chloride Removal and Monomer Impregnation of Bridge Deck Concrete by Electro-Osmosis", Report No.FHWA KS-RD-71-1, 1976.
106. Owens, P. L. "Fly ash and its usage in concrete", Concrete: The journal of the Concrete Society, 1979, 13: 21-26.
107. Stuart, K.D., Anderson, D.A., and Cady, P.D. "Compressive strength studies of portland cement motors containing fly ash and superplasticers", Cement and Concrete Research, 1980, 10: 823-832.
108. Oberholster, R.E., and Westra, W. B. "The effectiveness of mineral admixtures in reducing expansion due to alkali- aggregate reaction with Malmesbury Group aggregates", Proceedings, 5th International Conference on Alkali- Aggregate Reactions in Concrete, Cape Town, South Africa, 1981, Mar.30- Apr. 3.
109. Whiting, D., "Rapid Determination of the Chloride permeability of Concrete", Report No. FHW A-RD-811119, Federal highway Administration, Washington, D. C, 1981.
110. Goro, S., and Roy, D.M., "Diffusion of ions Through Hardened Cement Paste", Cement and Concrete Research., Vol. 11, No.516, 1981, pp. 751-757.
111. Manmohan, D., and Mehta, P.K. "Influence of pozzolanic, slag and chemical admixtures on pore size distribution and permeability of hardened cement pastes", Cement, Concrete and Aggregates, 1981, 3: 63-67.
112. Ramakishnan, V., Coyle, W.V., Brown, J., Tlustus, A., and Venkataramanujam, "Performance characteristics of concretes containing fly ash", In Proceedings Symposium on Fly Ash Incorporating in Hydrated Cement Systems. Edited by S.Diamond. Materials Research Society, Boston, MA, 1981. pp. 233-243.
113. Short, N. R., and Page, C. L. "The diffusion of chloride ions through portland and blended cement pastes", Silicates industriels, 1982, 47: 237-240.
114. Kantitakis, I.M. "Permeability of concrete containing pulverized fuel ash", Proceedings of 5th International Symposium on Concrete Technology, Nuevo Leon, Mexico, Mar. 1981, Department of Civil Engineering, University of Nuevo Leon, Monterrey, Mexico, 1982, pp. 311-322.
115. Brown, J.H. "The strength and workability of concrete with PFA substitution", Proceedings of the International Symposium on the Use of PFA in Concrete, University of Leeds, Leeds, U.K, Apr.14-16, 1982. Edited by J.G. Cabrera and A.R Cusens.Department of Civil Engineering, University of Leeds, Leeds, U.K, pp. 151-161.
116. Mather, K. "Current research in sulphate resistance at the Waterways Experiment Station", Proceedings of George Verbeck Symposium on Sulphate Resistance of Concrete. American Concrete Institute. Detroit, MI, Special Publication SP- 77, 1982, pp. 63-74.
117. Perenchio, W .F., and Marusin, S.L., "Short -Term Chloride Penetration into Relatively Impermeable Concretes", Concrete International, Vol. 5, No.4, April, 1983, pp. 37-41.
118. Whiting, D., "In Situ Measurement of the Permeability of Concrete to Chloride Ions", SP 82-25, Proceedings CANMET/ACI International Conference on In Situ/Nondestructive Testing of Concrete, ed. v. M. Malhotra, Ottawa, Canada, October, 1984, pp. 501-524.
119. Kasai, Y., Matsui, I., Fukushima, U., and Kamohara, H. "Air permeability and carbonation of blended cement mortars", Proceedings of 1st International Conference on the Use of Fly Ash, Silica Fume, Slag, and Other

Mineral By- products in Concrete, Montebello, PQ, July 31- Aug.5, 1983. Edited by V.M. Malhotra. American Concrete Institute, Detroit, MI, Special Publication SP-79, 1983, pp.435-451.

120. Sturrup, V.R., Hooton, R.D., and Clendenning, T.G. "Durability of fly ash concrete", In Proceedings, 1st International Conference on the Use of Fly Ash, Silica Fume, Slag, and Other Mineral By- products in Concrete, Montebello, PQ, July 31-Aug.5, 1983. Edited by V.M. Malhotra. American Concrete Institute, Detroit, MI,Special Publication SP- 79, pp.47-69.
121. Virtanen,j. "Freeze-thaw resistance of concrete containing blast furnace slag, fly ash and condensed silica fume", Proceedings of 1st International Conference on the Use of Fly Ash, Silica Fume, Slag, and Other Mineral By- products in Concrete,Montebello, PQ, July 31- Aug.5, 1983. Edited by V.M. Malhotra. American Concrete Institute, Detroit, MI, Special Publication SP- 79, 1983, pp.923-942.
122. Helmuth, R. A. "Water- reducing properties of fly ash in cement pastes, mortars,and concretes: Causes and test methods" Proceedings of Silica Fume, Slag, and Natural Pozzolans in Concrete, Madrid, Spain, Apr.21-25, 1986. Edited by V.M.Malhotra. American Concrete Institute, Detroit, MI, Special Publication SP-91, pp. 723-737.
123. Klieger, P., and Gebler, S. "Fly ash and concrete durability", Proceedings of Katharine and Bryant Mather International Conference on Concrete Durability, Atlanta, GA, Apr. 27- May 1, 1987. Edited by J .M. Scanlon. American Concrete Institute, Detroit, MI, Special Publication SP-100, Vol. 1, pp.1043-1069.
124. Farbiarz, J., and Carrasquillo, R. "Alkali- aggregate reaction in concrete containing fly ash", Proceedings of Katharine and Bryant Mather International Conference on Concrete Durability, Atlanta, GA, Apr. 27- May 1, 1987. Edited by J .M. Scanlon. American Concrete Institute, Detroit, MI, Special Publication SP-100, Vol. 1, pp.1787-1808.
125. Sivasundaram, V., Carette, G.G., and Malhotra, V.M "Structural concrete incorporating high volumes of ASTM Class F fly ash", ACI Materials Journal, 1989, 86(5): 507-514.
126. Carette, G.C., and Langley, W.S. "Evaluation of de-icing salt scaling of fly ash concrete", Proceedings, International Workshop on Alkali- Aggregate Reactions in Concrete: Occurrences, Testing and Control, Halifax, NS, 1990, CANMET, Ottawa, ON.
127. Sivasundaram, V., Carette, G.G., and Malhotra, V.M "Long term strength development of high volume fly ash concrete", Cement & Concrete Composites, 1990, 12: 263-270.
128. Dhir. R.K., Jones, M.R., Ahmed, H.E.H., and Seneviratne, A.M.G., "Rapid estimation of Chloride Diffusion Coefficient in Concrete", Magazine of Concrete Research, Vol.42, No.152, September, 1990, pp. 177-185.
129. Lemming, M.L., Ahroad, S.H., Zia,P., Schemmel, J.J, Elliot, R.P., and Naaman, A.E., "High Performance Concretes: An Annotated Bibliography 1974-1989", SHRP-C307,Strategic Highway Research Program, National Research Council, Washington, D.C.1990.
130. Suprenant, Bruce A., "Testing for Chloride Permeability of Concrete", Concrete Construction, July 1991,pp. 8-12.
131. Zia, P, Leming, M.L., Ahmad, S.H. "High Performance Concrete: A State-of-the-Art Report", SHRP-C317, Strategic Highway Research Program, National Research Council, Washington D.C.1991.
132. American Society for Testing Materials "Standard specifications for fly ash and raw or calcined natural pozzolan for use as a mineral admixture in portland cement concrete", ASTM, 1992, Philadelphia, PA, ASTM C 618-92a.
133. Nasser, K.W., and Lai, P.S.H. "Resistance of fly ash concrete to freezing and thawing", Proceedings of the 4th CANMET/ACI International Conference on the Use of Fly Ash, Silica Fume, Slag, and Other Mineral By-products in Concrete, Istanbul,Turkey, May 3- 8, 1992. Edited by V .M. Malhotra. American Concrete Institute, Detroit, MI, Special Publication SP-132, Vol. 1, pp.205-226.
134. Ramakrishnan, V ., Suheyl Akman, M., "Fly Ash, Silica fume, Slag and Natural Pozzolans in Concrete", Proceedings US -Turkey Workshop, Istanbul, May 9, 1992, pp.94-98.
135. Malhotra, V.M., Ramezanianpour, A.A., "Fly Ash in Concrete", MSL Division Report 94 -95 (IR), CANMET, Canada, 1994, pp.135 -140.
136. Naik, T .R.,Singh S.S, and Ramme, B., “Effect of Source and Amount of Fly Ash on Mechanical and durability Properties of Concrete” Durability of Concrete: Proceedings of Fourth CANMET / ACI International Conference, SP-170, V .M.Malhotra, ed., American Concrete Institute, Farmington Hills, Mich., 1997, pp.157-188.
137. Cahn, D.et al, "Atmospheric Co2and the U.S. Cement Industry", World Cement, August 1997, pp.64-68.
138. Naik, T .R.,Singh S.S, and Ramme, B., " Effect of Source and Amount of Fly Ash on Mechanical and durability Properties of Concrete", II Durability of Concrete:Proceedings of Fourth CANMETI ACI International

Conference, SP-170, V .M.Malhotra, ed., American Concrete Institute, Farmington Hills, Mich., 1997, pp.157-188.

139. Naik, T.R.,Singh S.S, and Ramme, B., "Effect of Source and Amount of Fly Ash on Mechanical and durability Properties of Concrete," Durability of Concrete:Proceedings of Fourth CANMENT/ACI International Conference, SP-170, V.M.Malhotra, ed., American Concrete Institute, Farmington Hills, Mich., 1997, pp.157-188.
140. ASTM Designation C 1202-97, Test method for Electrical Indication of Concrete' s Ability to Resist Chloride Ion Penetration, Annual Book of ASTM Standards, Section 4, Construction, Vol. 04.02, Concrete and Concrete Aggregates, ASTM,Philadelphia, PA, 1998.
141. Baweja, D., Roper, H., and Sirivivatnanon, V., "Chloride Induced Steel Corrosion in Concrete: Part I-Corrosion Rates, Corrosion Activity, and Attack Areas", Materials Journal, American Concrete Institute, Detroit, Volume 95, Issue 3, 1998.
142. Ghafoori, N., and Cesar A. Garcia M., "Compacted Non Cement Concrete Utilizing Fluidized Bed And Pulverized Coal Combustion By-Products", Materials Journal,American Concrete Institute, Detroit, Volume 95, Issue 5, 1998.
143. Berg, E.R., and Neal, 1.A., "Concrete Masonry Unit Mix Designs Using Municipal Solid Waste Bottom Ash", Materials Journal, American Concrete Institute, Detroit,Volume 95, Issue 4,1998.
144. Naik, T.R., and Singh, S.S., and Ramme, B.W., "Mechanical Properties and Durability of Concrete Made with Blended Fly Ash", Materials Journal, American Concrete Institute, Detroit, Volume 95, Issue 4, 1998.
145. Taikalsky, P .1., Smith, E., and Regan, R., "Proportioning Spent Casting Sand in Controlled-Low Strength Materials", Materials Journal, American Concrete Institute, Detroit, Volume 95, Issue 6, 1998.
146. Salem, R.M., and Burdette, E.G., "Role of Chemical and Mineral Admixtures on the Physical Properties and Frost-Resistance of Recycled Aggregate Concrete", Materials Journal, American Concrete Institute, Detroit, Volume 95, Issue 5, 1998.
147. Ghafoori, N., and Zhang, Z., "Sulfate Resistance of Roller Compacted Concrete", Materials Journal, American Concrete Institute, Detroit, Volume 95, Issue 4, 1998.
148. Shi, C., Stegemann, 1.A., and Caldwell, R.1., "Effect of Supplementary Cementing Materials on the Specific Conductivity of Pore Solution and Its Implications on the Rapid Chloride Permeability Test (AASHTO T277 and ASTM C1202) Results", Materials Journal, American Concrete Institute, Detroit, Volume 95, Issue 4; 1998.
149. Malhotra, V. M., Materials Technology Laboratory "Role of Supplementary Cementing Materials in reducing Greenhouse Gas Emissions", CANMET, pp.4-9,1998
150. Naik, T.R.,Singh S.S, Karus,R.N, and Hossain, M.M, "Deicing Salt Scaling Resistance of High-Volume Fly Ash Concrete Using Various Sources of Fly Ashes," Fly Ash, Silica Fume, Slag, and natural Pozzolans in Concrete: Proceedings of Sixth CANMET/ACI international Conference, SP-178,V.M.Malhotra, ed., American concrete Institute, Farmington Hills, Mich., 1998, pp.77-111.
151. Naik, T.R.,Singh S.S, Karus,R.N, and Hossain, M.M, "Deicing Salt Scaling Resistance of High- Volume Fly Ash Concrete Using Various Sources of Fly Ashes," Fly Ash, Silica Fume, Slag, and natural Pozzolans in Concrete: Proceedings of Sixth CANMENT/ACI international Conference, SP-178,V.M.Malhotra, ed., American concrete Institute, Farmington Hills, Mich., 1998, pp.77-111.
152. Baweja, D., Roper, H., and Sirivivatnanon, V., "Chloride Induced Steel Corrosion in Concrete: Part 2-Gravimetric and Electrochemical Comparisons", Materials Journal, American Concrete Institute, Detroit, Volume 95, Issue 3, 1999.
153. Zhang, M.H., Bilodeau, A., Malhotra, V.M., Kim, K.S., and Kim, l.C., "Concrete Incorporating Supplementary Cementing Materials: Effect of Curing on Compressive Strength and Resistance to Chloride-Ion Penetration", Materials Journal, American Concrete Institute, Detroit, Volume 96, Issue 2, 1999.
154. Arino, A.M., and Mobasher, B., "Effect of Ground Copper Slag on Strength and Toughness of Cementitious Mixes", Materials Journal, American Concrete Institute, Detroit, Volume 96, Issue 1, 1999.
155. Li, Z., Peng,. l., and Ma, B., "Investigation of Chloride Diffusion for High-Performance Concrete Containing Fly Ash, Microsilica, and Chemical Admixtures", Materials Journal, American Concrete Institute, Detroit, Volume 96, Issue 3, 1999.
156. Whiting, D., and Nagi, M., "Laboratory Evaluation of Nuclear Gage for Measurement of Water and Cement Content of Fresh Concrete", Materials Journal, American Concrete Institute, Detroit, Volume 96, Issue 1, 1999.
157. Zhao, T.l., Zhu, l.Q., and Chi P.Y., "Modification of Pore Chemicals in Evaluation of High-Performance Concrete Permeability", Materials Journal, American Concrete Institute, Detroit, Volume 96, Issue 1, 1999.

158. Gu, J., Beaudoin, J.J., Zhang, M.H., and Malhotra, V.M., "Performance of Steel Reinforcement in Portland Cement and High- Volume Fly Ash Concretes", Materials Journal, American Concrete Institute, Detroit, Volume 96, Issue 5, 1999.
159. Shi, C., "Pozzolanic Reaction and Microstructure of Chemical Activated Lime-Fly Ash Pastes", Materials Journal, American Concrete Institute, Detroit, Volume 95, Issue 5, 1999.
160. Baweja, D., Roper, H., Sirivivatnanon, V., "Specifications of Concrete For Marine Environments: A Fresh Approach", Materials Journal, American Concrete Institute, Detroit, Volume 96, Issue 4, 1999.
161. Hearn, N., "Effect of Shrinkage and Load-lnduced Cracking on Water Permeability of Concrete", Materials Journal, American Concrete Institute, Detroit, Volume 96, Issue 2, 1999.
162. Srinivas Yenamandra., " Properties of High Performance Concrete for Bridge Deck and Prestressed Girders", Master of Science Thesis, South Dakota School of Mines and Technology, 1999.
163. Bilodeau, A., and Malhotra, V.M., "High-Volume Fly Ash System: Concrete Solution for Sustainable Development", Materials Journal, American Concrete Institute, Detroit, Volume 97, Issue 1, 2000.
164. Myers, L.L., and Carrasquillo, R.L., "Mixture Proportioning for High-Strength High-Performance Concrete Bridge Beams", Special Publication, American Concrete Institute, Detroit, Volume 189,2000.
165. MacDonald, K.A., and Northwood, D.O., "Rapid Estimation of Water-Cementitious Ratio and Chloride Ion Diffusivity in Hardened and Plastic Concrete by Resistivity Measurement", Special Publication, American Concrete Institute, Detroit, Volume 191, 2000.
166. Parrott, L.1., "Curing Time Estimator for Portland and Portland/Fly Ash Concretes", Special Publication, American Concrete Institute, Detroit, Volume 192, 2000.
167. Vieira, M., A1meida, I.R., and Goncalves, A.F., "Influence of Moisture Curing on Durability of Fly Ash Concrete for Road Pavements", Special Publication, American Concrete Institute, Detroit, Volume 192,2000.
168. Saricimen, H., Maslehuddin, M., Shameem, M., AlGhamdi, A.J., and Barry, M.S., "Effect of Curing and Drying on Strength and Absorption of Concretes Containing Fly Ash and Silica Fume", Special Publication, American Concrete Institute, Detroit, Volume 192, 2000.
169. Collpardi, S., Corinaldesi, V., Moricone, G., Bonora, G., and Collepardi, "Durability of High-Performance Concretes with Pozzolanic and Composite Cements", Special Publication, American Concrete Institute, Detroit, Volume 192, 2000.
170. lain Bilodeau, V. Mohan Malhotra., "High-Volume Fly Ash System: Concrete Solutions for Sustainale Development", ACI Materials Journal, V .97, No.1,Jan-Feb2000, pp.41
171. Gretchen, K. Hoffman, " Western region Ash Group", fly Ash Usage in the Western United States, Url. http://www.wrashg.orglwestuse.htm.
172. Cahn, D. et al, "Atmospheric Co2 and the U.S. Cement Industry", World Cement,August 1997, pp.64-68.
173. ACI Committee 209, “Prediction of Creep, Shrinkage, and Temperature Effects in Concrete.” ACI 209R-92, Manual of Concrete Practice, American Concrete Institute, Detroit, MI, 1994.
174. Alfes, C. “Modulus of Elasticity and Drying Shrinkage of High-Strength Concrete Containing Silica Fume.” Fly Ash, Silica Fume, Slag, and Natural Pozzolansin Concrete. Proceedings of the Fourth International Conference, Istanbul Turkey; Ed. by Malhotra. V.M. (1992). American Concrete Institute, Detroit, Michigan.
175. Bloom, R., and Benture, A. “Free and Restrained Shrinkage for Normal and High Strength Concretes.” ACI Materials Journal, 1995, 92 (2), pp. 211-217.
176. Browne, R. D., “Thermal Movement of Concrete.” Concrete, 1972, 6 (11), pp. 51-53.
177. Fiorato, A. E. “PCA Research on High-Strength Concrete.” Concrete International, 1989, 11 (4), pp. 44-50.
178. Ngab, A. S., Slate, F.O., and Nilson, A. H. “Microcracking and Time-Dependent Strains in High Strength Concrete.” ACI Journal, 1981, 78 (4), pp. 262-268.
179. Shah, S.P., and Ahmad, S.H. "High Performance Concrete: Properties and Applications", McGraw-Hill Inc., New York, 1994.
180. Weiss, W. J., Yang, W., and Shah, S. P. “Shrinkage Cracking of Restrained Concrete Slabs.” Journal of Engineering Mechanics, 1998, 124 (7), pp. 765-774.
181. Wiegrink, K., Marikunte, S., and Shah, S. P. “Shrinkage Cracking of High-Strength Concrete.” ACI Materials Journal, 1996, 93 (5), pp. 409-415
182. Wolsiefer, J., Sivasundaram, V., Carette, G.G., and Malhotra, V.M., "Performance of Concretes Incorporating Various Forms of Silica Fume," Fifth Canmnet / ACI International Conference, Milwaukee, WI, 1995.
183. Vijaya Rangan, B., "High-Performance High-Strength Concrete: Design Recommendations", Concrete International, November 1998, Volume 20, No. 11, pp. 63-68.
184. Vijaya Rangan, B., and Yau Seng Hwee., "Studies on Commercial High-Strength Concretes", ACI Materials Journal, V. 87, No. 5, September-October 1990, pp. 440-445.

APPENDIX A

Details of Trial Mixes for Fresh and Hardened Concrete Properties for Bridge Deck Concrete

Note:

The following mix designation scheme is used. The first letter refers to the type of aggregate used: Q-Quartzite, L-Limestone, H-High Strength Girder Concrete. The second letter indicates a number that indicates the mix number. The next letters indicate whether the mix contains fly ash and/or silica fume: F-Fly Ash, S- Silica Fume. The number following S or F indicates the percentage of cement replaced with fly ash and/or silica fume. A zero indicates no fly ash or silica fume. The last letter with W indicates the water to cement ratio. All control mixes are referred to as CONTROL followed by the water to cement ratio.

Examples:

Q1CONTROLW0.4 - Mix no 1, with quartzite aggregate, with no cement replacement: Control, with water to cement ratio of 0.4.

Q2F15S7W0.52 - Mix no 2, with quartzite aggregate, with 15% of cement by weight replaced by fly ash, and with 7% of cement by weight replaced by silica fume, with water to cement ratio of 0.52.

L9F0S10W0.45 - Mix no 9, with limestone aggregate, with no fly ash, and with 10% of cement by weight replaced by silica fume, with water to cement ratio of 0.45

Table A1: Mixture Designations for Mixes with Quartzite Aggregate

Mixture Designation	Description
Q1CONTROLW0.4	Mix with no cement replacement : Control
Q2F15S7W0.52	Mix with 7% of cement by weight replaced by silica fume and 15% by fly ash
Q3F15S5W0.50	Mix with 5% of cement by weight replaced by silica fume and 15% by fly ash
Q4F20S5W0.54	Mix with 5% of cement by weight replaced by silica fume and 20% by fly ash
Q5F15S0W0.47	Mix with 15% of cement by weight replaced by fly ash
Q6F20S0W0.50	Mix with 20% of cement by weight replaced by fly ash
Q7F25S0W0.54	Mix with 25% of cement by weight replaced by fly ash
Q8F0S7W0.43	Mix with 7% of cement by weight replaced by silica fume
Q9F0S10W0.45	Mix with 10% of cement by weight replaced by silica fume
Q10F0S12W0.46	Mix with 12% of cement by weight replaced by silica fume

Note: Multiplication factor of 1.2 used for volume correction for fly ash addition

Table A2: Mixture Proportions for Mixes with Quartzite Aggregate

Mixture Designation	Mixture Proportions (lbs/cubic yard)							w/(c+f+sf)
	Cement pcy	Fly Ash pcy	Silica Fume pcy	Coarse Aggregate pcy	Fine Aggregate pcy	Water pcy	w/c	
Q1CONTROLW0.4	655	0	0	1725	1100	264	0.40	0.40
Q2F15S7W0.52	511	118	55	1725	1100	264	0.52	0.39
Q3F15S5W0.50	524	118	39	1725	1100	264	0.50	0.39
Q4F20S5W0.54	491	157	39	1725	1100	264	0.54	0.38
Q5F15S0W0.47	557	118	0	1725	1100	264	0.47	0.39
Q6F20S0W0.50	524	157	0	1725	1100	264	0.50	0.39
Q7F25S0W0.54	491	197	0	1725	1100	264	0.54	0.38
Q8F0S7W0.43	610	0	55	1725	1100	264	0.43	0.40
Q9F0S10W0.45	590	0	78	1725	1100	264	0.45	0.40
Q10F0S12W0.46	577	0	94	1725	1100	264	0.46	0.39

* Conversion Factor: pcy x 0.59 = kg/m^3

Table A3: Fresh Concrete Properties for Mixes with Quartzite Aggregate

Mixture Designation	Unit Weight		Air	Slump	
	lbs/ft^3	kg/m^3	%	inches	mm
Q1CONTROLW0.4	139.2	2229.6	8.0	4.00	102
Q2F15S7W0.52	141.2	2261.6	5.4	7.50	191
Q3F15S5W0.50	144.4	2312.9	4.4	5.25	133
Q4F20S5W0.54	140.8	2255.2	6.8	8.25	210
Q5F15S0W0.47	140.8	2255.2	7.0	7.50	191
Q6F20S0W0.50	140.8	2255.2	7.2	8.25	210
Q7F25S0W0.54	139.6	2236.0	7.6	9.00	229
Q8F0S7W0.43	143.6	2300.0	5.8	7.00	178
Q9F0S10W0.45	146.4	2344.9	4.8	4.25	108
Q10F0S12W0.46	144.4	2312.9	4.4	6.00	152

Table A4: 14- Day Compressive Strength and Static Modulus (Quartzite Aggregate)

Spec.	Age	Length		Diameter		Unit Weight		Static Mod. psi	Static Mod. Mpa	Compressive Strength	
ID #	days	in.	mm	in.	mm	pcf	Kg/m^3	(x10^6)	(x10^4)	psi	Mpa
Q1CONTROLW0.4-C1	14	12.00	304.8	6.01	152.6	142.2	2277.9	4.2	2.9	4955	34.2
Q1CONTROLW0.4-C2	14	12.00	304.9	6.00	152.5	145.1	2323.4	4.2	2.9	5320	36.8
*Q1CONTROLW0.4-C3	14	12.00	304.8	6.00	152.5	145.0	2322.8	5.3	3.7	5250	36.3
Averages		**12.00**	**304.8**	**6.00**	**152.5**	**144.1**	**2308.0**	**4.2**	**3.2**	**5175**	**35.8**
Q2F15S7W0.52-C1	14	12.00	304.8	6.00	152.4	145.2	2324.9	4.2	2.9	5110	35.3
Q2F15S7W0.52-C2	14	12.00	304.8	6.01	152.5	144.9	2321.0	4.2	2.9	5120	35.4
Q2F15S7W0.52-C3	14	12.00	304.8	6.00	152.5	145.0	2322.0	4.2	2.9	5175	35.8
Averages		**12.00**	**304.8**	**6.00**	**152.5**	**145.0**	**2322.6**	**4.2**	**2.9**	**5135**	**35.5**
Q3F15S5W0.50-C1	14	12.00	304.8	6.00	152.5	147.6	2364.1	4.2	2.9	5640	39.0
*Q3F15S5W0.50-C2	14	12.00	304.8	6.01	152.5	147.5	2361.7	4.2	2.9	4275	29.5
Q3F15S5W0.50-C3	14	12.00	304.8	6.01	152.5	150.0	2402.4	3.9	2.7	6020	41.6
Averages		**12.00**	**304.8**	**6.00**	**152.5**	**148.3**	**2376.1**	**4.1**	**2.8**	**5830**	**36.7**
Q4F20S5W0.54-C4	14	12.00	304.8	6.00	152.4	142.6	2284.0	4.2	2.9	4600	31.8
Q4F20S5W0.54-C5	14	12.00	304.8	6.00	152.4	142.6	2284.0	4.2	2.9	4795	33.1
*Q4F20S5W0.54-C6	14	12.00	304.8	6.00	152.4	142.6	2284.3	4.2	2.9	4050	28.0
Averages		**12.00**	**304.8**	**6.00**	**152.4**	**142.6**	**2284.1**	**4.2**	**2.9**	**4698**	**31.0**
Q5F15S0W0.47-C3	14	12.00	304.8	6.00	152.4	142.6	2284.0	4.7	3.2	5025	34.7
Q5F15S0W0.47-C4	14	12.00	304.8	6.00	152.4	142.6	2283.2	4.7	3.2	4900	33.9
Q5F15S0W0.47-C5	14	12.00	304.8	6.00	152.4	142.6	2283.2	4.7	3.3	4860	33.6
Averages		**12.00**	**304.8**	**6.00**	**152.4**	**142.6**	**2283.5**	**4.7**	**3.3**	**4928**	**34.1**

Table A4: 14- Day Compressive Strength and Static Modulus (Quartzite Aggregate)…continued

Spec. ID #	Age days	Length in.	Length mm	Diameter in.	Diameter mm	Unit Weight pcf	Unit Weight Kg/m^3	Static Mod. psi ($x10^6$)	Static Mod. Mpa ($x10^4$)	Compressive Strength psi	Compressive Strength Mpa
Q6F20S0W0.50-C2	14	12.00	304.8	6.00	152.4	142.6	2284.0	4.2	2.9	4420	30.5
Q6F20S0W0.50-C3	14	12.00	304.8	6.00	152.5	142.5	2282.6	4.2	2.9	4435	30.6
*Q6F20S0W0.50-C4	14	12.00	304.8	6.00	152.4	142.6	2283.2	4.2	2.9	4065	28.1
Averages		**12.00**	**304.8**	**6.00**	**152.4**	**142.6**	**2283.3**	**4.2**	**2.9**	**4428**	**29.8**
Q7F25S0W0.54-C2	14	12.00	304.8	6.00	152.4	140.0	2242.5	3.5	2.4	4175	28.8
Q7F25S0W0.54-C3	14	12.00	304.8	6.00	152.4	140.1	2243.2	3.5	2.4	3785	26.2
Q7F25S0W0.54-C5	14	12.00	304.8	6.00	152.4	140.0	2242.5	3.5	2.4	3430	23.7
Averages		**12.00**	**304.8**	**6.00**	**152.4**	**140.0**	**2242.8**	**3.5**	**2.4**	**3797**	**26.2**
Q8F25S0W0.54-C2	14	12.00	304.8	6.02	152.9	144.4	2312.7	4.7	3.2	6490	44.8
Q8F25S0W0.54-C3	14	12.00	304.8	6.01	152.7	144.5	2314.8	4.7	3.2	6410	44.3
Q8F25S0W0.54-C4	14	12.00	304.8	6.01	152.7	144.2	2309.0	4.7	3.2	6485	44.8
Averages		**12.00**	**304.8**	**6.01**	**152.7**	**144.4**	**2312.2**	**4.7**	**3.2**	**6462**	**44.7**
Q9F0S10W0.45-C3	14	12.00	304.8	6.01	152.6	147.3	2359.6	4.7	3.2	7230	50.0
Q9F0S10W0.45-C4	14	12.00	304.8	6.01	152.7	147.1	2356.1	4.7	3.2	7045	48.7
Q9F0S10W0.45-C5	14	12.00	304.8	6.01	152.7	147.2	2357.7	4.7	3.2	7050	48.7
Averages		**12.00**	**304.8**	**6.01**	**152.7**	**147.2**	**2357.8**	**4.7**	**3.2**	**7108**	**49.1**
Q10F0S12W0.46-C2	14	12.00	304.8	6.00	152.5	147.5	2362.5	5.0	3.4	8655	59.8
Q10F0S12W0.46-C3	14	12.00	304.8	6.00	152.5	147.6	2363.3	5.0	3.4	8835	61.0
Q10F0S12W0.46-C6	14	12.00	304.8	6.01	152.5	147.5	2361.7	5.0	3.4	8405	58.1
Averages		**12.00**	**304.8**	**6.00**	**152.5**	**147.5**	**2362.5**	**5.0**	**3.4**	**8632**	**59.6**

Note: *Specimen Not considered for calculation of average value as it is an outlier.

Table A5: 14-Day Flexural Strength (Quartzite Aggregate)

Spec. ID #	Age	Length		Breadth		Depth		Unit Weight		Maximum Load		Flexural Strength	
	days	in.	mm	in.	mm	in.	mm	pcf	kg/m^3	lbs	kgs	psi	Mpa
Q1CONTROLW0.4-B1	14	14.00	355.6	4.00	101.6	4.00	101.7	150.4	2408.4	3900.0	1769.0	730	5.0
*Q1CONTROLW0.4-B3	14	14.00	355.6	4.00	101.7	4.01	101.8	146.2	2341.3	3260.6	1479.0	610	4.2
*Q1CONTROLW0.4-B5	14	14.00	355.6	3.97	100.9	4.01	101.8	147.4	2361.2	4484.8	2034.3	840	5.8
Q1CONTROLW0.4-B6	14	14.00	355.6	4.01	101.8	4.00	101.7	146.2	2341.5	3750.1	1701.0	703	4.9
Averages		**14.00**	**355.6**	**4.00**	**101.5**	**4.01**	**101.7**	**147.5**	**2363.1**	**3848.9**	**1745.8**	**717**	**5.0**
*Q2F15S7W0.52-B1	14	14.00	355.6	4.04	102.6	4.05	102.9	143.3	2296.0	4300.7	1950.8	780	5.4
Q2F15S7W0.52-B2	14	14.00	355.6	4.07	103.3	4.06	103.1	142.0	2275.2	3579.7	1623.7	635	4.4
Q2F15S7W0.52-B3	14	14.00	355.6	3.98	101.2	4.03	102.4	146.0	2339.2	3353.6	1521.2	635	4.4
*Q2F15S7W0.52-B4	14	14.00	355.6	4.09	103.9	4.02	102.0	142.7	2286.5	3190.4	1447.1	580	4.0
Averages		**14.00**	**355.6**	**4.05**	**102.7**	**4.04**	**102.6**	**143.5**	**2299.2**	**3606.1**	**1635.7**	**635**	**4.4**
Q3F15S5W0.50-B1	14	14.00	355.6	4.03	102.2	4.00	101.7	146.0	2339.1	3830.3	1737.4	715	4.9
*Q3F15S5W0.50-B2	14	14.00	355.6	4.01	101.8	4.01	101.8	146.0	2338.6	3681.7	1670.0	690	4.8
Q3F15S5W0.50-B3	14	14.00	355.6	4.00	101.7	4.02	102.0	145.9	2336.7	3989.9	1809.8	740	5.1
Q3F15S5W0.50-B4	14	14.00	355.6	4.01	101.7	4.01	101.8	149.9	2401.9	4101.1	1860.2	765	5.3
Averages		**14.00**	**355.6**	**4.01**	**101.9**	**4.01**	**101.8**	**147.0**	**2354.0**	**3900.8**	**1769.3**	**740**	**5.1**
Q4F20S5W0.54-B1	14	14.00	355.6	4.00	101.6	4.00	101.6	142.7	2285.6	3300.0	1496.9	620	4.3
Q4F20S5W0.54-B2	14	14.00	355.6	4.00	101.6	4.01	101.7	142.5	2283.3	3100.0	1406.1	580	4.0
Q4F20S5W0.54-B3	14	14.00	355.6	4.00	101.7	4.00	101.7	142.4	2281.6	3100.0	1406.1	580	4.0
Averages		**14.00**	**355.6**	**4.00**	**101.6**	**4.00**	**101.7**	**142.6**	**2283.5**	**3166.7**	**1436.4**	**593**	**4.1**

Table A5: 14-Day Flexural Strength (Quartzite Aggregate)…continued

Spec. ID #	Age	Length		Breadth		Depth		Unit Weight		Maximum Load		Flexural Strength	
	days	in.	mm	in.	mm	in.	mm	pcf	kg/m^3	lbs	kgs	psi	Mpa
Q5F15S0W0.47-B1	14	14.00	355.6	4.00	101.6	4.00	101.6	146.5	2346.3	3991.7	1810.6	750	5.2
*Q5F15S0W0.47-B2	14	14.00	355.6	4.00	101.6	4.00	101.7	142.6	2284.2	2919.7	1324.4	545	3.8
Q5F15S0W0.47-B3	14	14.00	355.6	4.00	101.6	4.00	101.6	146.5	2347.0	3725.5	1689.9	700	4.8
*Q5F15S0W0.47-B4	14	14.00	355.6	4.00	101.6	4.00	101.7	142.6	2283.5	3425.6	1553.8	640	4.4
Averages		**14.00**	**355.6**	**4.00**	**101.6**	**4.00**	**101.7**	**144.6**	**2315.3**	**3515.6**	**1594.7**	**725**	**5.0**
*Q6F20S0W0.50-B1	14	14.00	355.6	4.00	101.6	4.00	101.6	139.6	2235.8	3200.4	1451.7	600	4.1
*Q6F20S0W0.50-B2	14	14.00	355.6	4.00	101.6	4.00	101.6	139.6	2235.8	4057.3	1840.4	760	5.3
Q6F20S0W0.50-B3	14	14.00	355.6	4.01	101.8	4.01	101.9	138.9	2224.6	3625.2	1644.4	675	4.7
Q6F20S0W0.50-B4	14	14.00	355.6	4.00	101.7	4.00	101.7	139.4	2232.4	3612.5	1638.6	675	4.7
Averages		**14.00**	**355.6**	**4.00**	**101.7**	**4.00**	**101.7**	**139.4**	**2232.2**	**3623.9**	**1643.7**	**675**	**4.7**
*Q7F25S0W0.54-B1	14	14.00	355.6	4.00	101.6	4.00	101.6	142.6	2284.7	3424.7	1553.4	640	4.4
Q7F25S0W0.54-B2	14	14.00	355.6	4.00	101.6	4.00	101.6	142.7	2285.1	3013.6	1366.9	565	3.9
Q7F25S0W0.54-B3	14	14.00	355.6	4.00	101.6	4.00	101.7	142.6	2284.2	2932.4	1330.1	550	3.8
Q7F25S0W0.54-B7	14	14.00	355.6	4.00	101.6	4.00	101.6	142.7	2285.1	3020.0	1369.8	565	3.9
Averages		**14.00**	**355.6**	**4.00**	**101.6**	**4.00**	**101.6**	**142.6**	**2284.8**	**3097.7**	**1405.1**	**560**	**3.9**
*Q8F25S0W0.54-B1	14	14.00	355.6	4.03	102.3	4.03	102.4	144.4	2313.2	4137.5	1876.7	760	5.3
Q8F25S0W0.54-B4	14	14.00	355.6	4.02	102.2	4.03	102.3	144.7	2317.3	4655.3	2111.6	855	5.9
Q8F25S0W0.54-B5	14	14.00	355.6	4.00	101.6	4.01	101.9	150.0	2402.7	4669.0	2117.8	870	6.0
Q8F25S0W0.54-B7	14	14.00	355.6	4.00	101.6	4.01	101.8	146.3	2343.0	4474.8	2029.7	835	5.8
Averages		**14.00**	**355.6**	**4.01**	**101.9**	**4.02**	**102.1**	**146.3**	**2344.0**	**4484.2**	**2034.0**	**853**	**5.9**

Table A5: 14-Day Flexural Strength (Quartzite Aggregate)…continued

Spec. ID #	Age	Length		Breadth		Depth		Unit Weight		Maximum Load		Flexural Strength	
	days	in.	mm	in.	mm	in.	mm	pcf	kg/m^3	lbs	kgs	psi	Mpa
Q9F0S10W0.45-B1	14	14.00	355.6	4.02	102.2	4.02	102.1	148.8	2383.2	4739.2	2149.7	875	6.0
Q9F0S10W0.45-B2	14	14.00	355.6	4.06	103.1	4.02	102.2	147.4	2360.6	4368.1	1981.3	800	5.5
Q9F0S10W0.45-B3	14	14.00	355.6	4.00	101.6	4.01	101.8	150.1	2404.6	4348.1	1972.3	815	5.6
Q9F0S10W0.45-B4	14	14.00	355.6	4.01	101.9	4.01	101.8	149.7	2397.3	4185.8	1898.6	780	5.4
Averages		**14.00**	**355.6**	**4.02**	**102.2**	**4.01**	**102.0**	**149.0**	**2386.4**	**4410.3**	**2000.5**	**818**	**5.6**
*Q10F0S12W0.46-B1	14	14.00	355.6	4.01	101.9	4.01	101.8	149.8	2399.2	4307.1	1953.7	805	5.6
Q10F0S12W0.46-B2	14	14.00	355.6	4.00	101.7	4.01	101.7	150.1	2404.0	4753.7	2156.2	890	6.1
*Q10F0S12W0.46-B3	14	14.00	355.6	4.00	101.7	4.00	101.7	150.2	2405.8	4445.6	2016.5	835	5.8
Q10F0S12W0.46-B5	14	14.00	355.6	4.00	101.7	4.00	101.7	150.1	2404.6	4894.1	2219.9	915	6.3
Averages		**14.00**	**355.6**	**4.01**	**101.7**	**4.00**	**101.7**	**150.1**	**2403.4**	**4600.1**	**2086.6**	**903**	**6.2**

Note: *Specimen not considered for the calculation of average value as it is an outlier.

Table A6: 28- Day Compressive Strength and Static Modulus (Quartzite Aggregate)

Spec. ID #	Age	Length		Diameter		Unit Weight		Static Mod.		Compressive Strength	
								psi	Mpa		
	days	in.	mm	in.	mm	pcf	Kg/m^3	(x10^6)	(x10^4)	psi	Mpa
Q1CONTROLW0.4-C4	28	12.14	308.4	6.01	152.5	142.4	2280.2	4.7	3.2	5685	39.3
Q1CONTROLW0.4-C5	28	12.16	308.9	6.00	152.5	142.4	2281.0	4.7	3.2	5935	41.0
*Q1CONTROLW0.4-C6	28	12.08	306.8	6.01	152.5	142.4	2280.2	4.2	2.9	5775	39.9
Averages		**12.13**	**308.0**	**6.00**	**152.5**	**142.4**	**2280.4**	**4.7**	**3.2**	**5798**	**40.1**
Q2F15S7W0.52-C4	28	12.09	307.1	6.01	152.7	142.1	2276.5	4.7	3.2	6170	42.6
Q2F15S7W0.52-C5	28	12.10	307.3	6.01	152.7	142.0	2274.7	4.7	3.2	6000	41.5
Q2F15S7W0.52-C6	28	12.12	307.8	6.01	152.8	144.5	2314.0	4.7	3.2	6250	43.2
Averages		**12.10**	**307.4**	**6.01**	**152.7**	**142.9**	**2288.4**	**4.7**	**3.2**	**6140**	**42.4**
Q3F15S5W0.50-C4	28	12.30	312.4	6.01	152.7	147.1	2356.3	5.3	3.6	7395	51.1
Q3F15S5W0.50-C5	28	12.14	308.4	6.01	152.7	147.2	2357.7	5.3	3.7	7225	49.9
Q3F15S5W0.50-C6	28	12.16	308.9	6.01	152.7	147.2	2356.9	5.3	3.6	7045	48.7
Averages		**12.20**	**309.9**	**6.01**	**152.7**	**147.2**	**2357.0**	**5.3**	**3.7**	**7222**	**49.9**
*Q4F20S5W0.54-C1	28	12.16	308.9	6.01	152.6	139.6	2236.6	4.0	2.8	5290	36.6
Q4F20S5W0.54-C2	28	12.14	308.4	6.01	152.7	139.5	2234.9	4.7	3.2	5570	38.5
Q4F20S5W0.54-C3	28	12.20	309.9	6.01	152.7	139.5	2235.0	4.7	3.2	5655	39.1
Averages		**12.17**	**309.0**	**6.01**	**152.7**	**139.6**	**2235.5**	**4.7**	**3.2**	**5505**	**38.0**
Q5F15S0W0.47-C1	28	12.02	305.2	6.02	152.8	141.7	2269.6	4.7	3.2	5810	40.1
Q5F15S0W0.47-C2	28	12.13	308.1	6.01	152.7	141.9	2273.5	4.7	3.2	5495	38.0
Q5F15S0W0.47-C6	28	12.15	308.6	6.02	152.8	141.7	2269.4	4.7	3.2	5560	38.4
Averages		**12.10**	**307.3**	**6.01**	**152.8**	**141.8**	**2270.8**	**4.7**	**3.2**	**5622**	**38.8**

Table A6: 28- Day Compressive Strength and Static Modulus (Quartzite Aggregate)…continued

Spec. ID #	Age	Length		Diameter		Unit Weight		Static Mod.		Compressive Strength	
								psi	Mpa		
	days	in.	mm	in.	mm	pcf	Kg/m^3	(x10^6)	(x10^4)	psi	Mpa
Q6F20S0W0.50-C1	28	12.15	308.6	6.02	153.0	141.3	2263.7	4.4	3.1	5175	35.8
Q6F20S0W0.50-C5	28	12.11	307.6	6.02	152.9	141.6	2268.0	4.7	3.2	5185	35.8
Q6F20S0W0.50-C6	28	12.16	308.9	6.02	153.0	143.9	2304.2	4.4	3.1	5000	34.6
Averages		**12.14**	**308.4**	**6.02**	**153.0**	**142.3**	**2278.6**	**4.5**	**3.1**	**5120**	**35.4**
Q7F25S0W0.54-C6	28	12.18	309.4	6.02	153.0	138.9	2224.0	4.2	2.9	4685	32.4
Q7F25S0W0.54-C1	28	12.10	307.3	6.01	152.8	139.4	2232.0	4.2	2.9	4875	33.7
Q7F25S0W0.54-C4	28	12.08	306.8	6.02	152.9	139.1	2228.0	4.2	2.9	4710	32.5
Averages		**12.12**	**307.8**	**6.02**	**152.9**	**139.1**	**2228.0**	**4.2**	**2.9**	**4757**	**32.9**
Q8F25S0W0.54-C5	28	12.11	307.6	6.01	152.6	144.6	2315.6	5.3	3.7	6840	47.3
Q8F25S0W0.54-C6	28	12.11	307.6	6.01	152.7	144.5	2314.8	5.3	3.7	7420	51.3
Q8F25S0W0.54-C1	28	12.01	305.0	6.01	152.7	141.9	2272.5	5.3	3.7	7045	48.7
Averages		**12.08**	**306.7**	**6.01**	**152.7**	**143.7**	**2300.9**	**5.3**	**3.7**	**7102**	**49.1**
Q9F0S10W0.45-C2	28	12.02	305.3	6.02	152.8	146.7	2350.2	5.3	3.6	8445	58.4
Q9F0S10W0.45-C1	28	12.08	306.8	6.01	152.7	146.9	2352.7	5.3	3.6	7925	54.8
Q9F0S10W0.45-C6	28	12.09	307.1	6.01	152.7	146.9	2352.9	5.3	3.6	7710	53.3
Averages		**12.06**	**306.4**	**6.01**	**152.7**	**146.8**	**2351.9**	**5.3**	**3.6**	**8027**	**55.5**
Q10F0S12W0.46-C4	28	12.01	305.1	6.02	153.0	144.0	2305.6	6.0	4.2	9130	63.1
Q10F0S12W0.46-C1	28	12.01	305.1	6.01	152.7	144.4	2312.7	6.0	4.2	8875	61.3
Q10F0S12W0.46-C5	28	12.23	310.6	6.02	152.9	144.0	2306.8	6.0	4.2	9070	62.7
Averages		**12.08**	**307.0**	**6.02**	**152.9**	**144.1**	**2308.4**	**6.0**	**4.2**	**9025**	**62.4**

Note: *Specimen not considered for the caluulation of average value as it is an outlier.

Table A7: 28-Day Flexural Strength (Quartzite Aggregate)

Spec. ID #	Age	Length		Breadth		Depth		Unit Weight		Maximum Load		Flexural Strength	
	days	in.	mm	in.	mm	in.	mm	pcf	kg/m^3	lbs	kgs	psi	Mpa
*Q1CONTROLW0.4-B4	28	14.00	355.6	4.00	101.6	4.00	101.7	146.5	2345.8	5138	2330	730	5.0
Q1CONTROLW0.4-B8	28	14.00	355.6	4.00	101.6	4.00	101.7	146.5	2346.5	5534	2510	1035	7.2
*Q1CONTROLW0.4-B2	28	14.00	355.6	4.00	101.6	4.00	101.7	146.5	2346.3	4193	1902	785	5.4
Q1CONTROLW0.4-B7	28	14.00	355.6	4.00	101.6	4.00	101.6	146.5	2347.0	5043	2287	945	6.5
Averages		**14.00**	**355.6**	**4.00**	**101.6**	**4.00**	**101.6**	**146.5**	**2346.4**	**4977**	**2257**	**990**	**6.8**
*Q2F15S7W0.52-B7	28	14.00	355.6	4.02	102.2	4.05	102.9	147.7	2366.0	4314	1957	785	5.4
Q2F15S7W0.52-B5	28	14.00	355.6	4.01	101.8	4.01	102.0	145.7	2334.2	4383	1988	810	5.6
*Q2F15S7W0.52-B6	28	14.00	355.6	4.02	102.2	4.02	102.1	148.9	2384.3	4037	1831	745	5.1
Q2F15S7W0.52-B8	28	14.00	355.6	4.02	102.2	4.05	102.9	143.9	2305.3	4765	2161	865	6.0
Averages		**14.00**	**355.6**	**4.02**	**102.1**	**4.03**	**102.5**	**146.6**	**2347.5**	**4375**	**1984**	**838**	**5.8**
*Q3F15S5W0.50-B8	28	14.00	355.6	4.02	102.2	4.02	102.1	148.8	2382.5	5017	2276	715	4.9
Q3F15S5W0.50-B5	28	14.00	355.6	4.01	102.0	4.01	101.9	149.5	2393.7	4297	1949	800	5.5
*Q3F15S5W0.50-B6	28	14.00	355.6	4.01	101.9	4.01	101.9	149.6	2395.7	5132	2328	955	6.6
Q3F15S5W0.50-B7	28	14.00	355.6	4.02	102.1	4.02	102.2	148.9	2385.4	4592	2083	850	5.9
Averages		**14.00**	**355.6**	**4.02**	**102.0**	**4.02**	**102.0**	**149.2**	**2389.3**	**4759**	**2159**	**825**	**5.7**
*Q4F20S5W0.54-B8	28	14.00	355.6	4.01	101.8	4.01	101.8	142.2	2277.9	4524	2052	845	5.8
Q4F20S5W0.54-B5	28	14.00	355.6	4.01	101.9	4.01	101.9	141.8	2271.7	3862	1752	720	5.0
Q4F20S5W0.54-B6	28	14.00	355.6	4.01	101.9	4.01	101.9	141.9	2272.8	4246	1926	790	5.5
Q4F20S5W0.54-B7	28	14.00	355.6	4.01	101.9	4.01	101.9	141.9	2272.2	3876	1758	720	5.0
Averages		**14.00**	**355.6**	**4.01**	**101.9**	**4.01**	**101.9**	**142.0**	**2273.7**	**4127**	**1872**	**743**	**5.1**

Table A7: 28-Day Flexural Strength (Quartzite Aggregate)...continued

Spec. ID #	Age	Length		Breadth		Depth		Unit Weight		Maximum Load		Flexural Strength	
	days	in.	mm	in.	mm	in.	mm	pcf	kg/m^3	lbs	kgs	psi	Mpa
*Q5F15S0W0.47-B5	28	14.00	355.6	4.02	102.0	4.01	101.8	145.7	2334.2	4026	1826	750	5.2
Q5F15S0W0.47-B8	28	14.00	355.6	4.01	101.9	4.01	101.8	145.9	2336.6	4695	2129	875	6.0
*Q5F15S0W0.47-B6	28	14.00	355.6	4.01	101.9	4.01	101.9	145.7	2333.5	3970	1801	740	5.1
Q5F15S0W0.47-B7	28	14.00	355.6	4.01	101.9	4.01	102.0	145.6	2331.9	4823	2188	895	6.2
Averages		**14.00**	**355.6**	**4.01**	**101.9**	**4.01**	**101.8**	**145.7**	**2334.0**	**4378**	**1986**	**885**	**6.1**
Q6F20S0W0.50-B8	28	14.00	355.6	4.01	101.9	4.01	101.9	141.9	2272.2	3962	1797	735	5.1
Q6F20S0W0.50-B6	28	14.00	355.6	4.02	102.0	4.01	101.9	141.8	2270.4	3584	1625	665	4.6
Q6F20S0W0.50-B7	28	14.00	355.6	4.01	101.9	4.02	102.1	141.6	2267.7	3640	1651	675	4.7
*Q6F20S0W0.50-B5	28	14.00	355.6	4.01	101.9	4.01	101.9	141.8	2271.7	3277	1486	610	4.2
Averages		**14.00**	**355.6**	**4.01**	**101.9**	**4.01**	**101.9**	**141.8**	**2270.5**	**3616**	**1640**	**692**	**4.8**
*Q7F25S0W0.54-B6	28	14.00	355.6	4.02	102.2	4.01	101.9	141.6	2267.7	2954	1340	550	3.8
Q7F25S0W0.54-B5	28	14.00	355.6	4.01	102.0	4.01	102.0	141.7	2269.9	3571	1620	665	4.6
Q7F25S0W0.54-B8	28	14.00	355.6	4.02	102.1	4.01	102.0	141.6	2267.7	3431	1556	635	4.4
*Q7F25S0W0.54-B4	28	14.00	355.6	4.02	102.1	4.02	102.1	141.3	2263.7	3863	1752	715	4.9
Averages		**14.00**	**355.6**	**4.02**	**102.1**	**4.01**	**102.0**	**141.6**	**2267.2**	**3455**	**1567**	**650**	**4.5**
Q8F25S0W0.54-B8	28	14.00	355.6	4.02	102.1	4.03	102.3	144.8	2318.6	4578	2076	845	5.8
Q8F25S0W0.54-B2	28	14.00	355.6	4.01	101.9	4.02	102.1	145.4	2328.9	4666	2117	865	6.0
Q8F25S0W0.54-B3	28	14.00	355.6	4.01	101.9	4.02	102.1	145.4	2329.0	4520	2050	835	5.8
Q8F25S0W0.54-B7	28	14.00	355.6	4.01	102.0	4.02	102.2	149.1	2387.3	4754	2156	880	6.1
Averages		**14.00**	**355.6**	**4.02**	**102.0**	**4.02**	**102.2**	**146.2**	**2341.0**	**4630**	**2100**	**856**	**5.9**

Table A7: 28-Day Flexural Strength (Quartzite Aggregate)...continued

Spec. ID #	Age	Length		Breadth		Depth		Unit Weight		Maximum Load		Flexural Strength	
	days	in.	mm	in.	mm	in.	mm	pcf	kg/m^3	lbs	kgs	psi	Mpa
Q9F0S10W0.45-B5	28	14.00	355.6	4.02	102.0	4.02	102.0	145.4	2328.4	5539	2512	1025	7.1
Q9F0S10W0.45-B8	28	14.00	355.6	4.02	102.0	4.01	101.9	145.6	2331.3	5409	2454	1005	6.9
Q9F0S10W0.45-B6	28	14.00	355.6	4.01	102.0	4.02	102.0	149.3	2391.3	5289	2399	980	6.8
*Q9F0S10W0.45-B7	28	14.00	355.6	4.02	102.0	4.01	101.9	145.5	2330.6	5097	2312	945	6.5
Averages		**14.00**	**355.6**	**4.02**	**102.0**	**4.01**	**102.0**	**146.4**	**2345.4**	**5334**	**2419**	**1003**	**6.9**
Q10F0S12W0.46-B4	28	14.00	355.6	4.03	102.3	4.03	102.4	148.2	2373.1	5340	2422	980	6.8
Q10F0S12W0.46-B7	28	14.00	355.6	4.03	102.4	4.03	102.4	144.4	2312.9	5628	2553	1030	7.1
Q10F0S12W0.46-B8	28	14.00	355.6	4.03	102.4	4.03	102.4	148.2	2373.1	5518	2503	1010	7.0
*Q10F0S12W0.46-B6	28	14.00	355.6	4.03	102.4	4.03	102.3	148.2	2373.1	6496	2946	1190	8.2
Averages		**14.00**	**355.6**	**4.03**	**102.4**	**4.03**	**102.4**	**147.2**	**2358.0**	**5745**	**2606**	**1007**	**7.0**

Note: *Specimen not considered for the calculation of average value as it is an outlier.

Table A8: Mixture Designations for mixes with Limestone Aggregate

Mixture Designation	Description
L1CONTROLW0.4	Mix with no cement replacement : Control
L2F15S7W0.52	Mix with 7% of cement by weight replaced by silica fume and 15% by fly ash
L3F15S5W0.50	Mix with 5% of cement by weight replaced by silica fume and 15% by fly ash
L4F20S5W0.54	Mix with 5% of cement by weight replaced by silica fume and 20% by fly ash
L5F15S0W0.47	Mix with 15% of cement by weight replaced by fly ash
L6F20S0W0.50	Mix with 20% of cement by weight replaced by fly ash
L7F25S0W0.54	Mix with 25% of cement by weight replaced by fly ash
L8F0S7W0.43	Mix with 7% of cement by weight replaced by silica fume
L9F0S10W0.45	Mix with 10% of cement by weight replaced by silica fume
L10F0S12W0.46	Mix with 12% of cement by weight replaced by silica fume

Note: Multiplication factor of 1.2 used for volume correction for fly ash

Table A9: Mixture Proportions for Mixes with Limestone Aggregate

Mixture Designation	Mixture Proportions (lbs/cubic yard)						w/c	w/(c+f+sf)
	Cement pcy	Fly Ash pcy	Silica Fume pcy	Coarse Aggregate pcy	Fine Aggregate pcy	Water pcy		
L1CONTROLW0.4	655	0	0	1725	1100	264	0.40	0.40
L2F15S7W0.52	511	118	55	1725	1100	264	0.52	0.39
L3F15S5W0.50	524	118	39	1725	1100	264	0.50	0.39
L4F20S5W0.54	491	157	39	1725	1100	264	0.54	0.38
L5F15S0W0.47	557	118	0	1725	1100	264	0.47	0.39
L6F20S0W0.50	524	157	0	1725	1100	264	0.50	0.39
L7F25S0W0.54	491	197	0	1725	1100	264	0.54	0.38
L8F0S7W0.43	610	0	55	1725	1100	264	0.43	0.40
L9F0S10W0.45	590	0	78	1725	1100	264	0.45	0.40
L10F0S12W0.46	577	0	94	1725	1100	264	0.46	0.39

* Conversion Factor: pcy x 0.59 = kg/m^3

Table A10: Fresh Concrete Properties for Mixes with Limestone Aggregate

Mixture Designation	Unit Weight		Air	Slump	
	lbs/ft^3	kg/m^3	%	inches	mm
L1CONTROLW0.4	139.6	2236.0	9.6	7.25	184
L2F15S7W0.52	141.6	2268.0	6.2	5.50	140
L3F15S5W0.50	139.6	2236.0	8.0	8.00	203
L4F20S5W0.54	140.4	2248.8	7.4	7.00	178
L5F15S0W0.47	143.2	2293.6	6.2	7.50	191
L6F20S0W0.50	145.6	2332.1	5.2	6.00	152
L7F25S0W0.54	141.6	2268.0	6.8	7.00	178
L8F0S7W0.43	144.0	2306.4	6.4	4.88	124
L9F0S10W0.45	142.8	2287.2	5.6	4.50	114
L10F0S12W0.46	144.8	2319.3	5.2	3.00	76

Table A11: 14- Day Compressive Strength and Static Modulus (Limestone Aggregate)

Spec. ID #	Age days	Length in.	Length mm	Diameter in.	Diameter mm	Unit Weight pcf	Unit Weight Kg/m^3	Static Mod. psi $(x10^6)$	Static Mod. Mpa $(x10^4)$	Compressive Strength psi	Compressive Strength Mpa
L1CONTROLW0.4-C4	14	12.02	305.3	6.06	153.9	144.0	2305.8	5.3	3.6	5760	39.8
L1CONTROLW0.4-C1	14	12.02	305.2	6.06	153.8	143.3	2294.4	5.2	3.6	5415	37.4
Averages		**12.02**	**305.2**	**6.06**	**153.9**	**143.6**	**2300.1**	**5.2**	**3.6**	**5588**	**38.6**
L2F15S7W0.52-C5	14	12.02	305.2	6.02	152.9	142.2	2277.8	5.3	3.6	6380	44.1
L2F15S7W0.52-C6	14	12.01	305.1	6.02	153.0	143.9	2304.4	5.3	3.6	6385	44.1
L2F15S7W0.52-C4	14	12.01	305.1	6.02	153.0	143.9	2305.2	5.3	3.6	6460	44.6
Averages		**12.01**	**305.1**	**6.02**	**153.0**	**143.3**	**2295.8**	**5.3**	**3.6**	**6408**	**44.3**
L3F15S5W0.50-C4	14	12.02	305.2	6.02	153.0	143.8	2303.9	4.7	3.2	5300	36.6
L3F15S5W0.50-C5	14	12.02	305.3	6.02	153.0	143.8	2303.7	4.7	3.2	5440	37.6
L3F15S5W0.50-C6	14	12.02	305.2	6.02	153.0	141.3	2263.4	4.7	3.2	5265	36.4
Averages		**12.02**	**305.2**	**6.02**	**153.0**	**143.0**	**2290.3**	**4.7**	**3.2**	**5335**	**36.9**
L4F20S5W0.54-C6	14	12.01	305.1	6.03	153.2	141.1	2259.2	4.7	3.2	5095	35.2
L4F20S5W0.54-C4	14	12.01	305.1	6.03	153.2	143.4	2297.0	4.7	3.2	5070	35.0
L4F20S5W0.54-C3	14	12.00	304.8	6.03	153.2	141.1	2260.2	4.7	3.2	5075	35.1
Averages		**12.01**	**305.0**	**6.03**	**153.2**	**141.9**	**2272.1**	**4.7**	**3.2**	**5080**	**35.1**
L5F15S0W0.47-C4	14	12.01	305.1	6.02	153.0	141.4	2264.2	4.2	2.9	4390	30.3
L5F15S0W0.47-C5	14	12.01	305.1	6.03	153.2	143.6	2299.7	4.2	2.9	4395	30.4
*L5F15S0W0.47-C6	14	12.02	305.2	6.03	153.2	140.9	2257.3	4.2	2.9	4725	32.6
Averages		**12.01**	**305.1**	**6.03**	**153.1**	**142.0**	**2273.7**	**4.2**	**2.9**	**4393**	**30.4**

Table A11: 14- Day Compressive Strength and Static Modulus (Limestone Aggregate)….continued

Spec.	Age	Length		Diameter		Unit Weight		Static Mod. psi	Static Mod. Mpa	Compressive Strength	
ID #	days	in.	mm	in.	mm	pcf	Kg/m^3	(x10^6)	(x10^4)	psi	Mpa
L6F20S0W0.50-C3	14	12.02	305.2	6.02	152.9	144.1	2307.4	4.7	3.2	4955	34.2
L6F20S0W0.50-C1	14	12.01	305.1	6.02	152.8	146.8	2351.1	4.7	3.2	4890	33.8
*L6F20S0W0.50-C2	14	12.01	305.0	6.02	152.9	146.7	2349.9	4.7	3.2	4485	31.0
Averages		**12.01**	**305.1**	**6.02**	**152.8**	**145.9**	**2336.1**	**4.7**	**3.2**	**4923**	**34.0**
L7F25S0W0.54-C2	14	12.02	305.2	6.02	152.8	141.6	2268.2	4.7	3.2	4570	31.6
L7F25S0W0.54-C1	14	12.01	305.0	6.02	152.9	144.2	2309.5	4.7	3.2	4660	32.2
L7F25S0W0.54-C5	14	12.02	305.2	6.02	152.9	144.1	2308.0	4.7	3.2	4605	31.8
Averages		**12.01**	**305.1**	**6.02**	**152.8**	**143.3**	**2295.2**	**4.7**	**3.2**	**4612**	**31.9**
L8F0S7W0.43-C4	14	12.01	305.0	6.03	153.1	143.7	2301.6	5.3	3.6	6660	46.0
L8F0S7W0.43-C5	14	12.01	305.1	6.03	153.1	143.8	2302.6	5.3	3.6	6925	47.9
L8F0S7W0.43-C6	14	12.01	305.0	6.03	153.0	141.3	2263.8	5.3	3.6	6750	46.6
Averages		**12.01**	**305.0**	**6.03**	**153.1**	**142.9**	**2289.4**	**5.3**	**3.6**	**6778**	**46.8**
*L9F0S10W0.45-C3	14	12.01	305.1	6.02	152.9	141.6	2267.8	5.3	3.6	7345	50.8
L9F0S10W0.45-C1	14	12.01	305.0	6.02	152.8	144.3	2310.5	5.3	3.6	7125	49.2
L9F0S10W0.45-C2	14	12.01	305.1	6.02	152.9	146.7	2349.9	5.3	3.6	7175	49.6
Averages		**12.01**	**305.1**	**6.02**	**152.9**	**144.2**	**2309.4**	**5.3**	**3.6**	**7150**	**49.4**
L10F0S12W0.46-C1	14	12.01	305.1	6.02	152.8	149.3	2390.7	5.3	3.6	7560	52.2
L10F0S12W0.46-C3	14	12.01	305.1	6.02	152.9	149.2	2390.1	5.3	3.6	7560	52.2
*L10F0S12W0.46-C5	14	12.01	305.1	6.02	152.8	149.3	2390.7	5.3	3.6	7070	48.9
Averages		**12.01**	**305.1**	**6.02**	**152.8**	**149.2**	**2390.5**	**5.3**	**3.6**	**7560**	**52.2**

Note:* Specimen not considered for the calculation of average value as it is an outlier.

Table A12: 14-Day Flexural Strength (Limestone Aggregate)

Spec. ID #	Age	Length		Breadth		Depth		Unit Weight		Maximum Load		Flexural Strength	
	days	in.	mm	in.	mm	in.	mm	pcf	kg/m^3	lbs	kgs	psi	Mpa
L1CONTROLW0.4-B5	14	14.00	355.6	4.02	102.1	4.02	102.1	145.2	2325.1	4356.3	1976.0	805	5.6
*L1CONTROLW0.4-B6	14	14.00	355.6	4.02	102.2	4.02	102.2	144.9	2320.5	3819.4	1732.4	705	4.9
L1CONTROLW0.4-B3	14	14.00	355.6	4.02	102.1	4.02	102.1	145.1	2324.0	4737.3	2148.8	875	6.0
L1CONTROLW0.4-B2	14	14.00	355.6	4.02	102.1	4.02	102.2	145.0	2323.4	4658.9	2113.2	860	5.9
Averages		**14.00**	**355.6**	**4.02**	**102.1**	**4.02**	**102.2**	**145.0**	**2323.3**	**4393.0**	**1992.6**	**847**	**5.9**
*L2F15S7W0.52-B3	14	14.00	355.6	4.02	102.2	4.03	102.4	144.6	2315.8	5317.1	2411.8	975	6.7
L2F15S7W0.52-B4	14	14.00	355.6	4.03	102.3	4.03	102.4	144.4	2313.1	4466.6	2026.0	820	5.7
L2F15S7W0.52-B2	14	14.00	355.6	4.03	102.3	4.03	102.4	144.4	2313.6	4566.6	2071.4	840	5.8
L2F15S7W0.52-B1	14	14.00	355.6	4.03	102.3	4.03	102.4	144.4	2313.6	4466.6	2026.0	820	5.7
Averages		**14.00**	**355.6**	**4.03**	**102.3**	**4.03**	**102.4**	**144.5**	**2314.0**	**4704.2**	**2133.8**	**827**	**5.7**
L3F15S5W0.50-B5	14	14.00	355.6	4.04	102.5	4.04	102.7	143.8	2303.3	3998.6	1813.7	730	5.0
L3F15S5W0.50-B7	14	14.00	355.6	4.03	102.4	4.03	102.4	144.3	2311.8	4080.0	1850.7	750	5.2
L3F15S5W0.50-B6	14	14.00	355.6	4.03	102.4	4.04	102.5	147.9	2368.7	4215.1	1911.9	770	5.3
L3F15S5W0.50-B8	14	14.00	355.6	4.03	102.4	4.03	102.4	148.1	2372.7	4096.8	1858.3	750	5.2
Averages		**14.00**	**355.6**	**4.03**	**102.4**	**4.03**	**102.5**	**146.0**	**2339.2**	**4097.6**	**1858.6**	**750**	**5.2**
L4F20S5W0.54-B6	14	14.00	355.6	4.02	102.0	4.02	102.1	141.5	2266.8	3974.4	1802.8	735	5.1
*L4F20S5W0.54-B1	14	14.00	355.6	4.02	102.0	4.02	102.0	137.7	2205.5	4362.7	1978.9	810	5.6
L4F20S5W0.54-B5	14	14.00	355.6	4.02	102.1	4.02	102.2	137.4	2201.6	4224.1	1916.0	780	5.4
Averages		**14.00**	**355.6**	**4.02**	**102.0**	**4.02**	**102.1**	**138.9**	**2224.6**	**4187.1**	**1899.2**	**758**	**5.2**

Table A12: 14-Day Flexural Strength (Limestone Aggregate)...continued

Spec. ID #	Age	Length		Breadth		Depth		Unit Weight		Maximum Load		Flexural Strength	
	days	in.	mm	in.	mm	in.	mm	pcf	kg/m^3	lbs	kgs	psi	Mpa
*L5F15S0W0.47-B1	14	14.00	355.6	4.02	102.0	4.02	102.2	149.0	2386.1	3944.3	1789.1	730	5.0
L5F15S0W0.47-B2	14	14.00	355.6	4.02	102.2	4.02	102.1	144.9	2321.5	4522.2	2051.2	835	5.8
L5F15S0W0.47-B3	14	14.00	355.6	4.02	102.1	4.02	102.2	145.0	2322.6	4655.3	2111.6	860	5.9
L5F15S0W0.47-B4	14	14.00	355.6	4.03	102.2	4.02	102.1	145.0	2322.0	4522.2	2051.2	835	5.8
Averages		**14.00**	**355.6**	**4.02**	**102.2**	**4.02**	**102.1**	**146.0**	**2338.0**	**4411.0**	**2000.8**	**843**	**5.8**
L6F20S0W0.50-B7	14	14.00	355.6	4.03	102.3	4.04	102.5	148.0	2371.2	4397.3	1994.6	805	5.6
*L6F20S0W0.50-B8	14	14.00	355.6	4.03	102.3	4.03	102.4	144.4	2313.3	5007.2	2271.2	920	6.4
*L6F20S0W0.50-B6	14	14.00	355.6	4.03	102.5	4.03	102.3	144.3	2311.1	5198.6	2358.0	950	6.6
L6F20S0W0.50-B5	14	14.00	355.6	4.02	102.0	4.03	102.2	145.1	2323.7	4572.3	2074.0	845	5.8
Averages		**14.00**	**355.6**	**4.03**	**102.3**	**4.03**	**102.4**	**145.5**	**2329.8**	**4793.9**	**2174.5**	**825**	**5.7**
*L7F25S0W0.54-B3	14	14.00	355.6	4.04	102.7	4.04	102.7	147.3	2359.0	5188.6	2353.5	940	6.5
L7F25S0W0.54-B2	14	14.00	355.6	4.05	102.9	4.04	102.6	139.5	2234.7	4372.7	1983.4	795	5.5
L7F25S0W0.54-B1	14	14.00	355.6	4.05	102.8	4.04	102.7	143.8	2303.7	4679.0	2122.4	850	5.9
L7F25S0W0.54-B4	14	14.00	355.6	4.04	102.7	4.04	102.5	143.8	2303.1	4281.6	1942.1	780	5.4
Averages		**14.00**	**355.6**	**4.05**	**102.8**	**4.04**	**102.6**	**143.6**	**2300.1**	**4630.5**	**2100.3**	**808**	**5.6**
*L8F0S7W0.43-B4	14	14.00	355.6	4.03	102.3	4.03	102.3	144.6	2315.7	5601.5	2540.8	1030	7.1
*L8F0S7W0.43-B3	14	14.00	355.6	4.03	102.4	4.03	102.3	148.3	2376.0	5775.6	2619.8	1060	7.3
L8F0S7W0.43-B2	14	14.00	355.6	4.03	102.3	4.03	102.3	140.7	2254.2	5002.6	2269.1	915	6.3
L8F0S7W0.43-B1	14	14.00	355.6	4.02	102.2	4.03	102.3	144.7	2317.3	4892.3	2219.1	900	6.2
Averages		**14.00**	**355.6**	**4.03**	**102.3**	**4.03**	**102.3**	**144.6**	**2315.8**	**5318.0**	**2412.2**	**908**	**6.3**

Table A12: 14-Day Flexural Strength (Limestone Aggregate)...continued

Spec. ID #	Age	Length		Breadth		Depth		Unit Weight		Maximum Load		Flexural Strength	
	days	in.	mm	in.	mm	in.	mm	pcf	kg/m^3	lbs	kgs	psi	Mpa
L9F0S10W0.45-B1	14	14.00	355.6	4.03	102.3	4.03	102.4	148.2	2373.1	5459.3	2476.3	1000	6.9
L9F0S10W0.45-B2	14	14.00	355.6	4.03	102.4	4.04	102.5	148.0	2370.2	5215.0	2365.5	955	6.6
L9F0S10W0.45-B3	14	14.00	355.6	4.02	102.1	4.03	102.2	144.9	2321.3	5026.4	2279.9	930	6.4
L9F0S10W0.45-B4	14	14.00	355.6	4.02	102.1	4.02	102.2	145.0	2322.0	4862.2	2205.5	900	6.2
Averages		**14.00**	**355.6**	**4.02**	**102.2**	**4.03**	**102.3**	**146.5**	**2346.7**	**5140.7**	**2331.8**	**928**	**6.4**
L10F0S12W0.46-B2	14	14.00	355.6	4.02	102.2	4.02	102.0	141.3	2263.7	5495.8	2492.9	1015	7.0
L10F0S12W0.46-B3	14	14.00	355.6	4.02	102.2	4.02	102.1	145.0	2322.0	6148.4	2788.9	1135	7.8
L10F0S12W0.46-B4	14	14.00	355.6	4.02	102.2	4.01	101.9	141.5	2265.9	5312.5	2409.7	985	6.8
L10F0S12W0.46-B1	14	14.00	355.6	4.02	102.2	4.02	102.2	144.9	2320.9	6293.0	2854.5	1160	8.0
Averages		**14.00**	**355.6**	**4.02**	**102.2**	**4.02**	**102.0**	**143.2**	**2293.1**	**5812.4**	**2636.5**	**1074**	**7.4**

Note: *Specimen not considered for calculation of average value as it is an outlier.

Table A13: 28- Day Compressive Strength and Static Modulus (Limestone Aggregate)

Spec. ID #	Age	Length		Diameter		Unit Weight		Static Mod. psi	Static Mod. Mpa	Compressive Strength	
	days	in.	mm	in.	mm	pcf	Kg/m^3	(x10^6)	(x10^4)	psi	Mpa
L1CONTROLW0.4-C3	28	12.01	305.1	6.01	152.7	141.9	2273.1	5.3	3.6	6005	41.5
L1CONTROLW0.4-C2	28	12.01	305.1	6.02	152.9	144.1	2308.5	5.3	3.6	6135	42.4
Averages		**12.01**	**305.1**	**6.02**	**152.8**	**143.0**	**2290.8**	**5.3**	**3.6**	**6070**	**41.9**
L2F15S7W0.52-C1	28	12.00	304.9	6.02	152.8	144.4	2312.1	5.3	3.6	8445	58.4
L2F15S7W0.52-C2	28	12.01	305.1	6.02	152.9	141.5	2266.1	5.3	3.6	8150	56.3
L2F15S7W0.52-C3	28	12.01	305.0	6.02	152.9	144.1	2307.2	5.3	3.6	8255	57.0
Averages		**12.01**	**305.0**	**6.02**	**152.9**	**143.3**	**2295.1**	**5.3**	**3.6**	**8283**	**57.2**
L3F15S5W0.50-C1	28	12.02	305.2	6.02	152.9	144.0	2305.6	5.3	3.6	5795	40.0
*L3F15S5W0.50-C2	28	12.01	305.1	6.02	152.9	141.5	2266.9	5.3	3.6	4955	34.2
L3F15S5W0.50-C3	28	12.02	305.3	6.02	152.8	144.2	2309.3	5.3	3.6	5860	40.5
Averages		**12.02**	**305.2**	**6.02**	**152.9**	**143.2**	**2294.0**	**5.3**	**3.6**	**5828**	**40.3**
L4F20S5W0.54-C1	28	12.01	305.1	6.01	152.7	141.9	2273.1	4.7	3.2	6060	41.9
*L4F20S5W0.54-C5	28	12.01	305.1	6.01	152.7	141.9	2272.7	4.7	3.2	5725	39.6
L4F20S5W0.54-C2	28	12.01	305.1	6.01	152.7	142.0	2274.4	4.7	3.2	6080	42.0
Averages		**12.01**	**305.1**	**6.01**	**152.7**	**141.9**	**2273.4**	**4.7**	**3.2**	**6070**	**41.9**
*L5F15S0W0.47-C3	28	12.01	305.0	6.02	152.8	141.7	2270.2	5.3	3.6	4855	33.5
L5F15S0W0.47-C2	28	12.02	305.2	6.02	152.9	144.0	2305.8	5.3	3.6	5270	36.4
L5F15S0W0.47-C1	28	12.02	305.3	6.02	152.9	141.4	2265.0	5.3	3.6	5270	36.4
Averages		**12.01**	**305.1**	**6.02**	**152.9**	**142.4**	**2280.3**	**5.3**	**3.6**	**5270**	**36.4**

Table A13: 28- Day Compressive Strength and Static Modulus (Limestone Aggregate)…continued

Spec. ID #	Age	Length		Diameter		Unit Weight		Static Mod.		Compressive Strength	
								psi	Mpa		
	days	in.	mm	in.	mm	pcf	Kg/m^3	(x10^6)	(x10^4)	psi	Mpa
L6F20S0W0.50-C4	28	12.01	305.1	6.02	152.8	146.8	2351.1	5.3	3.6	5490	37.9
L6F20S0W0.50-C6	28	12.02	305.2	6.02	152.8	146.7	2349.4	5.3	3.6	5630	38.9
L6F20S0W0.50-C5	28	12.01	305.1	6.02	152.9	146.7	2349.7	5.3	3.6	5365	37.1
Averages		**12.01**	**305.1**	**6.02**	**152.8**	**146.7**	**2350.1**	**5.3**	**3.6**	**5495**	**38.0**
L7F25S0W0.54-C4	28	12.01	305.1	6.02	152.9	144.2	2309.3	4.7	3.2	5485	37.9
L7F25S0W0.54-C3	28	12.02	305.3	6.02	153.0	143.9	2304.7	4.7	3.2	5265	36.4
L7F25S0W0.54-C6	28	12.01	305.0	6.02	152.9	146.8	2350.5	4.7	3.2	5415	37.4
Averages		**12.01**	**305.1**	**6.02**	**152.9**	**144.9**	**2321.5**	**4.7**	**3.2**	**5388**	**37.2**
*L8F0S7W0.43-C2	28	12.01	305.2	6.02	152.9	144.0	2305.8	5.3	3.6	8500	58.7
L8F0S7W0.43-C1	28	12.02	305.2	6.02	152.8	144.2	2308.9	5.3	3.6	8090	55.9
L8F0S7W0.43-C3	28	12.01	305.1	6.02	153.0	144.0	2306.0	5.3	3.6	7710	53.3
Averages		**12.01**	**305.2**	**6.02**	**152.9**	**144.0**	**2306.9**	**5.3**	**3.6**	**7900**	**54.6**
L9F0S10W0.45-C4	28	12.02	305.2	6.02	152.9	144.1	2307.6	5.3	3.6	8225	56.8
L9F0S10W0.45-C6	28	12.02	305.2	6.02	152.9	146.6	2347.8	5.3	3.6	8350	57.7
L9F0S10W0.45-C5	28	12.01	305.1	6.02	152.9	149.2	2390.1	5.7	3.9	8440	58.3
Averages		**12.01**	**305.2**	**6.02**	**152.9**	**146.6**	**2348.5**	**5.4**	**3.7**	**8338**	**57.6**
L10F0S12W0.46-C2	28	12.01	305.1	6.02	152.9	146.6	2347.5	6.0	4.2	8515	58.8
L10F0S12W0.46-C6	28	12.01	305.1	6.02	152.9	146.7	2349.4	6.0	4.2	8860	61.2
L10F0S12W0.46-C4	28	12.02	305.2	6.02	152.9	146.6	2347.3	6.0	4.2	8715	60.2
Averages		**12.01**	**305.1**	**6.02**	**152.9**	**146.6**	**2348.0**	**6.0**	**4.2**	**8697**	**60.1**

Note: *Specimen not considered for the calculation of average value as it is an outlier.

Table A14: 28-Day Flexural Strength (Limestone Aggregate)

Spec. ID #	Age	Length		Breadth		Depth		Unit Weight		Maximum Load		Flexural Strength	
	days	in.	mm	in.	mm	in.	mm	pcf	kg/m^3	lbs	kgs	psi	Mpa
L1CONTROLW0.4-B8	28	14.00	355.6	4.02	102.1	4.02	102.2	141.2	2262.3	4655.3	2111.6	860	5.9
L1CONTROLW0.4-B4	28	14.00	355.6	4.02	102.1	4.02	102.1	141.3	2263.9	4923.3	2233.2	910	6.3
*L1CONTROLW0.4-B1	28	14.00	355.6	4.02	102.1	4.03	102.3	141.2	2261.2	4364.5	1979.7	805	5.6
L1CONTROLW0.4-B7	28	14.00	355.6	4.02	102.1	4.02	102.1	145.2	2325.8	4703.6	2133.5	870	6.0
Averages		**14.00**	**355.6**	**4.02**	**102.1**	**4.02**	**102.2**	**142.2**	**2278.3**	**4661.7**	**2114.5**	**880**	**6.1**
*L2F15S7W0.52-B6	28	14.00	355.6	4.03	102.2	4.03	102.4	140.7	2254.3	6028.1	2734.3	1105	7.6
L2F15S7W0.52-B7	28	14.00	355.6	4.03	102.3	4.02	102.0	145.0	2322.9	5105.6	2315.9	945	6.5
L2F15S7W0.52-B5	28	14.00	355.6	4.03	102.4	4.04	102.7	136.3	2183.7	5350.8	2427.1	975	6.7
L2F15S7W0.52-B8	28	14.00	355.6	4.02	102.2	4.03	102.3	148.5	2379.3	5102.9	2314.6	940	6.5
Averages		**14.00**	**355.6**	**4.03**	**102.3**	**4.03**	**102.4**	**142.6**	**2285.0**	**5396.9**	**2448.0**	**953**	**6.6**
L3F15S5W0.50-B4	28	14.00	355.6	4.02	102.0	4.01	101.9	141.7	2270.2	5390.9	2445.3	1000	6.9
*L3F15S5W0.50-B3	28	14.00	355.6	4.02	102.0	4.01	101.8	141.9	2273.1	8049.0	3651.0	1495	10.3
L3F15S5W0.50-B2	28	14.00	355.6	4.02	102.1	4.02	102.2	145.0	2323.4	4684.5	2124.9	865	6.0
L3F15S5W0.50-B1	28	14.00	355.6	4.02	102.2	4.02	102.1	148.8	2384.1	4733.7	2147.2	875	6.0
Averages		**14.00**	**355.6**	**4.02**	**102.1**	**4.02**	**102.0**	**144.4**	**2312.7**	**5714.5**	**2592.1**	**913**	**6.3**
L4F20S5W0.54-B4	28	14.00	355.6	4.02	102.1	4.03	102.4	141.0	2257.9	4889.0	2217.6	900	6.2
*L4F20S5W0.54-B8	28	14.00	355.6	4.02	102.1	4.02	102.1	141.4	2265.1	4720.0	2141.0	875	6.0
L4F20S5W0.54-B3	28	14.00	355.6	4.02	102.1	4.02	102.1	141.4	2265.1	5050.0	2290.6	935	6.5
L4F20S5W0.54-B7	28	14.00	355.6	4.02	102.1	4.03	102.4	141.0	2257.9	5124.0	2324.2	940	6.5
Averages		**14.00**	**355.6**	**4.02**	**102.1**	**4.02**	**102.2**	**141.3**	**2262.7**	**4886.3**	**2216.4**	**925**	**6.4**

Table A14: 28-Day Flexural Strength (Limestone Aggregate) …..continued

Spec. ID #	Age	Length		Breadth		Depth		Unit Weight		Maximum Load		Flexural Strength	
	days	in.	mm	in.	mm	in.	mm	pcf	kg/m^3	lbs	kgs	psi	Mpa
L5F15S0W0.47-B7	28	14.00	355.6	4.03	102.3	4.01	101.9	145.2	2324.9	4824.0	2188.1	890	6.1
*L5F15S0W0.47-B6	28	14.00	355.6	4.02	102.1	4.02	102.0	141.4	2265.4	3798.0	1722.7	705	4.9
*L5F15S0W0.47-B8	28	14.00	355.6	4.02	102.2	4.04	102.6	148.1	2372.0	4058.0	1840.7	745	5.1
L5F15S0W0.47-B5	28	14.00	355.6	4.02	102.1	4.01	101.9	149.2	2390.4	4334.0	1965.9	800	5.5
Averages		**14.00**	**355.6**	**4.02**	**102.2**	**4.02**	**102.1**	**146.0**	**2338.2**	**4253.5**	**1929.4**	**845**	**5.8**
L6F20S0W0.50-B1	28	14.00	355.6	4.02	102.0	4.01	101.8	145.7	2333.0	4688.0	2126.4	870	6.0
L6F20S0W0.50-B3	28	14.00	355.6	4.01	101.9	4.01	101.9	149.4	2393.3	5100.0	2313.3	945	6.5
L6F20S0W0.50-B2	28	14.00	355.6	4.01	102.0	4.01	101.9	145.7	2333.0	4692.7	2128.6	870	6.0
*L6F20S0W0.50-B4	28	14.00	355.6	4.02	102.1	4.01	101.9	145.3	2327.8	4320.0	1959.5	800	5.5
Averages		**14.00**	**355.6**	**4.02**	**102.0**	**4.01**	**101.9**	**146.5**	**2346.8**	**4700.2**	**2132.0**	**895**	**6.2**
L7F25S0W0.54-B8	28	14.00	355.6	4.02	102.2	4.02	102.0	148.9	2384.9	4768.3	2162.9	880	6.1
*L7F25S0W0.54-B5	28	14.00	355.6	4.02	102.1	4.02	102.2	148.8	2383.2	5199.5	2358.5	960	6.6
L7F25S0W0.54-B6	28	14.00	355.6	4.02	102.1	4.02	102.1	145.2	2324.9	4838.5	2194.7	895	6.2
*L7F25S0W0.54-B7	28	14.00	355.6	4.02	102.1	4.02	102.0	149.0	2387.2	4530.4	2055.0	840	5.8
Averages		**14.00**	**355.6**	**4.02**	**102.1**	**4.02**	**102.1**	**148.0**	**2370.0**	**4834.2**	**2192.7**	**888**	**6.1**
L8F0S7W0.43-B5	28	14.00	355.6	4.02	102.2	4.02	102.0	149.0	2386.1	5717.3	2593.3	1055	7.3
*L8F0S7W0.43-B6	28	14.00	355.6	4.03	102.3	4.02	102.0	145.0	2323.1	5041.8	2286.9	930	6.4
*L8F0S7W0.43-B7	28	14.00	355.6	4.02	102.2	4.02	102.0	145.2	2325.5	6104.7	2769.0	1130	7.8
L8F0S7W0.43-B8	28	14.00	355.6	4.02	102.2	4.02	102.0	141.4	2264.3	5891.4	2672.3	1090	7.5
Averages		**14.00**	**355.6**	**4.02**	**102.2**	**4.02**	**102.0**	**145.1**	**2324.7**	**5688.8**	**2580.4**	**1073**	**7.4**

Table A14: 28-Day Flexural Strength (Limestone Aggregate) …..continued

Spec. ID #	Age	Length		Breadth		Depth		Unit Weight		Maximum Load		Flexural Strength	
	days	in.	mm	in.	mm	in.	mm	pcf	kg/m^3	lbs	kgs	psi	Mpa
L9F0S10W0.45-B8	28	14.00	355.6	4.02	102.1	4.02	102.1	148.9	2385.4	5378.2	2439.5	990	6.8
*L9F0S10W0.45-B6	28	14.00	355.6	4.02	102.1	4.02	102.1	145.1	2324.4	6280.6	2848.8	1160	8.0
L9F0S10W0.45-B7	28	14.00	355.6	4.02	102.1	4.02	102.1	145.1	2323.7	5393.7	2446.5	995	6.9
L9F0S10W0.45-B5	28	14.00	355.6	4.02	102.1	4.02	102.1	148.9	2385.4	5222.3	2368.8	965	6.7
Averages		**14.00**	**355.6**	**4.02**	**102.1**	**4.02**	**102.1**	**147.0**	**2354.7**	**5568.7**	**2525.9**	**983**	**6.8**
L10F0S12W0.46-B7	28	14.00	355.6	4.02	102.1	4.03	102.3	152.4	2441.2	5743.0	2605.0	1055	7.3
L10F0S12W0.46-B8	28	14.00	355.6	4.02	102.1	4.02	102.2	148.8	2383.8	6265.0	2841.8	1160	8.0
*L10F0S12W0.46-B5	28	14.00	355.6	4.02	102.2	4.02	102.2	152.5	2441.8	5425.0	2460.7	1000	6.9
L10F0S12W0.46-B6	28	14.00	355.6	4.02	102.1	4.01	101.9	153.0	2450.3	5625.4	2551.6	1040	7.2
Averages		**14.00**	**355.6**	**4.02**	**102.1**	**4.02**	**102.2**	**151.7**	**2429.3**	**5764.6**	**2614.8**	**1085**	**7.5**

Note: *Specimen not considered for the calculation of average value as it is an outlier.

Table A15: Chloride Permeability of Quartzite Mixes

Mix Id:	Age (days)	w/c	Cement		Fly Ash		Silica Fume		Air %	Coulombs	Average of Spec.	Cure History
			pcy	kg/m^3	pcy	kg/m^3	pcy	kg/m^3				
Q1CONTROLW0.4	14	0.403	655.0	388.4	0.0	0.0	0.0	0.0	8.0	7941	4	14 days continuos moist curing
Q2F15S7W0.52	14	0.403	655.0	388.4	118.0	70.0	55.0	32.6	5.4	6679	3	14 days continuos moist curing
Q3F15S5W0.50	17	0.403	524.0	310.7	118.0	70.0	39.0	23.1	4.4	3276	3	17 days continuos moist curing
Q4F20S5W0.54	16	0.403	491.0	291.2	157.0	93.1	39.0	23.1	6.8	6880	2	16 days continuos moist curing
Q5F15S0W0.47	15	0.403	557.0	330.3	118.0	70.0	0.0	0.0	7.0	10744	2	15 days continuos moist curing
Q6F20S0W0.50	14	0.403	524.0	310.7	157.0	93.1	0.0	0.0	7.2	11143	3	14 days continuos moist curing
Q7F25S0W0.54	14	0.403	491.0	291.2	197.0	116.8	0.0	0.0	7.6	14317	3	14 days continuos moist curing
Q1CONTROLW0.4	28	0.403	655.0	388.4	0.0	0.0	0.0	0.0	8.0	5719	3	28 days continuos moist curing
Q1CONTROLW0.4	37	0.403	655.0	388.4	0.0	0.0	0.0	0.0	8.0	5566	3	14 days continuos moist curing + air dried for 22 days + 1 day accelerated curing
Q2F15S7W0.52	47	0.403	655.0	388.4	118.0	70.0	55.0	32.6	5.4	533	2	Continuously moist cured for 28 days+air-dried for 7 days+12 day accelerated curing
Q2F15S7W0.52	43	0.403	655.0	388.4	118.0	70.0	55.0	32.6	5.4	713	2	Continuously moist cured for 28 days+air-dried for 7 days+12 day accelerated curing
Q3F15S5W0.50	51	0.403	524.0	310.7	118.0	70.0	39.0	23.1	4.4	1337	2	Continuously moist cured for 44 days + 7 days accelerated curing
Q4F20S5W0.54	49	0.403	491.0	291.2	157.0	93.1	39.0	23.1	6.8	1599	2	Continuously moist cured for 42 days + 7 days accelerated curing
Q5F15S0W0.47	48	0.403	557.0	330.3	118.0	70.0	0.0	0.0	7.0	4088	4	Continuously moist cured for 41 days + 7 days accelerated curing

Table A15: Chloride Permeability of Quartzite Mixes (...continued)

Mix Id:	Age (Days)	w/c	Cement		Fly Ash		Silica Fume		Air %	Coulombs	Average of Spec.	Cure History
			pcy	kg/m^3	pcy	kg/m^3	pcy	kg/m^3				
Q6F20S0W0.50	47	0.403	524.0	310.7	157.0	93.1	0.0	0.0	7.2	4548	2	Continuously moist cured for 40 days + 7 days accelerated curing
Q7F25S0W0.54	45	0.403	491.0	291.2	197.0	116.8	0.0	0.0	7.6	4059	3	Continuously moist cured for 38 days + 7 days accelerated curing
Q8F0S7W0.43	44	0.403	655.0	388.4	0.0	0.0	55.0	32.6	7.6	1642	3	Continuously moist cured for 39 days + 5 days accelerated curing
Q9F0S10W0.45	45	0.403	590.0	349.9	0.0	0.0	78.0	46.3	4.8	692	4	Continuously moist cured for 38 days + 7 days accelerated curing
Q10F0S12W0.46	43	0.403	577.0	342.2	0.0	0.0	94.0	55.7	4.4	132	3	Continuously moist cured for 36 days + 7 days accelerated curing

Conversion Factor:

1pcy = 0.593 * kg/m^3

Table A16: Chloride Permeability of Limestone Mixes

Mix Id:	Age days	w/c	Cement		Fly Ash		Silica Fume		Air %	Coulombs	Avg. of Spec.	ASTM Category	Cure History
			pcy	kg/m^3	pcy	kg/m^3	pcy	kg/m^3					
L1CONTROLW0.4	4	0.403	655.0	388.4	0.0	0.0	0.0	0.0	9.6	6340	3	High	3 days in water at 51 C
L2F15S7W0.52	4	0.403	655.0	388.4	118.0	70.0	55.0	32.6	6.2	481	2	Very Low	3 days in water at 46 C
L3F15S5W0.50	4	0.403	524.0	310.7	118.0	70.0	39.0	23.1	6.2	4478	2	High	3 days in water at 34 C
L4F20S5W0.54	5	0.403	491.0	291.2	157.0	93.1	39.0	23.1	7.4	2703	3	Moderate	3 days in water at 35 C
L5F15S0W0.47	4	0.403	557.0	330.3	118.0	70.0	0.0	0.0	6.2	4979	3	High	3 days in water at 40 C
L6F20S0W0.50	4	0.403	524.0	310.7	157.0	93.1	0.0	0.0	5.2	7249	3	High	3 days in water at 43 C
L7F25S0W0.54	4	0.403	491.0	291.2	197.0	116.8	0.0	0.0	6.8	7232	3	High	3 days in water at 44 C
L8F0S7W0.43	4	0.403	610.0	361.7	0.0	0.0	55.0	32.6	6.4	1089	3	Low	3 days in water at 44 C
L9F0S10W0.45	6	0.403	590.0	349.9	0.0	0.0	78.0	46.3	5.6	574	3	Very Low	5 days in water at 44 C
L10F0S12W0.46	5	0.403	577.0	342.2	0.0	0.0	94.0	55.7	5.2	354	3	Very Low	4 days in water at 44 C

Note :
Conversion Factor : I pcy = 0.593 x kg/m^3

Table A17: Chloride Permeability of Quartzite Mixes - 90 day tests

Mix Id:	Age days	w/c	Cement		Fly Ash		Silica Fume		Air %	Coulombs	Avg. of Spec.	ASTM Category	Cure History
			pcy	kg/m^3	pcy	kg/m^3	pcy	kg/m^3					
Q1CONTROLW0.4	97	0.403	655.0	388.4	0.0	0.0	0.0	0.0	8.0	4158	3	High	Continuously moist cured in water for 75 days:air dried for 22 days
Q2F15S7W0.52	102	0.403	655.0	388.4	118.0	70.0	55.0	32.6	8.0	1207	2	Low	Continuously moist cured in water for 73 days:air dried for 29 days
Q3F15S5W0.50	100	0.403	524.0	310.7	118.0	70.0	39.0	23.1	4.4	1219	3	Low	Continuously moist cured in water for 71 days:air dried for 29 days
Q4F20S5W0.54	100	0.403	491.0	291.2	157.0	93.1	39.0	23.1	6.8	1774	3	Low	Continuously moist cured in water for 69 days:air dried for 31 days
Q5F15S0W0.47	98	0.403	557.0	330.3	118.0	70.0	0.0	0.0	7.0	3475	2	Moderate	Continuously moist cured in water for 67 days:air dried for 31 days
Q6F20S0W0.50	99	0.403	524.0	310.7	157.0	93.1	0.0	0.0	7.2	6831	2	High	Continuously moist cured in water for 65 days:air dried for 34 days
Q7F25S0W0.54	96	0.403	491.0	291.2	197.0	116.8	0.0	0.0	7.6	4704	3	High	Continuously moist cured in water for 62 days:air dried for 34 days
Q8F0S7W0.43	97	0.403	610.0	361.7	0.0	0.0	55.0	32.6	5.8	1943	2	Low	Continuously moist cured in water for 60 days:air dried for 37 days
Q9F0S10W0.45	95	0.403	590.0	349.9	0.0	0.0	78.0	46.3	4.8	812	2	Very Low	Continuously moist cured in water for 58 days:air dried for 37 days
Q10F0S12W0.46	98	0.403	577.0	342.2	0.0	0.0	94.0	55.7	4.4	323	4	Very Low	Continuously moist cured in water for 55 days:air dried for 43 days

Note :
Conversion Factor : I pcy = 0.593 x kg/m^3

Table A18: Chloride Permeability of Limestone Mixes at 90-day

Mix ID:	Age (Days)	w/c	Cement		Fly Ash		Silica Fume		Air %	Coulombs	Avg. of Spec.	ASTM Category	Cure History
			pcy	kg/m^3	pcy	kg/m^3	pcy	kg/m^3					
L1CONTROLW0.4	96	0.403	655.0	388.4	0.0	0.0	0.0	0.0	9.6	6577	2	High	Continuously moist cured in water for 28 days:air dried for 68 days
L2F15S7W0.52	96	0.403	655.0	388.4	118.0	70.0	55.0	32.6	6.2	430	2	Very Low	Continuously moist cured in water for 28 days:air dried for 68 days
L3F15S5W0.50	95	0.403	524.0	310.7	118.0	70.0	39.0	23.1	8.0	615	3	Very Low	Continuously moist cured in water for 28 days:air dried for 67 days
L4F20S5W0.54	99	0.403	491.0	291.2	157.0	93.1	39.0	23.1	7.4	1785	3	Low	Continuously moist cured in water for 28 days:air dried for 71 days
L5F15S0W0.47	95	0.403	557.0	330.3	118.0	70.0	0.0	0.0	8.0	3553	3	Moderate	Continuously moist cured in water for 28 days:air dried for 67 days
L6F20S0W0.50	145	0.403	524.0	310.7	157.0	93.1	0.0	0.0	5.2	1455	3	Low	Continuously moist cured in water for 28 days:air dried for 117 days
L7F25S0W0.54	143	0.403	491.0	291.2	197.0	116.8	0.0	0.0	6.8	986	3	Very Low	Continuously moist cured in water for 28 days:air dried for 115 days
L8F0S7W0.43	154	0.403	610.0	361.7	0.0	0.0	55.0	32.6	6.8	685	4	Very Low	Continuously moist cured in water for 28 days:air dried for 126 days
L9F0S10W0.45	152	0.403	590.0	349.9	0.0	0.0	78.0	46.3	5.6	511	3	Very Low	Continuously moist cured in water for 28 days:air dried for 124 days
L10F0S12W0.46	154	0.403	577.0	342.2	0.0	0.0	94.0	55.7	5.2	373	4	Very Low	Continuously moist cured in water for 28 days:air dried for 126 days

Note :
Conversion Factor : I pcy = 0.593 x kg/m^3

APPENDIX B

Details of Trial Mixes for Fresh and Hardened Concrete Properties for Bridge Girder Concrete

Table B1: Mixture Designations for Bridge Girder Concrete

Mixture Designation	Description
H1CONTROL W0.28	Control mix with water to cement ratio as 0.28
H2CONTROLW0.30	Control mix with water to cement ratio as 0.30
H3CONTROLW0.32	Control mix with water to cement ratio as 0.32
H4F0S7W0.28	Mix with 7% of cement by weight replaced by silica fume and w/c = 0.28
H5F0S10W0.28	Mix with 10% of cement by weight replaced by silica fume and w/c = 0.28
H6F0S12W0.28	Mix with 12% of cement by weight replaced by silica fume and w/c = 0.28
H7F0S7W0.30	Mix with 7% of cement by weight replaced by silica fume and w/c = 0.30
H8F0S10W0.30	Mix with 10% of cement by weight replaced by silica fume and w/c = 0.30
H9F0S12W0.30	Mix with 12% of cement by weight replaced by silica fume and w/c = 0.30
H10F0S7W0.32	Mix with 7% of cement by weight replaced by silica fume and w/c = 0.32
H11F0S10W0.32	Mix with 10% of cement by weight replaced by silica fume and w/c = 0.32
H12F0S12W0.32	Mix with 12% of cement by weight replaced by silica fume and w/c = 0.32

Note: Multiplication factor of 1.2 used for volume correction

Table B2: Mixture Proportions for Bridge Girder Concrete

Mix Id.	% replace-ment	w/c	Mixture Proportions (lbs/cubic yard)					
			Cement	Silica Fume	Coarse Aggregate	Fine Aggregate	Water	w/(c+sf)
			pcy	pcy	pcy	pcy	pcy	
H1CONTROL W0.28	0	0.28	700	0	1725	1100	196	0.28
H2CONTROLW0.30	0	0.30	700	0	1725	1100	210	0.30
H3CONTROLW0.32	0	0.32	700	0	1725	1100	224	0.32
H4F0S7W0.28	7	0.28	651	59	1725	1100	182	0.26
H5F0S10W0.28	10	0.28	630	84	1725	1100	176	0.25
H6F0S12W0.28	12	0.28	616	101	1725	1100	172	0.24
H7F0S7W0.30	7	0.30	651	59	1725	1100	195	0.28
H8F0S10W0.30	10	0.30	630	84	1725	1100	189	0.26
H9F0S12W0.30	12	0.30	616	101	1725	1100	185	0.26
H10F0S7W0.32	7	0.32	651	59	1725	1100	208	0.29
H11F0S10W0.32	10	0.32	630	84	1725	1100	202	0.28
H12F0S12W0.32	12	0.32	616	101	1725	1100	197	0.28

Table B3: Plastic Properties of Concrete for Bridge Girders

Mix	Slump		Air	Unit Weight	
Id:	in.	mm	%	pcf	kg/m^3
H1CONTROL W0.28	4 3/4	121	10.0	137.6	2203.9
H2CONTROLW0.30	6	152	6.0	143.6	2300.0
H3CONTROLW0.32	3 3/4	95	9.8	137.6	2203.9
H4F0S7W0.28	4 3/4	121	11.6	135.6	2171.9
H5F0S10W0.28	5	127	11.0	133.6	2139.9
H6F0S12W0.28	2	51	10.0	135.6	2171.9
H7F0S7W0.30	7.5	191	10.6	127.6	2043.8
H8F0S10W0.30	5 3/4	146	6.2	143.6	2300.0
H9F0S12W0.30	6	152	2.4	152.0	2434.6
H10F0S7W0.32	7	178	6.4	142.4	2280.8
H11F0S10W0.32	7 3/4	197	4.0	147.6	2364.1
H12F0S12W0.32	3 3/4	95	3.2	148.0	2370.5
H4aF0S7W0.28	7	178	6.2	144.4	2312.9
H5aF0S10W0.28	5 1/2	140	3.8	147.6	2364.1
H6aF0S12W0.28	7 1/2	191	3.2	151.2	2421.8
H7aF0S7W0.30	7	178	5.8	144.8	2319.3
H1aCONTROL W0.28	8 1/2	216	4.0	147.6	2364.1
H2aCONTROLW0.30	3 3/4	95	3.8	150.4	2409.0
H3aCONTROLW0.32	7	178	7.0	141.2	2261.6

Note: Mixes having 'a' as subscript are mixes which have been repeated but have the same mix proportions as the original mix.

Table B4: 1-Day Compressive Strength for Bridge Girder Concrete

Spec. ID #	Age (days)	Length (inches)	Length mm	Diameter (inches)	Diameter mm	Unit Weight (pcf)	Unit Weight Kg/m^3	Compressive Strength psi	Compressive Strength Mpa
H1CONTROL W0.28A-2	1	8.01	203.4	4.02	102.1	153.1	2451.6	6540	45.2
H1CONTROL W0.28A-1	1	8.01	203.5	4.02	102.0	153.4	2456.4	6555	45.3
Averages		**8.01**	**203.4**	**4.02**	**102.0**	**153.2**	**2454.0**	**6548**	**45.2**
H2CONTROLW0.30A-1	1	8.01	203.4	4.02	102.0	153.3	2455.4	4735	32.7
H2CONTROLW0.30A-2	1	8.01	203.4	4.03	102.3	144.1	2308.0	5105	35.3
Averages		**8.01**	**203.4**	**4.02**	**102.1**	**148.7**	**2381.7**	**4920**	**34.0**
H3CONTROLW0.32A-1	1	8.01	203.5	4.04	102.6	143.1	2292.4	3510	24.3
H3CONTROLW0.32A-2	1	8.01	203.4	4.02	102.2	144.4	2313.0	3820	26.4
Averages		**8.01**	**203.5**	**4.03**	**102.4**	**143.8**	**2302.7**	**3665**	**25.3**
H4F0S7W0.28A-2	1	8.01	203.5	4.02	102.1	135.9	2176.6	4805	33.2
H4F0S7W0.28A-1	1	8.01	203.4	4.02	102.1	135.9	2177.2	4920	34.0
Averages		**8.01**	**203.4**	**4.02**	**102.1**	**135.9**	**2176.9**	**4863**	**33.6**
H5F0S10W0.28A-2	1	8.01	203.3	4.02	102.1	136.0	2178.0	5710	39.5
H5F0S10W0.28A-1	1	8.01	203.4	4.02	102.1	135.9	2176.9	5905	40.8
Averages		**8.01**	**203.4**	**4.02**	**102.1**	**135.9**	**2177.4**	**5808**	**40.1**
H6F0S12W0.28A-2	1	8.02	203.6	4.02	102.1	135.9	2176.6	5120	35.4
H6F0S12W0.28A-1	1	8.00	203.3	4.02	102.0	136.3	2183.4	5525	38.2
Averages		**8.01**	**203.5**	**4.02**	**102.1**	**136.1**	**2180.0**	**5323**	**36.8**
H7F0S7W0.30A-1	1	8.01	203.5	4.03	102.2	135.7	2173.0	6485	44.8
H7F0S7W0.30A-2	1	8.01	203.4	4.02	102.2	144.4	2312.5	5985	41.4
Averages		**8.01**	**203.4**	**4.02**	**102.2**	**140.0**	**2242.8**	**6235**	**43.1**

Table B4: 1-Day Compressive Strength for Bridge Girder Concrete (…continued)

Spec. ID #	Age (days)	Length (inches)	Length mm	Diameter (inches)	Diameter mm	Unit Weight (pcf)	Unit Weight Kg/m^3	Compressive Strength psi	Compressive Strength Mpa
H8F0S10W0.30-16	1	8.01	203.3	4.02	102.1	153.1	2452.2	6380	44.1
H8F0S10W0.30-15	1	8.01	203.4	4.02	102.1	153.0	2451.2	7170	49.5
Averages		**8.01**	**203.4**	**4.02**	**102.1**	**153.1**	**2451.7**	**6775**	**46.8**
H9F0S12W0.30-2	1	8.01	203.5	4.03	102.4	135.1	2164.4	6500	44.9
H9F0S12W0.30-1	1	8.01	203.4	4.02	102.1	136.0	2178.6	6145	42.5
Averages		**8.01**	**203.5**	**4.03**	**102.3**	**135.6**	**2171.5**	**6323**	**43.7**
H10F0S7W0.32-2	1	8.01	203.5	4.02	102.1	135.9	2176.7	4135	28.6
H10F0S7W0.32-1	1	8.00	203.3	4.01	101.9	135.4	2168.1	3920	27.1
Averages		**8.01**	**203.4**	**4.02**	**102.0**	**135.6**	**2172.4**	**4028**	**27.8**
H11F0S10W0.32-1	1	8.01	203.5	4.03	102.4	135.3	2166.5	4785	33.1
H11F0S10W0.32-2	1	8.02	203.6	4.03	102.4	135.1	2163.3	5010	34.6
Averages		**8.01**	**203.5**	**4.03**	**102.4**	**135.2**	**2164.9**	**4898**	**33.8**
H12F0S12W0.32-8	1	8.01	203.5	4.03	102.4	135.2	2164.9	5980	41.3
H12F0S12W0.32-9	1	8.01	203.5	4.03	102.4	135.3	2167.1	6430	44.4
Averages		**8.01**	**203.5**	**4.03**	**102.4**	**135.2**	**2166.0**	**6205**	**42.9**

Table B5: 3-Day Compressive Strength for Bridge Girder Concrete

Spec. ID #	Age (days)	Length (inches)	Length mm	Diameter (inches)	Diameter mm	Unit Weight (pcf)	Unit Weight Kg/m^3	Compressive Strength psi	Compressive Strength Mpa
H1CONTROL W0.28A-3	3	8.01	203.3	4.02	102.1	153.2	2454.1	7925	54.8
H1CONTROL W0.28A-7	3	8.02	203.6	4.02	102.1	152.8	2447.1	7560	52.2
Averages		**8.01**	**203.5**	**4.02**	**102.1**	**153.0**	**2450.6**	**7743**	**53.5**
H2CONTROLW0.30A-5	3	8.02	203.6	4.02	102.1	144.5	2314.6	6780	46.8
H2CONTROLW0.30A-3	3	8.00	203.3	4.02	102.0	144.7	2318.0	6700	46.3
Averages		**8.01**	**203.5**	**4.02**	**102.0**	**144.6**	**2316.3**	**6740**	**46.6**
H3CONTROLW0.32A-9	3	8.00	203.3	4.02	102.0	145.0	2321.7	5450	37.7
H3CONTROLW0.32A-8	3	8.01	203.4	4.02	102.0	153.3	2455.1	4970	34.3
Averages		**8.01**	**203.4**	**4.02**	**102.0**	**149.1**	**2388.4**	**5210**	**36.0**
H4F0S7W0.28A-7	3	8.01	203.5	4.02	102.2	144.4	2312.4	6495	44.9
H4F0S7W0.28A-10	3	8.01	203.4	4.02	102.2	144.2	2309.5	6445	44.5
Averages		**8.01**	**203.4**	**4.02**	**102.2**	**144.3**	**2310.9**	**6470**	**44.7**
H5F0S10W0.28A-7	3	8.01	203.6	4.02	102.1	152.8	2447.4	8190	56.6
H5F0S10W0.28A-10	3	8.01	203.5	4.03	102.2	152.6	2444.5	8060	55.7
Averages		**8.01**	**203.5**	**4.02**	**102.2**	**152.7**	**2446.0**	**8125**	**56.1**
H6F0S12W0.28A-10	3	8.02	203.6	4.03	102.3	152.3	2439.2	8475	58.6
H6F0S12W0.28A-8	3	8.02	203.8	4.04	102.6	151.3	2424.0	8590	59.4
Averages		**8.02**	**203.7**	**4.03**	**102.4**	**151.8**	**2431.6**	**8533**	**59.0**
H7F0S7W0.30A-6	3	8.02	203.6	4.04	102.5	152.1	2435.4	7795	53.9
H7F0S7W0.30A-3	3	8.02	203.8	4.03	102.4	143.6	2299.9	7845	54.2
Averages		**8.02**	**203.7**	**4.03**	**102.4**	**147.8**	**2367.6**	**7820**	**54.0**

Table B5: 3-Day Compressive Strength for Bridge Girder Concrete (…continued)

Spec. ID #	Age (days)	Length (inches)	Length mm	Diameter (inches)	Diameter mm	Unit Weight (pcf)	Unit Weight Kg/m^3	Compressive Strength psi	Compressive Strength Mpa
H8F0S10W0.30-14	3	8.01	203.4	4.02	102.0	153.3	2455.1	10260	70.9
H8F0S10W0.30-17	3	8.01	203.4	4.02	102.1	153.0	2451.2	9810	67.8
Averages		**8.01**	**203.4**	**4.02**	**102.1**	**153.2**	**2453.2**	**10035**	**69.3**
H9F0S12W0.30-9	3	8.00	203.3	4.02	102.1	136.0	2178.5	10235	70.7
H9F0S12W0.30-10	3	8.01	203.4	4.02	102.1	136.0	2178.5	10165	70.2
Averages		**8.01**	**203.3**	**4.02**	**102.1**	**136.0**	**2178.5**	**10200**	**70.5**
H10F0S7W0.32-6	3	8.01	203.5	4.02	102.0	136.2	2181.7	6275	43.4
H10F0S7W0.32-8	3	8.01	203.5	4.02	102.2	135.7	2173.0	6290	43.5
Averages		**8.01**	**203.5**	**4.02**	**102.1**	**135.9**	**2177.4**	**6283**	**43.4**
H11F0S10W0.32-5	3	8.01	203.4	4.02	102.1	144.5	2314.8	8355	57.7
H11F0S10W0.32-3	3	8.00	203.3	4.01	101.9	145.1	2324.2	7985	55.2
Averages		**8.01**	**203.3**	**4.02**	**102.0**	**144.8**	**2319.5**	**8170**	**56.5**
H12F0S12W0.32-6	3	8.01	203.3	4.01	101.8	136.8	2191.8	9985	69.0
H12F0S12W0.32-4	3	8.01	203.6	4.00	101.7	145.6	2331.6	10165	70.2
Averages		**8.01**	**203.4**	**4.01**	**101.8**	**141.2**	**2261.7**	**10075**	**69.6**

Table B6: 7-Day Compressive Strength for Bridge Girder Concrete

Spec.	Age	Length		Diameter		Unit Weight		Compressive Strength	
ID #	(days)	(inches)	mm	(inches)	mm	(pcf)	Kg/m^3	psi	Mpa
H1CONTROL W0.28A-5	7	8.01	203.4	4.02	102.1	153.1	2451.7	8865	61.3
H1CONTROL W0.28A-4	7	8.01	203.4	4.02	102.1	153.0	2451.2	8865	61.3
Averages		**8.01**	**203.4**	**4.02**	**102.1**	**153.1**	**2451.5**	**8865**	**61.3**
H2CONTROLW0.30A-6	7	8.02	203.8	4.02	102.1	152.7	2445.0	7875	54.4
H2CONTROLW0.30A-8	7	8.01	203.4	4.02	102.1	153.1	2451.4	8275	57.2
Averages		**8.01**	**203.6**	**4.02**	**102.1**	**152.9**	**2448.2**	**8075**	**55.8**
H3CONTROLW0.32A-6	7	8.01	203.5	4.03	102.3	143.8	2303.2	7450	51.5
H3CONTROLW0.32A-10	7	8.01	203.5	4.03	102.3	143.9	2305.3	5100	35.2
Averages		**8.01**	**203.5**	**4.03**	**102.3**	**143.9**	**2304.3**	**6275**	**43.4**
H4F0S7W0.28A-3	7	8.00	203.3	4.01	101.8	145.4	2329.5	8715	60.2
H4F0S7W0.28A-9	7	8.00	203.3	4.02	102.2	152.9	2448.8	8495	58.7
Averages		**8.00**	**203.3**	**4.02**	**102.0**	**149.2**	**2389.2**	**8605**	**59.5**
H5F0S10W0.28A-6	7	8.01	203.4	4.02	102.0	153.3	2454.9	11050	76.4
H5F0S10W0.28A-8	7	8.01	203.5	4.01	101.8	153.8	2463.3	11250	77.7
Averages		**8.01**	**203.5**	**4.01**	**101.9**	**153.5**	**2459.1**	**11150**	**77.0**
H6F0S12W0.28A-9	7	8.01	203.5	4.01	101.9	153.4	2457.5	11540	79.7
H6F0S12W0.28A-3	7	8.01	203.4	4.02	102.1	153.0	2450.9	11900	82.2
Averages		**8.01**	**203.5**	**4.02**	**102.0**	**153.2**	**2454.2**	**11720**	**81.0**
H7F0S7W0.30A-7	7	8.01	203.5	4.01	102.0	145.0	2321.7	10040	69.4
H7F0S7W0.30A-9	7	8.01	203.4	4.02	102.1	153.1	2451.4	10050	69.4
Averages		**8.01**	**203.4**	**4.02**	**102.0**	**149.0**	**2386.5**	**10045**	**69.4**

Table B6: 7-Day Compressive Strength for Bridge Girder Concrete (…continued)

Spec. ID #	Age (days)	Length (inches)	Length mm	Diameter (inches)	Diameter mm	Unit Weight (pcf)	Unit Weight Kg/m^3	Compressive Strength psi	Compressive Strength Mpa
H8F0S10W0.30-19	7	8.01	203.5	4.02	102.1	153.0	2450.4	11820	81.7
H8F0S10W0.30-12	7	8.01	203.5	4.02	102.0	153.2	2454.4	12745	88.1
Averages		**8.01**	**203.5**	**4.02**	**102.1**	**153.1**	**2452.4**	**12283**	**84.9**
H9F0S12W0.30-3	7	8.01	203.4	4.03	102.4	152.1	2436.2	12140	83.9
H9F0S12W0.30-4	7	8.01	203.5	4.04	102.5	151.8	2431.4	12120	83.7
Averages		**8.01**	**203.4**	**4.03**	**102.5**	**152.0**	**2433.8**	**12130**	**83.8**
H10F0S7W0.32-7	7	8.01	203.3	4.03	102.4	143.9	2305.0	7370	50.9
H10F0S7W0.32-4	7	8.01	203.5	4.02	102.1	144.5	2313.7	7800	53.9
Averages		**8.01**	**203.4**	**4.02**	**102.2**	**144.2**	**2309.3**	**7585**	**52.4**
H11F0S10W0.32-4	7	8.02	203.6	4.03	102.3	152.4	2440.7	9425	65.1
H11F0S10W0.32-6	7	8.01	203.4	4.02	102.2	152.8	2447.1	8655	59.8
Averages		**8.01**	**203.5**	**4.03**	**102.2**	**152.6**	**2443.9**	**9040**	**62.5**
H12F0S12W0.32-10	7	8.01	203.4	4.02	102.0	153.3	2455.6	11445	79.1
H12F0S12W0.32-1	7	8.01	203.4	4.02	102.2	152.7	2445.2	11400	78.8
Averages		**8.01**	**203.4**	**4.02**	**102.1**	**153.0**	**2450.4**	**11423**	**78.9**

Table B7: 28-Day Compressive Strength and Static Modulus for Bridge Girder Concrete

Spec. ID #	Age days	Length in.	Length mm	Diameter in.	Diameter mm	Unit Weight pcf	Unit Weight Kg/m^3	Static Mod. psi (x10^6)	Static Mod. Mpa (x10^4)	Compressive Strength psi	Compressive Strength Mpa
H1CONTROL W0.28A-8	28	8.01	203.6	4.02	102.1	152.9	2449.3	6.2	4.3	9535	65.9
H1CONTROL W0.28A-5	28	8.01	203.5	4.02	102.1	153.0	2450.3	6.2	4.3	10480	72.4
Averages		**8.01**	**203.5**	**4.02**	**102.1**	**153.0**	**2449.8**	**6.2**	**4.3**	**10008**	**69.2**
H2CONTROLW0.30A-9	28	8.00	203.3	4.02	102.0	153.4	2456.2	5.4	3.8	9115	63.0
H2CONTROLW0.30A-7	28	8.01	203.5	4.03	102.3	152.4	2440.8	5.4	3.7	8830	61.0
Averages		**8.01**	**203.4**	**4.02**	**102.2**	**152.9**	**2448.5**	**5.4**	**3.7**	**8973**	**62.0**
H3CONTROLW0.32A-5	28	8.01	203.5	4.02	102.1	153.0	2450.4	4.8	3.3	7525	52.0
H3CONTROLW0.32A-3	28	8.01	203.5	4.02	102.1	153.1	2451.9	5.4	3.7	8690	60.0
Averages		**8.01**	**203.5**	**4.02**	**102.1**	**153.0**	**2451.2**	**5.1**	**3.5**	**8108**	**56.0**
H4F0S7W0.28A-4	28	8.01	203.4	4.02	102.1	144.4	2313.0	5.4	3.7	9645	66.6
H4F0S7W0.28A-6	28	8.01	203.4	4.02	102.1	153.0	2451.2	6.2	4.3	9495	65.6
Averages		**8.01**	**203.4**	**4.02**	**102.1**	**148.7**	**2382.1**	**5.8**	**4.0**	**9570**	**66.1**
H5F0S10W0.28A-9	28	8.00	203.3	4.02	102.1	153.3	2455.1	6.2	4.3	11830	81.7
H5F0S10W0.28A-4	28	8.01	203.4	4.02	102.1	153.2	2453.6	5.4	3.7	11450	79.1
Averages		**8.00**	**203.3**	**4.02**	**102.1**	**153.2**	**2454.4**	**5.8**	**4.0**	**11640**	**80.4**
H6F0S12W0.28A-4	28	8.01	203.5	4.02	102.1	153.1	2451.9	6.2	4.3	14985	103.5
H6F0S12W0.28A-6	28	8.00	203.3	4.01	101.9	153.8	2462.8	6.2	4.3	14240	98.4
Averages		**8.01**	**203.4**	**4.01**	**102.0**	**153.4**	**2457.3**	**6.2**	**4.3**	**14613**	**101.0**

Table B7: 28-Day Compressive Strength and Static Modulus for Bridge Girder Concrete (…continued)

Spec.	Age	Length		Diameter		Unit Weight		Static Mod. psi	Static Mod. Mpa	Compressive Strength	
ID #	days	in.	mm	in.	mm	pcf	Kg/m^3	(x10^6)	(x10^4)	psi	Mpa
H7F0S7W0.30A-5	28	8.01	203.5	4.02	102.0	153.2	2454.3	6.2	4.3	11445	79.1
H7F0S7W0.30A-4	28	8.00	203.3	4.02	102.1	153.2	2453.2	6.2	4.3	11425	78.9
Averages		**8.01**	**203.4**	**4.02**	**102.1**	**153.2**	**2453.7**	**6.2**	**4.3**	**11435**	**79.0**
H8F0S10W0.30-9	28	8.01	203.4	4.02	102.0	153.3	2455.1	7.2	5.0	14205	98.2
H8F0S10W0.30-11	28	8.01	203.4	4.02	102.0	153.3	2455.2	7.2	5.0	13930	96.3
Averages		**8.01**	**203.4**	**4.02**	**102.0**	**153.3**	**2455.2**	**7.2**	**5.0**	**14068**	**97.2**
H9F0S12W0.30-6	28	8.01	203.3	4.02	102.2	152.7	2446.4	6.9	4.8	14350	99.2
H9F0S12W0.30-7	28	8.01	203.3	4.03	102.3	152.5	2442.6	6.9	4.8	14130	97.6
Averages		**8.01**	**203.3**	**4.03**	**102.3**	**152.6**	**2444.5**	**6.9**	**4.8**	**14240**	**98.4**
H10F0S7W0.32-10	28	8.01	203.5	4.02	102.1	144.5	2314.0	6.2	4.3	9970	68.9
H10F0S7W0.32-9	28	8.01	203.5	4.02	102.2	152.7	2446.0	6.2	4.3	9440	65.2
Averages		**8.01**	**203.5**	**4.02**	**102.1**	**148.6**	**2380.0**	**6.2**	**4.3**	**9705**	**67.1**
H11F0S10W0.32-9	28	8.01	203.4	4.01	101.9	153.5	2459.3	5.4	3.8	10670	73.7
H11F0S10W0.32-12	28	8.01	203.5	4.01	101.9	153.5	2458.3	5.4	3.8	9485	65.5
Averages		**8.01**	**203.4**	**4.01**	**101.9**	**153.5**	**2458.8**	**5.4**	**3.8**	**10078**	**69.6**
H12F0S12W0.32-7	28	8.00	203.3	4.02	102.2	152.9	2448.5	6.2	4.3	13375	92.4
H12F0S12W0.32-5	28	8.01	203.4	4.02	102.0	153.3	2455.6	6.2	4.3	13810	95.4
Averages		**8.01**	**203.3**	**4.02**	**102.1**	**153.1**	**2452.0**	**6.2**	**4.3**	**13593**	**93.9**

Table B8: 56-Day Compressive Strength and Static Modulus for Bridge Girder Concrete

Spec. ID #	Age days	Length in.	Length mm	Diameter in.	Diameter mm	Unit Weight pcf	Unit Weight Kg/m^3	Static Mod. psi $(x10^6)$	Static Mod. Mpa $(x10^4)$	Compressive Strength psi	Compressive Strength Mpa
H1CONTROL W0.28A-10	56	8.01	203.5	4.02	102.0	153.2	2454.4	6.2	4.3	10375	71.7
H1CONTROL W0.28A-9	56	8.01	203.4	4.01	101.8	145.5	2329.7	7.2	5.0	10310	71.2
Averages		**8.01**	**203.4**	**4.01**	**101.9**	**149.3**	**2392.1**	**6.7**	**4.6**	**10343**	**71.5**
H2CONTROLW0.30A-4	56	8.01	203.4	4.01	101.9	145.0	2322.6	6.2	4.3	9330	64.5
H2CONTROLW0.30A-10	56	8.01	203.5	4.01	101.9	145.2	2325.3	7.3	5.0	9500	65.6
Averages		**8.01**	**203.4**	**4.01**	**101.9**	**145.1**	**2324.0**	**6.7**	**4.7**	**9415**	**65.1**
H3CONTROLW0.32A-4	56	8.01	203.4	4.01	101.8	145.4	2328.6	6.2	4.3	9110	63.0
H3CONTROLW0.32A-6	56	8.01	203.5	4.02	102.1	144.5	2314.1	6.2	4.3	8865	61.3
Averages		**8.01**	**203.4**	**4.01**	**102.0**	**144.9**	**2321.3**	**6.2**	**4.3**	**8988**	**62.1**
H4F0S7W0.28A-5	56	8.01	203.4	4.02	102.0	144.9	2320.2	6.2	4.3	10860	75.0
H4F0S7W0.28A-8	56	8.01	203.5	4.02	102.0	144.7	2318.0	7.2	5.0	10655	73.6
Averages		**8.01**	**203.4**	**4.02**	**102.0**	**144.8**	**2319.1**	**6.7**	**4.6**	**10758**	**74.3**
H5F0S10W0.28A-3	56	8.01	203.4	4.02	102.1	136.1	2180.6	7.2	5.0	12815	88.6
H5F0S10W0.28A-5	56	8.01	203.3	4.02	102.0	136.4	2184.9	7.2	5.0	13030	90.0
Averages		**8.01**	**203.4**	**4.02**	**102.0**	**136.3**	**2182.7**	**7.2**	**5.0**	**12923**	**89.3**
H6F0S12W0.28A-5	56	8.01	203.4	4.01	101.8	145.4	2328.1	8.7	6.0	16245	112.3
H6F0S12W0.28A-7	56	8.01	203.3	4.01	101.8	145.4	2328.9	8.7	6.0	16640	115.0
Averages		**8.01**	**203.4**	**4.01**	**101.8**	**145.4**	**2328.5**	**8.7**	**6.0**	**16443**	**113.6**

Table B8: 56-Day Compressive Strength and Static Modulus for Bridge Girder Concrete (…continued)

Spec.	Age	Length		Diameter		Unit Weight		Static Mod. psi	Static Mod. Mpa	Compressive Strength	
ID #	days	in.	mm	in.	mm	pcf	Kg/m^3	(x10^6)	(x10^4)	psi	Mpa
H7F0S7W0.30A-8	56	8.00	203.3	4.01	101.8	145.4	2329.0	6.2	4.3	12875	89.0
H7F0S7W0.30A-10	56	8.00	203.3	4.01	101.8	145.6	2332.7	6.2	4.3	12895	89.1
Averages		**8.00**	**203.3**	**4.01**	**101.8**	**145.5**	**2330.9**	**6.2**	**4.3**	**12885**	**89.0**
H8F0S10W0.30-8	56	8.01	203.4	4.01	101.7	154.2	2469.5	8.7	6.0	14405	99.5
H8F0S10W0.30-2	56	8.01	203.4	4.01	101.8	145.5	2330.0	8.7	6.0	15465	106.9
Averages		**8.01**	**203.4**	**4.01**	**101.8**	**149.8**	**2399.7**	**8.7**	**6.0**	**14935**	**103.2**
H9F0S12W0.30-7	56	8.01	203.4	4.01	101.8	145.6	2331.6	7.3	5.0	14800	102.3
H9F0S12W0.30-5	56	8.00	203.3	4.01	101.9	145.3	2327.3	8.7	6.0	14250	98.5
Averages		**8.01**	**203.4**	**4.01**	**101.8**	**145.4**	**2329.4**	**8.0**	**5.5**	**14525**	**100.4**
H10F0S7W0.32-3	56	8.00	203.3	4.01	101.9	145.3	2327.1	6.2	4.3	9500	65.6
H10F0S7W0.32-5	56	8.00	203.3	4.01	101.8	145.4	2329.2	7.3	5.0	10300	71.2
Averages		**8.00**	**203.3**	**4.01**	**101.8**	**145.4**	**2328.2**	**6.7**	**4.7**	**9900**	**68.4**
H11F0S10W0.32-7	56	8.01	203.5	4.01	101.9	145.0	2321.7	7.3	5.0	12650	87.4
H11F0S10W0.32-8	56	8.01	203.3	4.02	102.0	144.9	2321.5	7.2	5.0	13110	90.6
Averages		**8.01**	**203.4**	**4.01**	**102.0**	**144.9**	**2321.6**	**7.2**	**5.0**	**12880**	**89.0**
H12F0S12W0.32-5	56	8.01	203.3	4.01	101.9	136.6	2188.4	7.3	5.0	14635	101.1
H12F0S12W0.32-3	56	8.01	203.3	4.01	101.9	145.3	2326.9	7.3	5.0	14250	98.5
Averages		**8.01**	**203.3**	**4.01**	**101.9**	**141.0**	**2257.7**	**7.3**	**5.0**	**14443**	**99.8**

Table B9: Compressive Strength and Static Modulus of recommended mix (H8) after accelerated curing

Spec. ID #	Age days	Length in.	Length mm	Diameter in.	Diameter mm	Unit Weight pcf	Unit Weight Kg/m^3	Static Mod. psi ($x10^6$)	Static Mod. Mpa ($x10^4$)	Compressive Strength psi	Compressive Strength Mpa
H8F0S10W0.30-8*	1	8.01	203.4	4.01	101.9	153.6	2460.9	6.2	4.3	8700	60.1
H8F0S10W0.30-4*	1	8.01	203.4	4.02	102.1	144.6	2315.6	6.2	4.3	8075	55.8
Averages		**8.01**	**203.4**	**4.02**	**102.0**	**149.1**	**2388.2**	**6.2**	**4.3**	**8388**	**58.0**
H8F0S10W0.30-3**	1	8.00	203.3	4.02	102.0	153.4	2456.4	7.2	5.0	11050	76.4
H8F0S10W0.30-2**	1	8.00	203.3	4.01	102.0	153.6	2460.9	7.3	5.0	10830	74.8
Averages		**8.00**	**203.3**	**4.02**	**102.0**	**153.5**	**2458.6**	**7.2**	**5.0**	**10940**	**75.6**
H8F0S10W0.30-1***	1	8.00	203.3	4.02	102.0	153.4	2456.8	7.2	5.0	11205	77.4
H8F0S10W0.30-5***	1	8.01	203.6	4.02	102.0	153.2	2453.2	7.2	5.0	11680	80.7
Averages		**8.01**	**203.4**	**4.02**	**102.0**	**153.3**	**2455.0**	**7.2**	**5.0**	**11443**	**79.1**
H8F0S10W0.30-6+	2	8.01	203.3	4.01	101.9	153.7	2462.0	7.3	5.0	13450	92.9
H8F0S10W0.30-7+	2	8.01	203.4	4.02	102.1	153.2	2453.2	7.2	5.0	12695	87.7
Averages		**8.01**	**203.4**	**4.02**	**102.0**	**153.4**	**2457.6**	**7.2**	**5.0**	**13073**	**90.3**
H8F0S10W0.30-16	1	8.01	203.3	4.02	102.1	153.1	2452.2	5.8	4.0	6380	44.1
H8F0S10W0.30-15	1	8.01	203.4	4.02	102.1	153.0	2451.2	5.8	4.0	7170	49.5
Averages		**8.01**	**203.4**	**4.02**	**102.1**	**153.1**	**2451.7**	**5.8**	**4.0**	**6775**	**46.8**
H8F0S10W0.30-13	2	8.00	203.3	4.02	102.0	153.5	2458.4	6.2	4.3	8845	61.1
H8F0S10W0.30-18	2	8.00	203.2	4.01	101.7	154.3	2470.9	6.2	4.3	9325	64.4
Averages		**8.00**	**203.3**	**4.01**	**101.9**	**153.9**	**2464.7**	**6.2**	**4.3**	**9085**	**62.8**

*Specimens subjected to accelerated curing for 6 hrs.
**Specimens subjected to accelerated curing for 12 hrs.
***Specimens subjected to accelerated curing for 18 hrs.
+ Specimens subjected to accelerated curing for 24 hrs.

Table B9: Compressive Strength and Static Modulus of recommended mix (H8) after accelerated curing (…continued)

Spec.	Age	Length		Diameter		Unit Weight		Static Mod. psi	Static Mod. Mpa	Compressive Strength	
ID #	days	in.	mm	in.	mm	pcf	Kg/m^3	(x10^6)	(x10^4)	psi	Mpa
H8F0S10W0.30-14	3	8.01	203.4	4.02	102.0	153.3	2455.1	6.2	4.3	10260	70.9
H8F0S10W0.30-17	3	8.01	203.4	4.02	102.1	153.0	2451.2	6.2	4.3	9810	67.8
Averages		**8.01**	**203.4**	**4.02**	**102.1**	**153.2**	**2453.2**	**6.2**	**4.3**	**10035**	**69.3**
H8F0S10W0.30-19	7	8.01	203.5	4.02	102.1	153.0	2450.4	6.2	4.3	11820	81.7
H8F0S10W0.30-12	7	8.01	203.5	4.02	102.0	153.2	2454.4	6.2	4.3	12745	88.1
Averages		**8.01**	**203.5**	**4.02**	**102.1**	**153.1**	**2452.4**	**6.2**	**4.3**	**12283**	**84.9**
H8F0S10W0.30-9	28	8.01	203.4	4.02	102.0	153.3	2455.1	7.2	5.0	14205	98.2
H8F0S10W0.30-11	28	8.01	203.4	4.02	102.0	153.3	2455.2	7.2	5.0	13930	96.3
Averages		**8.01**	**203.4**	**4.02**	**102.0**	**153.3**	**2455.2**	**7.2**	**5.0**	**14068**	**97.2**
H8F0S10W0.30-8	56	8.01	203.4	4.01	101.9	154.2	2469.8	8.7	6.0	14405	99.5
H8F0S10W0.30-2	56	8.01	203.4	4.01	101.9	145.5	2330.5	8.7	6.0	15465	106.9
Averages		**8.01**	**203.4**	**4.01**	**101.9**	**149.9**	**2400.1**	**8.7**	**6.0**	**14935**	**103.2**

Note:

1. Chloride Permeability of H8F0S10W0.30 after being subjected to accelerated curing for 24 hrs. at 70 C was found to be 158 Coulombs (ASTM Category: Very Low)
2. Chloride Permeability of H8F0S10W0.30 at 90-day was found to be 515 Coulombs. (ASTM Category: Very Low)

APPENDIX C

Details of Statistical Analysis for Accelerated Rapid Chloride Permeability Test

A NEW ACCELERATED RAPID CHLORIDE PERMEABILITY TEST FOR DURABILITY OF CONCRETE

INTRODUCTION

This paper presents the results of an experimental investigation to develop a new accelerated Rapid Chloride Permeability test. As we usually have to wait for 90 days to obtain the chloride permeability of concrete, there was a need to find the potential chloride permeability at a faster rate. So a relation between the rapid chloride permeability values obtained for the samples cured normally for 90 days (ASTM C 1202) and the specimens which were subjected to accelerated curing were established. A statistical analysis was done to enhance the obtained relationship. This relationship can be used in predicting the potential ninety-day rapid chloride permeability, when the accelerated cured test results are available.

ACCELERATED CURING AND CHLORIDE PERMEABILITY

In this type of curing, the specimens after being demolded were placed in a curing tank containing water maintained at a constant temperature of 38°C (100°F). After a few trials with different curing duration, it was decided to subject the specimens to 3 days of accelerated curing immediately after demolding the specimens at 24 hrs. After accelerated curing for 3 days, the specimens were tested for rapid chloride permeability as per ASTM C1202.

The specimens from the same concretes were subjected to Rapid Chloride Permeability test after 90 days. The specimens under went an average of 28 days of continuous moist curing and then air dried till they reached an age of 90 days. They were then tested for chloride permeability.

TEST RESULTS

The mixture designations used are given in Table A1, Appendix A and the actual mixture proportions used are given in Table A2, Appendix A. The fresh concrete properties are given in Table A3, Appendix A.

Chloride Permeability

The results of all tests conducted for chloride permeability are tabulated in Tables A15 and A17 and bar charts are shown in Figures 3.19, 3.21, 3.23 (Chapter 3). Initially it was expected that a significant reduction in chloride permeability would occur between the ages of 14 and 28-day. Mixes Q1CONTROLW0.4 through Q7F25S0W0.54 were tested after being subjected to 14 days of normal moist curing in cold water and mix Q1CONTROLW0.4 was also subjected to 28-day testing under the same conditions of curing. As can be seen from the results of the tests on mix Q1CONTROLW0.4 (Table A15, Appendix A), which showed 7941, and 5719 coulombs at 14 and 28-day (both high values). These values were considerably higher than the normal values because sufficient curing and drying did not take place. Therefore it was decided to subject the specimens to accelerated curing for seven days before testing and the results are given in Table A15, Appendix A.

The same concretes were subjected to rapid chloride permeability tests again after 90-day curing. The specimens were subjected to an average of 28 days of continuos moist curing and then air-dried till they reached an age of 90-days. They were then tested for chloride permeability. The results of these tests are tabulated in Table A17, Appendix A. The bar charts for the permeability values obtained are shown in Figure 3.21, Chapter 3. A comparative analysis of the results of the accelerated curing and 90-day test results shows a good correlation (Q2F15S7W0.52, Q3F15S5W0.50, Q4F20S5W0.54, Q8F0S7W0.43, Q9F0S10W0.45, Q10F0S12W0.46). The comparative bar charts are shown in Figure 3.23, Chapter 3.

STATISTICAL MODELS

Probability distributions are useful for modeling and analyzing real-world process. In some cases theoretical distributions closely fits the historical data that has been collected about a process. In other cases we make judgements about the fundamental nature of the process and choose an appropriate theoretical distribution without collecting data. The field of statistics concerned with making inferences about populations and population characteristics. Experiments are conducted with results that are subject to changes. The compression testing of a number of concrete cylinders is an example of a ‘statistical experiment’; a term that is used to describe any process by which

several chance observations were generated. The test results show considerable scatter under very carefully testing environment. It is therefore desirable to apply probabilistic or expected value procedures to insure adequate resistance of concrete structures.

REGRESSION ANALYSIS

Regression analysis is used to solve problems involving sets of variables when it is known that there exits some inherent relationship among the variables. The statistical aspect of the problem then becomes one of the arriving at the best estimate of relationship between variables, while correlation analysis is used to determine the degree of association between the variables. Some statistical assumptions need to be recognized before the application of linear regression analysis to an experimental statistics of data. In most applications, there is a clear distinction between the variables as far as their role in the experimental process is concerned. There is a single 'dependent variable' or response Y, which is uncontrolled in the experiment. The Y_i are random variables possessing the same variance σ^2. This response depends on the one or more 'independent or regressor variables' say $x_1,x_2,\ldots x_k$ which are measured with negligible error and indeed are often controlled in the experiment. Thus the independent variables $x_1,x_2,\ldots x_k$ are not random variables and therefore have no distributional properties.

REGRESSION MODEL FOR ACCELERATED RAPID CHLORIDE PERMEABILITY

A full model for predicting the Accelerated Rapid Chloride Permeability of the concrete was obtained using Regression Analysis. The dependent variable was Accelerated Rapid Chloride Permeability (Y) and the independent variable was ninety-day rapid chloride permeability values (X). Simple Linear regression was done on the above variables and the correlation coefficient was obtained as 0.96 that indicates strong regression. **Equation for the full log-log linear model is as follows**

$$\text{Log } Y = B_0 + B_1 Log(X)$$

Where, Y= Accelerated Rapid Chloride Permeability Values

X= Ninety-Day Rapid Chloride Permeability Values

B_0 and B_1 = Constants.

It was found after regression that the values of B_0 = -0.83 and B_1 = 1.22

ADEQUACY OF THE REGRESSION MODEL

The error introduced in the regression model is due to the variation between the values of Y within the given values of x. This component reflects mere random variation or pure experimental data. One of the ways of assessing the adequacy of the regression model is to determine $r^{2,}$ the ' multiple correlation coefficient squared'. r^2 expresses the proportion of the total variation in the values of the variable Y that can be accounted for or explained by a linear relationship with the values of the random variables x. The measure of linear association between two variable x and y is estimated by the sample correlation coefficient , r. The value of r varies between +1 and –1 . A value of r=1 implies a perfect linear relationship with a positive slope while a value of r=-1 results from a perfect linear relationship with a negative slope. But the value of r does not necessarily mean that a good relation exits. The following should also be considered for assessing the adequacy of the model.

- Normal probability plot of residuals(e_i) (Fig C1). If the residuals are normally distributed, then the plot should approximately be straight line (Fat Pencil test). (Fig C2).
- The standardized residuals $d_i = e_i / S_{y/x}$. If the residuals are normally distributed, then 95 % of the d_i should fall in the interval (-2, 2). (Table C1)

Figure C3 gives the Log-Log plot of the X and Y data points and the predicted values of accelerated rapid chloride permeability of the concrete (Y) using the proposed model. Regression statistics of the full model is given in Tables C2 and C3.

HYPOTHESIS TEST

The process of dichotomizing the outcomes of an experiment and the using the theory of probability to choose between the two alternatives is known as hypothesis testing. In this test two-tailed test was adopted.

Hypothesis Test on Model

Null Hypothesis - H_o: $\beta_1 = 0$ - There is no relation between Y and X.

Alternative Hypothesis - H_1: $\beta_1 \neq 0$ - There is a strong relation between Y and X.

The null hypothesis has to be rejected very strongly and the alternative hypothesis has to be accepted which will indicate that there is a strong linear relation between the Y and X values.

F (t)= [SSR/k]/ [SSE/n-k-1]

Where

SSR = Sum of squares about regression line

SSE = error of sum of squares for model

K = no of independent variables for model

n = sample size

F (T)= $f_{(\alpha,\nu1,\nu2)}$

If F (t) > F (T) then H_o is rejected

Where

α= Confidence level (95%)

$\nu1$= k degrees of freedom

$\nu2$=n-k-1 degrees of freedom

Significance Level test on model

F (t)= 93.95 and F (T)=5.32 since F (t)>F (T) Reject H_o

This implies that there exits a linear relationship between the dependent and the independent variables. The P value signifies the highest value of the confidence interval. The P value obtained for this model is 1.07 e-5 (Table C3) i.e. even if the value of 1-α is equal to 1.07e-5 there exits a strong relationship.

Hypothesis Test on R value

H_o: R= 0.

$H_{1:}$ r $\neq$ 0.

$$T(t) = T_{cal} = \frac{R\sqrt{n-2}}{\sqrt{1-R^2}}$$

Where

R= correlation coefficient.

n= sample size

t(t)=$t_{(n-2,\alpha/2)}$

If T(t) > t(t) or T(t) < - t(t)

then H_o is rejected

Where

α= Confidence level (95%)

n= sample size

Significance Level test on R

T (t)= 9.693 and t (t)=2.306 since T (t)>t (t) Reject H_o.

Even though we have taken less number of observations we strongly reject the null hypothesis this indicates a strong case of linear relation.

CONFIDENCE INTERVALS

A confidence interval establishes two values, a lower confidence limit and an upper confidence limit that define an interval estimate with pre-specified confidence. The confidence interval is formed by adding and subtracting the bound on the error of estimation from the point estimate. The bound on the error of estimation is (z or t times the standard error of the point estimate) where the z or t value depends on the level of confidence. It represents an interval, such a specified random variable will fall within that interval with the given level of confidence.

Confidence intervals about β_0

The confidence interval about β_0 is calculated by the formulae

$$\beta_0 \pm t_{n-2,\alpha/2} s_{y/x} \frac{\sqrt{\sum x_i^2}}{\sqrt{n\sum (x_i - \bar{x})^2}}$$

Therefore the confidence interval of β_0 is (-1.7924, 0.13097)

Confidence intervals about β_1

The confidence interval about β_1 is calculated by the formulae

$$\beta_1 \pm t_{n-2,\alpha/2} s_{y/x} \frac{1}{\sqrt{\sum (x_i - \bar{x})^2}}$$

Therefore the confidence interval of β_1 is (0.9332, 1.5158)

Using the technique similar to those above, the following 1-α confidence limits, for the mean of Y given specific paired value of x_k.

$$Y_1 \pm t_{n-2,\alpha/2} s_{y/x} \sqrt{1+\frac{1}{n}+\frac{(x_k-\bar{x})^2}{\sum(x_i-\bar{x})^2}}$$

the values of Y are given in Table C4. A confidence Band of a future value of Y (Accelerated Coulombs) (Fig. C4)

CONCLUSIONS

The results of the Rapid Chloride Permeability test carried out on specimens subjected to accelerated curing showed a good correlation with the results obtained from the tests carried out at 90 days. The correlation coefficient (R) obtained from the regression on full log-log model indicated very strong relationship and can be accepted for predicting the values. Hypothesis test (significance level test) done on model and r value was very good even though the sample size was small.

This equation can be used to predict the 90-day permeability for the quartzite aggregate concretes used in this project for any compressive strength, if the accelerated permeability value is known for that concrete. This is highly advantageous because we need not wait for 90 days to know the permeability of concrete used. Some preliminary tests done with limestone aggregate seemed to agree with the suggested equation, however further extensive testing is needed to develop a universal equation applicable to all aggregates.

Table C1: Predicted 90 Day Permeability Values using Log-Log Linear Model

Proposed Logarithmic Model: Log Y= b_0+b_1Log X							
90 Days Coulombs (X)	**Accelerated Coulombs (Y)**	**Log X**	**Log Y**	**Predicted Log Y**	**Residuals e_i**	**Standard Residuals d_i**	**Pred Y**
323	132	2.51	2.12	2.24	-0.12	-0.84	174.51
812	692	2.91	2.84	2.73	0.11	0.75	539.56
1207	533	3.08	2.73	2.94	-0.22	-1.50	876.67
1219	1337	3.09	3.13	2.95	0.18	1.24	887.35
1774	1559	3.25	3.19	3.15	0.05	0.31	1404.85
1943	1642	3.29	3.22	3.20	0.02	0.13	1570.44
3475	4088	3.54	3.61	3.51	0.11	0.74	3200.25
4158	5566	3.62	3.75	3.60	0.14	1.01	3986.66
4704	4059	3.67	3.61	3.67	-0.06	-0.40	4636.83
6831	4548	3.83	3.66	3.86	-0.21	-1.44	7321.69

Table C2: Summary of Regression Statistics of Model for Predicting 90 Day Permeability

Proposed Logarithmic Model: Log Y= b_0+b_1Log X									
Std Deviation Sy/x	b_0 (Intercept)	b_1 (X Variable)	Coef of Correlation r	R Square	Hypothesis Test on Model			Hypothesis Test on R Value	
					Significance F-P value	F(t)	F(T)	T(t)	t(t)
0.15	-0.83	1.22	0.96	0.92	1.07E-05	93.95	5.32	9.693	2.306

Table C3: Regression Statistics of the Logarithmic Model

Regression Statistics	
Multiple R	0.9599641
R Square	0.9215311
Adjusted R Square	0.9117224
Standard Error	0.1523191
Observations	10

ANOVA

	df	*SS*	*MS*	*F*	*Significance F*
Regression	1	2.179770091	2.179770091	93.9512	1.0709E-05
Residual	8	0.185608769	0.023201096		
Total	9	2.36537886			

	Coefficients	*Standard Error*	*t Stat*	*P-value*	*Lower 95%*	*pper 95%*
Intercept	-0.8307127	0.417036714	-1.991941481	0.08153	-1.79240174	0.131
X Variable 1	1.2244995	0.126330295	9.692841096	1.1E-05	0.9331811	1.5158

RESIDUAL OUTPUT

Observation	*Predicted Y*	*Residuals*	*Standard Residuals*
1	2.2418044	-0.12	-0.844177823
2	2.7320371	0.11	0.752528795
3	2.9428362	-0.22	-1.504855681
4	2.9480972	0.18	1.239725395
5	3.1476293	0.05	0.314863494
6	3.1960205	0.02	0.13476056
7	3.5051846	0.11	0.740393788
8	3.6006094	0.14	1.009233439
9	3.6662216	-0.06	-0.402502648
10	3.8646113	-0.21	-1.439969317

PROBABILITY OUTPUT

Percentile	*Y*
5	2.1206
15	2.7267
25	2.8401
35	3.1261
45	3.1928
55	3.2154
65	3.6084
75	3.6115
85	3.6578
95	3.7455

Table C4: 95% Confidence Region for Predicting Y given X

X	Y	Upper Band	Lower Band
2.60	2.35	2.80	1.91
2.85	2.66	3.06	2.26
3.02	2.87	3.25	2.49
3.21	3.10	3.47	2.73
3.32	3.24	3.60	2.87
3.45	3.39	3.77	3.02
3.56	3.53	3.91	3.15
3.62	3.60	3.99	3.22
3.71	3.71	4.11	3.32
3.81	3.84	4.24	3.43

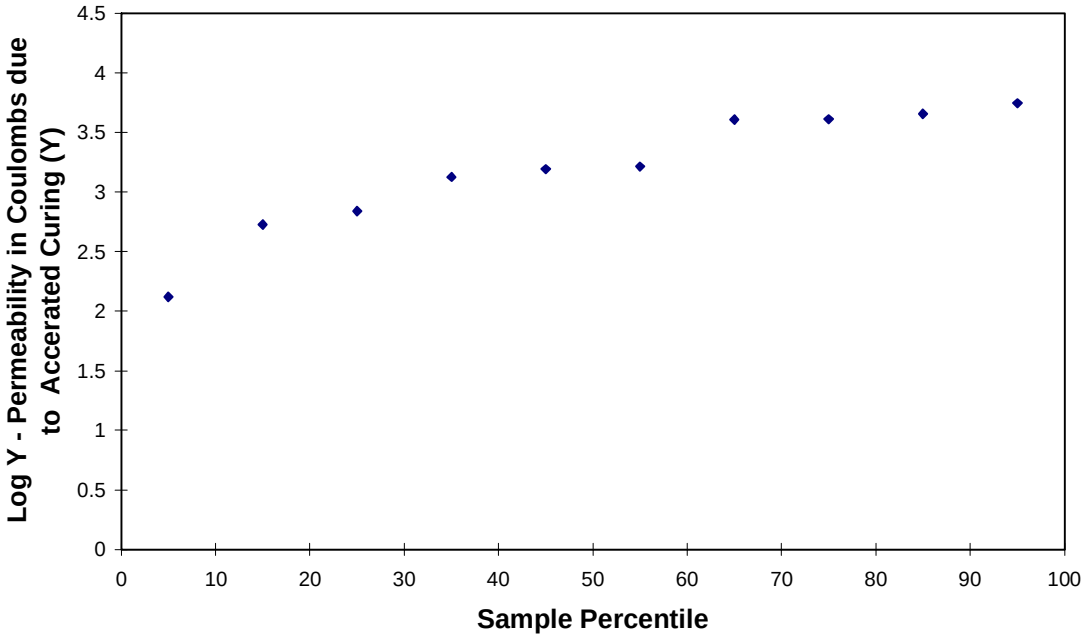

Fig C1: Normal Probability Plot of Residuals

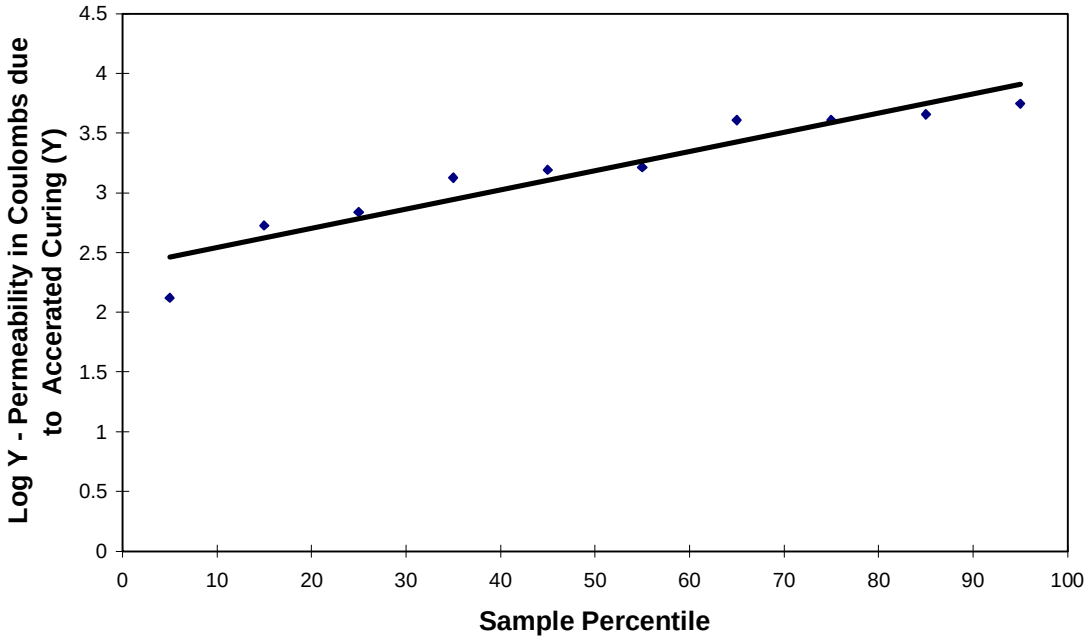

Fig C2: Fat Pencil Test on Normal Probability Plot

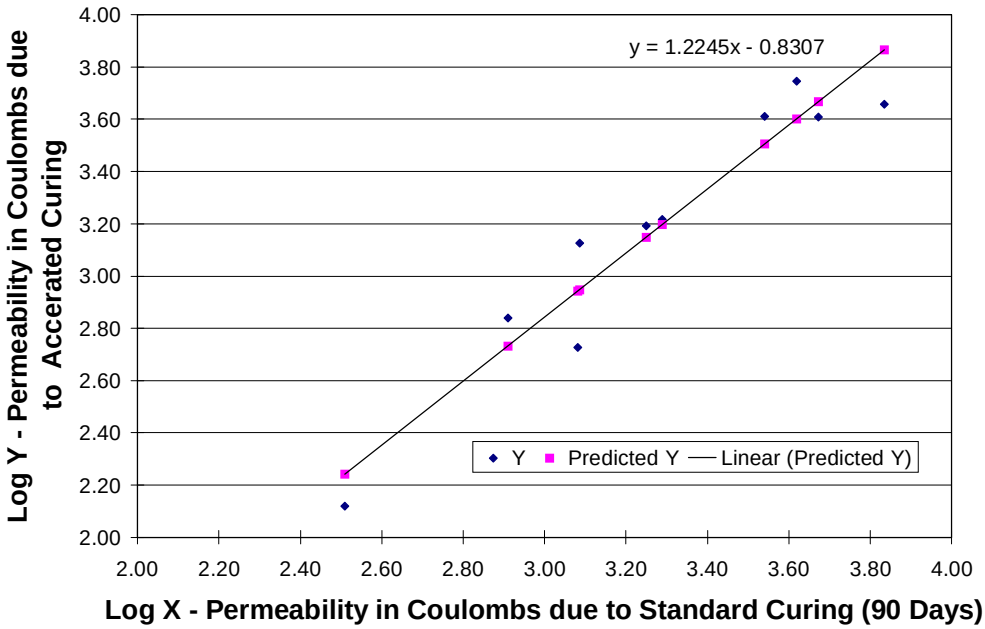

Fig. C3: Regression Analysis - Logarithmic Line Fit Plot

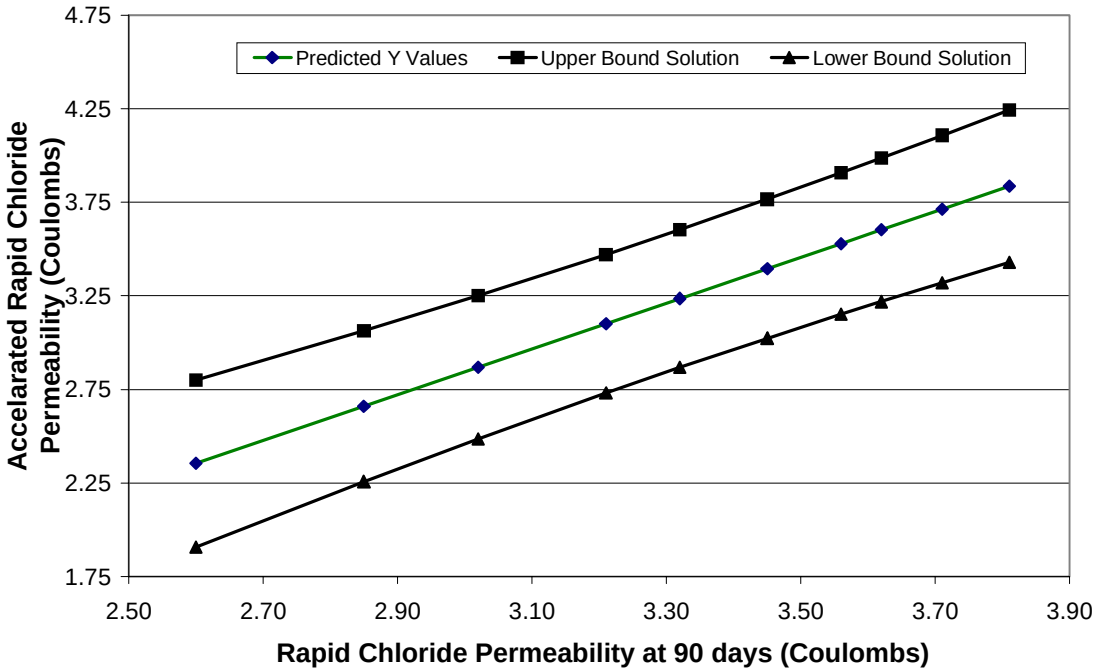

Figure C4: A confidence Band of a future value of Y (Accelerated Coulombs)

Dear Dr. Ramakrishnan,

I am sending you the report on the South Dakota Bridge that includes the final measurements using electromagnetic sensors am also attaching a supplement showing the calculation of losses in the high strength girder. I am sending you a copy of the same by fax and also sending you the final report by mail for your convenience. I am including few details of the final measurement in this letter.

A final set of measurements of the magnetoelastic sensors was attempted on 27 Nov 2001; readings for S3 and S4 were unambiguous and are summarized below. Data from sensor S1 9 nearest to the end of the beam) remained unavailable because of damage to the internal cable, sustained between 19 Jul 01 and 20 Jul 01, when the deck was poured and tamped. During the present visit difficulties were also experienced with sensor S2. The readings from S2 overranged , most likely due to an open circuit at some point. Because this sensor was functioning correctly after the pour on 20 Jul 01, the problem experienced with this sensor is probably due to factors related to external cable/connectors. However, due to deep snow, heavy winds, and freezing conditions on 27 Nov, no attempt was made to diagnose the location of the problem.

Readings for sensors S3 and S4 were obtained as follows. The steel/concrete temperature was measured using the type K thermocouple placed with the sensors during its fabrication. The measurement was made with a handheld thermocouple reader, yielding a value of –1.8 C. the discharge voltage was set to 150 V, the same as in previous measurements. The voltage set points between which the induced voltage was integrated were set to 0.574 and 0.757 volts, respectively, also matching the previous measurements. Three measurements of induced voltage were measured for each of the two sensors, as follows: S3 (2.6004,2.6022, 2.6013), and S4 (2.611,2.6121,2,6105). The mean values of 2.6013 and 2.6114 volts, respectively, were used in conjunction with the measured internal concrete/steel temperature to yield the following in-situ stresses: S3 =185.94 ksi and S4 = 187.88 ksi.

The corresponding forces in the cable are therefore 28447 and 28745 lbs , respectively. The average loss in prestress force is 5.5 % according to calculations from the measured values as shown in **Appendix I** .

It should be noted that the combination lock securing the instrumentation enclosure was frozen shut and all attempts of opening it failed. With the assistance of SDDOT personnel, the lock was removed with a bolt cutter. At the conclusion of the visit, SDDOT supplied a keyed lock , the keys to this lock were given to the lead project engineering in Sioux Falls, Mr. Craig Smith (SDDOT, P.O. Drawer L. Sioux falls, SD 57101-1927, 605 367 5680)

Please don't hesitate to contact me, if you need more information.

Yours sincerely,
Prof. Ming L. Wang
Director
Bridge Research Center
University of Illinois at Chicago
Chicago , IL –60607

Measurement of Prestressed Force of a High Strength Beam

By
Ming L. Wang
Department of Civil and Materials Engineering
University of Illinois – Chicago

Introduction

The field project in South Dakota demonstrates the application of magnetoelastic method to monitor strand stress in I-beams. These beams were fabricated by Gage Brothers Inc, SD, for a three span pre-tensioned concrete bridge. Figure 1 shows the cross-section of one of the I-beams. Each I-beam has 28 FW 0.5" 270 grade strands.

The purpose of this project was to develop a stress monitoring system for one strand of the beam shown in Fig. 1. Fig. 2 shows graphically the location of sensors along the strand. In order to avoid the possible damage and corrosion during construction and sensor's service period, a plastic dip (colored in yellow) was used to cover the steel covering of the sensor in the laboratory. After the sensor was installed on the strand, silicon sealant was used to fill the gap between the strand and the sensor.

Sensor Specifications

The sensors were designed at the University of Illinois at Chicago in the Civil Eng. laboratory and permeability function for each sensor was calibrated. Following are the specifications for the sensors used in the field test:

Cross-sectional area of 0.5" strand , A_f=0.153 in^2 = 98.71 mm^2

Effective area for 0.5" sensor , A_o = 0.332 in^2 =214.98 mm^2

Capacitor voltage Vcap =150 V , ΔV=0.272 V

Primary coil , 1700 turns, 18 gauge (0.01" in diameter) magnetic wire

Secondary coil , 700 turns, 38 gauge (0.004" diameter) magnetic wire.

According to the laboratory test results, optimal working point is calibrated at I_{avg} equal to 1.29 A, ΔI as 0.544 A and the corresponding permeability function is listed below.

$$\mu(\sigma,T) = 5.7113 - 2.4531\times10^{-5}\sigma^2 + 3.3558\times10^{-2}\sigma - 1.390\times10^{-2}T \qquad (1)$$

To solve the stress from above equation, we rewrite the equation as

$$\mu(\sigma,T) = k\sigma(\sigma-\sigma_0) + \alpha_1 T + \mu(0,0) \qquad (2)$$

thus stress can be expressed as

$$\sigma = \frac{1}{2}[\sigma_0 - \sqrt{\sigma_0^2 + 4(\mu - \mu_0 - \alpha_1 T)/k}] \qquad (3)$$

where σ_0 =-m1/m2=1367.98 ksi

k=m2=-2.4531$\times10^{-5}$

α_1 =-1.39 $\times10^{-2}$

$\mu(0,0)$ =5.7113

Here we have focused on the linear elastic region. The permeability equation (Eqn. 1) gives 2 roots for stress. The root out of elastic region is excluded because the yield stress for FW 0.5" strand is less than 500 ksi. Table I list some parameters obtained in the laboratory. Detailed description and analysis of the method is given in Appendix I.

TABLE I

PARAMETERS FOR THE SENSORS USED IN FIELD TEST

Sensor number	Resistant of primary coil (Ω)	Resistant of secondary coil (Ω)	U_{high}(V) optimal working point	U_{low}(V) Optimal working point	U_{int}(V) Electromotie force at T=23°C
1	18.3	73.7	0.802	0.530	1.3513
2	17.9	72.6	0.802	0.530	1.3562
3	18.0	73.7	0.802	0.530	1.3513
4	18.6	74.9	0.802	0.530	1.3583

Discussion :

The test was conducted at Gage Brothers Inc. in Sioux Falls, SD from May 16 to May 23. Three beams of length 54', 61' and 54' respectively, were fabricated in a 200' long prestressing 'bed' simultaneously. Four sensors were installed on the strand before the strand was tensioned up to 31,000 Lb. Figure 3 to Figure 5 show the sensors on the strand. As shown in Figure 6, a lab-top, a pulsed measuring device and a voltage controlled current source were used to measure the permeability of strand. Stress is calculated by inserting the permeability value into Equation 3. Table II is the measured results of forces along the strand at various stages of loading history.

Loading history includes the pouring of concrete in the test bed as shown in Fig. 7, after cutting the strand while resting in the concrete yard as shown in Fig. 8 and before pouring the concrete while resting at the bridge site as shown in Fig. 9. Fig. 10 shows the plot of Force vs Time for the sensors 1-4 during the complete test.

Conclusions :

1. The first measurement was taken after the strand was tensioned up to 31,000 lbs. From the results, it is seen that the stress is almost homogeneous along the four measured locations. As listed in Table II, the measured force is approximately 4% less than that of applied force (31,000 lbs). Considering the force applied at the end i.e. 160' away from measuring location, the measured value of stress is reasonable.
2. The second measurement taken 2 hours after the strand was tensioned showed no significant loss in stress.
3. The beam was cast on May 18, 2000. Third measurement was taken 6 days after the strand was tensioned. Stress loss of 1 % to 2% was measured during this period.

4. Concrete cylinders were cast using the same concrete as the I-beams and at the same time when the beams were fabricated. Strands were not released until the compressive strength of the concrete cylinder sample reached 8.75 ksi. On June 15, another measurement was taken after the strand was released. The value obtained from the first sensor showed stress loss to 97.7 ksi (14946 lbs in tension) that is half of the original stress value. This was because the measured location was 1' ¾" away from the end of beam where the released stress of the strand was zero. It is also seen from the results that there is an increase of about 0.5% to 1% in stress at other three locations even though the strand was released. This is due to the reason that the temperature went down to 12 C and a tensile force was applied to the strand by the concrete due to difference in their coefficient of expansion.
5. As seen from step 4 to step 5 there is an increase in force by 400 lbs when the beam was under its self weight at its final position at the construction site. However, the sensor that is 1'3/4" from the anchorage is further relaxed in tension of about 2100 lbs. This is attributed to the continuation of slippage between the strand and concrete. Several strain gages were also installed near the anchorage. These strain were covered by a thick layer of teflon for protection of strain gages against moisture. However, this cover prohibits the development of bond strength between the strand and the concrete.
6. There was an increase in force by 400 lbs after concrete was poured in the deck. Unfortunately, the wire of sensor 1 was damaged by the vibrator after pour of concrete.

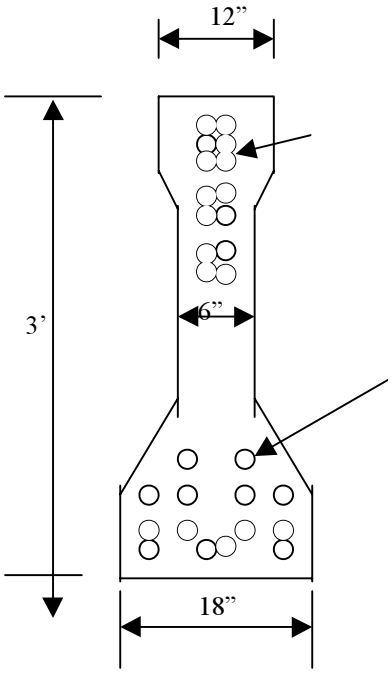

Figure 1. Cross section of the I-beam fabricated by Gage Brothers, Inc, SD

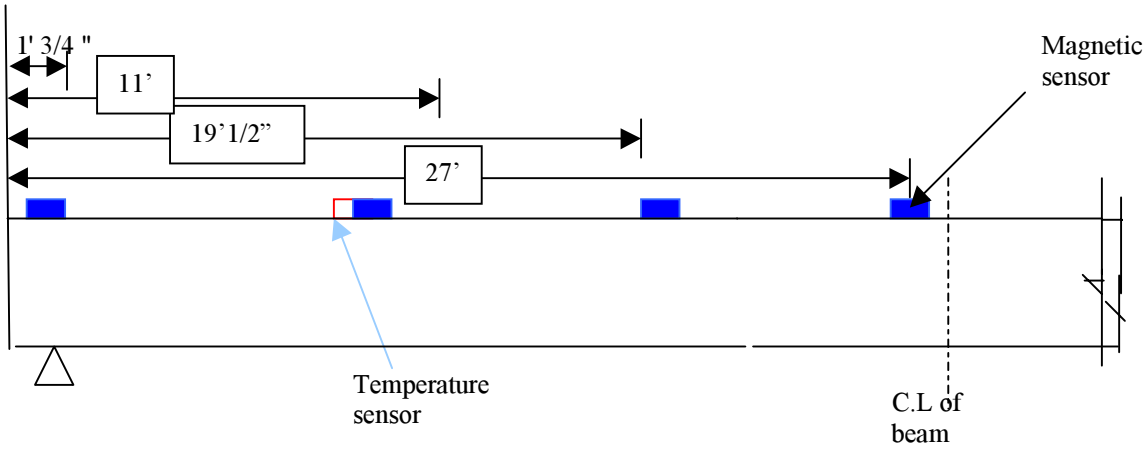

Figure 2. Sensor locations on the strand of a 54’ long simple supported I-beam

TABLE II: TEST RESULTS (Force Only)

Event	Schedule / Force	Sensor 1	Sensor 2	Sensor 3	Sensor 4
1	Tested after the strand was tensioned Strand un-released Concrete un-cast T=22 ° C (05/16/00)	29,300	29,391	29619	29656
2	2 hours after the strand was tensioned Strand un-released Concrete un-cast T=22 ° C (05/16/00)	29,272	28,700	28,714	28,760
3	6 days after the strand was tensioned , Strand unreleased 4 days after concrete was cast T=27.3 ° C (05/22/00)	28,934	28,554	28,639	28,825
4	30 days after the strand was tensioned Strand released 25 days after concrete was cast T=15.2 ° C at rest position (06/16/00)	14,946	28,714	28,760	29,085
5	Beam under it's self weight at final construction site Before pouring concrete on deck T = 15.4 C (6 p.m, 7/19/00)	12,820	29,121	29,180	29,463
6	Before pour of concrete on deck T= 15.0 C (10:30 a.m ,7/20/00)	13,089	29,133	29,189	29,464
7	After pour , deck formed T= 18.2 C (5 p.m , 07/20/00)	Wire damaged by vibrator	29,534	29,786	30,113
8	16 months from the casting, 11/27/01	Wire damaged by vibrator	Unable to take reading due to frozen connector	28,447	28,754

Figure 3. Magnetoelastic sensors installed on a strand

Figure 4. Magnetic sensor (colored in yellow) installed on a strand

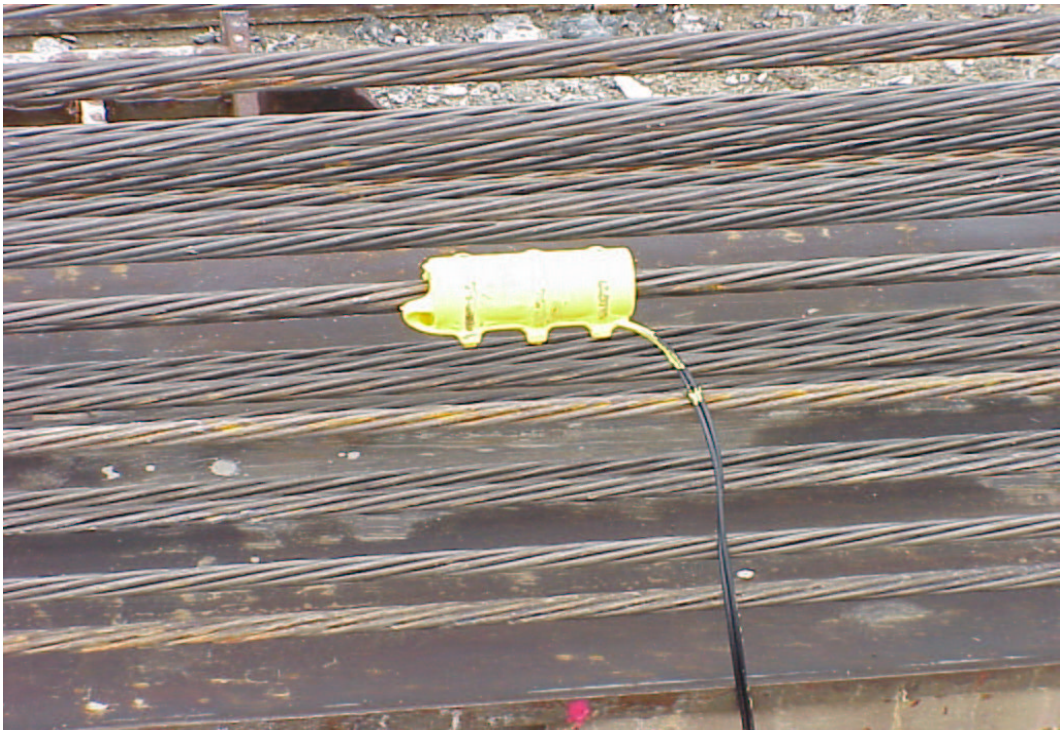

Figure . Magnetoelastic sensor on a tensioned strand

Figure 6. Field test facilities

Figure 7. Magnetoelastic sensors installed in a fabricated beam

Figure 8. Fabricated pre-tensioned I-beams

Figure 9. Final position of the beam at the site.

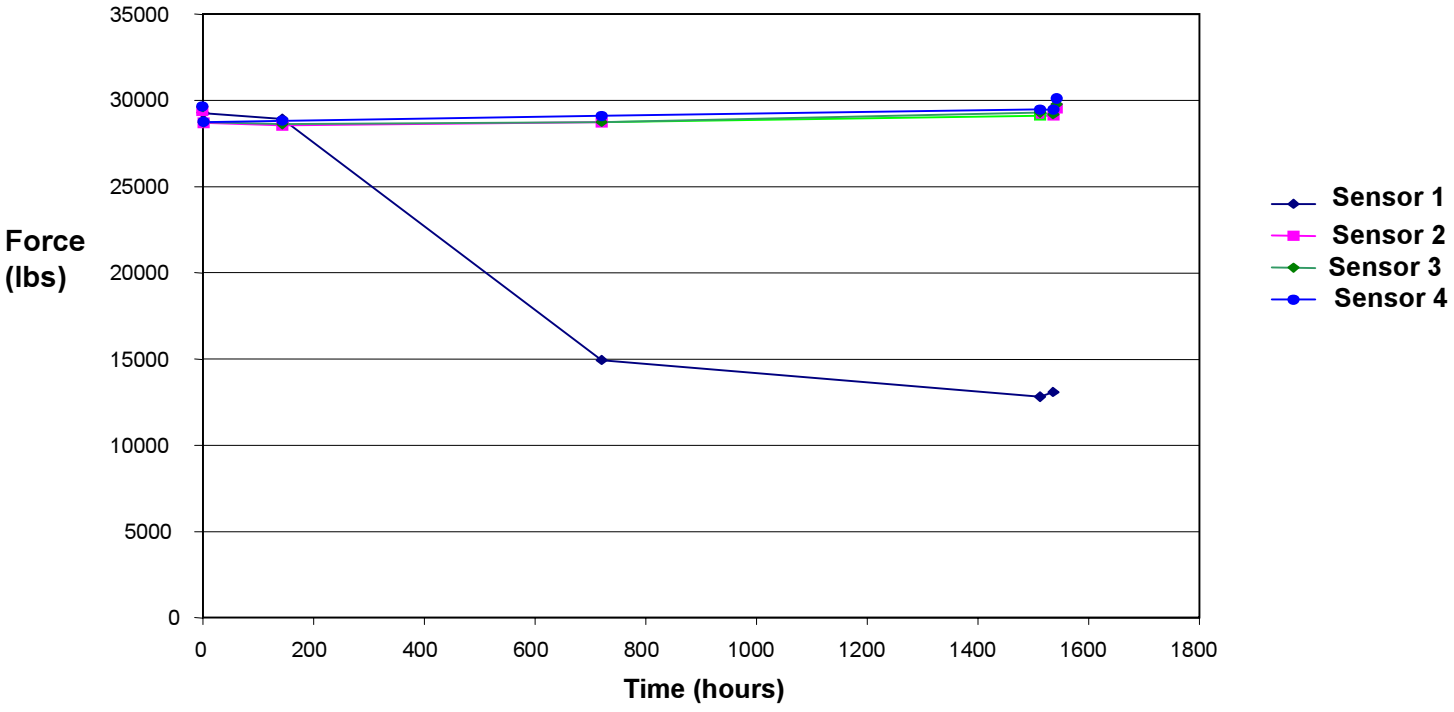

Fig. . i e vs Force for the sensors 1 - 4